Author:
Chambers, Adam Christian

Title:
The role of BCL-3 in apoptosis and therapy response in rectal cancer

The role of BCL-3 in apoptosis and therapy response in rectal cancer

Mr Adam Christian Chambers BMBS MSc MRCSEd

A dissertation submitted to the University of Bristol in accordance with the requirements for award of the degree of PhD in the School of Cellular and Molecular Medicine, Faculty of Biomedical Sciences.

January 2019 Words: 43256

Abstract

Colorectal cancer (CRC) is a major cause of cancer related mortality and is the second most common cause of cancer deaths in the UK (CRUK). Despite year on year improvements in survival, the five-year survival for all patients remains less than 60%. For locally advanced rectal cancer (LARC), surgical resection is a mainstay of management, alongside pre-operative long-course chemoradiotherapy (LCCRT). Tumour regression grade (TRG) in LARC is variable and patients' tumours that fail to regress with radiation have much poorer prognosis. Understanding why patients have a poor TRG is critical to improving survival from rectal cancer.

The proto-oncogene BCL-3 is upregulated in a subset of CRCs. BCL-3 expression predicts patient prognosis in advanced disease and has been shown to protect colon cancer cells from apoptosis. However, little is known regarding the role of BCL-3 in rectal cancer, specifically, concerning BCL-3's role in promoting tumour cell survival or in the response to irradiation.

Results reveal that BCL-3 is expressed in rectal cancer cells. BCL-3 suppression was shown to increase expression of the pro-apoptotic BH3-only BCL-2 family member Bim, leading to apoptosis. BCL-3 and p52 were identified at κB consensus sites on the BCL2L11 promoter. Moreover, BCL-3 suppression increased acetylated histone 3 abundance at the BCL2L11 promoter, suggesting BCL-3 loss, results in transcriptional activation of Bim. Additionally, BCL-3 protects rectal cancer cells from γ-irradiation and loss results in exacerbated and prolonged γH2AX foci formation.

These data suggest that BCL-3 plays an important role in the DNA damage response of CRC cells. Interestingly, immunohistochemistry of rectal cancer biopsies showed that BCL-3 expression may predict TRG to LCCRT. Excitingly, these data suggest a dual action for anti-BCL-3 therapeutics: targeting BCL-3 may be important for prevention and/or treatment, causing tumour cell death, whereas inhibiting BCL-3 function, in the subset of patients with increased BCL-3 expression in tumours, may increase the response to LCCRT and drive improvements in prognosis for these patients.

For Amalia and Cecily

Acknowledgements

I want to acknowledge all the members of the Williams and Paraskeva groups for guiding me through the PhD. Without all your help, it would not have been possible. Particularly, thanks to Danny, Rhys, Alex, Steve, Elle, Tray and Chris, who have all become true friends.

Thank you to my supervisor Ann, for giving me the opportunity and always knowing what to say or do when I needed advice.

I also want to acknowledge my funders, the MRC, David Telling Trust and the Elizabeth Blackwell Institute.

Finally, I want to thank my Wife, family and friends for putting up with me while I wrote up.

Author’s declaration

I declare that the work in this dissertation was carried out in accordance with the requirements of the University's Regulations and Code of Practice for Research Degree Programmes and that it has not been submitted for any other academic award. Except where indicated by specific reference in the text, the work is the candidate's own work. Work done in collaboration with, or with the assistance of, others, is indicated as such. Any views expressed in the dissertation are those of the author.

SIGNED: ..... DATE: .....

Table of Contents

Abstract ..... **ii**

Acknowledgements ..... **iv**

Author's declaration ..... **v**

Table of Contents ..... **vi**

List of Figures ..... **xii**

List of Tables ..... **xvi**

List of Abbreviations ..... **xvii**

1 Introduction **1**

1.1 Colorectal cancer **2**

1.2 Rectal cancer **5**

1.2.1 Current management of LARC 7

1.2.1.1 Surgical resection 7

1.2.1.2 Treatment and response with long-course chemo-radiotherapy in rectal cancer 8

1.3 Colorectal tumorigenesis **13**

1.3.1 Genetic drivers of colorectal cancer 14

1.3.2 Wnt pathway mutations 15

1.3.3 RAS/RAF pathway mutations 16

1.3.4 TP53 mutations 17

1.3.5 Transforming growth factor signalling 17

1.3.6 PI3 Kinase signalling 18

1.4 Epigenetic drivers of colorectal cancer **18**

1.5 The NF-κB signalling pathway **20**

1.5.1 An overview of NF-κB signalling 20

1.5.2 Canonical NF-κB signalling 24

1.5.3 Non-canonical NF-κB signalling 25

1.5.4 Atypical NF-κB signalling 28

1.6 B-cell lymphoma 3 (BCL-3) **31**

1.6.1 BCL-3 Structure 31

1.6.2 Translational control of BCL-3 32

1.6.3 Post-translational modification of BCL-3 33

1.6.4 BCL-3 Function 34
1.6.5 Control of NF-κB sub-units 34
1.6.6 Trans-activator or transrepressor 35
1.6.7 BCL-3 protein interactions 36
1.6.8 BCL-3 and the 'Hallmarks of Cancer' 37
1.6.8.1 Sustaining proliferative signalling 37
1.6.8.2 Activating invasion and metastasis 38
1.6.8.3 Evasion of Apoptosis 38
1.6.9 The role of BCL-3 in inflammation and immunity 39
1.7 Hypothesis and Aims 43
1.7.1 Project aims 44
2 Methods 45
2.1 Tissue Culture 46
2.1.1 Cultured Cells 46
2.1.1.1 SW1463 46
2.1.1.2 LS174T 46
2.1.1.3 HCA7/Parental 46
2.1.1.4 SW837 47
2.1.1.5 Fibroblast cell lines 47
2.1.1.6 Adenoma/Carcinoma protein expression screen cell lines 47
2.1.2 2D Cell Culture 47
2.1.3 Cell passage 48
2.1.4 3D Cell Culture 48
2.1.4.1 Human spheroid culture 48
2.1.4.2 Mouse organoid culture 49
2.1.4.3 Passaging mouse organoid cultures 50
2.2 Genetic Transfection 50
2.2.1 RNA Interference - siRNA 50
2.2.2 Stable overexpression of BCL-3 52
2.3 Functional Assays 53
2.3.1 Cell yield and survival assay 53
2.3.2 Crystal violet cell viability assay 54
2.4 Treatments 55
2.4.1 Pan-caspase inhibitor, QVD 55
2.4.2 BCL-3 small molecule inhibitors 55
2.4.3 Oxaliplatin 55
2.4.4 BCL2 Family inhibitor 56

2.4.5 Poly ADP Ribose Polymerase inhibitor 56
2.4.6 Transforming Growth Factor-Beta 57
2.4.7 Interleukin 6 57
2.4.8 Geneticin 57
2.4.9 Irradiation 57
2.5 Molecular Biology 59
2.5.1 RNA analysis 59
2.5.1.1 RNA extraction 59
2.5.1.2 Reverse Transcriptase Reaction 59
2.5.1.3 qRT-PCR 60
2.5.2 Protein analysis 61
2.5.2.1 Whole Cell Lysis 61
2.5.2.2 Whole Flask Lysis 61
2.5.2.3 3D Spheroid Culture Whole Cell lysis 62
2.5.2.4 Protein Concentration Assay 63
2.5.2.5 SDS-PAGE and Western Analysis 63
2.5.3 Immunofluorescent protein analysis 66
2.5.3.1 Transfection and irradiation of cells on coverslips 66
2.5.3.2 Coating of coverslips 66
2.5.3.3 Fixation and slide preparation 66
2.5.3.4 Confocal imaging of slides 68
2.5.4 Chromatin Immunoprecipitation (ChIP) 68
2.5.4.1 Chromatin crosslinking, fixation, lysis and sonication 68
2.5.4.2 Immunoprecipitation of chromatin 71
2.5.4.3 DNA clean-up 73
2.5.4.4 PCR and agarose gel electrophoresis 73
2.6 Data Analysis 75
3 Results 1: BCL-3 promotes cell-survival in colorectal tumour cells through supressing the BCL2 family, BH3-only pro-apoptosis protein Bim 76
3.1 Introduction 77
3.1.1 Apoptosis 77
3.1.2 The BCL-2 protein family 78
3.1.3 BCL2 interacting mediator of cell death (Bim) 79
3.1.4 Aims 81
3.2 Results 82
3.2.1 BCL-3 expression in rectal cancer cell lines 82

3.2.2 BCL-3 suppression increases levels of floating cells in colorectal tumour cells with high expression of BCL-3 83
3.2.3 BCL-3 suppression increases expression of the markers of intrinsic apoptosis 85
3.2.4 Apoptosis induced by BCL-3 suppression can be blocked using QVD (pan caspase inhibitor) 87
3.2.5 BCL-3 regulates Bim a pro-apoptotic member of the BCL2 family 89
3.2.6 Validation that Bim is regulated by BCL-3 91
3.2.7 Knockdown of Bim abrogates BCL-3 suppression-induced apoptosis 93
3.2.8 BCL-3 knockdown does not alter pAKT expression or pERK expression 95
3.2.9 Bim expression increases with BCL-3 and p52 suppression in HCA7 and SW1463 but not LS174T colorectal cancer cells 96
3.2.10 BCL-3 suppression increases levels of Bim mRNA 98
3.2.11 BCL-3 binds to the Bim promoter at NF-κB consensus sites 100
3.2.11.1 ChIP primer Design 100
3.2.11.2 Sonication Efficiency 102
3.2.11.3 Primer dimerisation 103
3.2.11.4 BCL-3 and p52 bind to the BCL2L11 promoter in colon and rectal cancer cell lines 105
3.2.11.5 BCL-3 suppression increases levels of active histone marks (acH3) at the BCL2L11 promoter 106
3.2.12 Response of a panel of colorectal cancer cell lines to ABT-737 .. 108
3.2.13 BCL-3 knockdown does not sensitise to treatment with ABT-737 110
3.3 Discussion 112

4 Results 2: BCL-3 protects colorectal cancer cells from γ-irradiation 116
4.1 Introduction 117
4.1.1 BCL-3 and NF-κB in therapy response 120
4.1.2 The tumour microenvironment and response to therapy 123
4.1.3 Aims 126
4.2 Results 127
4.2.1 BCL-3 expression may confer resistance to LCRT in rectal tumours 127
4.2.2 Optimisation of seeding densities for cell lines to be used in γ-irradiation cell viability experiments 129

4.2.3 Radiation dose response rates in 4 colorectal cancer cell lines .. 131
4.2.4 BCL-3 knockdown sensitises colorectal cells to γ-irradiation 133
4.2.5 BCL-3 suppression sensitises to oxaliplatin, a DNA damage inducing agent used in the management of rectal cancer 136
4.2.6 BCL-3 stable overexpression in a low basal expressing BCL-3 rectal cancer cell line 138
4.2.7 BCL-3 stable over-expression in rectal cancer cells does not alter cell viability following γ-irradiation 140
4.2.8 Automated spheroid area analysis accurately measures colorectal cancer spheroids embedded in Matrigel and is comparable to manual spheroid diameter measurement 142
4.2.9 BCL-3 expression in cells grown in 3D culture conditions 144
4.2.10 Fibrosis is a principal component of response to radiation in rectal cancer 146
4.2.11 BCL-3 expression is upregulated by IL-6 in rectal cancer cells ... 149
4.2.12 Investigating the role of CAFs on 3D growth and sensitivity to irradiation 151
4.2.13 Growth of SW1463 colorectal cancer spheroids is increased in co-culture with fibroblasts 154
4.2.14 Growth of rectal cancer spheroids (SW1463 and SW837) is increased with activated fibroblasts 156
4.2.15 Activated fibroblasts from normal and sporadic cancers potentially promote growth of SW1463 rectal spheroids 158
4.2.16 Co-culture of colorectal cancer spheroids with fibroblasts does not alter radiation sensitivity of the cancer spheroids 160
4.2.17 Conditioned media from activated fibroblasts results in a small increase in growth of rectal cancer spheroids 163
4.2.18 BCL-3 expression is promoted by treatment with conditioned media from fibroblasts in a rectal cancer cell line 166
4.2.19 BCL-3 suppression in 3D cultures was not possible using siRNA 168
4.2.20 BCL-3 inhibitors did not significantly reduce rectal cancer spheroid size 170
4.2.21 Analysing the effect of BCL-3 expression on the DNA damage response 172
4.2.21.1 BCL-3 suppression promotes increased and persistent γH2AX foci formation following radiation in HCA7/P colon cancer cells 172
4.2.21.2 BCL-3 suppression increases γH2AX formation in SW1463 cells 175

4.2.21.3 Does BCL-3 inhibit homologous recombination? 177
4.3 Discussion 179
5 Discussion 184
5.1 BCL-3 and apoptosis 185
5.2 BCL-3 and irradiation 188
6 Appendix 193
6.1 Appendix 1 194
6.1.1 ASPIRE STUDY PROTOCOL 194
6.2 Appendix 2 205
6.2.1 TNM staging of colorectal cancer 205
6.3 Appendix 3 207
6.3.1 Tumour regression grade (TRG) systems 207
6.4 Appendix 4 208
6.4.1 BCL2L11 gene sequence 208
6.5 Appendix 5 213
6.5.1 SDS-PAGE gel composition 213
6.6 Appendix 6 214
6.6.1 Automated spheroid assessment MATLAB script 214
7 References ..... Error! Bookmark not defined.

List of Figures

Figure 1.1 Age-specific incidence of colorectal cancer between 1974 and 2015 in England 2

Figure 1.2 Characteristics of colorectal cancer based on inherited genetic defects in comparison to sporadic colorectal cancer. 3

Figure 1.3 Anatomy of the colon and rectum 4

Figure 1.4 TNM staging of colorectal cancer 6

Figure 1.5 The adenoma-carcinoma sequence 14

Figure 1.6 Mutational burden in colorectal cancers and differences between non-hypermutator (nHM) and hypermutator phenotypes (HM). 15

Figure 1.7 Principal members of the NF-κB signalling pathway 22

Figure 1.8 The canonical NF-κB pathway 24

Figure 1.9 The non-canonical NF-κB signalling pathway 27

Figure 1.10 Atypical NF-κB homodimer signalling 30

Figure 1.11 Map of BCL-3 DNA 31

Figure 2.1 BCL-3 plasmid maps 53

Figure 2.2 Platinum-based chemotherapy compounds 56

Figure 3.1 Expression of BCL-3 in rectal cancer derived cell lines in comparison to a panel of colon carcinoma and adenoma derived cell lines 82

Figure 3.2 Suppression of BCL-3 increases cell death in rectal and colon cancer cells 84

Figure 3.3 BCL-3 suppression using siRNA induces increased cleavage of markers of intrinsic apoptosis: cleaved caspase-3 and cleaved PARP. 86

Figure 3.4 The pan-caspase inhibitor QVD blocks BCL-3 suppression induced apoptosis. 88

Figure 3.5 BCL-3 knockdown primarily alters Bim out of a panel of proteins critical for mitochondrial apoptosis. 90

Figure 3.6 Suppression of BCL-3 using differing siRNA sequences results in induction of Bim protein expression. 92

Figure 3.7 BCL-3 knockdown induced apoptosis is dependent on Bim. 94

Figure 3.8 BCL-3 suppression does not alter pAKT^{S473} levels in the colorectal cancer cell lines SW1463, HCA7/P and LS174T..... 95

Figure 3.9 Bim upregulation results from NF-κB2 suppression as well as BCL-3 suppression but not NF-κB1 97

Figure 3.10 BCL-3 suppression leads to increased levels of Bim mRNA. 99

Figure 3.11 The BCL2L11 promoter contains two putative NF-κB DNA binding sites 101

Figure 3.12 Validation of sonication efficiency using HCA7 carcinoma cells. ... 102

Figure 3.13 1% DMSO reduces primer dimer formation for primers with high GC content..... 104

Figure 3.14 BCL-3 and p52 are found at the BCL2L11 promoter. 105

Figure 3.15 Preliminary ChIP data suggests BCL-3 knockdown reduces abundance of acetylated Histone 3 at the BCL2L11 promoter. 106

Figure 3.16 Treatment of colorectal tumour cells with the BCL2 inhibitor ABT-737 109

Figure 3.17 ABT-737 treatment does not increase levels of apoptosis observed following BCL-3 suppression in colorectal tumour cells..... 111

Figure 4.1 BCL-3 expression in rectal cancers may predict response to neo-adjuvant radiation 128

Figure 4.2 Seeding densities for crystal violet cell viability assay in colorectal tumour cells 129

Figure 4.3 Sensitivity of colorectal cancer cells to γ-irradiation..... 132

Figure 4.4 BCL-3 knockdown increases radio-sensitivity in colorectal cancer cells 135

Figure 4.5 BCL-3 knockdown sensitises rectal cancer cells to an alternative DNA damaging agent, oxaliplatin. 137

Figure 4.6 BCL-3 over-expression in the SW837 rectal cancer cell line 139

Figure 4.7 SW837 stably over-expressing BCL-3 does not protect cells against γ-irradiation induced cell death 141

Figure 4.8 Automated spheroid area analysis in the rectal cancer cell line SW1463 143

Figure 4.9 BCL-3 expression in 3D culture conditions in a panel of colon and rectal cancer cell lines 145

Figure 4.10 Fibrosis is a major component of the response to radiation in rectal cancer and closely related to pathological tumour stage 148

Figure 4.11 Rectal cancer cells upregulate BCL-3 in response to IL-6 150

Figure 4.12 Colorectal cancer spheroids grow normally when co-cultured with low numbers of colon fibroblasts 153

Figure 4.13 Colorectal cancer spheroids require higher numbers of fibroblasts in co-culture to initiate increases in spheroid growth 155

Figure 4.14 Rectal cancer cells co-cultured with activated fibroblasts have increased growth 157

Figure 4.15 Co-culture of SW1463 rectal cancer spheroids with alternative fibroblasts results in increases in spheroid sizes. 159

Figure 4.16 Rectal cancer spheroids co-cultured with fibroblasts have increased radioresistance 162

Figure 4.17 Conditioned media from activated fibroblasts increases growth of SW1463 rectal cancer spheroids 165

Figure 4.18 BCL-3 expression is increased following exposure to CM from VC or TGFβ treated fibroblasts 167

Figure 4.19 Transfection of spheroids with BCL-3 siRNA in 3D does not alter radiation sensitivity 169

Figure 4.20 BCL-3 inhibitor non-significantly reduces growth of SW1463 rectal cancer spheroids 171

Figure 4.21 BCL-3 knockdown increases phosphorylated H2AX (γH2AX) foci formation following γ-irradiation 173

Figure 4.22 Rectal cancer cells SW1463 demonstrate increased γH2AX foci after BCL-3 suppression and irradiation. 176

Figure 4.23 BCL-3 suppression does not sensitise rectal cancer cells to Veliparib (PARP inhibitor) 178

Figure 5.1 Model of BCL-3 function in apoptosis in colorectal cancer cells 186

Figure 5.2 Model of BCL-3 function in DNA damaging therapy response..... 191

List of Tables

Table 2.1 γ-Irradiation dose 58

Table 2.2 Cell Lysis Buffer 61

Table 2.3 Buffers for Western Blot 64

Table 2.4 Antibodies for Western Blot 66

Table 2.5 Immunofluorescence antibodies 68

Table 2.6 ChIP buffers 71

Table 2.7 ChIP antibodies 72

Table 2.8 ChIP primers 74

Table 2.9 Touchdown PCR programme, TD-PCR 75

List of Abbreviations

CRC – colorectal cancer

IEC – intestinal epithelial cells

BCSP – bowel cancer screening programme

NHS – National Health Service

FAP – Familial Adenomatous Polyposis

APC – adenomatous polyposis coli

HNPCC – hereditary non-polyposis colorectal cancer

MMR – mismatch repair

MSI – microsatellite instability

MYH - MUTYH

MAP – MYH-associated polyposis

JPS – juvenile polyposis syndrome

PJS – Peutz Jeghers syndrome

MDT – multi-disciplinary team

CT – computed tomography scan

MRI – magnetic resonance imaging

TNM – Tumour Node Metastasis

LARC – locally advanced rectal cancer

CRM – circumferential resection margin

UICC – Union for International Cancer Control

TEM – transanal endoscopic microsurgery

CRUK – Cancer Research UK

TME – total mesorectal excision

AR – anterior resection

APR – abdominoperineal resection

TaTME – transanal total mesorectal excision

LARS – low anterior resection syndrome

SCPRT – short-course pre-operative radiotherapy

LCRT – long-course radiotherapy

LCCRT – long-course chemo-radiotherapy

MRC – Medical Research Council

NSABP – National Surgical Adjuvant Breast and Bowel project

EORTC – European Organisation for Research and Treatment of Cancer

FFCD – Federation Francophone de Cancerologie Digestive

TRG – tumour regression grade

MSKCC – Memorial Sloan Kettering Cancer Center

AJCC – American Joint Committee on Cancer

CAP – college of American pathologists

pCR – pathological complete response

OS – overall survival

DFS – disease free survival

cCR – clinical complete response

IWWD – international watch and wait database

HM - hypermutator

nHM – non-hypermutator

NICE – National Institute for Health and Care Excellence

LOI – loss of imprinting

KRAS – Kirsten Rat sarcoma virus

BRAF – B-rapid accelerating fibrosarcoma

EGFR – epidermal growth factor receptor

PI3K – phosphoinositide 3-kinase

TGFβ – transforming growth factor beta

SMAD – (small worm phenotype) mothers against decapentaplegic

Wnt – wingless

MLH1 – MutL homologue 1

NF-κB – nuclear factor kappa-light-chain-enhancer of activated B cells

IκB – inhibitor of kappa B

IKK - IκB kinase

NLS – nuclear localisation sequence

TAD – transactivation domain

RHD – Rel homology domain

ARD – Ankyrin repeat domain

NEMO – NF-κB essential modulator

NBD – NEMO binding domain

PEST – Proline glutamate serine and threonine

LZ – leucine zipper-like

DD – death domain

CC – coiled coil

HLH – helix-loop-helix

ZF – zinc-finger

RANK – receptor activator of nuclear factor κ B

BAFF – B-cell activating factor

TCR/BCR – T/B cell receptor

AOM - azoxymethane

DSS – dextran-sodium sulphate

LTβ - lymphotoxin beta

NIK – NF-κB inducing kinase

TRAF – TNF receptor associated factor

KO – knockout

ATM – ataxia telangiectasia mutated

CK2 – casein kinase 2

PID – processing-inhibitory domain

GWAS – genome-wide association studies

AP1 – activator protein 1

STAT – signal transducer and activator of transcription

SH3 – SRC homology 3

FYN – tyrosine kinase protein

GSK3 – glycogen synthase kinase 3

IL – interleukin

PMA – phorbol 12-myristate 12-acetate/phorbol ester

PTM – post-translational modification

TBLR1 - Transducin Beta Like 1 X-Linked Receptor

PSMB1 – proteosome subunit beta type-1

KAT – lysine acetyltransferase

JAB1 – Jun activation-domain binding protein 1

BARD1 – BRCA associated ring domain 1

BRCA – breast cancer type 1 susceptibility protein

HSP70 – heat shock protein 70

HDAC – histone de-acetylase

CtBP – C-terminal binding protein

MYC - myelocytomatosis

DDR – DNA damage repair

RA – rheumatoid arthritis

IBD – inflammatory bowel disease

RSV – respiratory syncytial virus

ATCC – American Type Culture Collection

DMEM – Dulbecco's Modified Eagles Medium

FBS – foetal bovine serum

EDTA – ethylenedianmine-tetraacetic acid

BSA – bovine serum albumin

RNAi – RNA interference

siRNA – short interfering RNA

GFP – green fluorescent protein

NAC – N-acetylcysteine

QVD – quinolyl-valyl-O-methylaspartyl-[-2,6-difluorophenoxy]-methyl ketone

DMSO – dimethyl sulfoxide

EGF – epidermal growth factor

PBS – phosphate buffered saline

ADM – advanced DMEM

ABT – Abbott Labs

PARP – poly-ADP ribose polymerase

Gy – Gray (measurement of irradiation dose)

cDNA – complimentary DNA

MMLV – moloney murine leukaemia virus

ddH_2O – double distilled water

TBP – tata-binding protein

PIC – protease inhibitor cocktail

EDTA – ethylenediaminetetraacetic acid

EGTA – ethylene glycol-bis(βaminoethyl ether)-N,N,N',N'-tetraacetic acid

WFL – whole flask lysate

WCL – whole cell lysate

TEMED – tetramethylethylenediamine

PVDF – polyvinylidene fluoride

TBS-T – Tris-buffered saline with tween 20

DAPI – 4',6-diamidino-2-phenylindole

MOMP – mitochondrial outer membrane permeability

SMAC/DIABLO – second mitochondria-derived activator of caspases/ direct IAP binding protein with low pl

AIF – apoptosis inducing factor

CARD – caspase recruitment domain

APAF1 – apoptotic protease-activating factor 1

ICAD – inhibitor of caspase-activated DNase

BH domain – BCL-2 homology domain

Bim – BCL-2 interacting mediator of cell death

DLC1 – dynein light chain 1

ER – endoplasmic reticulum

FOXO – forkhead box O

JNK – c-Jun N-terminal kinase

PGE2 – prostaglandin E2

Rb – retinoblastoma gene

PWM – position weight matrix

ChIP – chromatin immunoprecipitation

PCR – polymerase chain reaction

ROS – reactive oxygen species

DDR – DNA damage repair

BER – base-excision repair

NER – nucleotide excision repair

HR – homologous recombination

NHEJ – non-homologous end-joining

DSB – double strand break

SSB – single strand break

CDK – cyclin dependent kinases

ATR – ataxia telangiectasia and Rad3 related

DNA-PKcs – DNA-dependent protein kinase

PIKK – phosphatidylinositol 3-kinase-related kinase

BRCT – BRCA1 C terminus domain

MDC1 – mediator of DNA damage checkpoint protein 1

bFGF – basic fibroblast growth factor

CAF – cancer associated fibroblast

TM – tumour microenvironment

PDGF – platelet derived growth factor

EMT – epithelial-mesenchymal transition

α-SMA – alpha smooth muscle actin

FAP – fibroblast activating protein

SDF1 – stromal cell-derived factor 1

HGF – hepatocyte growth factor

NIHR – National Institute for Health Research

ECM – extracellular matrix

CRISPR – clustered regularly spaced palindromic repeat

1 Introduction

1.1 Colorectal cancer

Colorectal cancer (CRC) is a neoplasm that arises from the intestinal epithelial cells (IECs) lining the large bowel (colon and rectum). CRC is a major cause of cancer related mortality and is the second most common cause of cancer deaths in the UK (5). Despite year on year improvements in survival, the five-year net survival for male patients diagnosed with colon cancer is 58% (rectal cancer 58.6%), while in female patients it is 57.6% (rectal cancer 60.8%) (6). In the UK, incidence is greatest in older age groups; although, there has been a reduction in incidence in these age groups as a result of large-scale public health initiatives such as the Bowel Cancer Screening program (BCSP). Worryingly though, overall

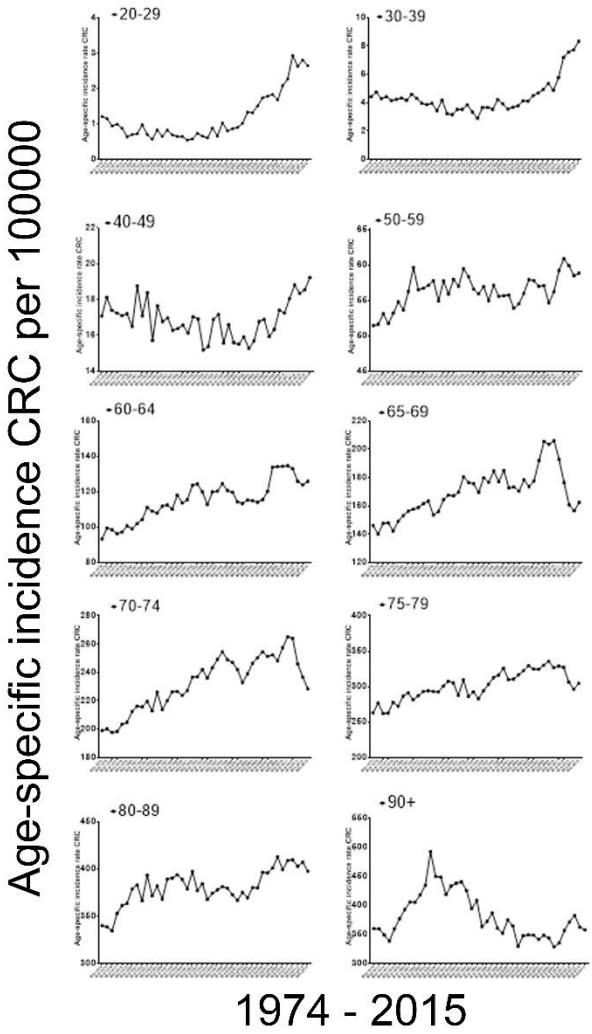

Figure 1.1 Age-specific incidence of colorectal cancer between 1974 and 2015 in England

CRC incidence is rising, particularly in younger populations (<50 years old) (Figure 1.1), similar to findings in other developed countries around the world (7). This disease remains a significant burden for patients and the NHS.

CRC can be subdivided into hereditary and sporadic forms (Figure 1.2). Of the hereditary forms, Familial Adenomatous Polyposis gene (FAP) is defined by germline mutations in adenomatous polyposis coli (APC), while other syndromes such as hereditary non-polyposis colorectal cancer (HNPCC or Lynch Syndrome) have germline defects in mismatch repair (MMR) genes leading to microsatellite instability (MSI (8)) and result in hyper-mutated tumours (9, 10). Other rarer polyposis syndromes that predispose to colorectal cancer include MYH-associated polyposis (MAP), juvenile polyposis syndrome (JPS) and Peutz Jeghers syndrome (PJS) (11). Sporadic colorectal cancers develop from a series of somatic mutations combined with epigenetic changes in previously normal tissue, known as the adenoma-carcinoma sequence (12), and as such they tend to develop in an older population due to the lead time of 10 to 15 years required to develop a carcinoma from an adenoma (See 1.3). Recently, significant work has been performed to characterise colorectal tumours based on consensus molecular subtypes (13).

	FAP	HNPCC	Sporadic
Germline defect	APC	MMR genes	nil
MSI	n/a	>90%	~15%
Tumour Initiation	accelerated	varied	long
Tumour Progression	varied	accelerated	varied
Prognosis	Poor	Good	Moderate
Age at diagnosis	~20-30yrs	~40yrs	>55

Figure 1.2 Characteristics of colorectal cancer based on inherited genetic defects in comparison to sporadic colorectal cancer.

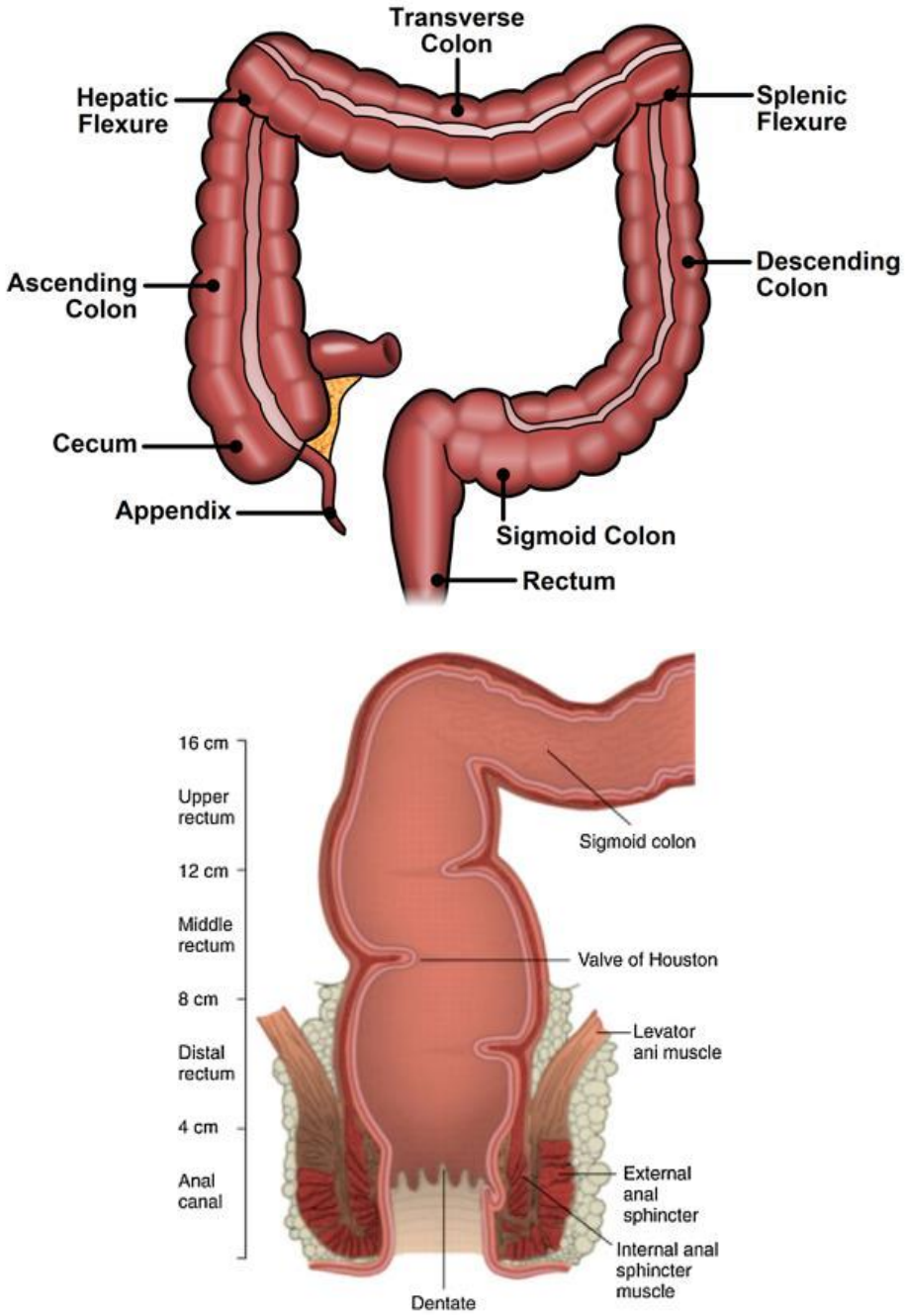

Figure 1.3 **Anatomy of the colon and rectum**

The rectum is the terminal portion of the large bowel that acts as a reservoir for storage of faecal matter. It is heavily colonised by bacteria which convert dietary fibre into short-chain fatty acids and is the final location where absorption of nutrients and water occurs. The rectum extends from the recto-sigmoid junction to the dentate line, where the anus originates. The rectum has portions covered by peritoneum and portions without a serosal covering, surrounded by pelvic organs, as it descends towards the anus.

Colorectal cancers (CRC) occur in patients with inherited genetic defects such as heterozygous APC mutation (FAP) or mutations in genes involved with MMR (HNPCC).

However, CRC more commonly develops sporadically with an accumulation of genetic and epigenetic defects leading to cancer. Adapted from Kinzler and Vogelstein 1996 (9) and Haggar and Boushey (14).

Colorectal cancer can be further subdivided based on anatomical location, which relates the tumour to its arterial supply, lymphatic and venous drainage.

1.2 Rectal cancer

The rectum is the terminal or distal-most portion of the large bowel that functions to store faecal matter and absorb the last nutrients and water contained within the stool. The rectum extends from the recto-sigmoid junction to the anus/dentate line and is around 15cm in length (Figure 1.3). Cancer of the rectum constitute around 30% of all colorectal malignancies and are managed differently to colonic tumours; this is due to the anatomy, such as the close proximity of the rectum to other pelvic organs (seminal vesicles/prostate in men and the vaginal vault in women), pelvic autonomic nerves, the lack of a serosal/peritoneal layer covering the majority of the rectum and the genetic differences of these tumours (15). The difference in genetics is thought to be primarily the difference between non-hypermutated and hypermutated tumours, of these, hypermutated tumours are significantly more common in the right of the colon (16).

Following diagnosis of a rectal lesion, staging of the tumour is critical to determine if it is early or advanced and the presence of metastatic disease. Staging of rectal cancer enables MDT (multi-disciplinary team) management decisions and all patients are offered standardised investigation including endoscopic evaluation (with biopsy for histopathological analysis), imaging including a computed tomography scan (CT) of the chest, abdomen and pelvis, a magnetic resonance imaging scan (MRI) of the pelvis (17) and additionally an endorectal ultrasound (EUS) (18). Subdivision into early disease, locally advanced and metastatic rectal

cancer uses the TNM staging system (Tumour Nodes Metastasis, Figure 1.4 and Appendix 2), enabling treatment stratification.

Locally advanced rectal cancer (LARC) is defined by the pathological extent of tumour (alongside lymph node involvement) leading to an increased risk of developing local recurrence, which has been the major cause of morbidity and mortality in these patients (19). Disease that threatens (within 1mm of mesorectal fascia) or involves the potential resection margin, is at high risk of local recurrence (20-22). These tumours, as defined by pelvic MRI, have a threatened (≤1 mm from mesorectal fascia) or compromised/breached mesorectal fascia/margin, but can also include very low tumours <5 cm from the anal verge (23). Pelvic MRI is critical

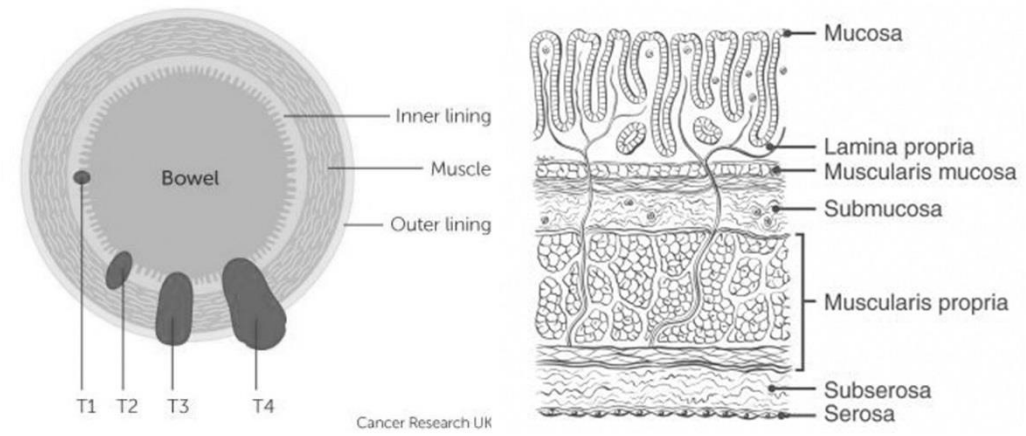

Figure 1.4 TNM staging of colorectal cancer

Tumours of the colon and rectum are staged according to depth of involvement of the bowel wall of the primary **T**umour, regional lymph **N**ode involvement and whether the cancer has **M**etastasised to distant locations (Appendix 2). Shown here is T stage, determining extent of the primary tumour. T1 tumours invade into submucosa, T2 tumours invade into muscularis propria, T3 tumours invade into the sub-serosa or into non-peritonealised peri-colic/rectal tissues and T4 tumours directly invade other organs or structures. Additional subclassifications have been developed which subdivide T1 and T3 lesions. Adapted from CRUK (www.cancerresearchuk.org) and UICC TNM staging (8th edition).

to this assessment and has be shown to be highly sensitive and capable of predicting clear resection margins (>1 mm circumferential resection margin (CRM)) in 92 % patients (24). LARC has a high rate of local recurrence and significant research effort has been directed at reducing this.

1.2.1 Current management of LARC

1.2.1.1 Surgical resection

Surgical management can be divided into those cases of early or advanced managed with curative intent and palliative disease. T1 tumours confined to the mucosa or submucosa would be suitable for local mucosectomy or full-thickness excision performed endoscopically or via TEM (transanal endoscopic microsurgery) (25). More advanced disease is managed with major resection. The aim of surgical resection of advanced rectal cancer is to achieve curative resection ensuring that the CRM is macro and microscopically free from tumour (R0 resection, resection margin positivity strongly predicts tumour recurrence); the identification and preservation of pelvic autonomic nerve plexi to ensure the preservation of urinary, bowel and sexual function; the preservation of the anal sphincter complex to enable faecal continence. Developments in surgical technique, pioneered by Richard Heald in the late 1970s, to improve local recurrence rates of advanced rectal cancer, resulted in the widespread adoption of rectal cancer resection along the mesorectal plane (termed Total Mesorectal Excision, TME) (26). The principle of TME is the same, no matter the surgical technique being utilised, and has been shown to significantly improve survival from rectal cancer (26-28). When performing TME, it is still unclear whether it is necessary to perform resection down to the level of the pelvic floor muscles or only resect to 2-5 cm below the tumour. Distal spread to lymph nodes below the tumour is thought to be minimal but increases with tumour stage (29, 30), however it is unknown if the surgeon needs to resect these more distal nodes along with the primary tumour.

Currently, there are two standard techniques for surgical removal of advanced rectal cancer; anterior resection (AR) resulting in bowel continuity or abdomino-perineal resection (APR, including extra-levator APR) resulting in permanent

stoma formation. The choice of which surgical procedure to perform depends primarily on the height of the tumour from the ano-rectal junction (dentate line) and the length of rectum distal to the tumour that enables colo-anal anastomosis, the extent of invasion of the tumour and the preferences of the patient.

Additional surgical techniques for performing TME, for advanced tumours less than T-stage 4, are currently being developed, such as the trans-anal TME (TaTME) operation (31, 32). The aim of TaTME is to improve the TME component in the distal pelvis and reduce rates of long-term surgical morbidity (such as low anterior resection syndrome – LARS) when TME can be difficult, particularly in male or obese patients and those patients who have undergone pre-operative radiotherapy. Critically, TaTME is still under evaluation to ensure its oncological safety and lack of inferiority with regard to morbidity and mortality in comparison to standard laparoscopic anterior resection (33).

Open or laparoscopic surgical resection using the mesorectal fascial plane for locally advanced rectal cancer is still the gold standard treatment providing a potential cure for this disease.

1.2.1.2 Treatment and response with long-course chemo-radiotherapy in rectal cancer

Alongside the technical developments in surgical technique over the past 50 years, there has been significant debate regarding the utility of radiotherapy with or without chemotherapy to achieve improvements in overall and disease-free survival and local or systemic recurrence. Therapy can be administered pre-operatively (neo-adjuvant) or post operatively (adjuvant). In rectal cancer, as opposed to colonic cancer, pelvic radiation was originally used to palliate patients with inoperable disease; although, early data suggested radiation therapy with X-rays improved overall and disease-free survival in resectable tumours (34). Given the propensity of rectal cancers to recur locally, radiation was subsequently used

as an adjuvant therapy to prevent this (35). Radiation is utilised in two alternative regimens (discussion of the actual method of delivery of radiation is beyond the scope of this project); firstly, short course preoperative radiotherapy (SCPRT), which consists of 25 Gy in 5 fractions followed by surgery at an interval of 1 week (developed from protocols used by VA Surgical Adjuvant Group and Toronto Group trials (36)). Secondly, long-course radiation (LCRT), initially described in the 1970s (37-39) and consists of 45 Gy (1.8 Gy fractions per day to limit toxicity) in 5 weeks plus a 5.4 Gy boost followed by surgery 6-8 weeks later. A recent meta-analysis found prolonging the interval to surgery may increase therapy response rates (40). Treatment with fluoropyrimidines was added to LCRT with the aim of improving radiation efficiency (LCCRT) (41-43).

Effort to reduce the high rates of local recurrence of rectal cancer using radiation led to a multi-arm study comparing surgery alone to adjuvant chemoradiotherapy, adjuvant radiation or adjuvant chemotherapy (44). This study showed that disease-free survival was significantly prolonged in the group receiving post-operative LCCRT compared to surgery alone; however, without prolonging overall survival and with no difference to those patients receiving post-operative radiation alone. Later studies showed significant reductions in local recurrence with LCCRT compared to LCRT alone (43). Additionally, this work showed reductions in cancer-related mortality and overall survival in patients undergoing adjuvant LCCRT. However, these studies were limited as the protocols used contained a drug, semustine, that was later shown to confer no benefit and lead to increased incidence of lymphoma (45).

Concurrently to these studies examining postoperative LCRT and LCCRT, research was being performed analysing the effect of pre-operative radiation to control local recurrence. Data from North America suggested that for more advanced tumours (Dukes' stage C) there was a reduction in local recurrence for

patients treated with SCPRT either as a single fraction or as multi-fractionated regimes (36, 46). These data were contrasted with data from a large randomised study in the UK analysing both single fraction (5 Gy) and multi-fractionated (20 Gy over 10 days), which showed no benefit to survival or local recurrence following SCPRT (47). Moreover, these studies were limited as they were performed before or during the improvements in surgical technique (meticulous TME/R0 resection) had been adopted. In the TME era, data from the Netherlands and Sweden has shown that SCPRT (25 Gy in 5 days) combined with surgical resection, ensuring TME, significantly reduced local recurrence over surgical TME alone (48-51). Additionally, the MRC-CR07 study showed SCPRT to be significantly better than the selective use of adjuvant LCRT, conferring benefits to local recurrence (61 % reduction) and disease-free survival (24 % improvement) (52).

So how did we get to the current management paradigm? The rectal cancer research community recognised that the addition of a radiosensitiser (5-fluorouracil) to LCRT was efficacious; however, it was also recognised that there was equipoise between SCPRT and neo-adjuvant LCCRT and when to utilise LCCRT to achieve the best reductions in local and distant recurrence as well as disease-free and overall survival.

The German Rectal Cancer and National Surgical Adjuvant Breast and Bowel Project (NSABP) groups showed that neo-adjuvant LCCRT compared to post-operative LCCRT decreased local relapse despite no improvements in disease-free or overall survival (53-55). Data from the EORTC (European Organisation for Research and Treatment of Cancer) and the FFCD (Federation Francophone de Cancerologie Digestive) 9203 trial showed decreased rates of local recurrence with LCCRT compared to SCPRT (56, 57). Although, data from the Polish colorectal study group, published at the same time, showed no difference in disease-free survival or overall survival between SCPRT and LCCRT, challenging findings from

EORTC and FFCD trials (58). However, a recent Dutch registry study analysing almost 6000 patients treated with either SCPRT or neo-adjuvant LCCRT found that there was a significantly higher chance of achieving a pathological complete response (pCR, see below) with LCCRT despite those tumours treated with LCCRT being of a more advanced stage (59), which corroborated a meta-analysis performed in 2009 (60). In summary, evidence from the past 60 years of research suggests that in the era of TME for rectal cancer neo-adjuvant LCCRT confers benefits to patients in reducing local recurrence and critically results in downstaging of tumours, although it is still unclear why there is limited benefit to overall survival rates.

Downstaging of the primary tumour is a term used to define a response to LCCRT (also downsizing or regression can be used). Assessment of this prior to resection can be made both clinically via endoscopy or radiologically. Post-operatively, downstaging of the tumour can be assessed pathologically, using a tumour regression grade (TRG). Various different grading systems are in use including Dworak's (61), MSKCC system, Mandard (62), AJCC (63) and Ryan TRG (64), all of which measure proportion of tumour mass replaced by fibrosis and residual tumour cells (65) (Appendix 3). It is well recognised that there is a broad range of response to neo-adjuvant LCCRT. While pathological complete response (pCR) is well defined as no residual tumour cells in the primary tumour or lymph nodes, non-response has no consensus definition but tumours show a range of absent/minimal regression (66). Rates of pCR are thought to be in the region of 12-15 % following LCCRT (67) with pCR accurately predicting long term OS and DFS following neoadjuvant therapy for rectal cancer (67, 68). All TRG systems predict recurrence, however the AJCC system was the most accurate in a study of 563 patients with T3/4 or N1 LARC (65). Although, the AJCC system may outperform other TRG grades in predicting patient survival, it fails to consider

pathological nodal status (ypN). ypN is a known determinant of poor prognosis despite good primary tumour response (69). Recent data suggests that a modified Dworak TRG system that takes into account nodal status, was a better predictor of survival compared to the other TRG systems (70). Additionally, TRG is also influenced by the length of delay to surgery; the Stockholm III trial analysed outcomes following SCPRT with or without delay to surgery and LCRT and showed that tumour regression could be augmented by allowing a 4-8 week delay to surgery in the SCPRT arm (71).

There remains an absolute need to understand and stratify which patients will most benefit from neo-adjuvant chemoradiotherapy and ideally achieve clinical complete response (cCR) and more importantly pCR (72). Furthermore, improving cCR rates may lead to more patients being considered for non-operative management or the 'watch and wait' approach as pioneered by the Habr-Gama group and others in the International watch and wait database (IWWD) consortium (73), where as many as 70% of patients with cCR do not undergo surgery (74). Recent data from a large international registry has suggested that for those patients with cCR undergoing a 'watch and wait' management strategy, 5-year disease specific survival was 93.8 % (95 % CI 90.9-95.9) (75). Data from this registry shows that in centres with longer follow up (median 3.7-7.1 years), rates of local regrowth are around 40 %, while in centres with shorter follow up (median 2.3 years) regrowth rates are around 15 %; clearly suggesting that close follow up for several years is necessary to catch all episodes of local tumour regrowth.

Therefore, the current use neo-adjuvant long-course chemoradiotherapy could be advocated in patients with high-risk locally advanced rectal cancer. LCRT is followed by surgery at 6-8 weeks to allow tumour regression/downstaging (as determined by a modified Ryan/AJCC TRG, Appendix 3). However, there are several questions that arise from this. Firstly, there are still many patients who have

a poor response or fail to respond at all to neo-adjuvant chemoradiation; therefore, it remains to be identified how best to both stratify use of radiation into those patients who would benefit most and improve the efficacy in patients who fail to respond. Secondly, predictive factors for response to therapy are not currently utilised and development of these is the key to future neo-adjuvant or adjuvant use; tumour biology, tumour microenvironment and the patient's genetic and lifestyle factors may all have roles to play with this. Thirdly, it is unclear if modulation of the tumour biology may facilitate improved responses to LCCRT. These questions should be also researched with the understanding that pre-operative use of radiation does carry associated risks; patients have increased bowel dysfunction post operatively (76, 77) and higher rates of sexual dysfunction (76) following radiation. Surgically, whilst operative time and blood loss are increased, there is also some limited evidence in small case series that the incidence of anastomotic leakage increases (28), although a Cochrane review and recent meta-analysis has refuted this (60, 78). Therefore, the correct use of radiation, in those patients who will have the best chance of benefit, is the ultimate goal. Alternatively, in those patients with a lower chance of achieving a pCR or good TRG, efforts should be made to enhance the efficacy of this therapy.

1.3 Colorectal tumorigenesis

Colorectal cancer is classically described as a multistep tumorigenic process (Figure 1.5) (79). Malignant tumours arise over the course of at least 10-15 years from pre-existing benign adenomas (80). The risk of developing colorectal cancer is determined by both environmental and genetic risk factors (81). Tumours arise as a result of mutational inactivation of tumour suppressor genes coupled with the activation of oncogenes (82). These mutations can occur in up to 100 genes in a typical colorectal malignancy but tend to involve a select number of cell signalling

pathways, with at least 4 or 5 ‘driver’ mutations required for malignant transformation.

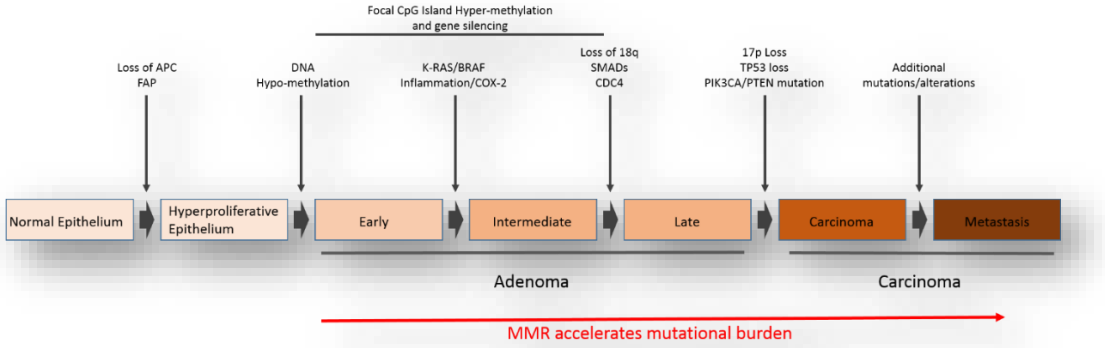

Figure 1.5 The adenoma-carcinoma sequence

The ‘adenoma-carcinoma sequence’ is a representation of the increasing burden of genetic and epigenetic changes that occur as normal colon progresses to becoming adenocarcinoma and metastasis. Critical early loss of APC or mutation of β-catenin is an initiating feature of colorectal cancer. Adenomas develop multiple further mutations, such as K-RAS or BRAF, and p53, which result in carcinoma, however these mutations do not need to be in a fixed order. Contiguous with these genetic changes are epigenetic changes such as DNA hypomethylation and CpG island hypermethylation which result in expression of oncogenes or silencing of tumour suppressor genes. Adapted from Hanahan and Weinburg 2011.

1.3.1 Genetic drivers of colorectal cancer

Throughout tumorigenesis cells will acquire mutations, which eventually lead to invasive carcinoma, but the order or sequence of acquisition of mutations is not fixed. Increasingly, understanding of all the mutations within CRCs has become more complex as high-throughput sequencing has been performed on greater numbers of tumours. Typically, sporadic CRC will develop mutations in the Wnt, RAS/RAF/MEK/ERK, TP53, PI3K and TGF-β signalling pathways as the primary driver mutations of this disease. These mutations combined with a small number of alternative driver mutations and epigenetic changes are the biological basis of colorectal cancer. Focus of the introduction will be on the Wnt signalling pathway as a critical determinant of tumorigenesis, the RAS/RAF transduction pathway and the p53 tumour suppressor gene.

1.3.2 Wnt pathway mutations

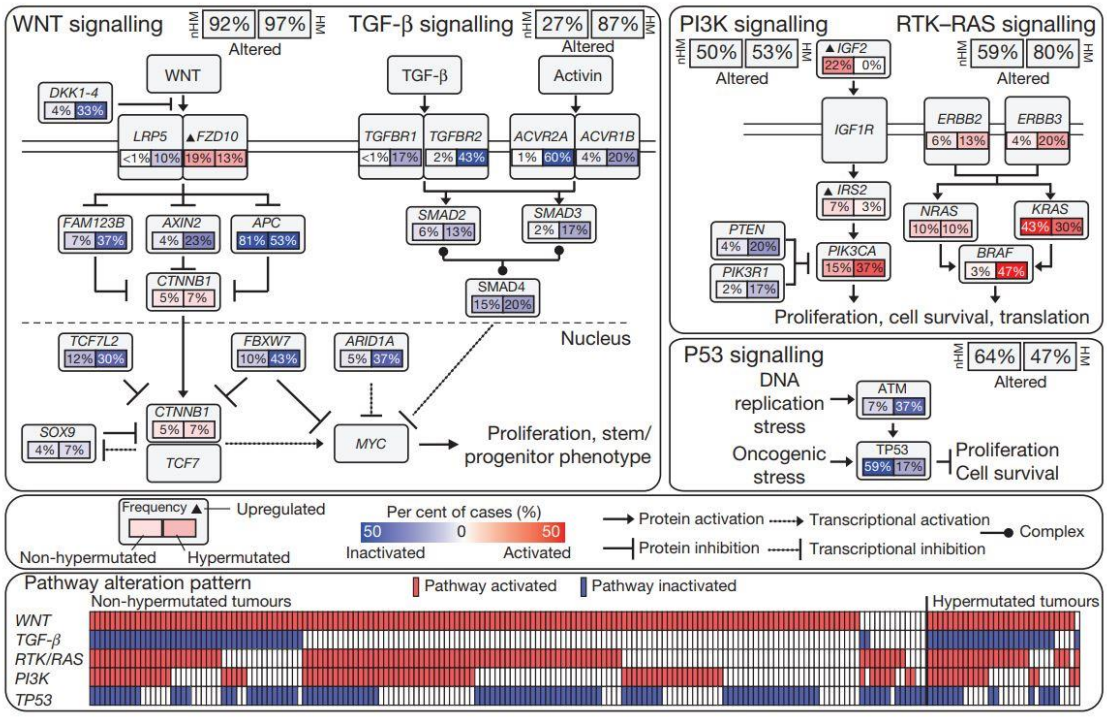

Figure 1.6 Mutational burden in colorectal cancers and differences between non-hypermutator (nHM) and hypermutator phenotypes (HM).

The rates of acquired mutations in colorectal cancer split according to pathway involved and by nHM or HM. The majority of colorectal tumours harbour WNT pathway mutations (81% have APC mutations in nHM tumours), TP53 muations (59% of nHM tumours), KRAS mutations (43% of nHM tumours). Adapted from The Cancer Genome Atlas Network Nature paper 2012

The canonical Wnt (Wingless) pathway is a critical pathway in colorectal tumorigenesis that regulates enterocyte stem cell homeostasis and embryological development in multiple tissue types but is also critical in cancer development (83). In colorectal cancer, almost all tumours harbour deficits in Wnt pathway genes, leading to constitutive activation of the pathway, principally through upregulation of β-catenin, which mimics a Wnt-on state (84). Germline (rare) and somatic (common) mutations in APC lead to aberrant phosphorylation of β-catenin reducing β-catenin degradation and leading to its nuclear accumulation where it functions as a cofactor for TCF/LEF driven transcription. APC is a critical early mutation in CRC development, recent data has suggested that even in the presence of other

mutated genes, restoration of functional APC within a tumour resulted in regression of tumour volume and a return to differentiated crypt architecture (85). Using mouse models, it has been further possible to validate that APC (and therefore the Wnt signalling pathway) is critical for the early development of CRC. $APC^{Min/+}$ mice (heterozygous truncated APC mutation leading to multiple intestinal neoplasia - Min) has very high penetrance with all mice developing high numbers of intestinal polyps and succumbing early to colonic tumours (86).

The Wnt signalling pathway is also critical for the development of the intestinal epithelium, driving the production and maintainence of the stem cell niche (87). Importantly, activated Wnt signalling also drives a cancer stem cell-like phenotype by promoting cell proliferation.

1.3.3 RAS/RAF pathway mutations

The RAS/RAF/MEK/ERK pathway is a signalling pathway, controlling proliferation, cellular differentiation and survival that transduces growth factor receptor signalling from cell surface to nucleus. Mutations in pathway members, such as Kirsten rat sarcoma virus (KRAS) or BRAF (B-Rapid Accelerating Fibrosarcoma, typically V600E substitution resulting in hyperactive protein), occur commonly in CRC and lead to independence from growth factor signalling (88). BRAF mutation is mutually exclusive of KRAS mutations and are commonly found in tumours with MMR deficiency (89, 90). Given that downstream signalling in BRAF and KRAS mutant tumours is thought to be similar, it suggests tumours containing these mutations may have similar phenotypes.

Colonic tumours are thought to have a 57% incidence of KRAS/BRAF mutation, while KRAS/BRAF mutations occur in 38% of rectal cancers (91), both of which leading to significantly worse patient prognosis (92). In wild-type KRAS tumours, cetuximab (a monoclonal antibody against EGFR (epidermal growth factor receptor also known as ERBB2) significantly improves patient survival (93, 94) and

is currently used as a first-line therapeutic agent for patients with metastatic CRC (NICE TA439, 2017). There is also some evidence to suggest that targeting EGFR in wild-type KRAS rectal tumours may improve response to radiation, although this is not used clinically (95).

1.3.4 TP53 mutations

It is suggested that p53 is an archetypical tumour suppressor gene and the 'guardian of the genome', highlighting this function, once p53 is mutated, cells develop genomic instability promoting cancer (96). Additionally, p53 null mice develop normally but carry a high burden of cancer (97), particularly following γ-irradiation (98).

p53 binds DNA at specific sequences and regulates transcription of genes that promote cell cycle arrest and apoptosis (for example p21 and Puma respectively). It plays a critical role in the response to DNA damage and when mutated, enables damaged cells to continue through the cell cycle, propagating the defect in daughter cells leading to tumorigenesis (99).

In colorectal tumours mutations in p53 or loss of 17p (carrying TP53) occur in just over half of all tumours and result in loss of the tumour repressor role of p53 (100). Mutations in p53 results in a significantly worse prognosis for patients (101), for example in rectal cancers it has been shown that p53 mutation results in poorer response to pre-radiation and a worse overall survival (102).

1.3.5 Transforming growth factor signalling

The transforming growth factor beta (TGFβ) family of cytokines are a key regulator of inflammation and immune homeostasis (103). In the intestinal epithelium TGFβ signalling has a complex role in tumorigenesis having effects as both a tumour suppressor and an oncogene (104). TGFβ cytokines activate signalling by causing

the assembly of receptor complexes at the cell surface that leads to the activation of the SMAD family of proteins (SMA and MAD-related protein) (105).

In colorectal cancer, mutations occur in several members of the TGFβ signalling pathway including receptors and downstream proteins. Mutations in the TGFβR2 gene occur as a result of microsatellite instability (106), while mutations effecting the SMAD proteins, particularly SMAD4 occur late in colorectal carcinogenesis as a result of loss of heterozygosity on chromosome 18q. Additionally, in sporadic CRC SMAD4 is mutated as a result of entire chromosomal deletions, frameshift, nonsense or missense mutation leading to its inactivation and loss of function as a tumour suppressor (105). Mutations in TGFβR2 lead to more favourable outcomes following treatment with fluorouracil-based treatments (5-fluorouracil or capecitabine) in MSI deficient CRC tumours (107).

1.3.6 PI3 Kinase signalling

The phosphoinositide 3-kinases (PI3K) phosphorylate the inositol ring of lipid substrates known as phosphatidylinositols and are thought to be ubiquitously deranged in cancer (108). The PIK3CA gene has been shown to be mutated in several cancers, particularly CRC (109). PIK3CA mutations predict poor response to standard therapy in CRC (110), while the same mutations have been shown to induce sensitivity to the anti-inflammatory drug, aspirin (111).

1.4 Epigenetic drivers of colorectal cancer

In addition to the genetic alterations commonly observed in CRC, there are also significant epigenetic changes that contribute to tumorigenesis (112). In broad terms, these epigenetic changes do not involve alteration of the DNA sequence but modification of histone proteins, DNA methylation and levels of RNA interference, which results in changes to gene expression and therefore cancer cell phenotype (113). In colorectal cancer it has been known for many years that

there is hypomethylation of cytosine residues throughout the genome (114) leading to genomic instability, activation of oncogenes and loss of imprinting (LOI) (112). In combination with global hypomethylation it is recognised that some genes, in particular tumour suppressors, undergo epigenetic silencing through focal CpG island hypermethylation, such as TP53, APC and MLH1 (115). Promotor hypermethylation has been particularly associated with MSI tumour subtype in sporadic carcinoma (116). Those sporadic cancers with hypermethylation have been further classified into a CpG Island Methylator Phenotype (CIMP).

1.5 The NF-κB signalling pathway

1.5.1 An overview of NF-κB signalling

The NF-κB proteins are key regulatory transcription factors in acute and chronic inflammation, the cellular stress response and immune response and were discovered in landmark work in 1986 (117). NF-κB signalling is rapidly activated following cellular stress stimuli such as infection, pro-inflammatory stimuli (118, 119), ionizing radiation (120) and chemical/physical stress . Importantly, NF-κB also undergoes activation by cancer-related inflammation (121, 122) where it can be activated in cancer stem cells (123) or in BRCA1 deficient breast cancers which have constitutive NF-κB activation (124).

The NF-κB proteins are a group of structurally-related subunits (RelA (p65), RelB, c-Rel, NF--κB1 and NF-κB2 (125, 126)). Structurally, all NF-κB subunits contain an N-terminal Rel homology domain (RHD), which mediates DNA binding, dimerisation of subunits and inhibitory protein binding (119).

NF-κB signalling is highly regulated. In unstimulated cells, NF-κB subunits are held predominantly within the cytoplasm due to binding of inhibitory proteins termed IκBs (inhibitor of kappa B). These inhibitory proteins, IκBα, IκBβ, IκBε, BCL-3, IκBz, IκBNS and the c-terminal portions of processed p100 and p105 (IκBδ and IκBγ respectively), function by binding to NF-κB subunits through their ankyrin repeat domains. Specific pathway activation will be discussed below; broadly however, activation occurs when IκBs are phosphorylated by IκB kinase (IKK) complexes resulting in ubiquitination and degradation of IκB. This releases the NF-κB subunit exposing the NLS (nuclear localisation sequence) and allowing the subunit to translocate and undergo dimerisation.

Dimerisation of NF-κB subunits into homo or hetero-dimers follows activation through either the canonical, non-canonical or atypical pathways, although this is perhaps an oversimplification. It is recognised that up to 15 differing NF-κB family complexes can be formed (127). Alternative dimer combinations may recognise individual κB sites with variable affinity leading to alternative gene regulatory programs for different dimers. Additionally, the subunits p50 and p52 lack transactivation domains (TADs), unlike RelA, cRel and RelB, meaning that, once bound to DNA, they require additional cofactors or interaction with a NF-κB subunit containing a TAD to activate transcription.

Specificity of NF-κB signalling is derived through several mechanisms including receptor and ligand specificity, IκB to NF-κB subunit specificity (128), κB target site

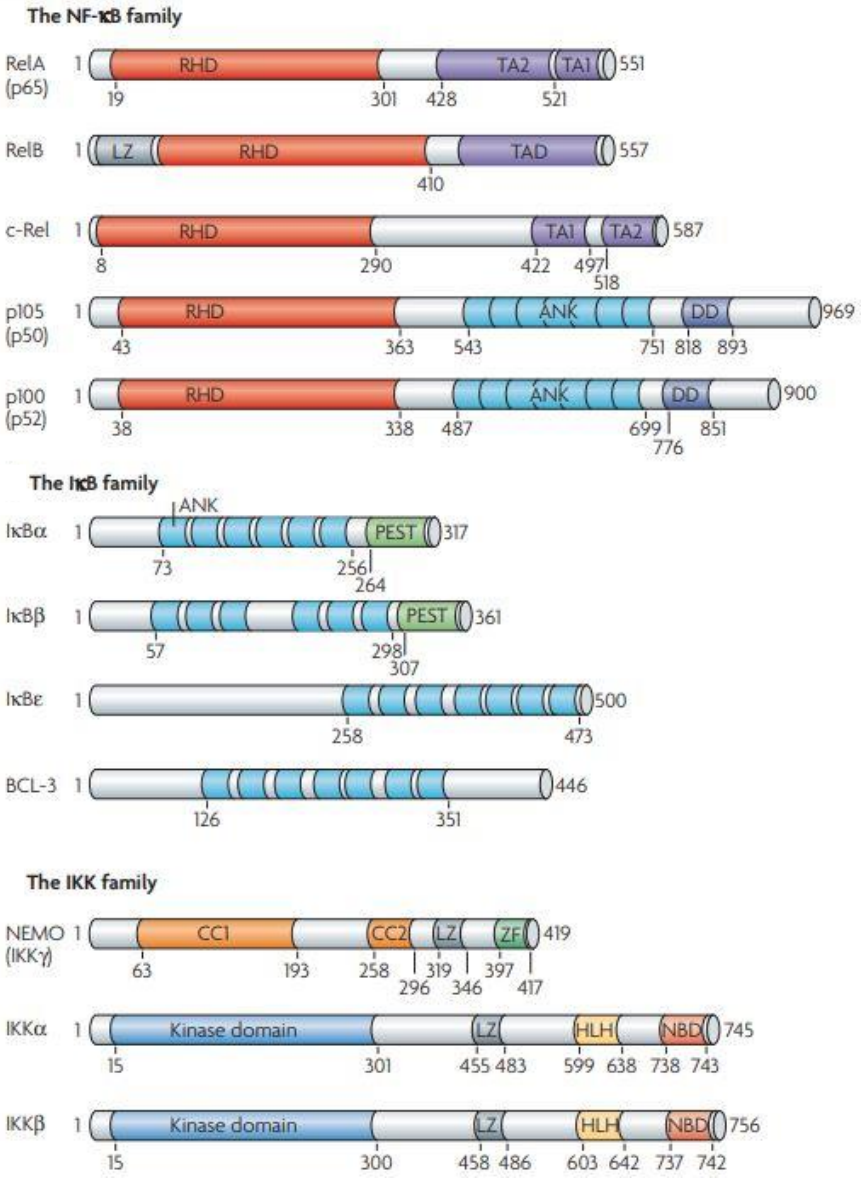

Figure 1.7 Principal members of the NF-κB signalling pathway

NF-κB signalling pathway members can be categorised as primary NF-κB subunits (RelA/p65, RelB, c-Rel, p105/p50 and p100/p52), Inhibitor of kappa B (IκB) proteins (IκBα, IκBβ, IκBε, BCL-3 and the c-terminal portions of p100 and p105 (IκBδ and IκBγ respectively) or IκB Kinase (IKK) proteins NEMO, IKKα and IKKβ. The main structural components of each protein are shown with amino acid residue positions beneath each gene map. Important structural domains for NF-κB subunits are the Rel Homology domain (RHD), Transactivation domain (TAD or TA1/2). In addition to these domains p100 and p105 subunits contain ankyrin repeat domains (ANK) like the IκB family members. Another important IκB domain is the PEST (proline P, glutamate E, serine S and threonine T) domains that IκBα and IκBβ contain, which enables protein-protein interaction. Other domains contained in the NF-κB protein family include leucine-zipper-like motifs (LZ), death domains (DD), coiled-coil (CC), NEMO-binding domain (NBD), helix-loop-helix (HLH) and zinc finger domains (ZF). Adapted from (4).

specificity, the epigenetic state of chromatin surrounding κB sites (particularly the acetylation state of histones (129)) (130, 131) and subunit dimer exchange on DNA through the course of an inflammatory stimulus (132, 133).

An important component of this complexity is the dimer-specific binding to κB regulatory sequences on DNA (134, 135). There are thought to be a number of κB consensus sites that have differing affinities for particular homo or hetero-dimers; κB DNA binding sites for heterodimers have a higher similarity between dimers, whereas homodimer binding sites have a higher rate of specificity for each homodimer (135). Minimal structural differences in p50 and p52, for example, can lead to differences in binding affinity for p50 and p52 homodimers to DNA (136). Moreover, it is known that the κB consensus sequence that a dimer binds to determines if there is activation or repression of transcription, for example p52 homodimers bound to BCL-3 exhibit either activation or repression of target genes depending on the κB sequence that the complex binds (137).

These different components of NF-κB signalling combine to give distinct pathways of activation, as will be discussed below.

1.5.2 Canonical NF-κB signalling

Initiation of canonical NF-κB signalling occurs through a variety of receptors, such as the TNF receptor super family, Toll receptors (see (138) for Toll-Like Receptor signalling review), interleukin (139) and T/B-cell antigen receptors (140) and their associated ligands (Figure 1.8). Canonical NF-κB activation is quick and leads to nuclear translocation of RelA/p65:p50 heterodimers (119).

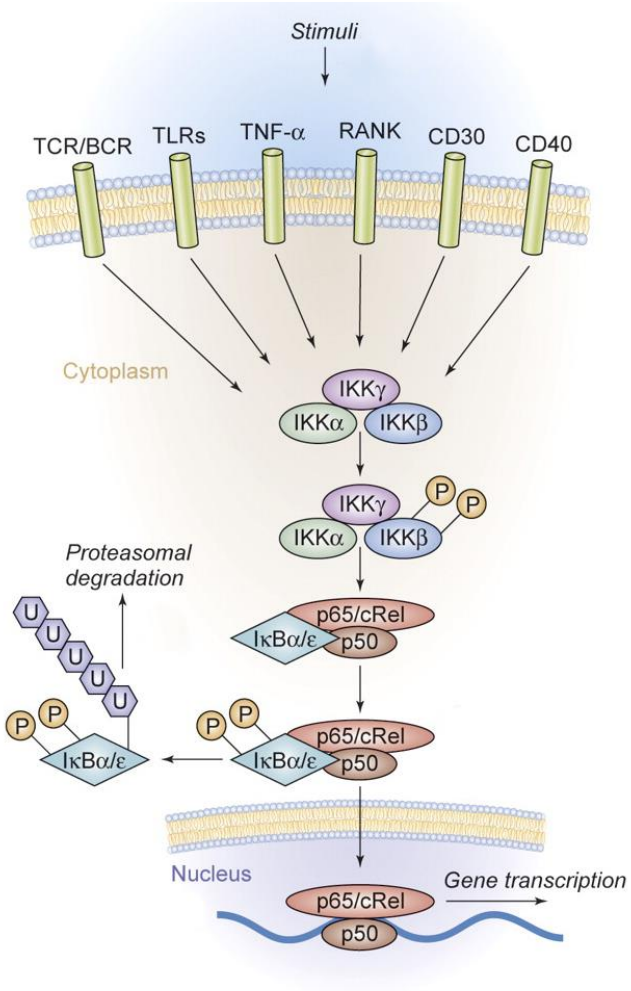

Figure 1.8 The canonical NF-κB pathway

The canonical NF-κB pathway is activated by diverse stimuli in diverse cell types with ligands binding at the cell surface to a number of different receptor families including T/B-cell receptors (TCR/BCR), Toll-like receptors (TLRs), tumour necrosis factor (TNF) family receptors, RANK, CD30 and CD40 receptors. These receptors activate the IKK complex containing IKKα, IKKβ and IKKγ/NEMO (NF-κB essential modulator), which subsequently phosphorylates IκB proteins leading to their ubiquitination and proteasomal degradation. Degradation of IκBs releases p65:p50 as well as other canonical heterodimers such as c-Rel:p50 enabling their translocation to the nucleus where they activate multiple genes leading to cell proliferation, cell survival, autophagy and a pro-inflammatory gene signature. Image adapted from (3)

The initial step in canonical pathway activation is post-translational modification and degradation of IκB proteins following stimulus. The IKK complex (made up of IKKα and IKKβ alongside a critical scaffold protein NF-κB essential modulator (NEMO) (141)) phosphorylates IκBα on serine 32 and serine 36 (142) or IκBβ on serine 19 and serine 23, leading to their poly-ubiquitination and degradation by the 26s proteosome (143). Additionally, the IKK complex facilitates the release of p50 from p105 through phosphorylation of p105 leading to its proteosomal degradation/processing. Release of the p65:p50 heterodimer, controlled by IκBα and IκBβ, results in its nuclear translocation where it binds to canonical κB motifs on DNA (4). Genes upregulated by the canonical pathway regulate cell survival, proliferation autophagy and inflammation (144).

The canonical pathway is important in cancer development. For example in colorectal cancer, mice with an IKKβ deletion in intestinal epithelial cells formed 75 % fewer colonic adenomas following AOM/DSS treatment (145). The underlying mechanism behind this was thought to be failed activation of the canonical NF-κB pathway following stimulation, showing a critical role for early tumour development by canonical NF-κB.

1.5.3 Non-canonical NF-κB signalling

Non-canonical NF-κB signalling is characterised by formation of p52:RelB heterodimers and is independent of IKKβ or NEMO (Figure 1.9) (119). The non-canonical pathway, while also being a receptor-mediated pathway, is activated by a more limited subset of TNF superfamily receptors than the canonical pathway, such as CD40, lymphotoxin β (LTβ), BAFF receptor and RANK amongst others (146). Ligands for these receptors result in recruitment of members of the TRAF family into cell membrane complexes leading to activation of NF-κB-inducing kinase (NIK) (147). NF-κB2/p100 resides in the cytoplasm of cells in a large

complex (kappaBsome) (148). NIK phosphorylates dimerised IKKα, which itself phosphorylates p100 (serines 176 and 180) enabling the proteolytic processing of p100 into p52 and a c-terminal domain that functions as an IκB protein (IκBδ) (149). Processed p52 complexes with RelB to form p52-RelB heterodimers (150) or can complex with itself to form p52 homodimers (see introduction 1.5.4 Atypical NF-κB signalling). Importantly, RelB is stabilised by both processed p52 and its precursor p100 (151). However unlike p100, p52 is unable to retain RelB in the cytoplasm leading to the nuclear accumulation of RelB-p52 heterodimers following p100 processing (152). RelB-p52 heterodimers are able to activate a gene specific transcriptional program (146) but have also been implicated in gene repression (153). Non-canonical NF-κB signalling is critical for development, as mice with NF-κB2 gene knockouts exhibit early post-natal mortality, have defects in antibody-mediated immunity and lymphoid architecture (154). Additionally, mice with a TRAF3 (TNF receptor-associated factor 3) deletion, which leads to constitutive

processing of p100 to form p52 (155), display early post-natal mortality, depletion of leukocyte numbers and hyposplenism (156). These models highlight the importance of p52 and the non-canonical signalling pathway in development and immune function. In cancer, elucidating the role of non-canonical signalling was initially challenging as IKKα knockout (KO) mice were not viable following the perinatal period (150). Despite this limitation, the non-canonical pathway is implicated in cancer development, for example, in diffuse large B-cell lymphoma, dysregulation of NIK results in uncontrolled proliferation of tumour cells (157).

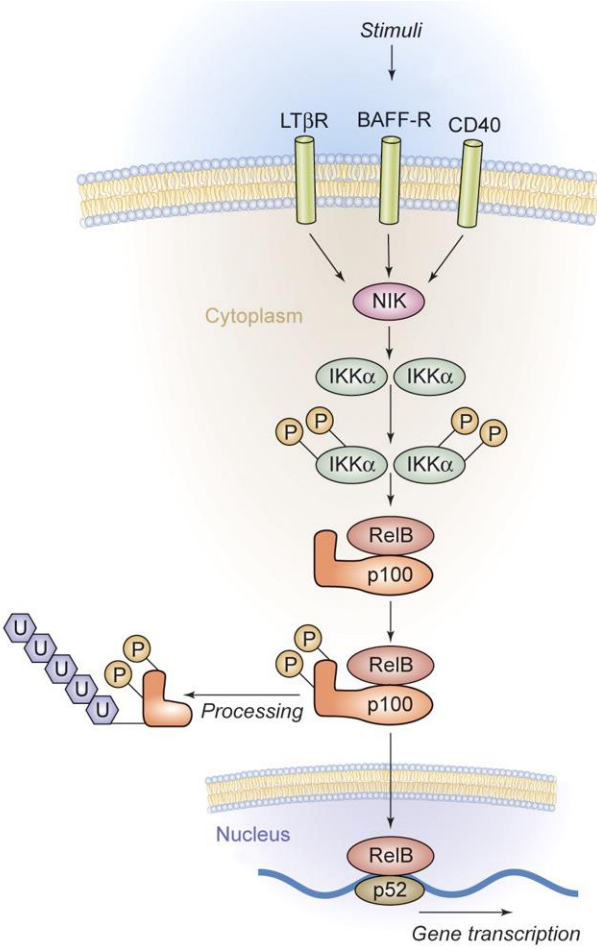

Figure 1.9 The non-canonical NF-κB signalling pathway

The non-canonical NF-κB signalling pathway is induced by a more specific group of ligands and their receptors including lymphotoxin β receptor (LTβR), B-cell activating factor receptor (BAFF-R), RANK (not shown) and CD40 receptors. Ligand recognition results in receptors recruiting members of the TRAF family to the cell membrane leading to activation of NF-κB inducing kinase (NIK). Activated NIK phosphorylates IKKα, which subsequently phosphorylates p100, leading to the proteolytic processing of p100 into p52 which translocates to the nucleus as a heterodimer with RelB. Image adapted from (3).

Additionally, constitutively active p52 is known to transform murine fibroblasts to become tumorigenic (158).

1.5.4 Atypical NF-κB signalling

The 'atypical' signalling pathway is not clearly defined in the literature. Some studies suggest that the atypical pathway consists of activation of canonical heterodimers in an IKK-independent mechanism directly through kinases such as ATM:Nemo (159), MEK1 (upregulated by p53 in response to cell stress) (160) or CK2 (casein kinase 2 in response to UV radiation) (161) (highlighting the multiplicity of canonical NF-κB activation). Alternatively, other authors use the 'atypical pathway' term to describe an NF-κB pathway that is dependent on involvement of a co-factor, the atypical IκB protein BCL-3 (Introduction 1.6 B-cell lymphoma 3 (BCL-3)). In this latter pathway, BCL-3 binds to processed p50 and p52 homodimers to activate or repress a subset of NF-κB regulated genes. p50 and p52 are thought to form strong homodimers with high affinity compared to other homodimer species (128). These homodimers bind to the majority of κB sites at gene promoter regions and binding is known to occur at multiple sites within the same promoter (162)).In difference to other NF-κB subunits, p50 and p52 lack TADs and subsequently require cofactors to induce activation of transcription (163).

The p50 protein is constitutively produced as a result of ubiquitin-independent 20s proteosomal degradation of p105 (164). Conversely, p52 is not constitutively processed due to possessing a processing-inhibitory domain (PID) at its c-terminal region, which requires NIK phosphorylation to undergo processing in an inducible manner. p50 homodimers have a predominantly repressive role (but also activating (165, 166)), occupying κB DNA sites when NF-κB signalling is not activated (163, 167, 168). BCL-3 has been shown to cooperate in transcriptional repression

induced by p50 homodimers (169). BCL-3 also associates tightly with p52 homodimers resulting in transcriptional activation by these dimers (170). Additionally, it is likely that BCL-3 plays a role in a subset of genes conditional on κB site and the presence of other co-regulatory proteins bound to the homodimers (137).

In summary, the atypical NF-κB pathway involves NF-κB dimers and their activation, not under the umbrella of the canonical or non-canonical pathways. For the purposes of this thesis the atypical NF-κB pathway will define p50 or p52 homodimers and their associated co-regulatory protein, BCL-3. This pathway is a critical component of the broader NF-κB response and plays a role in fine tuning of the canonical and non-canonical responses to an inflammatory stimulus. The role of BCL-3 in the atypical pathway will be discussed in detail below.

Atypical NF-κB pathway dimers contribute in a context specific mechanism to cancer development or suppression in a variety of tumours such as nasophryngeal (171), prostate (172)and hepatocellular carcinoma (173). Genome-wide association studies (GWAS) have shown that polymorphisms in important members of this NF-κB pathway contribute to the risk of developing colorectal cancer, further highlighting its critical role (174).

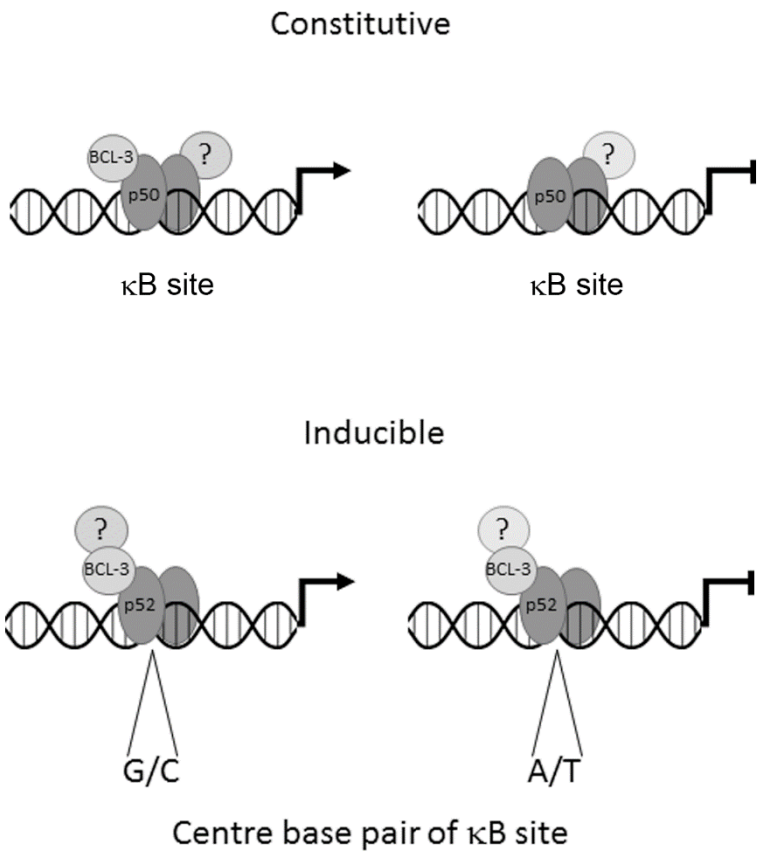

Figure 1.10 Atypical NF-κB homodimer signalling

Homodimers of p50 and p52 are processed products of p105 and p100 respectively. The p50 protein is processed\ constitutively from p105 following its phosphorylation and partial degradation by the proteosome. p52 is processed in an inducible manner following phosphorylation of p100 by kinases such as NIK. Homodimers of p50 bind to κB sites in DNA to repress or activate transcription with further dynamic regulation by BCL-3, which when bound, often leading to stabilisation of p50 homodimers on DNA and the activation of transcription. Homodimers of p52 bind to BCL-3 and activate or repress transcription based on the κB site that the complex binds to and the association of the complex with additional co-regulators. It is not known if the mechanism for each homodimer is functional See text for references.

1.6 B-cell lymphoma 3 (BCL-3)

BCL-3 is an atypical member of the IκB family of proteins (175) and was initially shown to be overexpressed in B cell chronic lymphocytic leukaemia which contain the translocation, t(14;19)(q32;q13.1) (176). BCL-3 is predominantly nuclear and functions as a co-regulator in multiple signalling pathways including AP1, STAT and NF-κB.

1.6.1 BCL-3 Structure

The *BCL-3* gene encodes a protein that contains 446 amino acids with a predicted molecular weight of 47 kDa. BCL-3 has seven ankyrin repeat domains (ARD) (Figure 1.3) as well as a proline-rich amino-terminal region and a proline and serine-rich carboxy-terminal region.

Structurally the ARD of BCL-3 has homology with the ARDs of both NF-κB1/p105 and IκB-α (177). However, in difference to the ARD of IκB-α, the BCL-3 ARD has an additional 2 residues in ANK1 leading to significantly different tertiary structures. Additionally, the BCL-3 protein has a seventh ARD, which replaces the PEST region (a 12 or more residue region rich in proline (P), glutamic acid (E),serine (S) and threonine (T) residues (178)) of IκB-α (179); PEST regions are regulatory regions controlling protein degradation and are commonly found in proteins with

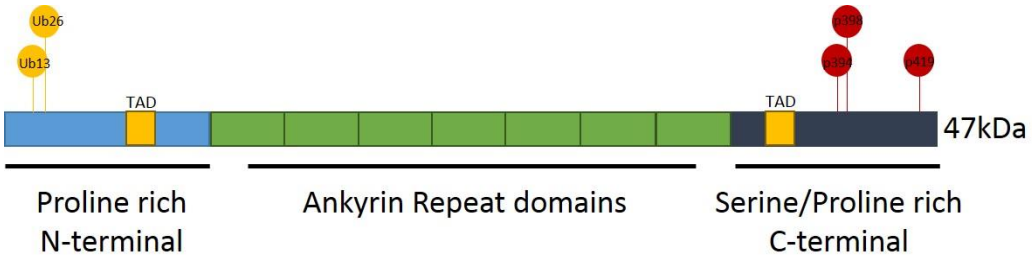

Figure 1.11 Map of BCL-3 DNA

BCL-3 has a proline rich N-terminus which contains groups of basic amino acids that act as Nuclear Localisation Sequences. N-terminal domain contains lysine (K) residues K13 and K26 that are sites of poly-ubiquitination (K48/K63 linked). BCL-3 has seven ankyrin repeat domains (ARD) which facilitate binding to NF-ΚB homodimers. Both the N and C-termini contain phosphorylation sites including the ones highlighted at serines 394/398/419. Kinases known to be active on these sites are AKT, GSK3 and ERK1. Adapted from Ohno et al 1990.

short intracellular half-lives. Specifically, the PEST region of IκB-α is modulated by phosphorylation, which controls its rapid degradation by the 26S proteasome (180, 181). Therefore, this structural difference of BCL-3 may lead BCL-3 to have a longer half-life than IκB proteins due to lack of this sequence.

BCL-3 has been reported to be predominantly nuclear because of two basic amino acid clusters near the N-terminus acting as weak nuclear localisation signals (NLS) (182). Additionally, the N-terminal proline-rich region of BCL-3 (amino acid residues 1-119) may also contain a binding site for proteins containing a SRC Homology 3 domain (SH3 domain) as it contains the amino acid motif X-P-p-X-P (X - aliphatic amino acid, P – proline). This domain is known to be an important mediator of protein-protein interactions and it may be that BCL-3 is able bind proteins such as STAT or PI3K through this motif (183, 184). The role of this domain has been corroborated by data analysing activated platelets where BCL-3 binds to the SH3 domain of FYN (tyrosine kinase protein) (185).

1.6.2 Translational control of BCL-3

The BCL-3 gene is thought to be relatively unusual in that it contains two CpG islands (186). These CpG island sequences (rich in levels of C and G nucleotides) mark sites of transcriptional initiation. The 5' CpG island was shown to be un-methylated in BCL-3 in contrast to the 3' island suggesting that the 5' island is the primary promotor site of BCL-3 (186). BCL-3 is a target gene of several pro-inflammatory transcription factors including canonical (187) and non-canonical NF-κB signalling (188), AP1 and STAT (signal transducer and activator of transcription). Induction of BCL-3 transcription, by these factors, occurs downstream of a number of cytokines such as TNF-α and interlukin-1α (IL-1α) (187), IL-2 (189), IL-4 (190), IL-6 (191), IL-9 (192), IL-10 (193) and IL-22 (194). Primarily, the upregulation of BCL-3 is mediated through the phosphorylation and activation of STAT3, which has been shown to bind to BCL-3 intronic enhancers

(195). STAT3 is known to be a GSK3 target and inhibition of STAT3 phosphorylation with a GSK3 inhibitor or in fact STAT3 inhibition itself, is shown to abrogate BCL-3 upregulation following STAT3 activation (196, 197).

In addition to STAT signalling, NF-κB signalling is thought to promote BCL-3 expression. The BCL-3 gene promoter contains a number of NF-κB consensus binding sites located -872 and -106 nucleotides upstream from the BCL-3 TSS. Transcription of BCL-3, by NF-κB, can be driven by TNFα, IL-1α and PMA (phorbol 12-myristate 13-acetate/phorbol ester) (187). In mice, knockout of p50 diminished expression of BCL-3 (162). Moreover, there are NF-κB consensus sites within intronic enhancer regions of the BCL-3 gene, suggesting that control of BCL-3 transcription by NF-κB not only relies on subunit binding to the BCL-3 promoter, but also to enhancers (198). Other work has identified that BCL-3 transcriptional control may require the atypical NF-κB subunit p52, which represses BCL-3 transcription, and that can be reversed by homodimer exchange on DNA by canonical NF-κB heterodimers (p65-p50) (199).

Unpicking the complexity surrounding BCL-3 transcription is challenging as it is clearly context and cell type dependent, but what is apparent is that BCL-3 is upregulated by a variety of cytokines, serving as a link between the STAT and NF-κB signalling pathways in response to cellular stress.

1.6.3 Post-translational modification of BCL-3

Post-translation modification (PTM) of proteins is a primary mechanism by which function, and abundance/degradation are controlled in the cell. BCL-3 is extensively phosphorylated predominantly at its C-terminal domain, in which there are 22 possible phosphorylation sites (serine, threonine and tyrosine). Binding of BCL-3 to p50 or p52 was thought to be prerequisite for its phosphorylation to take place (200, 201). However, more recent data has shown that phosphorylation of

BCL-3 is mediated by GSK-3 or ERK1 (202, 203), and occurs in both the cytoplasm and nucleus, leading to proteosomal degradation.

Ubiquitination also plays an important role in BCL-3 sub-cellular localisation and degradation. The enzyme CYLD (homozygous loss of CYLD results in cylindroma) acts on BCL-3 in the cytoplasm to remove K63 (lysine 63) ubiquitin chains (204). This inhibits BCL-3 nuclear translocation and binding to NF-κB homodimers. Degradation of BCL-3 also requires ubiquitination, although this appears to be via K48 ubiquitination as has been shown to occur predominantly in the nucleus via the PSMB1 subunit of the 20s proteasome (201). Ubiquitination also occurs on lysine residues 13 and 26 and is independent of phosphorylation by GSK3 when ubiquitination is performed by the E3 ligase, TBLR1 (201).

In addition to these documented PTMs, it is likely that BCL-3 is a substrate for other unstudied kinases or is modified by not only phosphorylation or ubiquitination. For example, BCL-3 has 2 putative sites for ATM phosphorylation (Ser-Gln, SQ amino acid domain at positions 369 and 404) (205), linking its post-translational modification to the DNA damage response.

1.6.4 BCL-3 Function

Functionally BCL-3 differs from the other IκB proteins (IκB-α, IκB-β and IκB-epsilon) which bind to NF-κB proteins in the cytoplasm inhibiting their nuclear translocation and subsequent transcriptional activity. Important to note are the contrasts in reported function of BCL-3, suggested to be a consequence of differing tissue models, cancer vs normal tissue, and differing experimental conditions.

1.6.5 Control of NF-κB sub-units

First thought to inhibit nuclear translocation of p50 homodimers (206), binding of BCL-3 to p50 homodimers was later shown to unmask the NLS of p50 allowing translocation of the complex into the nucleus (182, 207). Furthermore, p50 protein

with a mutated NLS was shown to be predominantly cytoplasmic even when bound to BCL-3 highlighting the importance of the p50 NLS following binding to BCL-3 (207). Structural data suggests that BCL-3 may bind basic NLS residues less stably as the ankyrin repeats 1, 2 and 3 required for this interaction are less acidic, compared to IκB-α resulting in this alteration to BCL-3 function (179).

1.6.6 Trans-activator or transrepressor

Initial work, using in-vitro gel retardation assays, showed that bacterially derived BCL-3 inhibited p50 homodimer-DNA binding (177), but not p50-p65-DNA binding (208), in a manner dependent on the ARD of BCL-3 involving either repeats 1, 6 or 7 (175); ARD binding was later corroborated by other groups (207, 209, 210). BCL-3 was later shown to directly bind with p50 homodimers to genes inducing repression (169). The ability of BCL-3 to act as a repressor is thought to be concentration dependant. While binding of p50 homodimers to κB promotor sites competitively displaces transactivating p65:p50 heterodimers; when BCL-3 was co-transfected with p50, increasing concentrations of BCL-3 reversed the repressive nature of the p50 homodimers whilst still inhibiting p65:p50 heterodimer transactivation (162, 211). BCL-3 may mediate this function by selectively removing p50 homodimers from DNA allowing the binding of heterodimers and transactivation of the target gene (208). Controversially, the opposite effect was observed by another group examining the same cells and utilizing similar methods, suggesting perhaps multiple modes for BCL-3 transactivation depending on context (212). Additionally, data suggests BCL-3 is a transactivator when bound to p52 homodimers (212, 213). Critical to the role of BCL-3 as a transcriptional activator is the fact that BCL-3 has TADs (170), which given that both p50 and p52 lack this domain, allows BCL-3 to transform the repressive homodimers into transcriptional activators.

Therefore, in summary, it appears that BCL-3 has four primary mechanisms of gene interaction with p50/p52 homodimers; firstly through destabilisation of repressive p50/p52 homodimers bound to DNA (214, 215); secondly by forming a ternary activating/repressive complex on DNA (specificity of which is determined directly by the κB sequence bound by the ternary complex (137) and by the binding of additional co-factors (216)) and thirdly by un-masking NLS domains on p50 that allows it to translocate and dissociate NF-κB heterodimers from DNA. Fourthly, it is likely that BCL-3 alongside p50 or p52 homodimers, is part of the temporal NF-κB response to a stimulus, utilising the repressive nature of these complexes to control the expression of target genes following initial transcription by canonical NF-κB proteins (217).

1.6.7 BCL-3 protein interactions

BCL-3 has been shown to form additional and alternative protein-protein interactions as well as the interaction with p50/p52. BCL-3 functions as a bridging factor between NF-κB homodimers and other co-regulators, such as Tip60 (KAT5), Jab-1, Pirin and Bard-1 (216). This adds a further dimension to the regulation of transcription by BCL-3, with some co-regulators resulting in repression of target genes and others in transactivation. Further protein-protein interactions have been documented such as with Hsp70, HDAC1 and 3, CtBP1 and CtBP2 (218, 219).

Acetylation is known to play an important role in other NF-κB family subunits such as p65, where acetylation results in reduced binding of p65/p50 heterodimers to κB sites on the DNA (220). It is unknown if the bridging role that BCL-3 plays, with proteins such as Tip60 and HDAC1/3, facilitates acetylation of p50 or p52 homodimers, which would further define control of homodimer transactivation in the nucleus. Evidence exists to show that p50 can be acetylated and that this acetylation results in enhanced binding to κB sites (221).

Thus BCL-3 has multiple functions ranging from activation of p50/p52 subunits in the cytoplasm, their nuclear import and modulation of homodimer transactivation through facilitating binding of different transcriptional co-regulators. It also is suggested that BCL-3 has contrasting functions depending on the pathological model used, in particular there is a significant reversal of function in inflammation models (222), which could be explained by investigation of co-factor binding and post translational modification of chromatin surrounding NF-κB dimers (223).

1.6.8 BCL-3 and the 'Hallmarks of Cancer'

Cancer cells display certain hallmarks that are prerequisites for tumorigenesis and have been discussed in a series of landmark papers over the past 20 years and updated in 2011 (224). The multistep nature of colorectal carcinogenesis leads to tumours developing aberrations in these critical aspects of cell physiology that ultimately leads to cancer and its metastasis. BCL-3 has been implicated in a number of these 'hallmarks of cancer'.

1.6.8.1 Sustaining proliferative signalling

Cancer cells can disregard the homeostatic cues that govern normal cells ability to grow and importantly stop growing. Cancers acquire the ability for self-sustaining proliferation through a number of different means, including dysregulation of cancer cell cell-cycle, increased growth factor production, stimulation of cells within the microenvironment resulting in increased pro-proliferative paracrine signalling and the deregulation of growth factor receptors leading to hypersensitivity to growth factors (224, 225). The effect of BCL-3 on tumour growth/proliferation has been observed in different tumour types. In colorectal cancer cells, BCL-3 induces the post-translational stabilisation of c-Myc, mediated by ERK1/2 increased tumour xenograft size (226); while BCL-3 over expression was shown to induce cell cycle progression, mediated by Cyclin-D1 in hepatocellular carcinoma (227, 228), malignant melanoma (229) and breast cancer (230). The converse was also true,

as suppression of Cyclin-D1 by p53 was shown to be dependent on BCL-3 suppression (231). Furthermore, proliferation of skin cancer cells was shown to be abrogated when nuclear translocation of BCL-3 was blocked by its upstream regulator, CYLD (204).

1.6.8.2 Activating invasion and metastasis

Invasion into surrounding tissues is a defining feature of malignant cells followed by metastasis to distant organ sites, which is often the fatal event of solid malignancy (224). In breast cancer models, it has been demonstrated that BCL-3 drives metastasis of tumour cells (232, 233). In HER2 positive breast tumour cells, BCL-3 KO resulted in an 80% reduction of metastatic burden in mice following tail-vein injection of tumour cells (233). While in the MMTV-PyMT mouse model of mammary adenocarcinoma, BCL-3 suppression using Dox-inducible shRNA resulted in the reduction in lung metastasis, through targeting Smad3 stability in the TGF-β signalling pathway (232). Additionally, a clinical study examined immunohistochemistry from paired normal and tumour tissue in hepatocellular carcinoma and showed BCL-3 expression results in advanced tumour node metastasis; this was shown to have contributed to the poorer prognosis observed in these patients (227).

1.6.8.3 Evasion of Apoptosis

BCL-3 has been shown to regulate cellular apoptosis through different mechanisms in different cell lines. Studies examining colorectal and cervical tumour cell lines has shown BCL-3 to be an important down-stream regulator of apoptosis by the AP1 complex, following UV-radiation (234). In HEK293 cells, BCL-3 stabilizes CtBP1 (an anti-apoptotic protein) leading to the repression of target pro-apoptotic genes, and was also shown to protect breast carcinoma cells from undergoing apoptosis after UV-radiation (235).

BCL-3 has been shown to prevent apoptosis by inhibiting proteins such as Smac/Diabolo and p53 activity (through upregulation of HDM2) (236-239). Although, even in p53-null backgrounds BCL-3 suppression was able to initiate apoptosis through targeting the expression of DNAPKcs, proteins critical for DNA damage repair (DDR) (236).

Evidence from this and other groups showed BCL-3 to be a potent survival factor in colorectal cancer (2, 188), through activating the pro-survival AKT/PKB pathway (2). Given that BCL-3 is upregulated in a subset of colorectal malignancies (188, 240, 241), it maybe that resistance to therapy is propagated through BCL-3 and its anti-apoptotic effects on tumour cells, thus making it an attractive target in cancer therapy.

In hepatocellular carcinomas, BCL-3 is frequently overexpressed in tumour tissue, compared to normal tissue, in conjunction with p50 and p52 NF-κB subunits (242). However, recently published data, using a hepatocyte specific BCL-3 over-expression mouse model, showed that BCL-3 expression promoted hepatocyte death following an inflammatory insult and mice developed fewer hepatocellular carcinomas (243). This study also highlighted that BCL-3 overexpression reduced the influx of certain populations of immune cells into the liver ($CD8^+$ t cells, B cells and leukocytes), protecting against induced inflammation. It may be that hepatocellular carcinomas are particularly sensitive to alterations in canonical NF-κB signalling and that repression of canonical NF-κB occurs when BCL-3 is overexpressed in combination with atypical NF-κB homodimers, leading to abrogation of apoptosis in this context.

1.6.9 The role of BCL-3 in inflammation and immunity

NF-κB signalling is recognised to have contrasting function depending on the biological context (244), which appears to be consistent with the role of BCL-3 in cancer compared to its role in non-malignant, inflammatory models; the presence

of BCL-3 appears to ameliorate inflammation in these alternative non-malignant models. BCL-3 KO mice have defects in lymphoid organs, including displaying aberrant development of Peyer's patches, which would affect intestinal immune surveillance and response to certain pathogens (245).

BCL-$3^{-/-}$ has been studied in a variety of different inflammatory models, including pancreatitis, colitis, dermatitis and rheumatoid arthritis. In a mouse model of acute pancreatitis, where pancreatic inflammation is stimulated using cerulin or sodium taurocholate, results showed that BCL-$3^{-/-}$ mice had increased levels of oedema and necrosis in their pancreata (246). This finding, that BCL-3 KO increases the severity of inflammation, has been corroborated in an inflammatory bowel disease model (IBD; Crohn's disease and ulcerative colitis) (222). In a contact hypersensitivity model of atopic dermatitis, BCL-$3^{-/-}$ mice had worsened inflammation following topical oxalazone treatment, which appeared to be mediated through increased cytokine production.(247). Earlier evidence, for this mechanism, comes from an important paper published in Science by Carmody et al. This paper examined the expression of pro-inflammatory cytokines in murine immune cells (macrophages and dendritic cells) devoid of BCL-3 (248). BCL-3 acted to repress canonical NF-κB transcription of target cytokines (such as TNF-α, CXCL1, CXCL2, IL-1β and IL-10) leading to significantly increased expression after inflammatory stimuli in the BCL-3 KO cells, corroborating earlier evidence (249). What was particularly interesting about this study was that not all cytokines responded in the same way to BCL-3 KO. In cytokines that showed an early spike in transcription following lipopolysaccharide (LPS), BCL-3 KO had a significant impact on their production; while cytokines such as IL-6 showed a slower increase in transcription that was unchanged in BCL-$3^{-/-}$ cells, compared to BCL-3 WT controls. This data suggests that BCL-3 KO affects different aspects (early and late) of the NF-κB driven response to inflammation. Interestingly, IKKβ KO in

intestinal epithelial cells worsens the histological severity of colonic inflammation and led to the animals loosing greater amounts of weight (145). If BCL-3 knockout leads to increased binding of canonical NF-κB dimers (248), then it is unclear why the phenotype observed with BCL-3 knockout is similar to the phenotype observed when canonical NF-κB has been inactivated by IKKβ deletion.

In converse to the data above, another recent study showed that BCL-3 over-expression, specifically in $CD4^+$ T-cells (including T regulatory cells), results in a pancolitis of the large bowel of mice (250, 251). This cell-type specific effect was corroborated by work in $CD4^+$ cells in a rheumatoid arthritis (RA) model, which showed over-expression of BCL-3 in these cells was implicated in the pathogenesis of RA (252). Interestingly, BCL-$3^{-/-}$ T cells failed to induce colitis when transferred into $Rag1^{-/-}$ mice (253), suggesting an inability of BCL-$3^{-/-}$ T cells to respond to the microbiota-derived and antigen-specific signals that drive colitis in this model.

Following induction of inflammation there is a concomitant induction of BCL-3 in a variety of tissue types. This is likely to represent a feedback loop, in place to regulate pathways such as NF-κB and modulate their function following a stimulus. Evidence for this comes from a number of sources; in respiratory syncytial virus (RSV) infection of airway epithelial cells, BCL-3 is initially upregulated leading to inhibition of NF-κB and STAT transcription by acting as a bridging factor to HDAC1, which is transcriptionally repressive (219). Furthermore, BCL-3 represses STAT3 regulating proteins (201); Repression of STAP2 by BCL-3 and p50 homodimers in conjunction with CtBP on the STAP2 promoter can diminish STAP2 dependent BRK kinase signalling that phosphorylates and activates STAT3 (254). BCL-3 is upregulated in tissue from patients with IBD (250). Although, further data from IBD patients has shown that in B cells isolated from diseased tissue, CpG sites in the BCL-3 gene are commonly methylated, and therefore repressed (255).

Despite these data showing the role of BCL-3 as both a pro-inflammatory and an anti-inflammatory mediator in non-cancer tissue, it does still appear that BCL-3 has similar control over regulation of apoptosis (discussed below in Results 3.1.1) in non-malignant tissue compared to the role of BCL-3 in cancers.

BCL-$3^{-/-}$ granulocytes, isolated following pulmonary transplant in mice, had higher levels of apoptosis, as measured by annexin V (256). This links to other data showing BCL-3 KO cells in mice colons had increased caspase-3 cleavage following dextran-sodium sulphate (DSS) induced colitis (222), suggesting these cells were undergoing more apoptosis.

In summary, BCL-3 has alternative roles in inflammation depending on which cell type it is expressed in and whether all tissues have lost or gained expression. It is suggested, that KO of BCL-3 reduces the ability of cells to upregulate survival programmes following an inflammatory insult leading to concomitant rise in apoptosis; this results in a worse grade of histological inflammation and tissue damage propagating worse inflammation, suggesting it may be the pro-survival role of BCL-3, following stress/insult, which is critical to its function.

1.7 Hypothesis and Aims

BCL-3 is an atypical IκB protein that functions as a co-factor with atypical NF-κB homodimers, p52 and p50, to regulate atypical NF-κB driven transcriptional activation and repression depending on the cell type and context. There is clear evidence to show upregulation of BCL-3 in a subset of colorectal cancers, which correlates with poorer patient prognosis (240). Previous work, from this lab, shows BCL-3 promotes evasion of apoptosis in colon cancer cells but the role of BCL-3 in promoting cell survival is not fully understood and to date nobody has investigated the function of BCL-3 in the difficult to treat rectal cancers (257).

The management of LARC involves neo-adjuvant LCCRT to control the local spread of disease where the resection margins are compromised or threatened. It is essential to understand the response of LARC to neo-adjuvant LCCRT as poor response determines a significantly worse patient prognosis. Understanding the drivers of a poor response would enable patients to be stratified into those patients who should receive therapy, those patients who should receive therapy including additional adjunctive medication and those patients where response will always be poor, and therapy should be avoided by progressing straight to surgical resection.

BCL-3 expression is upregulated in a IL-6/STAT3 dependent manner (195). The tumour stromal contains large numbers of activated fibroblasts known as cancer associated fibroblasts (CAFs) which secrete IL-6 as a principal cytokine. Fibrosis is a primary response following irradiation in rectal cancers but, as discussed earlier, response is often incomplete; leaving tumour cells surrounded by large amounts of activated fibroblasts.

It is hypothesised that BCL-3 expression, upregulated by fibrosis in rectal cancers, promotes evasion of apoptosis and hence tumour survival. Additionally, it is hypothesised that BCL-3 expression would decrease the response to irradiation in rectal cancers, contributing to the poor prognosis reported in earlier studies.

1.7.1 Project aims

Understand the role of BCL-3 in rectal cancers and analyse if BCL-3 protects cells from undergoing apoptosis in these cells.

Identify the mechanism by which BCL-3 promotes evasion of apoptosis if observed in rectal cancer cells.

Establish if BCL-3 plays a role in the response to irradiation in rectal cancer.

Analyse rectal cancer tissue for BCL-3 expression and correlate to tumour response grade (TRG).

Investigate the role of CAFs in promoting BCL-3 expression and growth or response to therapy of cancer cells in a 3D spheroid model system.

Investigate, in-vitro, the role of BCL-3 in the DNA damage response and to determine a mechanism for this function.

2 Methods

2.1 Tissue Culture

2.1.1 Cultured Cells

2.1.1.1 SW1463

This cell line was obtained from the American Type Culture Collection (ATCC, VA, USA) and were checked for mycoplasma infection prior to use. SW1463 are derived from a 66 year old female patient with a Dukes' C adenocarcinoma of the rectum (258). This cell line has homozygous mutations in KRAS (259), SMAD4 (13), TP53, APC and SOX9 (260). SW1463 are MMR proficient.

2.1.1.2 LS174T

This cell line was established from a right sided Dukes' B colonic tumour from a 58 year old female patient (261). LS174T is MMR deficient cell line (hMSH6) (262) and concomitantly is wild-type for TP53 (263) and has a mutation in TGFβR2 (264). The cell line also has mutations in KRAS (259), PIK3CA (265), β-catenin (266) and E-cadherin (267) while being wild-type APC (260). Importantly, in the context of apoptosis, LS174T have mutant BAX, which results in the absence of the protein (264).

2.1.1.3 HCA7/Parental

The HCA7/Parental (herein known as HCA7/P) cell line was a kind gift from Susan Kirkland (Imperial College London, UK). HCA7/P were isolated from a Dukes' B hepatic flexure adenocarcinoma of the colon in a 58 year old woman (268). HCA7/P is a MMR deficient cell line with a mutation in MSH3 and hypermethylation of MLH1 (269). This cell line has a heterozygous deletion at exon 8 codon 300 leading to a frameshift mutation in p53 (270). Furthermore, HCA7/P has mutations in HER3 (ERBB3) and TGFβR2 (260). Interestingly, as well as being β-catenin WT (266), HCA7/P have indeterminate APC status, previous studies thought APC was WT (271), but a more recent paper has highlighted frameshift mutations in APC

that result in a significantly truncated protein, which would likely result in loss of β-catenin regulatory activity (260, 266).

2.1.1.4 SW837

This rectal cancer cell line was isolated from a 53 year old male patient with a Dukes' C adenocarcinoma of the rectum (258). This cell line has mutations in APC, KRAS and ATM (260), with a point mutation in exon 7 of TP53 (270). SW837 are MMR proficient.

2.1.1.5 Fibroblast cell lines

The fibroblast cell lines were isolated by members of the lab in the 1980s (Dr A Hague). They were obtained from patients with both FAP and sporadic tumours. FAP fibroblasts were JW and JD cells, while SC and CM were grown from sporadic adenocarcinomas. The SW cell line was obtained from normal tissue adjacent to a colorectal cancer.

2.1.1.6 Adenoma/Carcinoma protein expression screen cell lines

The following cell lines were only used in screens of protein expression amongst a selection of adenoma and carcinoma cells. The adenoma cell lines AA/C1, AN/C1, AA/C1/10C and RG/C2 cell lines were isolated and cultured originally by this group as described previously (272-274). The carcinoma lines HT29, HCT116, HCT15, SW480, SW620 and LOVO were all available from existing laboratory stocks, obtained from ATCC.

2.1.2 2D Cell Culture

All 2D carcinoma cell lines were cultured in Dulbecco's Modified Eagles Medium ((DMEM), Life Technologies, UK); 500 mL DMEM supplemented with 50 mL (10 %) Foetal Bovine Serum (FBS, Life Technologies, UK), 2mM glutamine (Life Technologies, UK) and penicillin/streptomycin solution (100 units/mL penicillin and 100 μg/mL streptomycin, Life Technologies, UK). For adenoma cell lines 500 mL

DMEM was supplemented with 100 mL (20 %) FBS, penicillin/streptomycin solution (100 units/mL penicillin and 100 μg/mL streptomycin), with the addition of insulin, 0.2 units/mL (Sigma–Aldrich, Dorset, UK) and hydrocortisone 1 μg/mL (Sigma-Aldrich, Dorset, UK). 25 cm^3 tissue culture flasks (T25 flasks, Corning, NY, USA) were used to maintain stock cells. Cells were maintained in incubators at 37 ˚C in 5 % CO_2 and medium was changed every 3-4 days.

2.1.3 Cell passage

Cells were passaged, and ratio split when cultures were sub-confluent. Firstly, medium was removed, and cells were washed with phosphate buffered saline (PBS). Next, cells were incubated with 2 mL Trypsin/EDTA (0.1 % w/v of trypsin (Dibco, Becton Dickinson, Oxford, UK) and 0.1 % w/v of ethylenediamine-tetraacetic acid (EDTA) (Sigma–Aldrich, Dorset, UK) in PBS) at 37 ˚C until cell-cell and cell-flask contacts were disrupted. Trypsin/EDTA was neutralised by adding 8 mL of 10 % DMEM to the flask and cell suspension was removed into a universal. Cell suspensions were centrifuged at 3000 rpm for 3 min. The supernatant was removed, and cells were suspended in further 10 % DMEM. Cells were syringed to provide single cells and were then diluted to ensure a ratio split of 1:6–1:20 depending on cell line. Cells could also be counted at this point using a haemocytometer and used in downstream experiments.

2.1.4 3D Cell Culture

2.1.4.1 Human spheroid culture

3D culturing of colorectal cancer cell lines from single cell suspensions embedded in Matrigel (BD Biosciences, California, USA) was adapted from methods published by Sato et al. 2009 (275). A single-cell suspension was produced from 2D cell culture by trypsinisation (as described above 2.1.3), re-suspended in 5 mL PBS and syringed prior to being strained through a 40 μm nylon cell strainer (Falcon, Fisher Scientific, USA). The single cells were counted using a

haemocytometer and seeded into ice-cold Matrigel (200–500 cells/50 µL of Matrigel, around 2-5 µL PBS/cell suspension in Matrigel). 50 µL aliquots of Matrigel/cell suspension was then pipetted (using pre-chilled pipette tips (-20 ˚C) to ensure Matrigel does not polymerise inside pipette) into pre-warmed (37 ˚C), 24-well tissue culture plates (24-well plate, Corning, NY, USA) (see Figure 6). 48-well plates (Corning, NY, USA) were also used with 20 µL Matrigel/cell suspension per well. Polymerisation of Matrigel is achieved by incubating the plates at 37 ˚C for 10-20 min until the gel has set. The gel is then bathed in 500 µL (24-well plate) or 250 µL (48-well plate) organoid medium per well. Medium for organoid culture has been adapted from Sato et al. 2009 (275) and consists of Advanced DMEM/F12 ((ADM/F12) Life Technologies, UK) supplemented with Bovine Serum Albumin 0.1 % (BSA. Sigma–Aldrich, Dorset, UK), 2 mM glutamine, 100 units/mL penicillin, 100 µ/mL streptomycin and 10 mM Hepes (Sigma–Aldrich, Dorset, UK). This medium was aliquoted into 48.5 mL units and stored at -20 ˚C. Prior to use the medium was defrosted and further supplemented with 1 mL of 1:50 B27 (Life Technologies, UK), 500 µL of 1:100 N2 (Life Technologies, UK) and 100 µL of 1:500 N-acetyl cysteine (Sigma–Aldrich, Dorset, UK) (Appendix 1). Medium changes were performed one week following plating and thereafter every three-four days.

2.1.4.2 Mouse organoid culture

Mouse small intestinal crypts were isolated from 6-week-old C57BL/6 BCL-3 null (BCL-$3^{-/-}$) and control mice in triplicate by Dr. D Legge. Briefly, small intestines were excised from the mice after culling, washed with ice-cold PBS, the villi were scraped into a 50 mL falcon tube and incubated with 25 mM EDTA/PBS, for 30 min. Crypts were collected and resuspended in Matrigel (50µL with 75 µL of crypt suspension) and polymerised as above (Methods 2.1.4.1). Crypts were maintained on 500 µL ADM/F12 supplemented as above with the addition of EGF

0.5 µL/1000 µL ((stock 100 ng/µL) Peprotech, #AF-100-15), Noggin 20 µL/1000 µL ((stock 5 µg/µL) Peprotech #250-38), mR-Spondin 5 µL/1000 µL ((stock 100 µg/µL) R&D Systems #3474-RS). Medium was changed every three days.

2.1.4.3 Passaging mouse organoid cultures

Organoid cultures once they had reached a size where there was significant apoptotic debris within the lumen of each organoid (between 10-14 days after seeding). To passage Matrigel/crypt mixtures were mechanically broken up using cold PBS and a p1000 pipette. For each 100 µL Matrigel at least 2 mL PBS was used. PBS was supplemented with cold ADM/F12 1:4 ratio. This mixture was placed into a 15 mL falcon tube and centrifuged at 600 rpm for 3 min. After discarding the supernatant, the pellet was suspended in a further 4 mL of PBS/ADM/F12 and mechanically dissociated using a p200 pipette until organoids were hardly visible (around 5-10 cycles of pipetting up and down). The mixture was centrifuged at 600 rpm for 3 min and the supernatant discarded. A single further wash was performed and again the crypts spun down at 600 rpm for 3 min. The pellet was then suspended in the desired quantity of Matrigel on ice before being seeded into 24-well plates and supplemented with 500 µL of mouse organoid medium, as above.

2.2 Genetic Transfection

2.2.1 RNA Interference - siRNA

Transient knockdown of target genes was performed using RNA interference (RNAi). RNAi will be achieved using small interfering RNA (siRNA) introduced into cells in suspension using Lipofectamine RNAiMAX (Life Technologies, UK). Sub-confluent cells were medium changed onto 10 % DMEM free of penicillin and streptomycin antibiotics, to encourage exponential growth 12–24 hours prior to being trypsinised. Cells were trypsinised, counted and seeded in well plates or

tissue culture flasks and transfected in suspension with human siRNA (as per manufacturer's instructions). Sequences targeting BCL-3 siRNA (Sequence A: target sequence 'AGACACGCCUCUCCAUAUU'; Sequence D: target sequence 'CCGUGCAGCUCUUGCUAGA', Dharmacon, UK) or non-targeting siRNA (target sequence 'UAAGGCUAUGAAGAGAUAC', Dharmacon, UK), Bim siRNA (Sequence 2: target sequence Sense 'UGACCGAGAAGGUAGACAA', anti-sense 'UUGUCUACCUUCUCGGUCA', Ambion, UK), NF-κB1 siRNA (SMARTpool: target sequences #1 Sense 'CCAAACAGUUCACCUAUUA', Antisense 'UAAUAGGUGAACUGUUUGG', #2 Sense 'GGACGUGUCUGAUUCCAAA', Antisense 'UUUGGAAUCAGACA-CGUCC', #3 Sense 'GGUGAUGGAUCUGAGUAUA', Antisense 'UAUACU-CAGAUCCAUCACC', #4 Sense 'GUAGACACGUACCGACAGA', Antisense 'UCUGUCGGUACGUGUCUAC'), NF-κB2 siRNA (SMARTpool: target sequences #1 Sense 'CCAAACAGUUCACCUAUUA', Antisense 'UAAUAGGUGAACUG-UUUGG'; #2 Sense 'GGACGUGUCUGAUUCCAAA', Antisense 'UUUGGAAUC-AGACACGUCC'; #3 Sense 'GGUGAUGGAUCUGAGUAUA', Antisense 'UAUACUCAGAUCCGUCACC'; #4 Sense 'GUAGACACGUACCGACAGA', Antisense 'UCUGUCGGUACGUGUCUAC', Dharmacon, UK) were used compared to non-targeting control siRNA sequences. All sequences were prepared in nuclease-free water at 100 μM concentrations and stored at -20 °C. For a 12.5 cm^3 tissue culture flasks (T12.5 flask), initially, RNAiMAX 5 μL/flask is mixed with 250 μL/flask of Opti-MEM reduced serum medium (Life Technologies, UK) and concomitantly 1 μL siRNA is mixed with 250 μL/flask Opti-MEM, for a final concentration of 50 nM siRNA/T12.5 flask. Mixtures were incubated at room temperature for 10 minutes. The RNAiMAX mixture is added dropwise to the siRNA while swirling gently, allowing the RNAiMAX and siRNA to form complexes at room temperature for 20 min. 500 μL of complexes in Opti-MEM was then added to

1.5 mL of single-cell suspension of 1-2x10^6 cells in 10 % DMEM pen/strep free media in T12.5 flasks and allowed to incubate at 37 ˚C for 16 hr. After 16 hr, medium is aspirated and replaced with standard 10 % DMEM. Protein suppression is confirmed by western analysis at the time points of interest, taken from the introduction of siRNA to the cells.

2.2.2 Stable overexpression of BCL-3

The overexpression of BCL-3 was achieved by the transfection of a plasmid containing the human BCL-3 cDNA, under the control of a heterologous promoter. In order to over-express BCL-3, plasmids containing FLAG-tagged BCL-3^{WT} and BCL-$3^{ANK\ M123}$ (kind gift by Dr Alain Chariot (Liege, Belgium) (218)) or GFP-tagged BCL-3 (BCL-3^{GFP}) (Origene, Rockville USA) were used. The mutant BCL-3 construct (BCL-$3^{ANK\ M123}$) contains three point mutations leucine>alanine at residues 168, 171 and isoleucine>alanine at residue 173, located between ankyrin repeats 1 and 2 leading to lack of binding of BCL-3 to p50 or p52 (201). SW837 cells were used as they have low expression of BCL-3. SW837 initially underwent dose response to geneticin (G418 see methods 2.4.8) with doses ranging from 100-500 µg/mL to ascertain the correct selection dose for these cells. A dose of 400 µg/mL G418, with twice weekly medium changes, resulted in loss of any viable cells, and was selected. SW837 cells were transfected in T25 flasks as per manufacturer's instructions. Initially, 250 µL of Opti-MEM with 10 µL Lipofectamine 2000 (Life Technologies, UK) or 250 µL of Opti-MEM with 5 µg of pcDNA3.1 empty vector control plasmid or expression plasmid were incubated for 5 min, after which they were added together dropwise to allow complexes to form for 20 min.

Following this, the complxes were added to cells and topped up with 2 mL of Opti-MEM. Cells were incubated with transfection reagents overnight, after which medium was replaced with fresh DMEM 10 %. 72 hr later DMEM containing 400 µg/mL G418 was introduced to the cells for selection. Two separate flasks of transfected cells per plasmid (flask A or B) were selected for 2 weeks before being passaged and analysed separately in downstream applications (western blot, 2D and 3D growth assays). Selected cells containing plasmids were maintained on

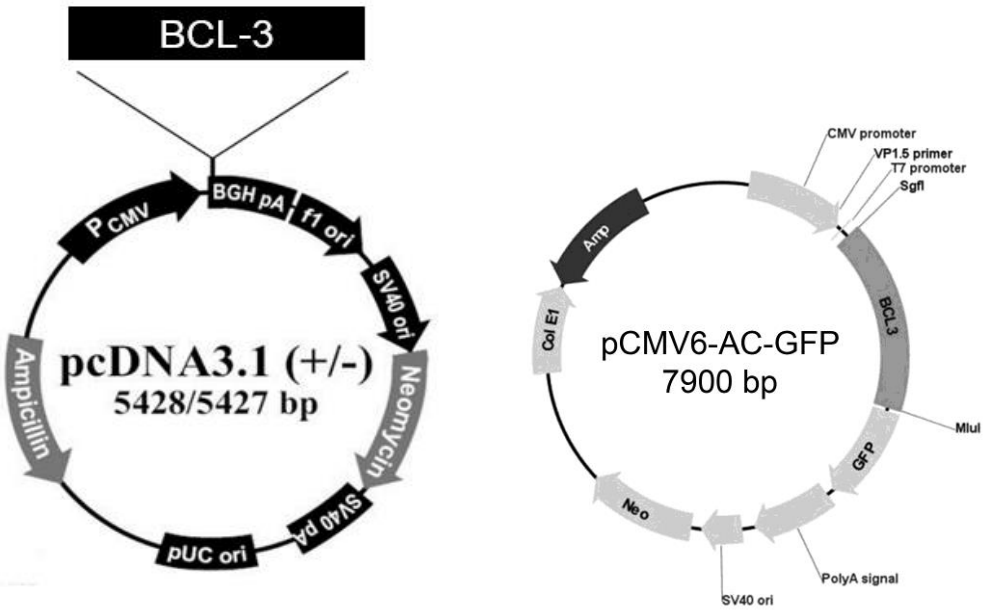

Figure 2.1 BCL-3 plasmid maps

A Map of pcDNA3.1 plasmid with inserted BCL-3 sequence (BCL-3^{WT}, and BCL-$3^{ANK\ M123}$). **B** Map of pCMV6-AC-GFP plasmid to produce BCL-3^{GFP}. Plasmids contained genes for geneticin/neomycin and ampicillin resistance for selection in mammalian and bacterial cells, respectively.

200 µg/mL G418 long-term.

2.3 Functional Assays

2.3.1 Cell yield and survival assay

To determine changes to cell yield and apoptosis after transfection colorectal adenoma/cancer cells were seeded in T12.5 or T25 flasks. Cells were incubated for 48 or 72 hr. At these time-points medium was collected for floating cell counting.

Medium containing the detached (floating cells) was removed and stored for counting; this apoptosis assay was validated in this laboratory as floating cells are known to be predominantly those that have undergone apoptosis in vitro (276). Remaining adherent cells were trypsinised (as above 2.1.3) and were counted to measure cell yield per flask. Cells were counted using a haemocytometer with at least four counts made per flask and an average taken of these. The proportion of apoptotic cells was determined by dividing the total number of floating cells counted by sum of number of floating cells and number of attached cells counted (276).

2.3.2 Crystal violet cell viability assay

A crystal violet cell viability assay was used to assess cell viability in 2D culture systems. Cells were grown in 6-well tissue culture plates (Corning, NY, USA) and transfected or treated with irradiation as described (Methods 2.2 & 2.4). At set time-points (2 or 3 weeks) cells were washed twice with PBS (2 mL/well). Cells were then fixed with 2 mL/well of 4 % paraformaldehyde for 10 minutes. A further wash with 2 mL of PBS was carried out. A 0.5 % w/v solution of crystal violet (Sigma, UK) with distilled water was made and 2 mL/well placed on the cells for 10 minutes. Crystal violet solution was removed, and plates were washed in warm tap water to remove excess stain. Plates were allowed to dry briefly. 2 mL of 10 % v/v solution of acetic acid with distilled water was made and used to elute intracellular crystal violet from the cells with a 10 minute incubation on a rocker. A sample of 100 µL of the crystal violet/acetic acid solution was pipetted into each well of a 96-well plate (Corning, NY, USA) and read using a microplate reader (Bio-Rad, Hemel Hempsted, UK) at 595 nm absorbance. This assay was also a scaled down into a 24-well plate setup using a 4-fold reduction in all volumes used above.

2.4 Treatments

2.4.1 Pan-caspase inhibitor, QVD

Drug treatment with quinolyl-valyl-O-methylaspartyl-[-2,6-difluorophenoxy]-methyl ketone (Q-VD-OPh or QVD, Calbiochem, USA), an irreversible broad-spectrum caspase inhibitor, was used to inhibit apoptosis. Cells were treated with 10uM QVD diluted in medium from 10 mM stock (DMSO) stored at -20 °C. 24 hr after seeding cells were treated with QVD or DMSO and after a further 24 or 48 hours cells were processed for downstream applications.

2.4.2 BCL-3 small molecule inhibitors

BCL-3 inhibitors (BCL-3i) were a kind gift from Dr. Richard Clarkson (Cardiff University, Wales). Two inhibitors were obtained herein known as BCL-3iA and BCL-3iB. These drugs inhibit the interaction of BCL-3 with its NF-κB subunit binding partners p50 and p52; the inhibitors do this by interacting with the ankyrin repeats of BCL-3, known to be critical for its interaction with either p50 or p52 (176). Established spheroid cultures were treated with medium containing BCL-3iA (stock concentration 100 mM in DMSO stored at -20 °C and working concentration ranged from 0.01 to 100 μM) or BCL-3iB (stock concentration 100 mM in DMSO and working concentration ranged from 0.01 to 100 μM) every two days compared to vehicle control (DMSO) until the end of the experiment at two weeks from seeding spheroid cultures.

2.4.3 Oxaliplatin

Oxaliplatin (Sigma, UK) is a platinum-based compound (Figure 2.2) used as a first-line agent in colorectal cancer (1). Platinum containing compounds cause a variety of Pt-DNA adducts that result in either inter-strand or intra-strand crosslinks resulting in inhibition of DNA replication, cell cycle arrest and apoptosis (277). Oxaliplatin induces DNA intra-strand crosslinks between GG and GA bases

particularly targeting the N7 position of guanosine (278). A stock solution of 10 mM oxaliplatin in DMSO was made up (stored at -4 °C) and a range of concentration used experimentally (1-100 μM in medium). Cells were treated with oxaliplatin or vehicle control for 72 hr prior to downstream applications.

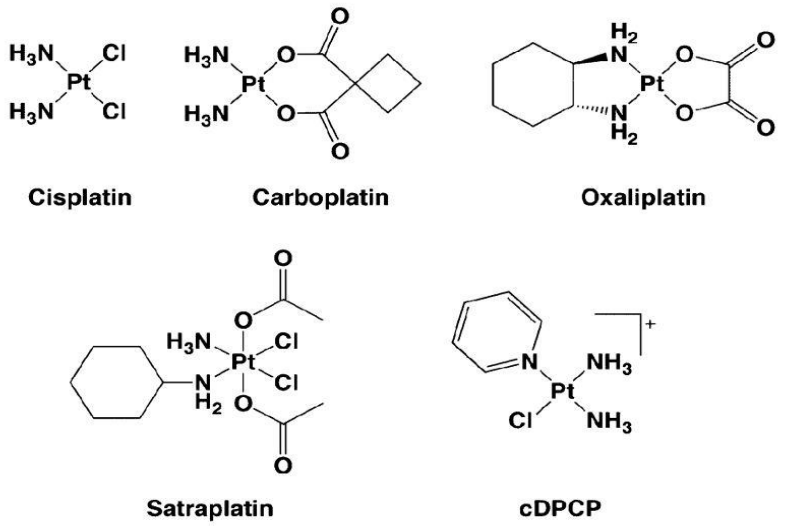

Figure 2.2 Platinum-based chemotherapy compounds

Oxaliplatin is a platinum containing compound that forms platinum (Pt) to DNA crosslinks, particularly on the N7 residue of guarnidine. Adapted from Todd and Lippard (1)

2.4.4 BCL2 Family inhibitor

The BCL2 inhibitor ABT-737 (Selleckchem, USA) is an orally bioavailable BH3 mimetic inhibitor of BCL2, BCLxl and BCLw but importantly not of MCL-1. BCL2 and related multi-domain pro-survival proteins are anti apoptotic through their interaction with the multi-BH3 domain pro-apoptotic and BH3-only proteins. Inhibition of this interaction results in increased apoptosis. Stock solution of 20 mM ABT-737 in DMSO was made and stored at -20 °C. Cells were treated (dose range 0.001-50 μM) at 72 hr after seeding for a period of 24 hr before returning cells to 10 % DMEM or the cells were harvested for downstream applications.

2.4.5 Poly ADP Ribose Polymerase inhibitor

Veliparib (ABT-888, Selleckchem, USA) inhibits PARP1 and PARP2 function in the DNA damage response and leads to synthetic lethality in cells with homologous

recombination DDR pathway deficiencies (such as BRCA1 mutations in breast cancer). Veliparib was dissolved at 10 mM in DMSO and stored at 10 mM at -20 ˚C. Cells were treated with a range of doses (0.01-100 μM) for 72 hr prior to use in downstream applications.

2.4.6 Transforming Growth Factor-Beta

Transforming Growth Factor-beta (TGFβ, R&D Systems, USA) was used to promote fibroblast activation and differentiation into a cancer associated fibroblast phenotype. TGFβ was dissolved in sterile water with 4 mM HCl and 1 % w/v BSA. TGFβ was stored at -20 °C at 2 μg/mL. Cells were treated with TGFβ at 10 ng/mL for 72 hr prior to being used in downstream applications

2.4.7 Interleukin 6

Interleukin 6 (IL-6, Life Technologies, UK) is a small 20 kDa cytokine produced early in a transient manner in response to infection and inflammation (279). IL-6 was purchased from Sigma and dissolved in water. IL-6 was used at 25 ng/mL in all experiments.

2.4.8 Geneticin

Geneticin (G418, Sigma UK) is a aminoglycoside antibiotic that was origionally isolated as a product of Micromonospora rhodorangea (280). Cells containing the neo-gene from Tn5 encoding an aminoglycoside 3'-phosphotransferase are resistant to G418. Therefore, G418 is used for selection of cells that have been transfected with a plasmid containing this resistance gene. Typical doses are around 400 μg/mL for selection.

2.4.9 Irradiation

Cells were seeded and grown for 48 hours prior to irradiation. The radiation source is a Caesium-137 (Cs-137) irradiator. Prior to irradiation, cells were treated with 0.25 mM Hepes buffer (Sigma–Aldrich, UK). Cells were taken to the irradiator

alongside control cells to ensure identical environments throughout treatment. Cells were exposed to irradiation doses of 1, 2.5, 5, and 10 Gy (Table 2.1). 24 hours following irradiation the medium was aspirated and refreshed with fresh 10% DMEM. Cells were incubated for two-three weeks and medium was changed twice a week. Cell viability was assessed using a crystal violet cell viability assay as above (2.3.2).

Distance from Source	1 Gy	2.5 Gy	5 Gy	10 Gy
25cm	51	128	255	510
40cm	130	325	650	1300
60cm	292	731	1462	2924

Table 2.1 γ-Irradiation dose

Distance from Caesium-137 source and time required for dose of irradiation. Time in seconds. Radiation dose in Gray (Gy).

2.5 Molecular Biology

2.5.1 RNA analysis

2.5.1.1 RNA extraction

Cells were placed on ice and washed twice with 2 mL ice-cold PBS. 1 mL of ice-cold TRI Reagent® (Sigma–Aldrich, Dorset, UK), which contains guanidine thiocyanate and phenol, was placed onto the cells and incubated for a couple of minutes to allow dissolution of the cells, following which cells were scraped and put in Eppendorf tubes. Following this, a liquid phase separation step was performed using 200 μL chloroform (BDH, UK), after vigorous shaking for 15 sec it was incubated for 10 minutes and then centrifuged at 11500 g for 10 min at 4 ˚C to split the liquid into three phases. RNA is then precipitated using 500 μL isopropanol shaken and left for 15 min, followed by pelleting at 11500 g for 10 min at 4 ˚C. The pellet is washed in 70 % v/v ethanol in ddH_2O followed by centrifugation at 8500 g for 5 min at 4 ˚C. The RNA pellet is then suspended in 100 μL ddH_2O.

RNA clean-up was performed as per manufacturers' instructions using RNeasy Mini Kit (Qiagen, Germany) spin columns, including on-column treatment with DNase I for 15 min. Cleaned RNA was eluted from the spin-columns and RNA concentration and quality was measured using a NanoDrop (Thermo Scientific, Germany) spectrophotometer at 260-280 nm UV. RNA was considered free of contaminants and pure if 260:280 ration was >1.8. RNA was stored at -80 ˚C.

2.5.1.2 Reverse Transcriptase Reaction

Complementary DNA (cDNA) was synthesised by reverse transcriptase using the RNA dependent DNA polymerase moloney murine leukaemia virus (MMLV), to generate a single stranded DNA product from the mRNA template. RNA (2 μg) was incubated with 0.5 μg (1 μL) oligo dT primer for 5 minutes at 70 ˚C after which it

was cooled quickly by placing directly onto ice to stop secondary structure reformation. To the RNA, MMLV buffer (5 µL), RNasin (RNase inhibitor, 25 units) and dNTPs (Deoxunucleotide mixture, 5 µL) was added to the reaction mixture. MMLV Reverse Transcriptase or ddH_2O control were added to form duplicate tubes, to examine for evidence of contaminating DNA. These mixtures were then heated to 40 ˚C for 1 hr, before dilution with 175 µL DNAase-free water and storage at -20 ˚C.

2.5.1.3 qRT-PCR

The quantitative real-time polymerase chain reaction (qRT-PCR) reaction was used to measure the relative abundance of the gene of interest compared to a housekeeping gene, such as the gene, TATA-binding protein (TBP). Reaction mixtures per sample were made in triplicate for each of the Reverse Transcriptase or singularly for ddH_2O controls, which contained 6.25 µL SYBR Green (DNA reporter molecule. Qiagen, Germany), 1.25 µL primer set, 3 µL ddH_2O and 2 µL cDNA. Fluorescence data was collected in real time and analysed using MxPro software to determine relative abundances of each primer in comparison to the housekeeping gene. Primers used were to BCL-3 (Cat number QT00008050), Bim (Cat number QT01013831) and TBP (Cat number QT00000721) (Quantitect primers, Qiagen, UK). Standard curves were performed of each primer used.

2.5.2 Protein analysis

2.5.2.1 Whole Cell Lysis

Cells were transferred from the incubator to ice, where the medium was removed. Cells were washed twice with ice-cold PBS and aspirated, ensuring all liquid was full removed. 100 µL/flask ice-cold cell lysis buffer (Cell Signalling Technology, MA, USA) containing PIC (cOmplete^{TM}, Mini Protease Inhibitor Cocktail tablets, Roche Switzerland) (Table 2.2) was added to cells and cells placed on ice, on a rocker for 10 min. Cells were scraped from the flask and transferred to a pre-chilled Eppendorf tube on ice. Samples were vortexed for 5 seconds and then transferred to a chilled centrifuge. Samples were centrifuged at 18500 g, 4 ˚C for 10 min. The supernatant was then transfer to a second, clean, chilled Eppendorf and stored at -80 ˚C until protein assay.

Cell Lysis Buffer	
Tris-HCL (pH7.5)	20 nM
NaCl	150 mM
Na_2EDTA	1 mM
EGTA	1 mM
Triton	1 % w/v
Sodium pyrophosphate	2.5 mM
Beta-glycerophosphate	1 mM
Na_3VO_4	1 mM
leupeptin	1 µg/mL

Table 2.2 Cell Lysis Buffer

10 mL of lysis buffer is made by adding 1 mL of 10xlysis buffer to 9 mL PBS and adding 1xPIC tablet. Aliquoted into 1 mL and stored at -20 °C.

2.5.2.2 Whole Flask Lysis

To determine differences in the expression of proteins known to be markers of apoptosis (cleaved caspase-3 and cleaved PARP) whole flask lysates (WFL) were

prepared containing both the adherent and the floating cell population. The medium collected containing floating cells was collected; adherent cells were washed twice with ice-cold PBS, which was collected and collated with the original media. Media and PBS washes were then centrifuged at 3000 g for 3 minutes to pellet the floating cells. 100 μl/flask of ice-cold cell lysis buffer (Table 5.1) was added to each flask. The cell pellet of floating cells and cellular debris was lysed with a 50 μl portion of the lysis buffer already added to flasks. This was then removed and added back to the respective flask to create the WFL. Adherent cells were then scraped and the preparation of the cell lysate processed as above (Section 2.5.2.1).

2.5.2.3 3D Spheroid Culture Whole Cell lysis

To collect protein from 3D spheroid cultures a method was used (optimised from (281)) in order to remove traces of Matrigel which was found to contaminate protein concentration assays. Medium was aspirated and spheroids growing in Matrigel were dislodged and broken up using 4 mL/100 µL Matrigel of ice-cold 4 °C PBS with 5 mM EDTA and a PIC tablet (1 tablet/20 mL) and transferred into 15 mL Falcon tubes (Thermo Fisher Scientific, MA, USA). The conical tubes were then rotated for 30 minutes at 4 °C. Following this, the spheroid/PBS solution was centrifuged gently for 5 minutes at 1000 rpm. The supernatant was removed leaving a loose, spheroid pellet, which was suspended in a further 4 mL of cold PBS/EDTA 1 % and centrifuged as above. The PBS/EDTA was aspirated carefully by tilting the Falcon tube to ensure complete removal of PBS/EDTA while not disturbing the spheroid pellet. 50 μL of cell lysis buffer was added to the pellet and incubated on ice for 10 minutes with vortexing 3 times. The cell lysis was transferred to new Eppendorf tubes and centrifuged at 15000 g, 4 ˚C for 10 minutes. The supernatant was transfer to a clean, chilled Eppendorf tube and stored at -80 ˚C.

2.5.2.4 Protein Concentration Assay

Protein concentration of cell lysates was determined using a Bio-Rad DC protein assay kit (Bio-Rad, Hemel Hempsted, UK), according to manufacturer's instructions and is based upon the Lowry protein assay. Protein concentration were compared to a series of BSA standards and concentration was assessed using a microplate reader (Bio-Rad, Hemel Hempsted, UK) at 720 nm absorbance. Following elucidation of protein concentrations, concentrated samples of 100 μg protein/25 μL were made for western blotting by adding 25 μL of 5X Laemmli buffer (Table 2.3) to a 100 μL volume of distilled water/cell lysate mix (depending on protein concentration) and boiling for 5 minutes using a heat block, 100 ˚C. Samples were stored at -20 °C.

2.5.2.5 SDS-PAGE and Western Analysis

This method of gel electrophoresis was originally described by Laemmli in 1970 (282). Samples were run on either 9 % or 12.5 % acrylamide gels to ensure correct resolution of target proteins for subsequent analysis. Gels were cast (Appendix 5 for gel constituents) and polymerisation of acrylamide catalysed chemically by the addition of tetramethylethylenediamine (TEMED) and ammonium persulphate (APS). Samples were run through the gel for 1 hour at 180 V. Proteins were then transferred to a membrane to enable further analysis (283). Transfer took place onto Immobilon-P polyvinylidene fluoride (PVDF) membrane (EMD Millipore, USA) using 100 V for 1 hour 30 minutes, while 'transfer sandwich' was immersed in transfer buffer (see Table 2.3 for buffers).

Buffer	Constituents
Running	192 mM Glycine 25 mM Tris 0.1 % SDS

Transfer	192 mM Glycine 25 mM Tris 20 %/v Methanol
Blocking	10 mM Tris-HCl (pH 8) 150 mM NaCl 5 % low fat milk powder
Washing (TBS-T)	10 mM Tris-HCl (pH 8) 150 mM NaCl 0.2 % Tween-20
Laemmli 5x	312.5 mM Tris-HCl (ph6.8) 50 % (v/v) Glycerol 5 % (v/v) 2-mercaptoethanol 10 % (w/v) SDS 0.01 % Bromophenol blue

Table 2.3 Buffers for Western Blot

Membranes were then blocked for 1 hour in 5 % milk/TBS-T to eliminate non-specific antibody binding. Primary antibodies (Table 2.4) were diluted in 0.05 % milk buffer (Table 2.3) before being added to membranes and incubated at 4 ˚C overnight on a rotator. Membranes were washed (3x10 minutes in TBS-T). Secondary antibody (specific for the species primary antibody was raised in) was diluted in 0.05 % milk buffer added and further incubation at room temperature occurred for 1 hour on a rotator. Membranes were washed again (3x10 minutes in TBS-T). Protein expression was determined by horseradish peroxidase (HRP) chemi-luminescence using a Luminol system (KPL, MD, USA) according to the manufacturer's protocol. X-ray films (Kodak Diagnostic Film X-Omat, Kodak, UK) were used to detect chemi-luminescence with exposure times of 2 seconds to 45 minutes depending on protein. Processing was completed using a Compact X4 Film Processor (X-ograph Imaging Systems Ltd, UK).

Primary antibody	Dilution	Species	Catalogue Number	Manufacturer

BCL-3	1:1000	Rabbit	23959-1-AP	Proteintech, Manchester, UK
BCL-3 (for mouse cells)	1:1000	Rabbit	sc-185	Santa Cruz Biotechnology, CA, USA
NF-κB1 (p105/p50)	1:200-1000	Mouse	sc-8414	Santa Cruz Biotechnology, CA, USA
NF-κB2 (p100/p52)	1:1000	Mouse	05-361	EMD Millipore, Herts, UK
RelA (p65)	1:10000	Rabbit	D14E12XP	Cell Signalling Technology, MA, USA
BCL2	1:1000	Rabbit	sc-492	Santa Cruz Biotechnology, CA, USA
BCL-XL	1:1000	Mouse	sc-509	Santa Cruz Biotechnology, CA, USA
BCL-$_W$	1:1000	Rabbit	n/a	Gift Ben Edde, UoB
MCL-1	1:2000	Rabbit	sc-819	Santa Cruz Biotechnology, CA, USA
BAK	1:500	Mouse	556382	BD Transduction Laboratories
BAX	1:1000	Rabbit	sc-493	Santa Cruz Biotechnology, CA, USA
Bim	1:1000	Rabbit	17003	Chemicon (now EMD Millipore, Herts, UK)
Puma	1:1000	Rabbit	4976	Cell Signalling Technology, MA, USA
BAD	1:1000	Rabbit	9292s	Cell Signalling Technology, MA, USA
Total AKT	1:1000	Rabbit	9272	Cell Signalling Technology, MA, USA
p-AKT (S473)	1:1000	Rabbit	4058	Cell Signalling Technology, MA, USA

Cleaved PARP	1:10000	Rabbit	AB32064	Abcam, Cambridgeshire, UK
Cleaved caspase-3	1:1000	Rabbit	9664	Cell Signalling Technology, MA, USA
α Smooth Muscle Actin (αSMA)	1:1000	Rabbit	19245	Cell Signalling Technology, MA, USA
α-Tubulin	1:10000	Mouse	T9026	Sigma-Aldrich, Dorset, UK
α-Tubulin for mouse cells	1:2000	Rabbit	2125s	Cell Signalling Technology, MA, USA

Table 2.4 Antibodies for Western Blot

2.5.3 Immunofluorescent protein analysis

2.5.3.1 Transfection and irradiation of cells on coverslips

Cells were transfected in suspension (detailed above in section 2.2.1) with 50 nM BCL-3 siRNA or control siRNA and seeded onto 18 mm^2 glass coverslips (coverslips were coated with poly-L-lysine, see below, (section 2.5.3.2)) placed into 6-well plates (Corning, NY, USA). Cells were incubated for 72 hours from onset of transfection, at this point medium was spiked with 80 µL 1 M Hepes and cells were transferred to the irradiator and 2.5 Gy γ-irradiation delivered. Fixation of cells was started at exact 30 min, 6 hr, 12 hr or 24 hr post the end of the irradiation dose.

2.5.3.2 Coating of coverslips

Poly-L-lysine (Sigma-Aldrich, Dorset, UK) was used to coat glass coverslips prior to seeding cells; to promote cell adhesion to the glass for SW1463 cells. Coverslips were immersed in 0.001 % Poly-L-Lysine solution for 1 hr after which they were washed twice in sterile filtered water and then dried ready for use.

2.5.3.3 Fixation and slide preparation

Medium was aspirated, and coverslips washed twice with ice-cold PBS. Cells were fixed and permeabilised using 4 % (w/v) paraformaldehyde containing 0.1 % Triton

X-100 (Sigma-Aldrich, Dorset, UK) for 15 min. Paraformaldehyde/Triton X-100 was removed within a fume-hood and coverslips were washed three times with PBS for 5 min/wash. Any residual formadehyde was quenched using 0.1375 M glycine for 5 min at room temperature, followed by a further PBS wash for 5 min. A solution of 1 % w/v bovine serum albumin (BSA) in PBS was used to block the coverslips for 15 min. Coverslips were then removed from wells and inverted cell-side down onto a 70 μL drop of primary antibody (Table 2.5), including separately an isotype control, diluted in 1 % BSA in PBS, which were placed on a length of Parafilm® (Sigma-Aldrich, Dorset, UK). Coverslips were incubated with primary antibody for 1 hr at room temperature, following this, coverslips were placed back into wells and three washes of 5 min with PBS completed. The coverslips were removed from the wells and inverted onto a 70 μL drop of secondary antibody (Table 2.5). Incubation with secondary antibody was for 1 hr at room temperature with coverslips by foil to limit bleaching by light. After incubation, coverslips were placed once again within the wells and a further three 5 min washes with PBS performed. On the second wash, DAPI (4',6-diamidino-2-phenylindole, Sigma-Aldrich, Dorset, UK) at 1:10000 was added to the wash and incubated with the coverslips for the duration of the wash. Coverslips remained covered from light throughout wash periods. To mount coverslips, 15 μL of Mowiol (Sigma-Aldrich, Dorset, UK) with 2.5 % 1,4diazabicyclo-[2,2,2]-octane (DABCO, Sigma-Aldrich, Dorset, UK) was placed onto a glass slide and coverslips inverted onto this. Mowiol was left to harden overnight in the dark before imaging.

Primary antibody	Dilution	Species	Catalogue Number	Manufacturer
BCL-3	1:200	Rabbit	sc-185	Santa Cruz, Biotechnology, CA, USA
BCL-3	1:100	Rabbit	23959-1-AP	Proteintech, Manchester, UK

γH2AX	1:500	Mouse	05-636	EMD Millipore, Herts, UK
Isotype control IgG	1:200 or 1:100 (as primary)	Rabbit Mouse	12-370 12-371	EMD Millipore, Herts, UK
Secondary antibody	**Dilution**	**Species**	**Catalogue Number**	**Manufacturer**
Alexa Fluor 488	1:10000	Goat anti-rabbit	A11034	Invitrogen, Thermo Fisher Scientific, MA, USA
Alexa Fluor 594	1:10000	Goat anti-mouse	A11032	Invitrogen, Thermo Fisher Scientific, MA, USA

Table 2.5 Immunofluorescence antibodies

2.5.3.4 Confocal imaging of slides

A Leica confocal microscope (Leica DMI 6000, Inverted confocal microscope, Wolfson Imaging Suite, University of Bristol) was used to obtain images at 40x and 63x magnification. Care was taken to ensure that observed fluorescence was a true reading and not background signal. IgG isotype control primary antibodies were used that lacked specificity to the target but matched the class, species and concentration of the target. Furthermore, BCL-3 suppression using siRNA was used to determine the correct signal for BCL-3, following optimisation of the lazar intensity with IgG control fluorescence. By ensuring that there was no significant fluorescence within the IgG controls, calibration of the laser intensity for the BCL-3 signal was possible. γH2AX foci were counted manually and an average number of foci/nucleus for each condition was obtained.

2.5.4 Chromatin Immunoprecipitation (ChIP)

2.5.4.1 Chromatin crosslinking, fixation, lysis and sonication

Cells were medium changed 24 hr prior to being fixed when between 60-80 % confluent. If transfected, cells were fixed at 72 hr post initiation of transfection. To fix, media was aspirated from cells and washed once with 4 mL room temperature

PBS. Cells were then incubated at room temperature for 10 min with fresh 1 % formaldehyde (CH_2O) (Pierce™ 16 % formaldehyde (w/v), 1 mL in 15 mL PBS. Thermo Fisher Scientific, MA, USA). CH_2O was removed into a waste jar and the unreacted CH_2O was quenched with glycine to stop further cross-linking. Quenching was performed with 5 mL of 0.1375 M glycine per flask and cells incubated at room temperature for 5 min. Flasks were then placed on ice and the cells washed twice with 5 mL/flask of ice-cold PBS. All residual PBS was removed and 500 µL of cold cytoplasmic lysis buffer (Table 2.6) was added to each flask. Cells were scrapped and recovered into a 1.5 mL Eppendorf tube and incubated on ice for 10 min with brief vortexing twice. Lysates were centrifuged at 700 g for 5 min at 4 °C and the supernatant (cytoplasmic fraction) aspirated and discarded into a waste pot. The pellet was suspended in a further 500 µL of cold cytoplasmic lysis buffer and then centrifuged again at 700 g for 5 min at 4 °C. Following aspiration and discarding of the supernatant (residual cytoplasmic fraction) without disturbing the nuclear fraction pellet, the pellet was suspended in 500 µL of room temperature nuclear lysis buffer (Table 2.6) and incubated on ice for 10 min. Lysates were transferred to a sonicator (Diagenode Bioruptor, Belgium) and sonicated for 30 sec for between 15-20 cycles in iced-water. Sheared chromatin was checked to ensure sonication had resulted in a smear around a DNA 500bp marker (Promega, USA) as visualised on a 1.5 % agarose gel.

2 µL per condition of sheared chromatin was added to 45 µL CSTLB (Table 2.6) and incubated with 1 µL RNase A (10 mg/mL) (EMD Millipore, Herts, UK) at 37 °C for 30 min. Following this 1 µL Proteinase K (10 mg/mL) (Sigma-Aldrich, Dorset, UK) was added and a further incubation for 2 hr at 62 °C completed. 5x Orange G (Sigma-Aldrich, Dorset, UK) was added to samples at a 1:5 ratio and the sonicated samples run with a 100 bp DNA marker (Promega, WI, USA) alongside

unsonicated samples on a 1.5 % agarose gel. After confirmation of chromatin shearing efficiency samples could be stored at -80 °C.

ChIP Buffers	Constituents
Cytoplasmic Lysis Buffer	10 % Glycerol 10 mM Tris-HCl pH8 1.5 mM $MgCl_2$ 0.5 % NP-40 1xProtease Inhibitor Cocktail Tablet/10 mL
Nuclear Lysis Buffer	1 % SDS 50 mM Tris- HCl pH8 10 mM EDTA 1xProtease Inhibitor Cocktail Tablet/10 mL
CST Lysis Buffer (CSTLB) **used as Dilution Buffer**	1xCell Signalling Technology lysis buffer (see above) 20mM Tris-HCl pH7.5 150 mM NaCl 1 mM Na_2EDTA 1 mM EGTA 1 %Triton 1xProtease Inhibitor Cocktail Tablet/10 mL
Elution Buffer	1 % SDS 50 mM Tris- HCl pH8 10 mM EDTA
Wash Buffer 1	0.1 % SDS 0.1 % deoxycholate 1 % Triton X-100 0.15 M NaCl 1 mM EDTA 0.5 mM EGTA 20 mM HEPES pH 7.6
Wash Buffer 2	0.1 % SDS 0.1 % deoxycholate 1 % Triton X-100

	0.5 M NaCl 1 mM EDTA 0.5 mM EGTA 20 mM HEPES pH 7.6
Wash Buffer 3	0.25 M LiCl 0.5 % sodium deoxycholate 0.5 % NP-40 1 mM EDTA 0.5 mM EGTA 20 mM HEPES pH 7.6
Wash Buffer 4	1 mM EDTA 0.5 mM EGTA 20 mM HEPES pH 7.6
TAEx50	**2 M Tris acetate** 100 mM Na_2EDTA Mixed 1:50 with ddH_2O before use

Table 2.6 ChIP buffers

2.5.4.2 Immunoprecipitation of chromatin

Samples were, thawed on ice, then centrifuged at 14000 g for 15 min to pellet any insoluble material and precipitated SDS. Supernatant was transferred to a fresh Eppendorf tube. Using a NanoDrop (Thermo Fisher Scientific, MA, USA) spectrophotometer, DNA concentration was measured (A_{260}) against the nuclear lysis buffer devoid of SDS as a blank. DNA is thought to be 'pure' if the A_{260}:A_{280} ratio was above 1.6. Sample concentrations were equalised by diluting the more concentrated sample to the concentration of the weaker sample using nuclear lysis buffer, devoid of SDS.

Antibody	Amount (stock concentration)	Species	Catalogue Number	Manufacturer
BCL-3	3 µg (200 µg/mL)	Rabbit	sc-185	Santa Cruz, Biotechnology, CA, USA
BCL-3	3 µg (48 µg/150 µL)	Rabbit	23959-1-AP	Proteintech, Manchester, UK
IgG	3 µg (1 µg/µL)	Rabbit Mouse	12-370 12-371	EMD Millipore, MA, USA
Acetylated H3	1 µL (1 µg/µL)	Rabbit	06-599B	EMD Millipore, MA, USA
Ser5 RNA Polymerase II	2 µL (0.7 µg/µL)	Rabbit	AB5131	Abcam, Cambridgeshire, UK
NF-κB2/p52	3 µg (1 µg/µL)	Mouse	05-361	EMD Millipore, MA, USA

Table 2.7 ChIP antibodies

25 µg of chromatin for each antibody to be used for ChIP was transferred to a fresh Eppendorf tube and diluted to a total volume of 500 µL with CSTLB (Table 2.6). Each sample was pre-cleared with 1 µg species specific IgG antibody (EMD Millipore, Herts, UK) and 5 µL of Protein A or G beads (A – Rabbit, G - Mouse) (Dynabeads®, Thermo Fisher Scientific, MA, USA) and incubated for 3 hr on a rotator at 4 °C. After this time, the samples were briefly centrifuged and placed onto a magnetic rack on ice (Dynamag-2 magnetic particle concentrator, Thermo Fisher Scientific, MA, USA). After 30 sec, the chromatin was retrieved into a new Eppendorf tube. 5 µL of chromatin was salvaged from each experimental condition to be processed later as the input sample. 1-5 µg of primary antibody (Table 2.7) was added to the chromatin and rotated in the cold room at 4 °C overnight. The following day, 20 µL of Protein A or G beads were added to each Eppendorf tube and incubated on a rotator for 3 hr. Samples were retrieved and briefly centrifuged before being placed on the magnetic rack on ice. After 30 sec, the liquid was removed from each Eppendorf tube and discarded. Sequential washes of the Dynabeads were then performed using the ChIP wash buffers (Table 2.6). Each

wash was followed by a 5 min rotation at 4 °C before Eppendorf tubes were placed back onto the magnetic rack on ice. Washes were 2x Buffer 1, 1x Buffer 2, 1x Buffer 3 and 2x Buffer 4. After the final incubation of 5 min, samples were transferred to new Eppendorf tubes and the liquid was discarded. At room temperature, 100 µL of elution buffer was added to each Eppendorf tube containing beads and incubated at 65 °C for no longer than 16 hr (typically around 12-14 hr) to reverse CH_2O cross-linking. This was followed by a treatment with 1 µL RNase A at 37 °C for 30 min and then with 1 µL proteinase K at 55 °C for 2 hr. Both incubations were performed on a shaking heated incubator (Accutherm™, Labnet International, NJ, USA) at 1200 rpm, which maintained the Dynabeads in solution. Samples were then cooled to room temperature before a DNA clean-up step.

2.5.4.3 DNA clean-up

The QIAquick PCR purification kit (Qiagen, Germany) was used to clean DNA ready for PCR as per manufacturer's instructions. Samples were placed onto spin columns after pH had been corrected using 3 µL of 3 M sodium acetate, to a pH<7.5. Samples were centrifuged for 1 min at 13000 rpm and the flow-through discarded. A further wash was performed, and samples centrifuged again for 1 min at 13000 rpm. DNA was eluted from membranes and stored at -20 °C.

2.5.4.4 PCR and agarose gel electrophoresis

Immunoprecipitated chromatin was analysed using end-point PCR, as well as qRT-PCR. PCR was carried out using primers (

Primer set name	Forward	Reverse
BCL2L11(1)	GGGAGGCTAGGGTACACTTC	CAGGCTCGGACAGGTAAAGG

BCL2L11(1b)	GAGCGGGAGGCTAGGGTA	AGGCTCGGACAGGTAAAGG
BCL2L11(2)	CGGGTTGGGGTAGGTGAG	TGGCGTGTTTACCGGAGTA
BCL-3	GGGAGAGAACCAGAGAGACG	GTTGAGTCCGGGTCACTGAG
GAPDH	TCGAACAGGAGGAGCAGAGAGCGA	TACTAGCGGTTTTACGGGCG
Bimoff	GAGGTGGTGGGGAGAAATGA	TTCCAGCCCCTTTCCCTAAG

Table 2.8) designed in the lab (with kind

Table 2.8 ChIP primers

Primer set name	Forward	Reverse
BCL2L11(1)	GGGAGGCTAGGGTACACTTC	CAGGCTCGGACAGGTAAAGG
BCL2L11(1b)	GAGCGGGAGGCTAGGGTA	AGGCTCGGACAGGTAAAGG
BCL2L11(2)	CGGGTTGGGGTAGGTGAG	TGGCGTGTTTACCGGAGTA
BCL-3	GGGAGAGAACCAGAGAGACG	GTTGAGTCCGGGTCACTGAG
GAPDH	TCGAACAGGAGGAGCAGAGAGCGA	TACTAGCGGTTTTACGGGCG
Bimoff	GAGGTGGTGGGGAGAAATGA	TTCCAGCCCCTTTCCCTAAG

help from Dr. A Greenhough), to genomic DNA, using online software, the UCSC genome browser and Primer3 (284, 285). For end-point PCR, a 50 µL reaction mix was made per ChIP sample; consisting of 25 µL Promega Master Mix (Promega, WI, USA), 2 µL primer pair, 1 µL ChIP sample or ddH_2O control, 21 µL ddH_2O and 0.5 µL DMSO (additive to reduce primer dimerization) (Sigma-Aldrich, Dorset, UK).

The touchdown PCR (TD-PCR, Table 2.9 (286)) programme was used to amplify DNA templates, after which 5x Orange G (Sigma, UK) was added in a 1:4 ratio. Samples were run alongside DNA markers on an 1-2 % ethidium bromide (Bio-rad, UK) agarose (Geneflow, National Diagnostics, UK) gel (1-2 % in 1xTAE) for 40 min at 200 V and imaged using a UV light box. For qRT-PCR, a standard protocol (Methods 2.5.1.3) was used but immunoprecipitated chromatin used, in place of cDNA with the primers designed for use with genomic DNA (

Table 2.8). For one reaction mix 12.5 µL SYBR Green (Qiagen, Germany), 10 µL

Primer set name	Forward	Reverse
BCL2L11(1)	GGGAGGCTAGGGTACACTTC	CAGGCTCGGACAGGTAAAGG
BCL2L11(1b)	GAGCGGGAGGCTAGGGTA	AGGCTCGGACAGGTAAAGG
BCL2L11(2)	CGGGTTGGGGTAGGTGAG	TGGCGTGTTTACCGGAGTA
BCL-3	GGGAGAGAACCAGAGAGACG	GTTGAGTCCGGGTCACTGAG
GAPDH	TCGAACAGGAGGAGCAGAGAGCGA	TACTAGCGGTTTTACGGGCG
Bimoff	GAGGTGGTGGGGAGAAATGA	TTCCAGCCCCTTTCCCTAAG

ddH_2O, 1 µL primer pair and 1.5 µL ChIP sample was used. Results were compared to IgG control to ascertain fold-change in DNA abundance between conditions. Additionally, as with end-point, PCR samples were mixed 4:1 with Orange G and run on an agarose gel, as above, to check for primer-dimerisation. Gels were visualised on a UV light-

Step	Time	Temperature (°C)	Cycles
Activation	2 min	95	35 cycles, annealing temperature decreases every 4 cycles
Denaturation	25 sec	94	
Annealing	35 sec	64 decreasing to 55	

box.

Extension	35 sec	72	
End	10 min	72	-

Table 2.9 Touchdown PCR programme, TD-PCR

2.6 Data Analysis

Data including statistical analysis was performed in the Graphpad Prism 7 software. Parametric data was represented as means and standard deviations (SD) analysed with either a Student's t-test or for multiple means an ANOVA. Non-parametric data represented as medians and interquartile range (IQR) and was analysed with a Wilcoxon Signed Rank test or for multiple conditions a Kruskall Wallis test. Spheroid population data was noted to be log normally distributed and was summarised as medians (IQR) and analysed with Kruskall Wallis. The number of γH2AX foci/nuclei are known to be Poisson distributed (287) and summarised as mean (SD).

Leica Application Suite Lite (Leica, USA) software was used to analyse image data alongside the MATLAB software for automated image analysis.

Adobe Photoshop 6 (Adobe, USA) was used to create all figures.

3 Results 1: BCL-3 promotes cell-survival in colorectal tumour cells through supressing the BCL2 family, BH3-only pro-apoptosis protein Bim

3.1 Introduction

Elimination of old or damaged cells is a critical component of development, homeostasis and disease (288). Cellular elimination is controlled principally by a process known as apoptosis, or programmed cell death (289). Initially described as individual cell separation, condensation, fragmentation and phagocytosis (289), apoptosis was subsequently found to be a highly regulated process (290); whilst also having a basic mechanism that is evolutionarily conserved (291). Apoptosis is split into two main pathways, the intrinsic and extrinsic apoptotic pathways (292). Evasion of apoptosis is well recognised as a major component of tumour development and therapy resistance in cancer; and is one of the original 'hallmarks of cancer' (224).

3.1.1 Apoptosis

The intrinsic pathway is mediated by mitochondria and is initiated by diverse cytotoxic stimuli such as DNA damage, growth-factor deprivation or viral infection (293). Activation of this pathway leads to mitochondrial outer membrane permeability (MOMP), which allows release of factors such as cytochrome c, but also Smac/DIABLO, apoptosis-inducing factor (AIF) and procaspases from the intermembrane space (294, 295). On release from mitochondria, cytochrome c binds to Apaf-1 leading to activation of the caspase cascade and cell death. Caspases are proteolytic, cysteinyl aspartate enzymes, stored in the cytoplasm as zymogens (inactive pro-forms of the enzyme). The release of cytochrome c, in the intrinsic pathway, allows the dATP/ATP dependent binding of procaspase-9 to the Caspase Recruitment Domain (CARD) of apoptotic protease-activating factor-1 (Apaf-1) to form the apoptosome (296). Binding of procaspase-9 to Apaf-1 cleaves caspase-9 which in turn cleaves other members of the caspase family (caspase-3 and caspase-8) setting off the cleavage cascade. Initially, cleaved caspase-9 activates procaspase-3 by cleaving it at the Asp175 residue forming intermediate

cleavage products which are subsequently auto-cleaved at the Asp25 residue, by active caspase-3. This auto-cleavage results in a powerful amplification of the apoptotic signal and means the cell is unable to escape from the apoptotic cascade. As an effector caspase, cleaved caspase-3 then proteolytically degrades numerous proteins (such as poly ADP ribose polymerase (PARP), inhibitor of caspase-activated DNase (ICAD) and structural proteins) within the cell resulting in the apoptotic phenotype observed by Kerr et al published in 1972. These events are tightly controlled by the balance of pro-survival and pro-apoptotic members of the BCL-2 family. This family of proteins consists of over 20 related members that share BCL-2 Homology (BH) domains (288) and have been classically subdivided into 3 classes.

3.1.2 The BCL-2 protein family

BCL-2 with its related members, are critically important in apoptosis as upstream, negative regulators of cytochrome c release and its downstream effects of caspase-3 cleavage (297). The pro-survival members BCL-2, BCL-w, BCL-x_L, MCL-1 and A1, share three or four BH domains (293). Of these, the BH1, BH2 and BH3 domains form a hydrophobic groove on the surface of pro-survival BCL-2 members that is able to bind the BH3 domain of Bax and Bak, preventing their activation; furthermore, the groove can bind the BH3-only domains of the BH3-only class (298). The Bax family (Bax/Bak) of multi-BH domain proteins (1-3 BH domains) (299) reside on mitochondrial membrane or in the cytoplasm and upon activation, form pores that enable permeabilisation of the mitochondrial outer membrane, which allows the release of cytochrome c (discussed above) (300).

There is controversy about how BCL-2 family of proteins function to inhibit apoptosis, with two main models; the direct (301) and the indirect (302) activation models. In the direct activation model BH3-only proteins (Bim, Bid (301) and purportedly Puma (303)) interact directly with Bax/Bak leading to their

oligomerisation and MOMP. Other BH3-only proteins do bind Bax/Bak directly but this results in abrogation of binding with pro-survival BCL-2-like proteins. The indirect model suggests that BH3-only members act to antagonise pro-survival BCL-2-like proteins and inhibit their function; in the case of 'sensitizer' BH3-only proteins this allows the release of 'activator' BH3-only members like Bim and Bid from BCL-2-like members enabling them to bind directly to Bax/Bak (304). Importantly, work has shown that both models are necessary for full apoptotic activity of the BH3-only proteins, in particular Bim (305). Binding results in neutralisation of the BCL-2-like family and activation of Bax or Bak. In addition to this, the BH3-only proteins are recognised to have specific binding affinities for each of the pro-survival BCL-2 members, highlighting some degree of context dependency (300, 302, 304).

3.1.3 BCL2 interacting mediator of cell death (Bim)

The pro-apoptotic BH3-only family of proteins are united by the solitary inclusion of a BH3 domain in the protein and include the members Bim, Bid, Puma, Noxa, Bad and Bik. The BH3-only protein Bim is thought to be one of the more important and potent of the family members (306). Bim, or BCL-2 interacting mediator of cell death, has three commonly recognised isoforms (Bim^{EL}, Bim^{L} and Bim^{S}). Bim is a promiscuous binding partner for all the BCL-2-like anti-apoptotic family members; highlighting the important functional role Bim plays in apoptosis from many different signals, as well as the potency of Bim (302, 305).

Critical to Bim function is the BH3 domain. Bim indirectly activates Bax by binding to and inhibiting the pro-survival BCL2 proteins (BCL-2, BCL-w or BCL-$_{XL}$). It does this by utilising the BH3 domain, present in all three Bim isoforms to interact with the hydrophobic groove that is central to the pro-survival proteins' function (306), as Bim with mutated BH3 domains were unable to bind this groove (307). Alongside Bim's role as an indirect activator of Bax, (as well as truncated Bid, (tBid), which

enables crosstalk between the extrinsic and intrinsic mitochondrial apoptosis pathways (290)) it functions as a direct activator of Bax (299, 305), inducing conformational change in Bax and its oligomerisation.

Bim expression and function is regulated by a number of different mechanisms including transcriptionally, post-translational modification and protein sequestration. Early studies of Bim showed it to be predominantly localised to intracytoplasmic membranes, independent of Bim association with BCL2 (306). Later data, highlighted that it is Bim^{EL} and Bim^{L} which bind to dynein light chain 1 (DLC1), leading to the suppression of Bim apoptotic activity (308). Furthermore, the sequestration of Bim, with DLC1, is dependent on phosphorylation of Bim, as phosphorylation by JNK on threonine 56 counteracts this interaction, leading to release of Bim from DLC1 and its functional activation (309).

Additional phosphorylation events also control Bim degradation and therefore apoptotic function (310). Bim is principally a target of activated ERK, but also AKT kinases, both of which lead to Bim phosphorylation, subsequent ubiquitination and proteosomal degradation. In colorectal tumours with BRAF mutations, Bim is repressed through phosphorylation by constitutively active ERK1/2 and is subsequently degraded (311). Moreover, suppression of Bim by PGE_2 in early colorectal tumours (a subset have upregulated by COX2) is also thought to be through ERK1/2 signalling (312). Moreover, inactivation of ERK1/2 by upstream action of a protein phosphatase on MAPK, induces Bim leading to apoptosis (313). Bim^{EL} is also phosphorylated on serine 87 by AKT leading to its degradation (314). Importantly, de-phosphorylation of these sites by protein phosphatase 2A is a potent apoptotic mechanism in endoplasmic reticulum (ER) stress (315) but, additionally, could play a role in general protein regulation.

Bim is also tightly controlled at the transcriptional level and is primarily regulated by FoxO1 (316) and FoxO3a (317-320) as part of the AKT signalling pathway. In

this pathway, phosphorylated AKT (activated) phosphorylates FoxO1 or FoxO3a leading to their nuclear to cytoplasmic translocation and silencing of the transcriptional function of these proteins. Other transcription factors that are thought to regulate Bim include E2F1 as part of the Rb pathway (321) and CHOP-C/EBPα following ER stress (315).

3.1.4 Aims

BCL-3 nuclear expression in colorectal tumours has been shown to confer a worse prognosis for patients (240). Additionally, in-vitro data from this group has identified BCL-3 to be a survival factor in colon cancer cells (257) as discussed in the introduction (Section 1.6.8). There is however limited data on if and how BCL-3 regulates the apoptosis pathway directly in rectal cancer cells. The aim of this work was to establish whether BCL-3 protected rectal cancer cells from undergoing apoptosis and the potential mechanism involved.

3.2 Results

3.2.1 BCL-3 expression in rectal cancer cell lines

To establish the validity of the BCL-3 antibody and expression of BCL-3 in rectal cancer cells compared to colon cancer cells and adenoma cells, BCL-3 expression was analysed in a panel of cells (Methods 2.1.1). It was important to determine expression of BCL-3 in rectal cancer cells compared to adenoma or colon cells firstly to identify if BCL-3 is expressed in rectal cancer cells and to identify which cell lines to use for future experiments. BCL-3 was detected using western blotting, which identified the characteristic smear of BCL-3 protein, at around 55 kDa, that results from its multiple post-translational modifications, particularly phosphorylation (203). Western blot identified that SW837 were a low expressing rectal cancer cell line while SW1463 were high BCL-3 expressers (Figure 3.1).

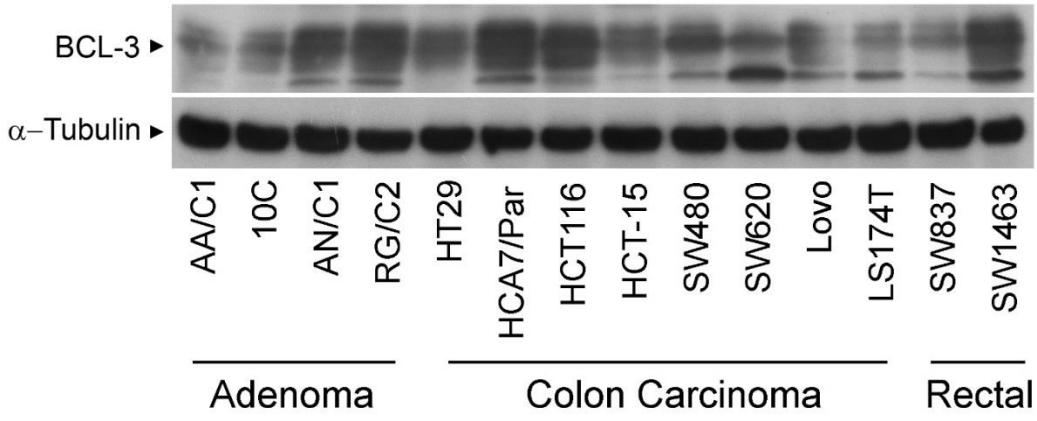

Figure 3.1 Expression of BCL-3 in rectal cancer derived cell lines in comparison to a panel of colon carcinoma and adenoma derived cell lines.

Western blot analysis was used to compare BCL-3 expression in two rectal cancer cell lines SW837 and SW1463 to a panel of colon adenoma and carcinoma cell lines. Validation of protein concentration assay and equal loading was confirmed with α-Tubulin.

3.2.2 BCL-3 suppression increases levels of floating cells in colorectal tumour cells with high expression of BCL-3

Previous work from this group supports the published view that BCL-3 is a pro-survival, oncogene in colon cancer and other solid malignancies (257, 322). Additionally, previous work by this group has shown that the shed or floating cell fraction is predominantly apoptotic in colorectal cancer cell lines (Methods 2.3.1). BCL-3 was suppressed to determine whether altered cell survival in rectal cancer cells (SW837 and SW1463) compared to control high BCL-3 expressing cells (HCA7/P and LS174T). To suppress BCL-3 cells were transfected with siRNA (50nM, Sequence A) (257). Cell counts of adherent and floating cells were performed (Figure 3.2) and the percentage of floating cells calculated as a percentage of the total adherent cells per flask. Results showed that numbers of floating cells increased at 48 and 72 hours in three out of four of the cell lines, with statistical significance achieved in the SW1463, HCA7/Par and LS174T cell lines at 72 hr and at 48 hr in the HCA7/Par and LS174T cell lines. In the low BCL-3 expressing SW837 cell line, BCL-3 suppression failed to increase floating cell numbers at either time point. Protein was harvested to analyse the efficiency of BCL-3 knockdown with siRNA for each experiment. Western analysis confirmed BCL-3 knockdown in all cell lines at 48 and 72 hr. These data confirmed that in high BCL-3 expressing rectal cancer cells and colon cancer cells, suppression of BCL-3 increases cell death as measured by proportion of shed floating cells.

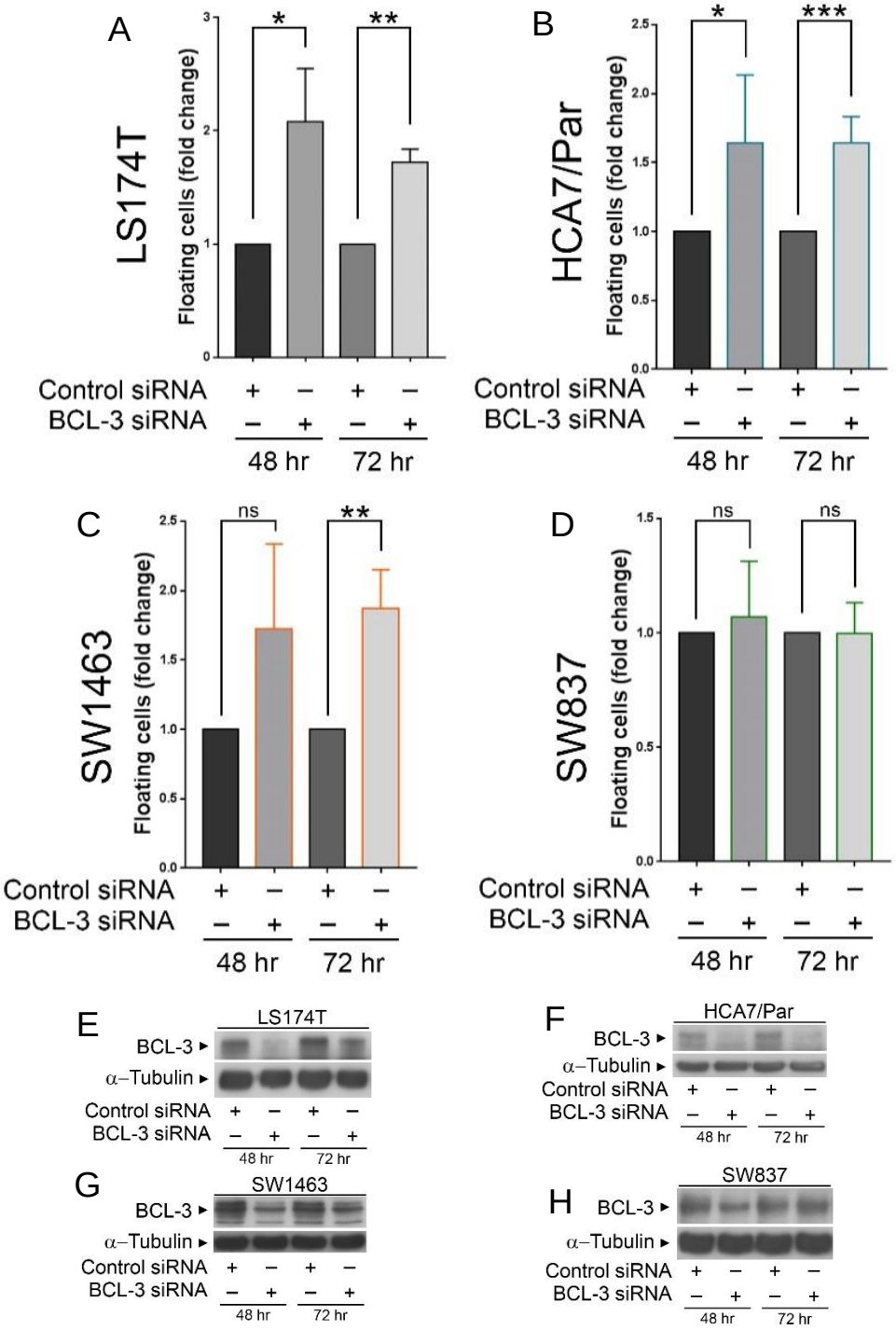

Figure 3.2 Suppression of BCL-3 increases cell death in rectal and colon cancer cells

BCL-3 was suppressed in colon (LS174T (A), HCA7/P (B)) and rectal cancer cells (SW1463 (C), and SW837 (D)) with siRNA. At 48 and 72 hours following transfection adherent and floating cells were counted. Results showed there was significant increases in floating cell numbers, predominantly at the 72 hour time-point, following BCL-3 knockdown except in the SW837 cell line (D), which are a low BCL-3 expressing cell line. BCL-3 knockdown was verified using western blot (E-H). Graphs show combined data from 3 independent experiments (mean and standard deviation (SD)). Statistical analysis was performed on GraphPad Prism 7 software using a Student's T-Test (* :P<0.05, ** : P<0.01, *** : P<0.001, NS : non-significant).

3.2.3 BCL-3 suppression increases expression of the markers of intrinsic apoptosis

Dying cells undergo a undergo a cascade of events leading to cell death via a number of mechanisms including apoptosis (programmed cell death). Molecular markers can be utilised to determine the mechanism of apoptotic death. To validate that the increase in floating cells was as a result of increased apoptosis in cells with suppressed BCL-3. Whole flask lysates (WFL; the combined population of adherent and floating cells, methods 2.5.2.2) were harvested and western analysis used to probe for molecular markers of apoptosis, cleaved caspase-3 (Intrinsic apoptosis (296)) and cleaved PARP (specific cleavage product of apoptosis (323) (Figure 3.3). BCL-3 was knocked down using siRNA in LS174T, SW1463 and HCA7/P cells, which had shown statistically significant fold increases in floating cells previously. WFL was collected at 48 hr following transfection. Results showed that BCL-3 suppression increased levels of cleaved caspase-3 and cleaved PARP suggesting induction of intrinsic apoptosis. Interestingly, LS174T (Figure 3.3 C) carcinoma cells have very low levels of basal apoptosis and this was mirrored with relatively lower levels of cleaved-PARP and cleaved caspase-3 compared to the other cell lines analysed. Cleaved-PARP was chosen as a more robust marker of apoptosis induction in these colon and rectal cancer cell lines for future experiments. These results suggest that suppression of BCL-3 increases apoptosis in both rectal and colon cancer cell lines.

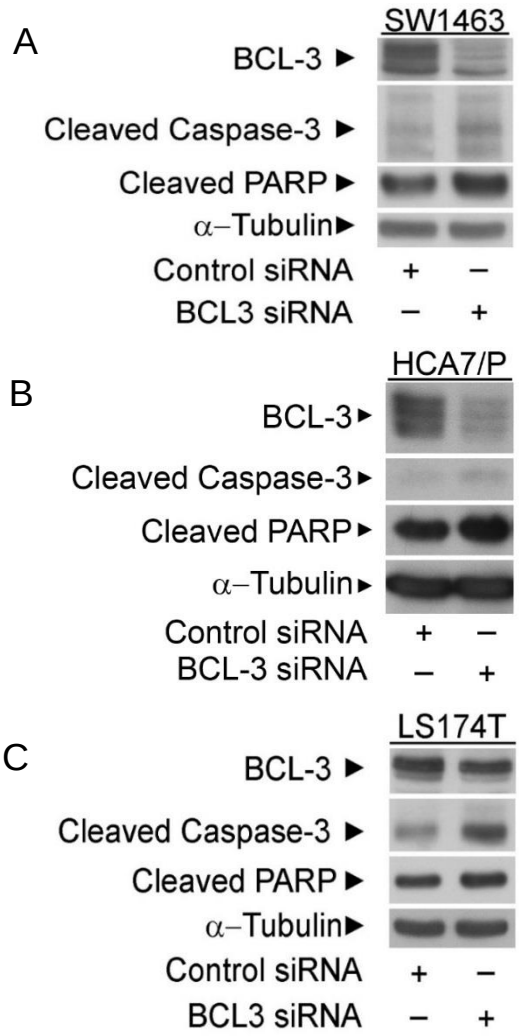

Figure 3.3 BCL-3 suppression using siRNA induces increased cleavage of markers of intrinsic apoptosis: cleaved caspase-3 and cleaved PARP.

SW1463 (A), HCA7/P (B) and LS174T (C) colorectal cancer cells were transfected with BCL-3 siRNA or Control siRNA. At 48 hours from transfection attached and floating cells were pooled to create WFL. Markers of apoptosis (Cleaved Caspase-3 and Cleaved PARP) were detected using western blot. Results showed BCL-3 suppression increased the induction of cleaved caspase-3 and cleaved PARP suggesting the induction of intrinsic apoptosis on BCL-3 suppression. Exemplary data of n=3 experiments.

3.2.4 Apoptosis induced by BCL-3 suppression can be blocked using QVD (pan caspase inhibitor)

The pan-caspase inhibitor quinolyl-valyl-O-methylaspartyl-[-2,6-difluorophenoxy]-methyl ketone (Q-VD-OPh or QVD) blocks the cleavage of caspases, which blocks the downstream effects of MOMP and inhibits apoptosis (324). To confirm that increases in floating cells and expression of markers of apoptosis following BCL-3 suppression was through induction of apoptosis, QVD was used to inhibit this process. Colorectal cancer cells, SW1463, HCA7/P and LS174T were transfected with BCL-3 siRNA or control siRNA (50 nM). 24 hr following transfection QVD (10 μM) was added to inhibit apoptosis induced by BCL-3 knockdown (Methods 2.4.1). Cell counts were performed 72 hr following transfection, to measure adherent and floating cells. It was observed, that while the number of floating cells increased following BCL-3 knockdown, this was abrogated by treatment with QVD (Figure 3.4). Furthermore, western blots of whole flask lysates showed upregulation of cleaved caspase-3 and cleaved PARP, which was almost completely abrogated with QVD treatment. Taken together, these data show that BCL-3 suppression increases levels of apoptosis in both colon and rectal tumour cells with high basal levels of BCL-3 expression.

Interestingly it was noted that when samples were treated with QVD a further band, recognised by cleaved caspase-3 antibody, appeared on the immunoblot. This band was at the 20kDa marker, which could be an intermediate caspase-3 cleavage product (Figure 3.4). When caspase-3 is cleaved initially by the apoptosome, this is carried out by caspase-9 leading to a p20 product that is further cleaved to the final fully active caspase-3 by auto-cleavage (303). This observation suggests that QVD blocks this auto-cleavage leading to a build-up of the 20 kDa band on western blot.

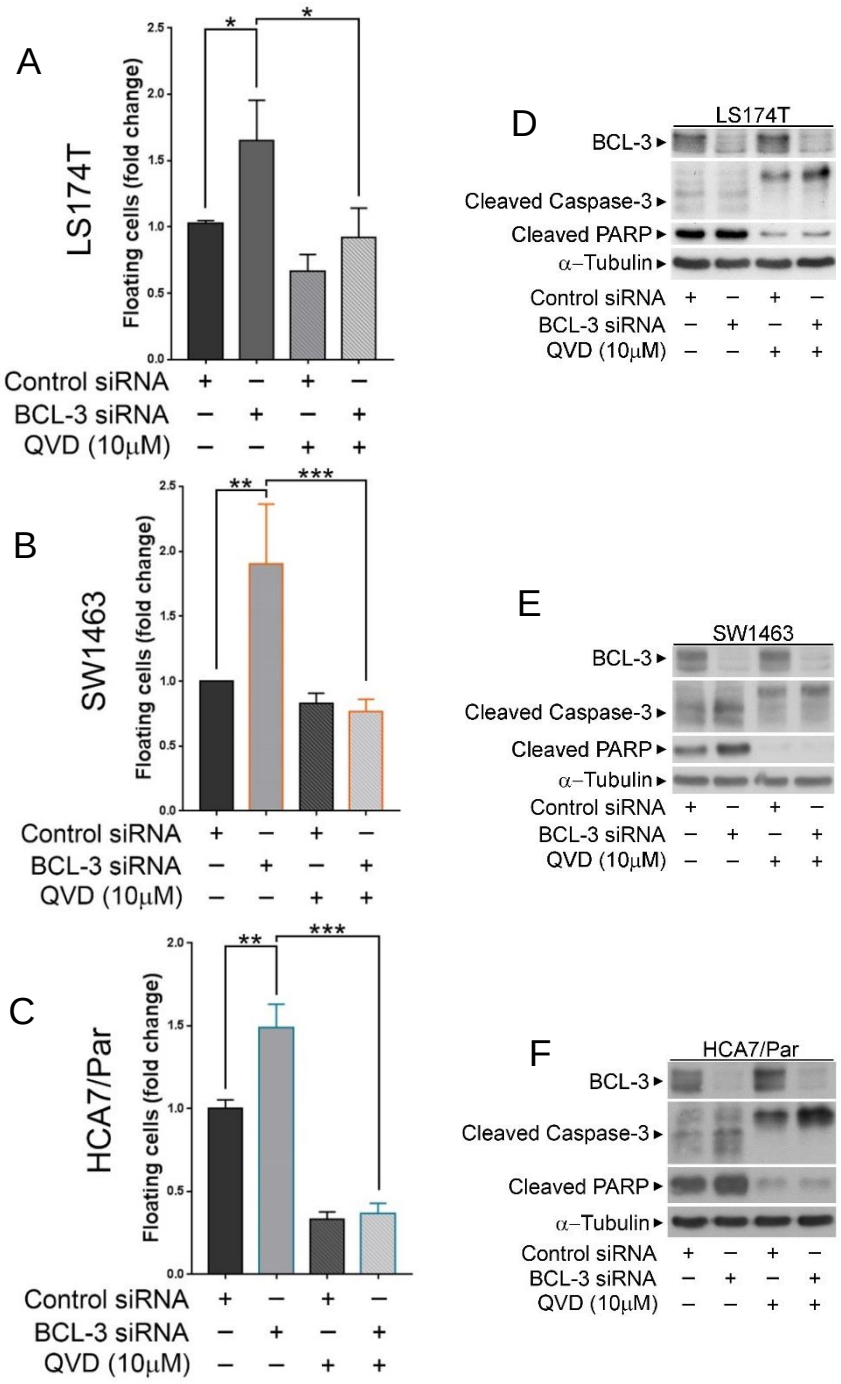

Figure 3.4 The pan-caspase inhibitor QVD blocks BCL-3 suppression induced apoptosis.

LS174T (A), SW1463 (B) and HCA7/Par (C) cells were transfected with BCL-3 or control siRNA and treated with QVD (10 μM) or vehicle control at 24 hr. Adherent and floating cells were counted. Protein lysates were collected for adherent cells (Whole Cell Lysate, WCL) and pooled adherent and floating cells (Whole Flask Lysate, WFL). BCL-3 suppression increased proportions of floating cells, which was abrogated by treating cells with QVD (A-C). Western analysis confirmed induction of molecular markers of apoptosis, which was blocked by treatment with QVD. Counting experiments shown are the combined data from 3 independent experiments (mean and SD) (A-C). Western blots shown are exemplar blots from n=3 experiments (D-F). Statistical analysis was performed on GraphPad Prism 7 software using a Student's T-Test (* :P<0.05, ** : P<0.01, *** : P<0.001, NS : non-significant).

3.2.5 BCL-3 regulates Bim a pro-apoptotic member of the BCL2 family

The BCL2 protein family are important regulators of apoptosis (325). The canonical NF-κB pathway regulates BCL-x_L a pro-survival member of the BCL2 family of proteins (326). Although, the role of BCL-3 as a regulator of the BCL2 protein family is unknown in colorectal tumour cells. Therefore, to determine whether apoptosis seen with BCL-3 knockdown a panel of BCL-2 proteins was analysed. (Figure 3.5). These included members from all three classes of the BCL-2 family of proteins. The three colorectal cell lines LS174T, SW1463 and HCA7/P, where apoptosis induction had been observed, were transfected in suspension with BCL-3 siRNA (50nM Sequence A, Methods 2.2.1). Whole cell lysates were obtained at 48 and 72 hours following transfection. Results showed that the pro-apoptotic, BH3-only protein Bim was regulated, with BCL-3 suppression inducing Bim levels in all three carcinoma cell lines at both time-points (Figure 3.5 A-C). Moreover, it appeared that all three isoforms (Bim^{EL}, Bim^{L} and Bim^{S}, formed by alternative splicing (327)) were upregulated by BCL-3 suppression, suggesting that BCL-3 may be regulating Bim at the transcriptional level. Interestingly, the protein panel also revealed that in two of the cell lines (SW1463 and LS174T (Figure 3.5 A&B)) there was downregulation of BCL-w, a pro-survival member of the BCL-2-like family, with no clear regulation in HCA7/P (Figure 3.5 C). Other noted protein regulation, was of the pro-survival BCL-2-like protein MCL-1. It appeared that MCL-1 was up-regulated at the 48 hr time-point with BCL-3 suppression. Furthermore, it was confirmed that the LS174T cell line did not have Bax expression as a result of mutation (Figure 3.5 B). The Bax gene is known to contain microsatellite repeats which leave it susceptible to mutation in tumours with deficient mismatch repair (MMR) (264, 328).

These data suggest that BCL-3 suppression may be leading to apoptosis through upregulation of the pro-apoptotic BH3-only protein, Bim rather than through other members of the BCL2 family. Bim can sequester and inhibit the majority of the pro-survival members of BCL2 proteins as well as binding directly to activate the pro-apoptotic proteins BAX and BAK, making Bim a critical regulator of apoptosis.

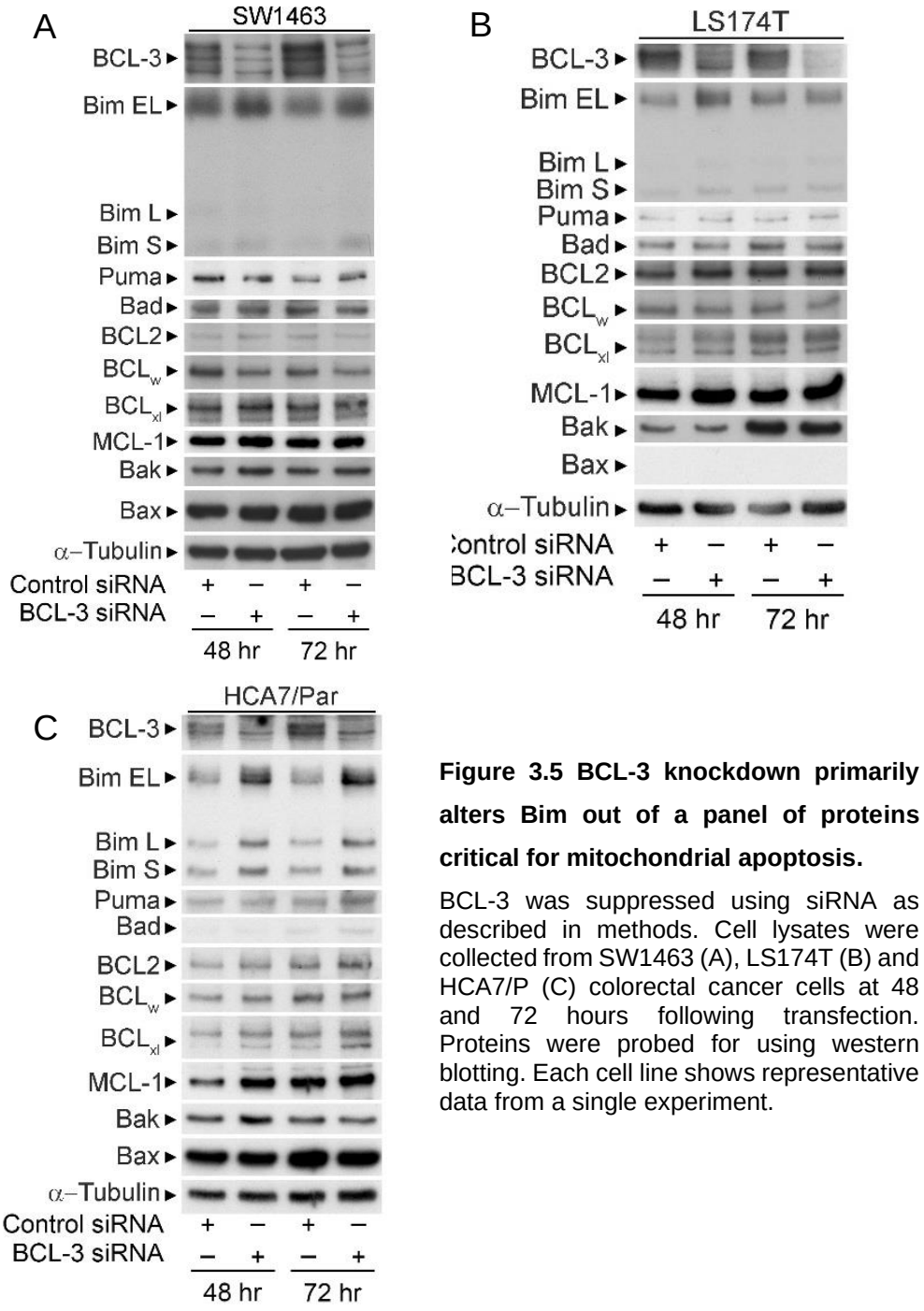

Figure 3.5 BCL-3 knockdown primarily alters Bim out of a panel of proteins critical for mitochondrial apoptosis.

BCL-3 was suppressed using siRNA as described in methods. Cell lysates were collected from SW1463 (A), LS174T (B) and HCA7/P (C) colorectal cancer cells at 48 and 72 hours following transfection. Proteins were probed for using western blotting. Each cell line shows representative data from a single experiment.

3.2.6 Validation that Bim is regulated by BCL-3

It was important to ensure that the observed effect of BCL-3 suppression on Bim protein expression was not as a result of off-target effects from a single siRNA sequence (sequence A). Gene suppression using short interfering RNA or siRNA takes advantage of conserved mechanisms of gene regulation and defence against external RNA (329). siRNA functions to degrade target mRNA following transcript specific sequence identification; however, despite being highly reproducible, it is recognised that off-target effects may occur even with minimal sequence homology, resulting in hybridisation of siRNA and other transcripts (330). Therefore, BCL-3 was suppressed using a second sequence (50nM sequence D) and compared to control siRNA or standard target sequence (sequence A) (Figure 3.6 A-C); both these two target sequences have been previously validated and shown to induce efficient knockdown of BCL-3 (257). Cell lysates were analysed with western analysis and despite only partial suppression, results confirmed increased expression of Bim with each sequence of siRNA targeting BCL-3. Interestingly, in SW1463 cells, Bim upregulation was more pronounced following BCL-3 suppression with sequence D (Figure 3.6 C), although BCL-3 siRNA sequence A did clearly result in Bim upregulation too. These data suggest that the observed effect on Bim from BCL-3 suppression was not an off-target effect of a single BCL-3 siRNA sequence.

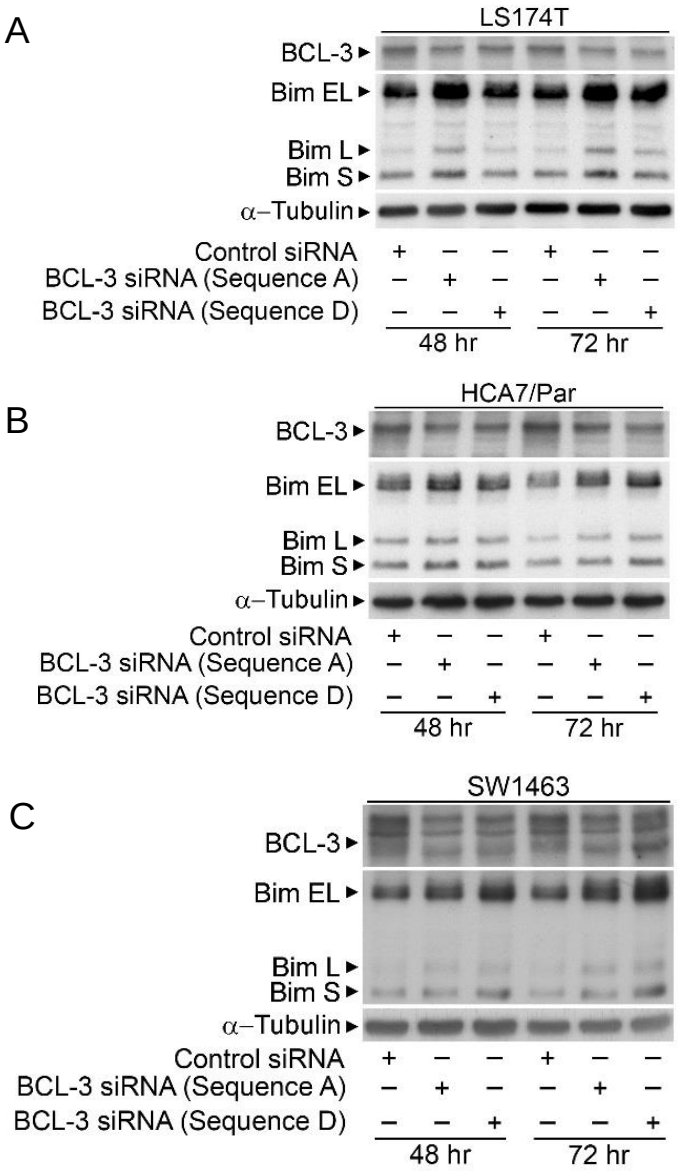

Figure 3.6 Suppression of BCL-3 using differing siRNA sequences results in induction of Bim protein expression.

To ensure that regulation of Bim by BCL-3 suppression was not sequence specific, colorectal cancer cell lines (LS174T, HCA7/P and SW1463) were transfected according to described methodology (see methods). Cells were transfected in suspension with two alternative sequences of siRNA targeting BCL-3 (sequence A and D), which had been previously validated by our group as the optimal sequences for BCL-3 protein suppression (2). Cells were lysed at 48 and 72 hours post-transfection and BCL-3 and Bim protein expression analysed using western blotting. α-Tubulin expression was used as a loading control.

3.2.7 Knockdown of Bim abrogates BCL-3 suppression-induced apoptosis

To determine if the increase in apoptosis of colorectal cancer cells observed following suppression of BCL-3 was dependent on regulation of Bim expression, a co-transfection experiment was performed. SW1463, HCA7/P and LS174T colorectal carcinoma cells were transfected in suspension with BCL-3, Bim or a combination of both siRNA sequences. Total siRNA was controlled for by adjusting the amount of control siRNA in the single transfected conditions (BCL-3 or Bim) to ensure maximum siRNA was no more than 100 nM (Methods 2.2.1). At 72 hr following transfection adherent and floating cells were collected and counted. The percentage of floating cells was then determined. Results show the increase in apoptosis induced by BCL-3 suppression was abrogated by Bim knockdown in all the cell lines tested (Figure 3.7). Western blot was used to confirm protein knockdown of BCL-3 and Bim in the WCL. Furthermore, abrogation of apoptosis was confirmed by cleaved PARP at the molecular level in WFL in co-transfected cells (Figure 3.7). These observations suggest that the increase in floating cells and therefore apoptosis is dependent on Bim expression as when Bim expression is reduced the effect of BCL-3 suppression on apoptosis is abrogated.

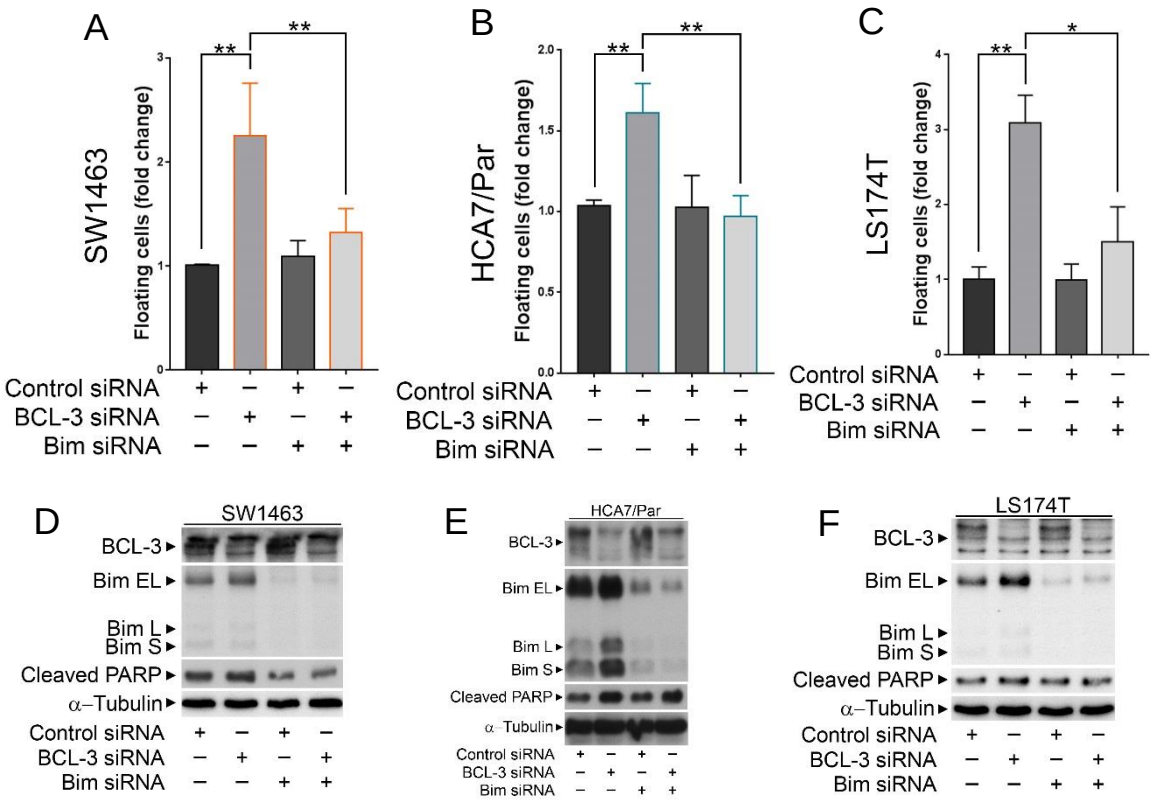

Figure 3.7 BCL-3 knockdown induced apoptosis is dependent on Bim.

SW1463 (A), HCA7/P (B) and LS174T (C) colorectal cancer cells were transfected with BCL-3, Bim, control siRNA or co-transfected with both siRNA sequences. Total siRNA as well as concentration of each manufacturer siRNA (BCL-3: Ambion, Bim: Dharmacon, Methods 2.2.1). Cells were counted 48 hours after transfection. BCL-3 suppression significantly induced apoptosis, which was abrogated by co-suppression of Bim (A-C). WCL and WFL were harvested and western blot performed to analyse expression of BCL-3, Bim and cleaved-PARP (D-F). α-Tubulin expression was used as a loading control. Counting experiments are combined data from n=3 independent experiments (mean and SD) and western blots are exemplary from n=3 experiments. Statistical analysis was performed on GraphPad Prism 7 software using a Student's T-Test (* :P<0.05, ** : P<0.01, *** : P<0.001, NS : non-significant).

3.2.8 BCL-3 knockdown does not alter pAKT expression or pERK expression

AKT is known to have anti-apoptotic functions which are partially mediated through phosphorylation of the Forkhead Box O (FoxO) transcription factor (318). A principle target of FoxO transcription is Bim (317, 331). When FoxO is phosphorylated this results in its nuclear exclusion and eventual degradation, resulting in reduced Bim transcription (332). Previous work from this group has shown that BCL-3 expression modulated levels of phosphorylated AKT (pAKT) in the cell lines SW480 and HCT116 (257). It was hypothesised that BCL-3 suppression may negatively regulate pAKT expression, thereby reducing FoxO phosphorylation and activating Bim gene transcription, western analysis was performed to probe for pAKT (serine 473). Colorectal cancer cells SW1463, HCA7/P and LS174T were transfected in suspension with BCL-3 siRNA compared to control siRNA as described in methods. Protein was harvested 48 and 72 hr following transfection and western blot performed. Results showed that there was no consistent regulation of pAKT by BCL-3 suppression at either 48 or 72 hr from transfection (Figure 3.8). These data suggest that, in the colorectal cancer cell lines SW1463, HCA7/P and LS174T, the effects of BCL-3 suppression, on Bim upregulation, are not mediated through the AKT-FoxO-Bim axis.

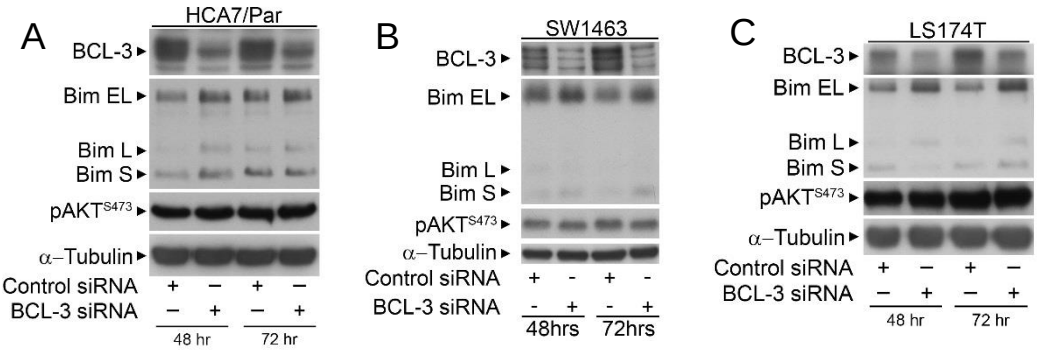

Figure 3.8 BCL-3 suppression does not alter pAKT^{S473} levels in the colorectal cancer cell lines SW1463, HCA7/P and LS174T

HCA/P (A), SW1463 (B) and LS174T (C) cells were transfected in suspension with BCL-3 or control siRNA (50 nM). Whole cell lysates were collected at 48 and 72 hr from transfection initiation. Western analysis was performed and showed that after suppression of BCL-3, Bim expression was indeed induced; however, pAKT^{S473} expression was unchanged in all three cell lines analysed. Equal loading confirmed with α-Tubulin expression. Westerns are exemplary images from n>3 independent experiments. Note SW1463 BCL-3 and Bim blot used in Figure 3.5.

3.2.9 Bim expression increases with BCL-3 and p52 suppression in HCA7 and SW1463 but not LS174T colorectal cancer cells

BCL-3 is an important co-factor in atypical NF-κB signalling where it regulates transcription by the atypical NF-κB homodimers p50 and p52. Previous observations showed that BCL-3 was not altering pAKT levels in SW1463, HCA7/P and LS174T colorectal cancer cells. It was hypothesised that the effect of BCL-3 suppression on Bim up-regulation may be through regulation of the atypical NF-κB homodimers. To examine if NF-κB1 or NF-κB2 suppression had similar effects on Bim expression compared to BCL-3 suppression siRNA was used to all three genes. Therefore, SW1463, LS174T and HCA7/P cells were transfected with BCL-3, NF-κB1 and NF-κB2 siRNA and compared to control siRNA. Protein lysates were collected at 72 hr following transfection. Western blot was used to examine protein expression. Results showed that Bim expression was induced by both BCL-3 and NF-κB2 knockdown but not NF-κB1 suppression in HCA7/P and SW1463 cells (Figure 3.9 A&B). Interestingly, this was not the case in LS174T carcinoma cells, where NF-κB2 suppression reduced Bim levels in comparison to both control and BCL-3 transfected cells. These observations suggest that, in HCA7/P and SW1463 cells, BCL-3 and p52 both repress Bim expression. In LS174T cells it may be that BCL-3 suppression induces Bim by an alternative mechanism.

Further analysis highlighted that NF-κB2 knockdown resulted in the induction of BCL-3 in all the cell lines analysed but NF-κB1 suppression did not have the same effect on BCL-3 (Figure 3.9 A-C).

These data suggest that BCL-3 and p52 suppression have mirrored effects in HCA7/P and SW1463 carcinoma cells resulting in upregulation of Bim. To analyse this further qRT-PCR experiments were performed to assess mRNA levels after BCL-3 suppression.

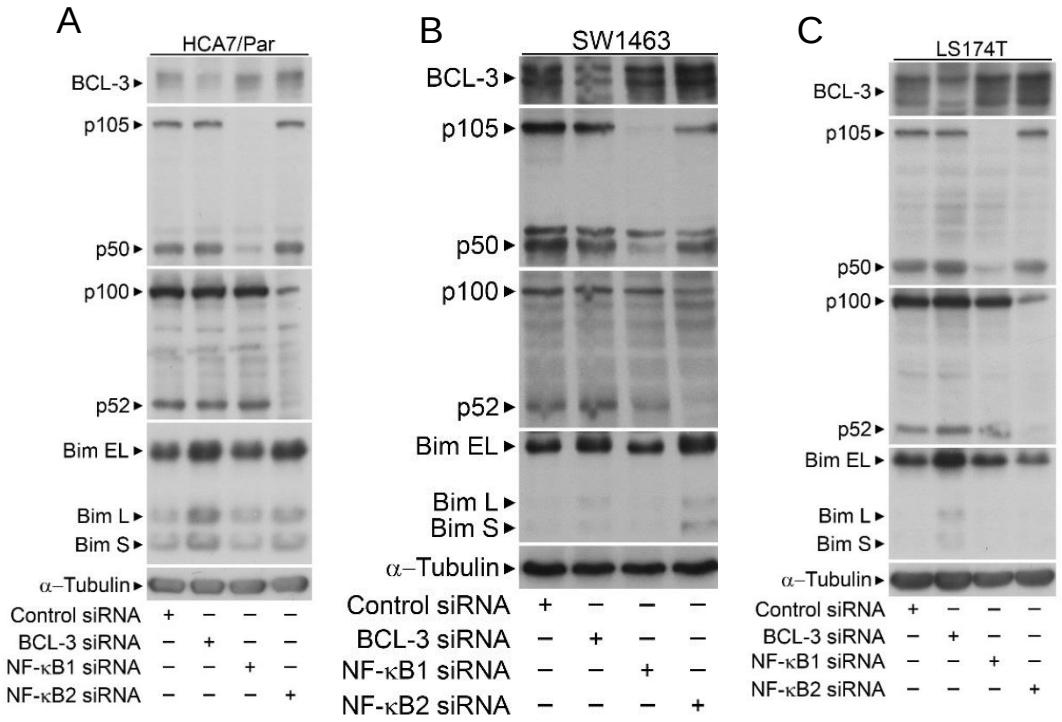

Figure 3.9 Bim upregulation results from NF-κB2 suppression as well as BCL-3 suppression but not NF-κB1

HCA7/P, SW1463 and LS174T cells were transfected in suspension as described (Methods 2.2.1). 50 nM siRNA of each siRNA was used to supress BCL-3, NF-κB1 and NF-κB2, 72 hr following transfection initiation whole cell lysates were harvested and western analysis performed. Results showed that NF-κB2 suppression as well as BCL-3 suppression increased Bim expression, while NF-κB1 knockdown failed to induce Bim expression in SW1463 and HCA7/P cells but not in LS174T cells. Western blots are exemplar data representative of n=3 independent experiments.

3.2.10 BCL-3 suppression increases levels of Bim mRNA

BCL-3, when acting as an NF-κB co-regulator, is known to have repressive roles on gene transcription (199), which would corroborate the effect observed. The results obtained so far indicate that BCL-3 suppression results in upregulation of all Bim isoforms in those colorectal cell lines analysed with high basal BCL-3 expression. SW1463 and HCA7/P cells were used as previous experiments had shown apoptotic response and Bim upregulation was greatest in these cell lines. Additionally, Bim was regulated by both BCL-3 and p52 in these cells. To determine if the regulation of Bim protein expression by BCL-3 suppression was at the transcriptional level, qRT-PCR was performed to measure levels of Bim mRNA. HCA7/P and SW1463 were transfected with 50 nM siRNA (BCL-3 vs control) and left for 48 and 72 hours to achieve maximal knockdown of BCL-3. The early time-point of 48 hr was utilised to capture changes in mRNA level, which would be expected to occur prior to protein alterations. mRNA was purified using a Qiagen PCR kit after which cDNA was synthesised before being incubated with the qRT-PCR reaction mixture (primers used BCL-3, Bim and TBP as the housekeeping gene). Primers used for qRT-PCR were designed to identify all three of the main Bim isoforms created by alternative splicing. It was observed that BCL-3 suppression significantly induced expression of Bim mRNA at both 48 and 72 hr after transfection in HCA7/P (1.80 fold increase at 48 hr and 1.83 fold increase at 72 hr) and SW1463 cells (1.67 fold increase at 48 hr and 1.43 fold increase at 72 hr) (Figure 3.10). BCL-3 mRNA was confirmed to be significantly reduced by transfection (data not shown). These data suggest that upregulation of Bim is through denovo gene transcription in these colorectal cancer cells. Further experiments would be performed to assess if BCL-3 was found at regulatory regions in the Bim promoter.

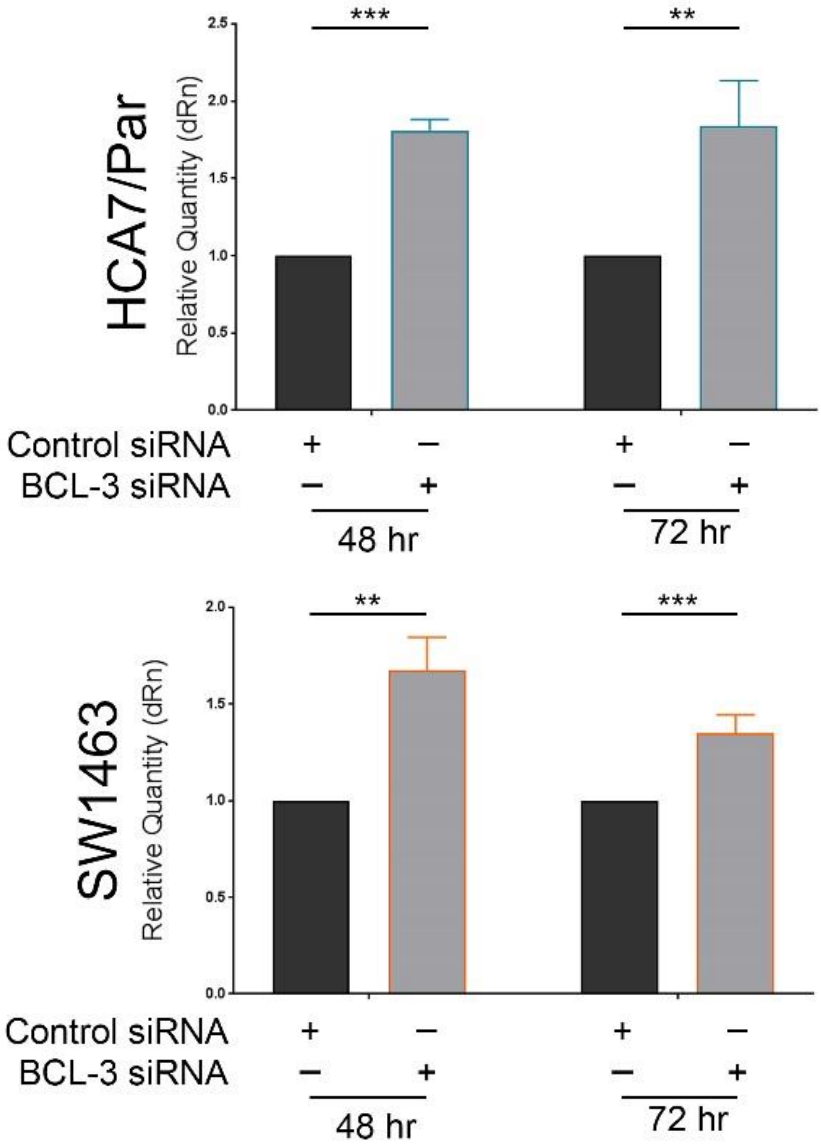

Figure 3.10 BCL-3 suppression leads to increased levels of Bim mRNA.

SW1463 and HCA7/P cells were transfected in suspension with BCL-3 siRNA. Total cellular RNA was extracted from cells at 48 and 72 hours post transfection. qRT-PCR was performed using primers to Bim and TBP (housekeeping primer). Results showed that BCL-3 suppression significantly increased Bim mRNA levels in SW1463 and HCA7/P cells at both time-points. Data is mean and SD of 3 biological replicates with Relative Quantity (dRn) normalised to the housekeeping gene. Statistical analysis was performed on GraphPad Prism 7 software using a Student's T-Test (* :P<0.05, ** : P<0.01, *** : P<0.001, NS : non-significant).

3.2.11 BCL-3 binds to the Bim promoter at NF-κB consensus sites

3.2.11.1 ChIP primer Design

BCL-3 is well recognised to repress transcription when bound to atypical NF-κB homodimers in the nucleus (Introduction 1.6.6). Bim is known to be regulated by non-canonical NF-κB signalling with RelB-p52 complexes identified at putative NF-κB consensus sequences present at the BCL2L11 promoter (153). Data shown previously identified that BCL-3 and p52 regulated Bim expression in SW1463 and HCA7/P cells (Figure 3.6). Additionally, BCL-3 suppression regulated Bim mRNA levels suggesting modulation of transcription (Figure 3.10). Chromatin immunoprecipitation (ChIP) was used to determine whether BCL-3 regulated Bim transcription by binding to the BCL2L11 gene. BCL-3 binds to DNA through its association with NF-κB homodimers (see introduction 1.6.4 for references). NF-κB dimers bind to DNA on κB consensus sites, which can vary in their sequence. It was unclear if specific consensus sequences (such as those site in the Bim promoter shown to bind non-canonical dimers (153)) enable atypical/homodimer binding as NF-κB DNA binding sequences are distinct for each subunit. As p52 suppression had induced Bim expression mirroring the effect of BCL-3 suppression but p50 knockdown had not induced Bim, an NF-κB consensus site on the BCL2L11 promoter that was potentially more specific to p52 was sought.

The genomic DNA sequence of BCL2L11 was downloaded from the UCSC Genome browser (http://genome.ucsc.edu/ using Human Genome December 2013 GRCh38/hg38 Assembly) (Appendix 4). To identify possible p52 homodimer binding sequences, the online program JASPAR (http://jaspar.genereg.net/ database containing transcription factor DNA-binding preferences, modelled as position weight matrices (PWM), under a creative commons attribution) was mined to identify the DNA-binding PWM. The p52 PWM was identified (Figure 3.11). These sequences were then used to analyse the BCL2L11 gene promoter region. Results identified a number of putative NF-κB DNA-binding sites within 5000 bases (5 kb) that matched the p52 homodimer PWM obtained from JASPAR. Primers were designed using Primer3 software (http://primer3.ut.ee/) with optimum primer size of 150 bp and choosing primers with minimal predicted self-complementarity to minimise primer dimer and secondary structure formation. Primers were chosen for PCR to include those NF-κB regions closest to the BCL2L11 transcription start

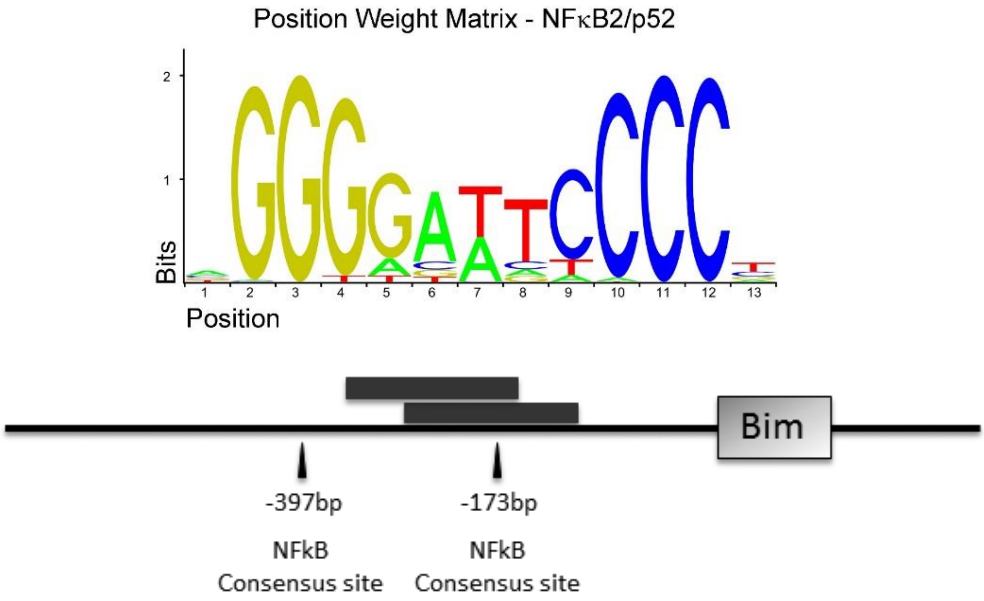

Figure 3.11 The BCL2L11 promoter contains two putative NF-κB DNA binding sites

Analysis of the BCL2L11 gene using NF-κB p52 homodimer consensus sequences identified a number of possible DNA-binding sites within the BCL2L11 promoter. Online software JASPAR was used to identify p52 consensus binding sequences. These sequences were then used to identify areas of the Bim promoter region for ChIP experiments.

site (TSS). Additionally, primers were designed to NF-κB consensus sites in the BCL-3 promoter region as BCL-3 is recognised to be a target of transcriptional repression by p52 (199) and therefore, would act as a positive control; furthermore, primers were designed to a region close to the BCL2L11 gene with no identified NF-κB consensus sites, which would act as a negative control.

3.2.11.2 Sonication Efficiency

Initial experiments were performed in HCA7/P and SW1463 cells growing, exponentially, in basal conditions (10 % DMEM, T25 flasks). Chromatin was sonicated (15-20 cycles, 30 sec/cycle) into fragments of between 100-500 bp lengths (Figure 3.12), as these are considered optimal for the downstream PCR steps following IP; too large fragments may result in false positive detection, while over-sonication may result in too smaller fragment size and false negative results. Chromatin sonication was checked to ensure optimal fragment size by running samples on a 1.5 % agarose gel (Figure 3.12).

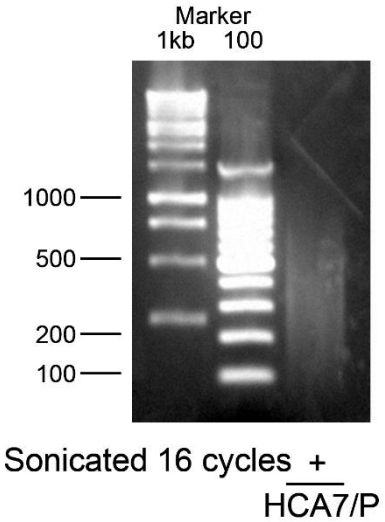

Figure 3.12 Validation of sonication efficiency using HCA7 carcinoma cells.

HCA7/P carcinoma cells were grown in 2xT25 flasks until 60-80 % confluent. Cells were fixed using 4 % paraformaldehyde for 10 min. The nuclear compartment was isolated and lysed, following which nuclear lysates were sonicated for 16 cycles. Sonicated DNA was then resolved on an 1.5 % agarose gel for 40 min at 200 V. Results showed that 16 cycles of sonication was sufficient to fractionate DNA into fragments of between 100-500 bp.

3.2.11.3 Primer dimerisation

It was noted that there was significant primer-dimer formation, likely as a result of too high 3' self-complementarity of the primers. This can be an issue in PCR due to a number of reasons including template that is found at very low levels leading exponential amplification of small fragments resulting in utilisation of PCR reagents and reduction in PCR of the true template.

As significant primer dimer had been observed, in the primers of interest, it was necessary to try and reduce this by optimising the PCR reaction conditions. Additives to PCR reactions can minimise primer dimer by optimising the reaction conditions. DMSO works by disrupting base pairing in primers with high GC content (333). Using the ChIP samples prepared from HCA7/P cells it was possible to test if the addition of DMSO would improve the reaction efficiency and abrogate primer dimer formation of the primers of interest. 1 % or 3 % v/v DMSO was added in to the reaction mixtures (Methods 2.5.4.4). It was observed, that the addition of the PCR additive DMSO 1 % v/v resulted in improved PCR efficiency and reduced primer dimer formation for primers designed to the BCL2L11 and BCL-3 promoter (Figure 3.13 A&D). Additionally, it was clear that the addition of 3 % v/v DMSO resulted in worse PCR efficiency and significant primer dimer formation again (Figure 3.13 B&E). A further primer to the BCL2L11 promoter was designed, as described above, with increased stringency on Primer3 software (http://primer3.ut.ee/) to ensure that there was reduced self-complementarity of the designed primers (complimentary 3' bases (1-2) and any complimentary bases (3-4)) (Figure 3.13 C). This primer, BCL2L11 (1b), was used in PCR with the same optimised reaction mixture and led to further reduction in primer-dimer formation. Additionally, primers to a putative κB site in a non-promoter region of Bim (Bimoff) and GAPDH (Figure 3.13 F&G) acted as controls with results showing no binding of BCL-3 to these regions. Ongoing PCR experiments were performed with the

optimised primer to the Bim promoter (BCL2L11 (1b)) and reaction mixture with the addition of 1% DMSO.

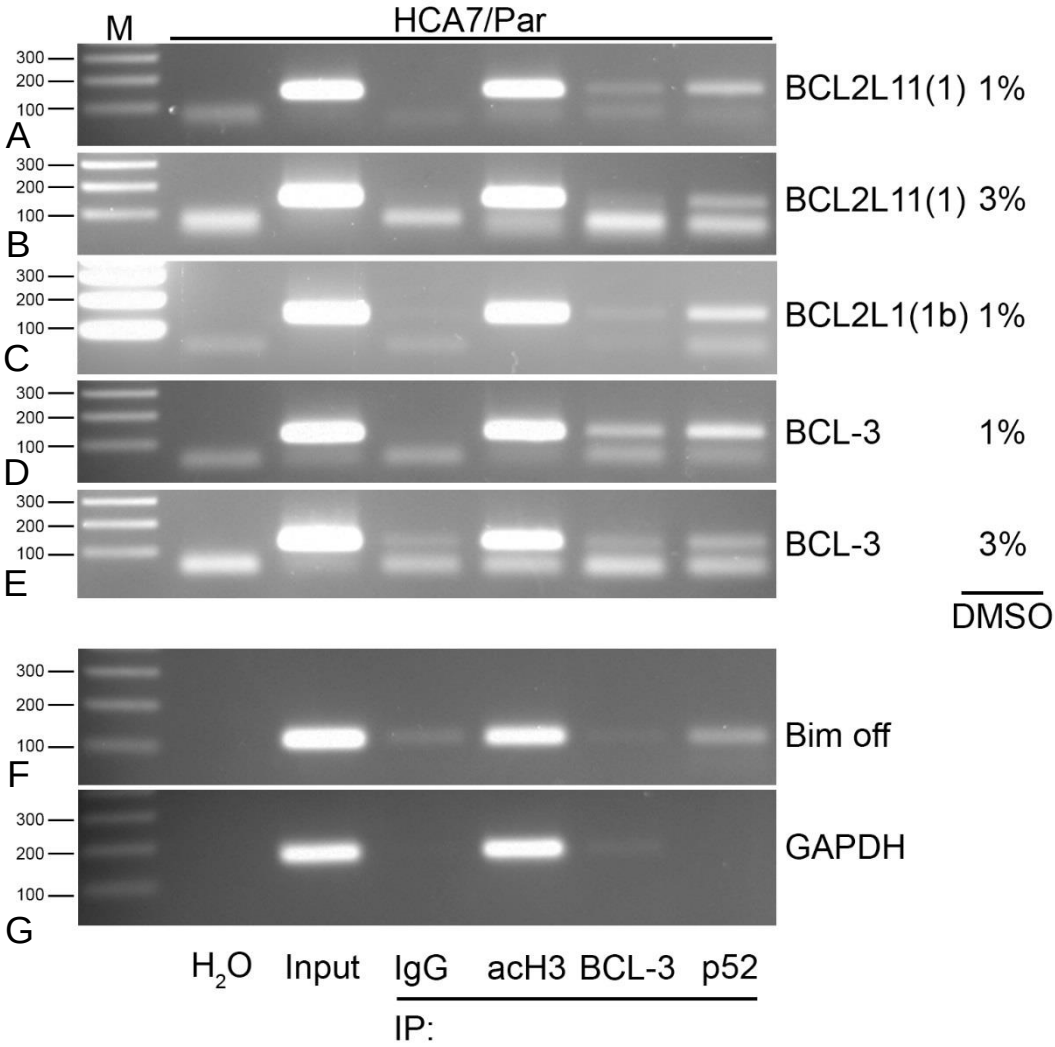

Figure 3.13 1% DMSO reduces primer dimer formation for primers with high GC content.

HCA7/P carcinoma cells were grown and fixed as before. End-point PCR was performed with ChIP samples. 1 or 3 % v/v DMSO was added to the reaction mixtures and PCR was run as in methods 2.5.4.4. PCR products were analysed on a 2 % agarose gel. It was observed that 1 % v/v DMSO resulted in more efficient PCR reaction with reduced primer dimer formation for both primers tested (A&D compared to B&E). Interestingly, increasing DMSO to 3 % resulted in a less efficient reaction and much greater primer dimer formation (B&E). Furthermore, a second primer (BCL2L11b) to the same BCL2L11 promoter region was designed, with significantly lower 3' or any self-complementarity resulting in less primer dimer formation compared to the original BCL2L11 primer (A&C). p52 bound to the positive control region in the BCL2L11 gene (F) but not to GAPDH, while BCL-3 bound to neither region (F or G).

3.2.11.4 BCL-3 and p52 bind to the BCL2L11 promoter in colon and rectal cancer cell lines

Further experiments were performed to investigate if BCL-3 was found at the Bim promoter in rectal cancer cells. To do this, the optimised primer to NF-κB p52 consensus site in the Bim promoter (BCL2L11 (1b)) was compared to a GAPDH primer in a second cell line (SW1463). ChIP was performed as before on HCA7/P and SW1463 cells and end-point PCR (Methods 2.5.4.4) to analyse the immunoprecipitated chromatin. Products were run on a 2 % agarose gel for 40 min. It was observed that BCL-3 and p52 were identified at the BCL2L11 promoter (BCL2L11 (1b)) in both SW1463 and HCA7/P CRC cells (Figure 3.14 A and B). Importantly, BCL-3 or p52 were not found at the GAPDH promoter, which acted as a negative control (Figure 3.14 C). Additionally, there was no signal observed in IgG control immunoprecipitates, suggesting that the results from the BCL-3 and p52 pulldown is specific. These results confirm that BCL-3 and p52 are found at the Bim promoter in both colon and rectal cancer cell lines.

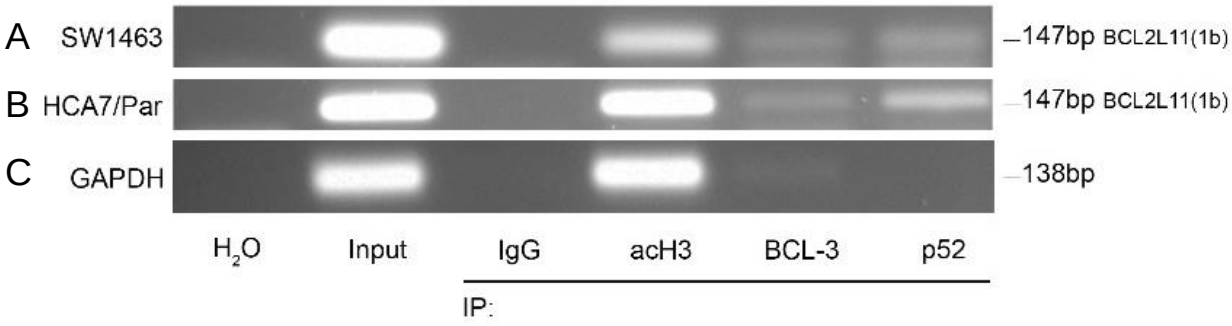

Figure 3.14 BCL-3 and p52 are found at the BCL2L11 promoter.

HCA7/P and SW1463 carcinoma cells were grown in exponential phase. Cells were fixed with 4 %paraformaldehyde for 10 min. Sonicated chromatin was immunoprecipitated with IgG, acH3, BCL-3 and p52 antibodies overnight and collected on Dynabeads. Input and ChIP samples underwent PCR in comparison to H_2O control. Products were run on a 2 % agarose gel at 200 V for 40 min. These preliminary results identified that BCL-3 and p52 were both found bound to the BCL2L11 promoter (SW1463 A and HCA7/P B) but not to the GAPDH promoter. Data shown is exemplary data from n=5 ChIP experiments.

3.2.11.5 BCL-3 suppression increases levels of active histone marks (acH3) at the BCL2L11 promoter

BCL-3 is known to interact with the histone modifying enzymes TIP60/KAT5 (216) and HDAC1 (219). Having identified that BCL-3 binds to the promoter region of BCL2L11, it was necessary to understand if BCL-3 modulated chromatin marks that signify active gene transcription. It is recognised that acetylated histone 3 (acH3) is an important histone modification that signifies active transcription (334). Additionally, phosphorylated Pol2 at serine 5 is found at promoters and marks

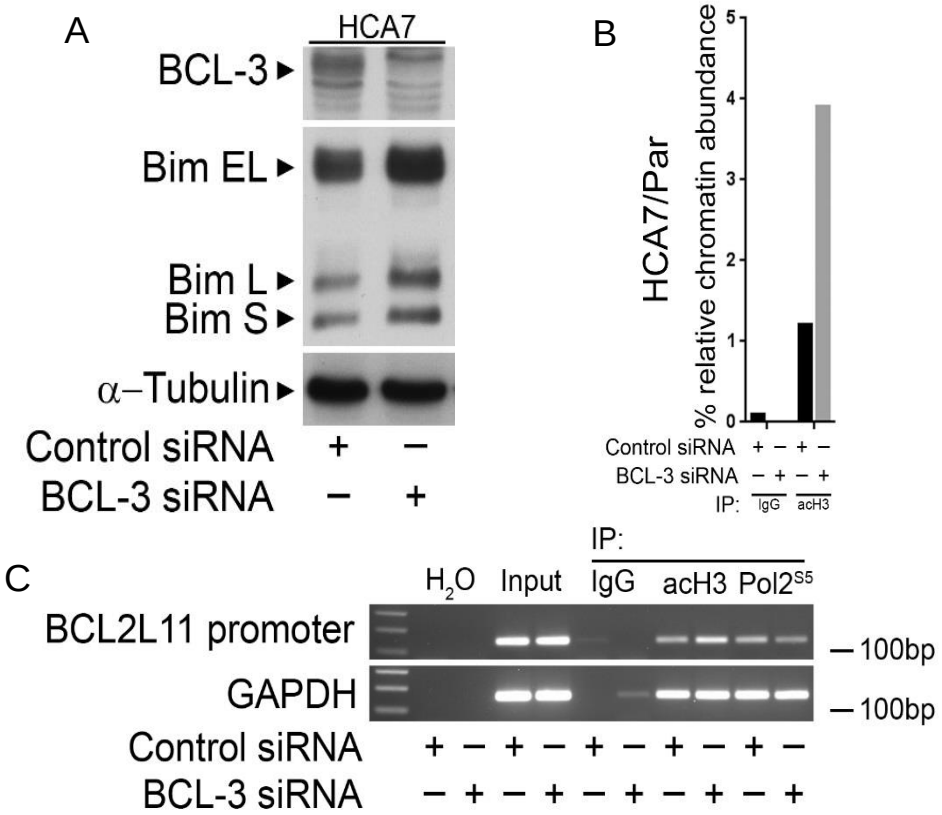

Figure 3.15 Preliminary ChIP data suggests BCL-3 knockdown reduces abundance of acetylated Histone 3 at the BCL2L11 promoter.

BCL-3 was suppressed in HCA7/P cells using siRNA and compared to cells treated with control siRNA (50 nM). At 72 hr following transfection, cells were processed for downstream applications; whole cell lysates were taken for western blot and 2xT25 flasks were fixed with 4 % paraformaldehyde for chromatin immunoprecipitation. Western blot was used to confirm BCL-3 knockdown and Bim induction, α-Tubulin was used as a loading control. Chromatin immunoprecipitation was performed on fixed and sonicated samples using antibodies to acH3, Pol2S5 and IgG. After ChIP, end-point PCR and qRT-PCR were performed. End-point PCR products were run on an 2 % agarose gel. qRT-PCR data was processed using MXPro software and results exported to Graphpad Prism 7 software.

transcriptional initiation (335). Therefore, ChIP was performed to ascertain if BCL-3 knockdown effected levels of acH3, with IP also performed to assess for alterations in Pol2S5. In HCA7/P carcinoma cells, BCL-3 siRNA (50 nM) was transfected in suspension and compared to control siRNA. BCL-3 knockdown was confirmed at 72 hr with western blot (Figure 3.15 A). The results show that BCL-3 knockdown increased levels of acetylated histone 3 at the BCL2L11 promoter consistent with the transcriptional activation observed previously (Figure 3.15 B and C). Although, there was no significant alteration to Pol2S5 at the Bim promoter with BCL-3 suppression. These data suggest that BCL-3 could play a direct role in chromatin modification, leading to alteration of transcription, a role that is incompletely understood.

3.2.12 Response of a panel of colorectal cancer cell lines to ABT-737

Targeting evasion of apoptosis by colorectal tumour cells is an attractive therapeutic prospect, as it would enable sensitisation of tumour cells to currently used chemo-radiation or enable novel targeted therapies. Moreover, colorectal cancers are known to have increased levels of BCL2 and BCL-x_L, which may limit the effectiveness of BCL-3 suppression on cancer cell apoptosis (336-338). Mechanistic studies of drugs targeting BCL2 dependent apoptosis, such as ABT-737, have suggested that they do not directly induce apoptosis in target cells but help to sensitise these cells to apoptotic stimuli, by tipping the balance towards the pro-apoptotic proteins, thereby allowing increased MOMP and apoptosis (339). Therefore, as BCL-3 suppression was shown to induce Bim expression, a hypothesis was considered; by blocking the effect of the pro-survival BCL2 proteins there would be sensitisation of colorectal cancer cells to BCL-3 knockdown resulting in reduced survival compared to BCL-3 suppression alone. To test this hypothesis, it was important to understand the IC50 values for the colorectal cell lines being used, so as to enable correct dosing throughout the BCL-3 knockdown experiments. Colorectal tumour cells SW1463, SW837, HCA7/P and LS174T were seeded into 48 well plates and allowed to grow for 48 hr before being treated with ABT-737 at logarithmically varying doses, based on micromolar concentrations described in the literature (339). Following 24 hr of treatment standard media was placed onto cells and cells allowed to grow until a week had passed since seeding. Cells were then fixed and stained with crystal violet as per methods. Concentrations of eluted crystal violet in acetic acid were analysed to ascertain changes to total proportion of viable cells per condition. Results showed that IC50 values ranged from just under 10 μM to around 20 μM for the cell lines tested. To

ascertain if BCL-3 would be sensitised by ABT-737 it was decided to use sub-IC50 concentrations in the following experiments.

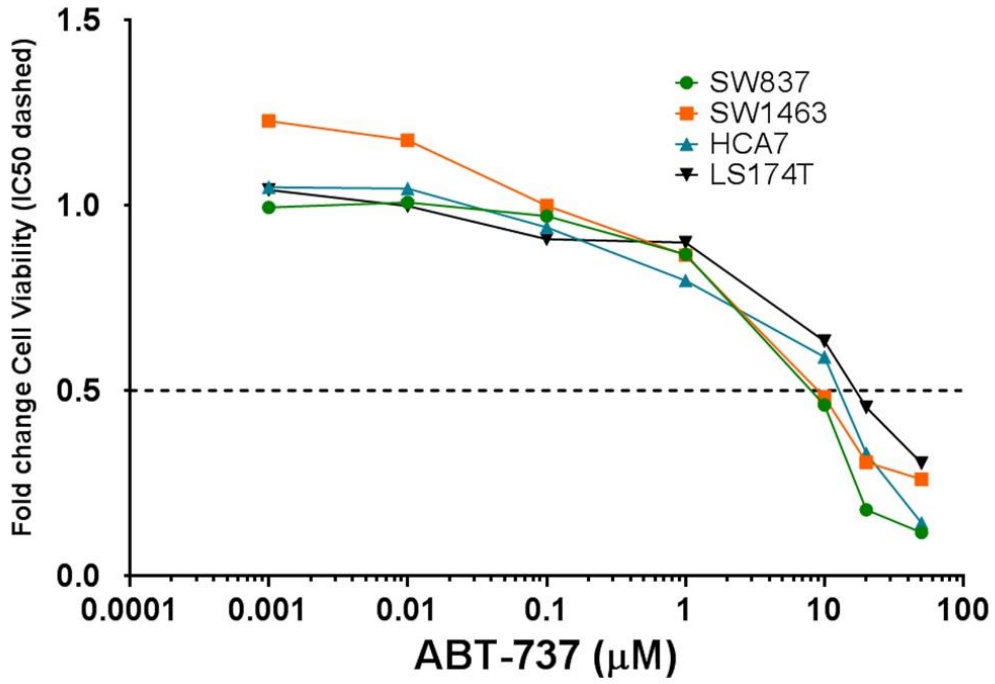

Figure 3.16 Treatment of colorectal tumour cells with the BCL2 inhibitor ABT-737

SW1463, SW837, HCA7/P and LS174T cells were seeded into 48 well plates for 48 hr prior to being treated with ABT-737 or vehicle control (DMSO). ABT-737 treatment was for 24 hr following which cell media was changed to standard 10% DMEM and cells incubated until seven days following seeding. A crystal violet cell viability assay was then performed and absorbance of crystal violet in solution measured using a microplate reader. Data shown is the mean fold change of cell viability, following treatment normalised to the vehicle control, of two independent experiments, for each cell line, plotted on a semi-log graph. Dashed line indicates the IC50 line. Observed IC50 values calculated using non-linear regression for cell lines analysed were SW1463 10.55 μM (95 % CI 10.73-12.35), , SW837 10.19 μM (95 % CI 7.38-14.34 μM), HCA7/P 14.59 μM (95 % CI 10.74-19.52), LS174T 18.5 μM (95 % CI 11-50.98). Analysis of IC50 values performed using Graphpad Prism software.

3.2.13 BCL-3 knockdown does not sensitise to treatment with ABT-737

Having analysed the general effect of ABT-737 on the viability of colorectal cancer cells, the aim was to translate these data into those cells where BCL-3 had been suppressed to ascertain if there was any benefit to concurrent treatment with a BCL2 inhibitor following BCL-3 suppression. As the effect on Bim expression following BCL-3 knockdown was greatest in SW1463 and HCA7/P cells (Figure 3.17), these cell lines were chosen for the ongoing experiments. Cells were transfected as before in suspension and seeded into 24 well plates, or T12.5 flasks (for protein lysate collection). At 48 hr following transfection cells were treated with sub-IC50 values of ABT737 or vehicle control. Cells were fixed at seven days following transfection and stained with crystal violet. It was observed that there was no significant additive effect of ABT-737 treatment on reduction in cell viability in either cell line tested (SW1463 or HCA7/P) following BCL-3 suppression. Western analysis of lysates taken following BCL-3 suppression and ABT-737 treatment showed BCL-3 suppression induced Bim (Figure 3.17). Interestingly, in the SW1463 cell line, ABT-737 treatment resulted in Bim protein induction, particularly Bim^{EL}, this was not the case in HCA7/Par cells.

Taken together, these data suggest that BCL2 inhibitors combined with BCL-3 suppression may not be therapeutically efficacious in colorectal cancers with high BCL-3 expression, the possible reasons for this will be discussed below.

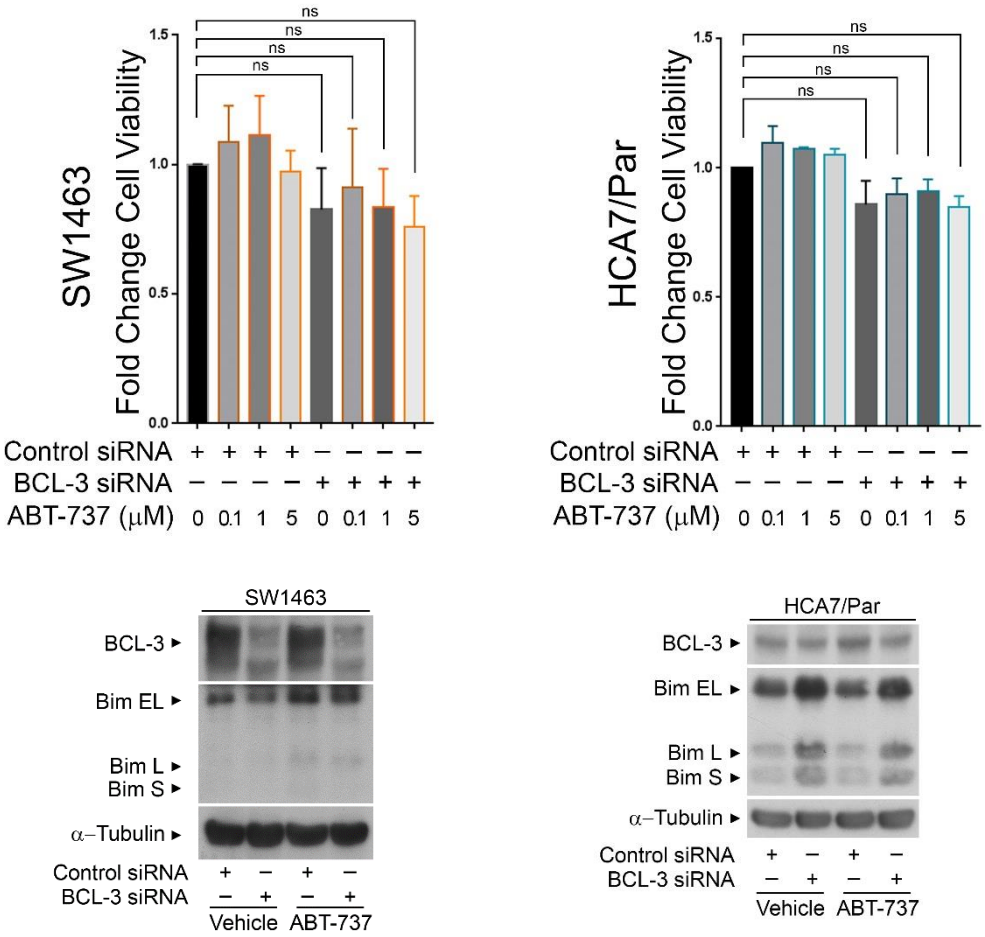

Figure 3.17 ABT-737 treatment does not increase levels of apoptosis observed following BCL-3 suppression in colorectal tumour cells.

Colorectal cancer cells SW1463 and HCA7/P were seeded into 48 well plates and BCL-3 was suppressed using siRNA in suspension as described in methods. Following 48 hr of transfection medium was replaced with 10 % DMEM containing either ABT-737 (0.1, 1 or 5 μM) or vehicle control (DMSO) for 24 hr treatment. At this time point medium was again removed and replaced with standard 10% DMEM, cells seeded in T12.5 flasks concurrently were lysed at this point also. Cells seeded for western analysis were treated with ABT-737 at 5 μM. Statistical analysis of cell viability data showed non-significance at all doses of ABT-737 compared to control, in both cell lines. Western blots are exemplary from n=3 experiments. Statistical analysis was performed on GraphPad Prism 7 software using a Student's T-Test (* :P<0.05, ** : P<0.01, *** : P<0.001, NS : non-significant).

3.3 Discussion

It is recognised that BCL-3 expression promotes evasion from apoptosis in several different cell types and under different conditions (discussed in introduction 1.6.8.3). However, although BCL-3 has been previously shown to promote tumour cell survival in colon cancer cells (257), its role in promoting cell survival in rectal cancer cells was unknown. In addition, there is limited data on the mechanism underpinning the regulation of apoptosis by BCL-3. Therefore, initially BCL-3 expression in two rectal cancer cells was compared to a panel of colon and adenoma cell lines and the high BCL-3 expressing cell line was taken forward for further experiments. It is shown that loss of BCL-3 promotes apoptosis in rectal cancer cells (confirmed as apoptosis by blocking caspase cleavage using QVD). This is potentially important as it suggests targeting BCL-3 in those cancers with higher expression could increase that rate of cell death of tumour cells, leading to tumour regression. A possible limitation of this study was the number of rectal cancer cell lines included and it would also be interesting to examine further rectal cancer cell lines for BCL-3 expression and assess if other high BCL-3 expressing lines exhibit the same response to BCL-3 suppression.

The BCL2 family proteins are critical regulators of apoptosis. Much work has shown that Bim expression and function is controlled through PTM (309, 311, 312). Interestingly, using RNAi results showed that BCL-3 suppression consistently increased Bim protein and mRNA expression, suggesting loss of BCL-3 was increasing Bim transcription. Importantly, apoptosis following loss of BCL-3 was dependent on the increase in Bim expression. Bim is a BH3-only protein that functions as a critical and potent pro-apoptotic regulator by binding to pro-survival BCL2 family members (reviewed in section 3.1.3). Bim has been shown to be an important regulator of apoptosis in colorectal tumour cells (311) although this study was confined to BRAF mutant cancers. The cell lines used for this study do not

have BRAF mutations, implicating Bim as a critical regulator of apoptosis in a wider range of CRC cells, not only BRAF mutant CRC cells. Further investigation could be performed to assess whether KRAS WT, mutant or BRAF mutations alter the response to BCL-3 suppression in cancer cells. Given that BCL-3 functions as a co-regulator with atypical NF-κB homodimers, investigations were performed to assess if suppression of NF-κB1 and NF-κB2 resulted in regulation of Bim. The results identified that Bim expression was increased following NF-κB2 knockdown but not NF-κB1. These data should be interpreted with the understanding that the siRNA targets the full-length NF-κB1 or NF-κB2 transcripts. Therefore, it may be that the effect of NF-κB2 knockdown on Bim is driven by suppression of the full-length NF-κB2 rather than the processed p52 protein itself. Full length NF-κB2 is known to have bona fide IκB functions and the siRNA would target these functions (340).

Given that Bim protein expression was increased by both BCL-3 and NF-κB2 suppression experiments, qRT-PCR was performed following BCL-3 suppression and showed upregulation of Bim mRNA. Therefore, in-silico analysis was performed to analyse the BCL2L11 gene for NF-κB consensus sites, this was to enable primer design for ChIP analysis. The κB consensus sites found on DNA are known to be specific to particular NF-κB dimers (133, 135); although, it is unknown if BCL-3 alters which κB consensus site the homodimers can bind to (whether interaction with BCL-3 can change the specificity of hetero- or homodimer binding). ChIP was performed to assess if BCL-3 and/or p52 bound to the regulatory regions of Bim previously implicated as important for its expression (153). Results indicated that BCL-3 was found at the Bim promoter alongside p52 in basal conditions. This led me to propose that BCL-3 may be repressing Bim transcription by binding to NF-κB consensus sites in the Bim promoter under basal unstimulated conditions.

The findings suggest that supressing BCL-3 led to release of transcription repression and Bim transcription. The data presented above suggests that BCL-3 suppression reduces cell viability despite expression levels of other BCL2 family proteins.

This is the first data to show that apoptosis induced by BCL-3 suppression is Bim dependent in rectal cancer. Moreover, this is the first data to show that BCL-3 and p52 are found at the same NF-κB consensus site within the BCL2L11 gene promoter. Previous studies have shown that Bim transcription is repressed by non-canonical NF-κB heterodimers through association with HDAC4, leading to resistance to apoptosis and therapy resistance (153). Results showed that histone 3 acetylation increases following BCL-3 loss and it may be that BCL-3 is promoting repressive chromatin through facilitating histone modification (discussed in final discussion 5). Clinically, it is known that a proportion of tumours have upregulated BCL-3 expression which would be contributing to evasion of apoptosis and therapy resistance through Bim suppression and it may be that targeting BCL-3 in rectal tumours is attractive therapeutically.

The data shown above have shown that BCL-3 suppression directly upregulates the pro-apoptotic BCL2 family protein Bim. Bim leads to apoptosis through binding to pro-survival members of the BCL2 family. The pro-survival BCL2 family members, such as BCL2 and BCL-x_L, are drivers of colorectal tumorigenesis, progression and therapy resistance, highlighting these proteins as attractive therapeutic targets (341, 342). Inhibition of the pro-survival members of the BCL2 family is possible using small molecule inhibitors (ABT-737, ABT-263 and ABT-199) that occupy the hydrophobic pocket of BCL-2, BCL-x_L and BCL-w, competitively inhibiting binding of the BH3 α-helix and inducing apoptosis (339). It was hypothesised that the effect of Bim upregulation on apoptosis could be increased with combined treatment with a BCL2 family inhibitor (343, 344).

However, the data showed no additional effect of BCL2 inhibition when combined with BCL-3 knockdown. Though the mechanism is not determined, this could be because MCL-1 is highly expressed in these cell lines and it could be that MCL-1 is driving the resistance to ABT-737 in these cells (345). The BCL2 inhibitors have similar efficacies for inhibiting BCL-2 members, except MCL-1, with later inhibitors (ABT-199) being more protein specific (346). Additionally, it may be that un-sequestering Bim from BCL2 or BCL-x_L, by using the ABT-737 (343), has no additional effect when Bim has been significantly upregulated by BCL-3 suppression. Further work could assess if specific MCL-1 inhibition or use of a BCL2 inhibitor that also targeted MCL-1, resulted in increased sensitivity to apoptosis in cells following Bim upregulation by BCL-3 suppression.

In summary, BCL-3 regulates Bim expression in colorectal cancer cells leading to increased apoptosis. It was shown that BCL-3 binds to the Bim promoter, alongside p52, where it appears to have a repressive effect on Bim transcription. Interestingly, there was no synergy or added effect of ABT-737 treatment in these colorectal cancer cell lines. As stated above there is preliminary evidence that BCL-3 suppression may increase chromatin accessibility. Chromatin remodelling drugs have been used to increase the efficacy of conventional drugs in cancer treatment (data for HDAC inhibitors for example has shown increased radiosensitivity in colorectal cancer cells) (347). This led to the investigation as to whether inhibition of BCL-3 function could alter the response of colorectal cancer cells to conventional therapy. Targeting BCL-3 in colorectal cancers would be an attractive therapeutic option to promote apoptosis in these cells, a focus of possible future work.

4 Results 2: BCL-3 protects colorectal cancer cells from γ-irradiation

4.1 Introduction

In rectal cancer, patients are typically treated with DNA damaging agents such as irradiation and platinum-based drugs (oxaliplatin or cisplatin) (18). In locally advanced rectal cancer, the DNA damaging treatment is neo-adjuvant long course chemo-radiation. However, there are a significant proportion of patients who fail to respond to neoadjuvant therapy and as a result have significantly poorer prognosis (Introduction 1.2.1.2). Understanding what drives the response to DNA damaging therapy in tumour cells is critical to improving the efficacy of therapy and, with the utilisation of biomarkers, could lead to the stratification of patients into those who will benefit and should receive therapy and those who are poor responders and could progress straight to surgery.

As well as its use as a therapeutic agent, cells are exposed to DNA damage through three main mechanisms, environmental agents (UV-radiation, ionising radiation and genotoxic chemicals), cellular metabolism and its associated products (ROS, hydroxyl radicals and H_2O_2) and the occasional spontaneous disintegration of some chemical bonds in DNA (hydrolysis of nucleotide residues and deamination of bases) (348). The outcomes of DNA damage are significant, including cell-cycle arrest (required to prevent replication of damaged DNA and propagation of the DNA damage to daughter cells through mitosis (349)), cell fate decisions (apoptosis if DNA damage is too severe and un-repairable) and alterations to gene transcription (350). Upstream of these cellular effects is a cascade of processes initiated by the DNA damage known as the DNA damage response (DDR).

Critically, no single repair process can facilitate the repair of all the different types of damage and all pathways are highly conserved due to the existence of DNA damage from the very origin of DNA itself (348). There are four main DDR pathways in mammals, base-excision repair (BER), nucleotide excision repair

(NER, encompassing global genome NER (GG-NER) and transcription coupled NER (TCR)), error-free homologous recombination (HR) and error-prone non-homologous end joining (NHEJ, encompassing canonical and alternative NHEJ). An additional DDR pathway is mismatch repair (MMR) which repairs incorrectly matched bases following replication and is important pathway when deranged in a number of cancers including CRC (351). These repair mechanisms can be broadly divided into repair pathways for single strand break (SSB) or double strand break (DSB), although there is significant overlap. DSB are significant lesions to overcome for the cellular DDR machinery and are highly toxic (352).

DSBs are induced by irradiation, free-radicals, chemicals, replication fork collapse with SSB and during repair of inter-strand DNA crosslinks. Irradiation results in the formation of both simple and complex DSBs. Additionally, irradiation also results in large numbers of SSB and base abnormalities, which also necessitate repair via appropriate DDR pathways (353). Repair pathway choice is highly regulated following DNA damage. It is highly dependent on cell cycle phase (354), which controls which proteins are recruited to DSB to perform end resection or initiate end joining (355). HR requires template DNA to repair DNA with high-fidelity, restricting HR to S/G2 phases of the cell cycle. NHEJ operates throughout the cell cycle but is particularly dominant in G0/1. Additionally, the regulation of repair pathway choice is made through alterations in NHEJ and HR protein expression and protein PTM by cyclin dependent kinases (CDKs). CDKs mediate the phosphorylation of target genes (for example CtIP, EXO1), which results in the increased resection of DNA ends in cycling cells favouring the resection dependent pathways (HR, SSA and alt-NHEJ) (356).

Pathway choice is also regulated by proteins such as 53BP1 and BRCA1; for example, 53BP1 is capable of blocking resection of DNA ends by preventing CtIP from binding DNA, directing repair into NHEJ. Additionally, while it appears that

pathway choice and execution are isolated, actually, it should also be recognised, that repair pathways are intricately interlinked with many of the proteins performing roles in either repair pathway (ATM, MRN complex and BRCA1), providing cross-talk between the two pathways to ensure that DNA is repaired if one fails or compete with each other for DSB sites (350, 357, 358). For example it is thought that alternative-NHEJ (alt-NHEJ) takes over from the HR pathway in HR-deficient tumours (359).

Briefly, the DDR process involves the sensing of DNA damage, transduction of this signal and activation of effector proteins to alter cellular function (350). Initially, DSB sensing involves a number of different complexes depending on mechanism and type of damage (MRN complex, RPA complex, sirtuins, Ku complex and PARP1) (360). Activation of each complex results in alternate downstream signalling cascades and alternative mechanisms of repair (HR, c-NHEJ and alt-NHEJ). Additionally, the kinetics of complex recruitment to DNA damage determines mechanism of repair (361). NHEJ proteins PARP1 and Ku70/80 are quickly and independently recruited to DSB sites (360), whilst recruitment of HR dependent proteins occurs over a slower timescale.

Following lesion sensing, the PI3K-like protein kinases (PIKK) are activated creating a signal-transduction cascade. Proteins such as ATM (Ataxia telangiectasia mutated), ATR (ATM and Rad3-related) and DNA-PKcs (DNA-dependent protein kinase)) are activated by DNA damage sensors. ATM, for example, is activated following binding to the MRN complex, where it is acetylated (by a co-factor, Tip60 (362)) and auto-phosphorylated (363). Activated PIKK proceed to phosphorylate a large number of substrate proteins including checkpoint control proteins and histones such as H2AX.

H2AX is one of the core histones (H2B, H3 and H4 being the other members) forming the octermeric nucleosome that facilitates chromatin organisation. H2AX

has a S-Q-E motif, which is recognised by activated PIKK following DNA damage, leading to phosphorylation on serine 139 (then known as γH2AX) (364-366). Inhibition of PIKK results in absent γH2AX foci formation and absent irradiation induced foci (IRIF) downstream of γH2AX (367); highlighting that H2AX phosphorylation is a critical early event that coordinates the DDR. γH2AX formation is proportional to the quantity of radiation and maximal concentrations are seen at 30 minutes following irradiation dose (368).

γH2AX has several roles at DSB, including de-compaction of chromatin and recruitment of additional repair factors. Firstly, γH2AX interacts with proteins, such as the SNF2/SWI2 family member, INO80 that remodel chromatin in the region of the DSB, in an ATP-dependent manner, to make it more accessible to the DDR machinery (369, 370). Secondly, recruitment of MDC1 to γH2AX is mediated through the BRCT domain in MDC1 (371). MDC1 is phosphorylated by ATM (372) and then coordinates the additional recruitment of large numbers of effector proteins such as RNF8 (373, 374), 53BP1 (375), RAD50 or Rad51 and BRCA1 (367) into IRIF facilitating repair of the lesion. Measurement of γH2AX foci and the IRIF associated with γH2AX is a valuable tool in radiation biology research.

4.1.1 BCL-3 and NF-κB in therapy response

The role of BCL-3 in response to therapy is yet to be fully elucidated. As discussed previously (Introduction 1.6.4), BCL-3 is an important cell survival factor in colorectal tumours (240, 257). There is limited evidence on the role of BCL-3 in the response of cancers to DNA damaging agents. Studies in breast cancer cells showed BCL-3 over-expression was protective against DNA damage induced apoptosis following cisplatin and UV-C irradiation (239). Additionally, an RNAi study in C.elegans revealed that the BCL-3 orthologue, C04F12.3, played a role in cell cycle response and sensitivity following γ-irradiation (376). BCL-3 interacts with

proteins important in DDR such as BARD1, TIP60 (216) or HDAC1 (219), although how this interaction effects the DNA damage response has not been studied. These data highlight that if BCL-3 does play a role in the DNA damage response it may be well-conserved through different species. There is also evidence in a keratinocyte model of skin carcinogenesis that UV radiation induces the activation of BCL-3:p52 or BCL-3:p50 complexes within the nucleus of exposed cells; suggesting that BCL-3 may be part of an atypical NF-κB dependent response to this DNA damaging agent (377). However, the impact of NF-κB signalling is still being elucidated.

Understanding of the NF-κB signalling pathway in response to DNA is best understood in canonical signalling and poorly understood in non-canonical or atypical signalling. Genotoxic stress, such as the DSBs caused by irradiation (amongst other DNA damaging agents), results in activation of NF-κB signalling (120, 378). The canonical NF-κB pathway has been shown to be the principle pathway activated, which is consistent with the evidence that NF-κB prevents apoptosis, promoting cell survival after cell stress. It appears that there are several different mechanisms by which canonical NF-κB activation exerts its effects following irradiation. In response to DNA damage, canonical NF-κB pathway subunits are directly activated in a mechanism dependent on ATM (Ataxia Telangiectasia Mutated) (379, 380). Additionally, it has been shown that canonical NFκB pathway activation occurs as a result of mutations to DDR pathways within tumours, such as BRCA1 deficiency (124). The mechanism behind this is complex. It was initially examined in cells lacking functional ATM protein (AT cells), which failed to activate NF-κB following treatment with DNA damage inducing agents such as IR, camptothecin or etoposide. This complemented work showing IκBα degradation was unchanged in AT cells, unlike control cells which showed early degradation of IκBα, in response to radiation (380). Other NF-κB pathway

members involved include the IκB kinase (IKK) complex, p50 and NEMO. The IKK complex is central to the activation of canonical NF-κB signalling. Data from breast carcinoma cells has shown that DNA damage induced activation of ATM results in the NEMO dependent activation of p65 (381). This appears specific to ATM, as ATR and DNA-PKcs do not cause the same activation of NF-κB. Further work showed that SUMOylated NEMO is phosphorylated by ATM at serine 85 (159), leading to its non-degradative ubiquitination, nuclear export (along with a proportion of ATM) and the subsequent activation of IKKα and IKKβ; thereby, leading to activation of canonical NF-κB signalling (159, 382). Moreover, PARP1 plays a critical role in this model, acting as a scaffold to assemble ATM, PIASy and NEMO, leading to the signalling cascade as described (383). p50 is known to be phosphorylated on serine 329 leading to fine tuning of genes undergoing transcription by activated canonical heterodimers, although this may only occur in response to certain types of DNA damage (384, 385). Therefore, canonical NF-κB activation, with subsequent upregulation of targets such as BCL2, CIAP2 and IL-8 (386), is a critical and conserved response to DNA damage, particularly DSBs.

What is the translation of these studies clinically? Data is contradictory from different cell types. Some studies suggest that levels of activated p65 do not predict response to radiation in rectal cancer patients (387). Whilst others have shown increased expression of canonical subunits, such as p65, in pre-therapy biopsy specimens correlated with shortened overall patient survival; although, p65 expression again did not correlate with the clinical/pathological response to radiation (TRG) (386, 388). In other malignancies, such as glioblastoma, in patients with higher expression of activated canonical signalling proteins (phosphorylated p65) the response to radiation is reduced (389). Therefore, while p65 expression predicts overall survival and is upregulated by radiation, p65 expression does not predict clinical/pathological response to radiation suggesting that p65 impacts

survival independent of radiation response (itself a predictor of survival). Given the different outcome in different cancers, it is likely the effect is context specific.

Other NF-κB subunits have been implicated in radiation response in rectal cancer. In a small retrospective study, patients carrying a nucleotide polymorphism of the NF-κB1 (p105/p50) gene promoter, rs28362491 (DEL/DEL) had an increased sensitivity to chemo-radiation (390). This polymorphism occurs 94bp upstream of the NF-κB1 TSS and results in reduced expression of NF-κB1 on stimulation by LPS (391). This suggests that reduced expression of NF-κB1 following inflammatory stimuli may result in increased sensitivity to radiation in rectal cancer.

There is clearly an exciting opportunity in understanding what role BCL-3 and the atypical NF-κB signalling pathway play in response to radiation in colorectal cancer, given the paucity of data currently published.

4.1.2 The tumour microenvironment and response to therapy

The TM is a major component of malignancy, as mutated epithelial cells alone do not constitute a tumour (392). The TM represents the complex interaction between the malignant cells and other non-malignant cells (for example endothelial, immune and stromal cells) and proteins (393). Importantly there is a reciprocal relationship between these two populations (malignant and non-malignant) of cells with bi-directional pro-tumour signalling contributing to therapeutic resistance of the malignant population (394). Large proportions of fibroblasts within cancers are thought to be cancer-associated fibroblasts (CAFs; also known as tumour-associated fibroblasts, reactive stromal fibroblasts or peritumoral fibroblasts) which are perpetually activated by cancer cells through a paracrine mechanism (for example secretion of bFGF (basic fibroblast growth factor), PDGF (platelet derived growth factor) and TGF-β (395)). Following stromal activation, a proportion of

cancers then become addicted to the CAF-derived signals within the TM leading to a positive feedback loop.

CAFs are recognised to initiate and promote cancer progression, drive metastasis (396), epithelial-mesenchymal transition (EMT) of tumour cells and promote resistance to therapy, utilising cell-cell contact as well as the secretion of signalling molecules (397-399). The origin of CAFs is still controversial but they are thought to be derived from a number of different cell populations, from different tissues, including differentiation of resident fibroblasts or the recruitment of mesenchymal stem cells (MSC) but also may include adipocytes, stellate cells, pericytes and other circulating stem cells (400). CAFs can be identified by upregulation of markers such as α-smooth muscle actin (αSMA) (401), as well as S100A4, vimentin and fibroblast activation protein (FAP) (398). Morphologically, CAFs are distinct cells that have large spindle shapes with abundant stress fibres and well organised transmembrane associated fibronectin containing fibres connected to actin microfilaments (known as the fibronexus) (401).

CAFs are thought to promote or be indicative of poorer outcomes or more aggressive tumour biology. Clinically, the expression of markers suggestive of a CAF phenotype in advanced CRC have been associated with higher rates of vascular invasion (402). Additionally, high expression of CAF markers such as α-SMA in CRC resulted in patients having a poorer OS (403) and high ratios of stromal cells to carcinoma cells is also associated with poorer prognosis and tumour recurrence in CRC (394). In rectal tumours the TM is thought to be important in the development of local recurrence following neoadjuvant therapy (404). Stroma with high expression of CAF markers (αSMA, FAPα, CD26 and SDF1) predicted tumour regrowth and therefore local recurrence in LARC following LCRT (405, 406). Neo-adjuvant therapy itself also leads to fibroblast activation resulting in secretion of paracrine signals that contribute to poorer prognosis (407).

Following irradiation fibroblasts secrete higher levels of growth factors such as HGF and FGF (408). Neo-adjuvant therapy also results is the significant formation of stroma or fibrosis within the TM, a feature that is measured using TRG (409).

CAFs also directly propagate persistent inflammation within the tumour. CAFs are recognised to facilitate tumour-promoting inflammation through several mechanisms including direct production of pro-inflammatory chemokines/cytokines and the secretion of factors that attract multiple immune cell types into the tumour. This signalling results in direct upregulation a number of signalling pathways in tumour cells including NF-κB (410, 411), PI3K/AKT and JAK/STAT3, which contributes to a variety hallmark capabilities (392). CAFs promote activation of these signalling pathways through secretion of a multitude of proteins; results from microarray data from pancreatic, skin, cervical and breast tumours showed significant upregulation of pro-inflammatory genes such as COX-2, IL-1β, IL-6 and members of the CXCL family of chemokines, by the respective tissue specific CAF (410). IL-6 is a principal cytokine secreted by CAFs. IL-6 is a pleotropic cytokine that regulates cells by binding to the IL-6R leading to the recruitment and homo-dimerisation of glycoprotein 130 (gp130) (412). This leads to phosphorylation and dimerisation of STAT3 and its translocation to the nucleus where it activates transcription of target genes. IL-6 signalling has effects on inflammation, immune cell coordination and haematopoiesis (413). In breast cancer it has been shown that IL6 is a key cytokine secreted from CAFs (414) while in colorectal cancer, CAF-derived IL6 stimulates proliferation of tumour xenografts (415). BCL-3 is known to be upregulated in a subset of colorectal cancers (240). However, the mechanisms driving BCL-3 upregulation in these tumours is not clear. BCL-3 is a STAT3 target and is therefore likely to be downstream of cytokines such as IL-6. IL-6 has been shown to consistently upregulate BCL3 in a bank of myeloma cell lines (416) purportedly in a STAT3/HS4 dependent manner (191). It was

hypothesised that BCL-3 expression in CRC may be related to CAFs and to tumour response to radiation.

4.1.3 Aims

The aims of this chapter are to elucidate the role BCL-3 plays in the response of colorectal tumour cells to DNA damaging agents, such as irradiation or oxaliplatin, and understanding what role CAFs play in BCL-3 regulation of therapeutic resistance using a 3D spheroid model of CRC.

4.2 Results

4.2.1 BCL-3 expression may confer resistance to LCRT in rectal tumours

BCL-3 has been shown to be upregulated in a subset of colorectal tumours but its effect on the response of tumours to therapy is unknown. To examine whether BCL-3 expression related to response to LCRT in rectal cancer, samples from the ASPIRE cohort study (IRAS 141548) (Appendix 1 for protocol) were used. Biopsy samples were obtained at diagnosis and tumour samples were obtained following surgical resection after neo-adjuvant LCRT. Patients were followed to assess response to therapy. Therapy response was analysed using the American Joint Committee on Cancer/College of American Pathologists (AJCC/CAP) tumour regression grade (TRG) by gastro-intestinal pathologists at each of the sites recruiting patients. The AJCC TRG (TRG 0-3, Appendix 3) classifies tumour response according to the ratio of remaining tumour cells and fibrosis in tumour samples (62). Biopsy and tumour samples were fixed in formalin and processed by Southmead Histology Department (Claire Blunt MSc). Immunohistochemical analysis was performed using antibodies to BCL-3 (Table 2.5). Preliminary results of a small initial group of patients (n=13) showed that BCL-3 staining appeared to correlate with response to LCRT (Figure 4.1), with minimal BCL-3 staining relating to a good response to irradiation (TRG1) while strong BCL-3 staining correlated with poor therapeutic response (TRG3). Despite these interesting results it is important to note that further analysis of the full cohort is ongoing and results will be analysed and published in full when available. However, these preliminary findings suggest that BCL-3 high expression may correlate with response to therapy and therefore may play a role in protecting tumour cells from LCRT in rectal cancer and warrant further investigation.

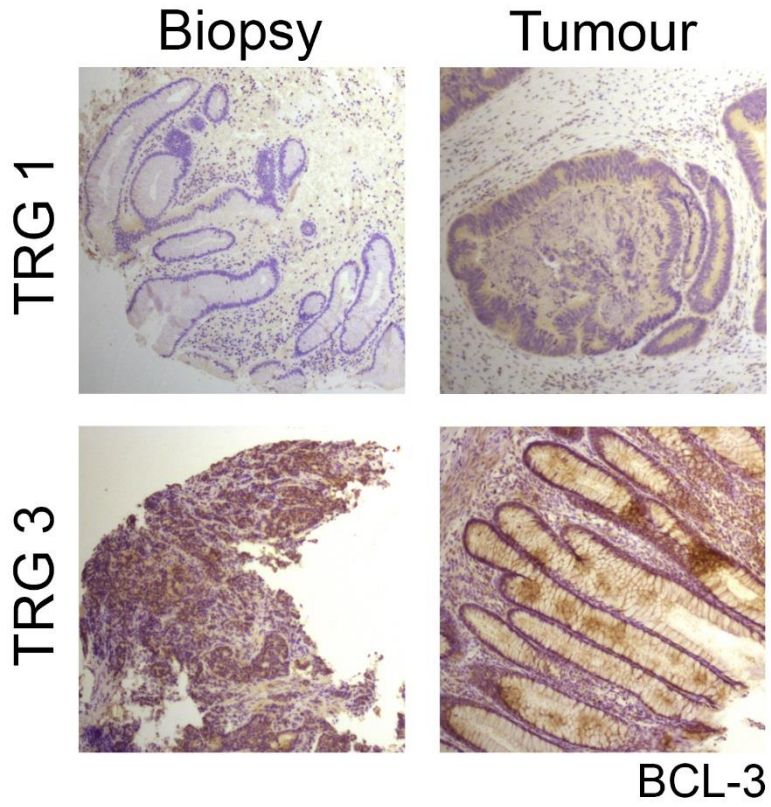

Figure 4.1 BCL-3 expression in rectal cancers may predict response to neo-adjuvant radiation

To ascertain if expression of BCL-3 in rectal tumours correlated with TRG following neoadjuvant radiation in rectal cancers, samples were used from the ASPIRE cohort study. Biopsy and tumour samples were stained with antibody to BCL-3 and imaged using widefield light microscopy. BCL-3 staining was scored as none – 0, minimal – 1, moderate – 2 and strong – 3. TRG was assessed by pathologists at each participating centre of the ASPIRE cohort study. Preliminary results showed that in some patients BCL-3 expression correlated with TRG, high BCL-3 expression with high TRG. Results are exemplary data from the initial 10 patients analysed in the ASPIRE trial.

4.2.2 Optimisation of seeding densities for cell lines to be used in γ-irradiation cell viability experiments

The aim of the following experiments was to determine the impact of BCL-3 expression on the radiation sensitivity of colorectal cancer cells. Leading on from earlier work, a high (SW1463) and low (SW837) BCL-3 expressing rectal cancer cell line was compared to colon carcinoma cells (HCA7/P and LS174T). I used an in-vitro model to assess cell viability following irradiation in combination with BCL-3 knockdown as it had been identified that BCL-3 may play a role in response to irradiation in rectal tumours, from the ASPIRE study (Figure 4.1). To maintain cells in an actively growing phase the seeding density of cells into plates was critical. Therefore, optimisation of seeding densities in 6 well plates was performed.

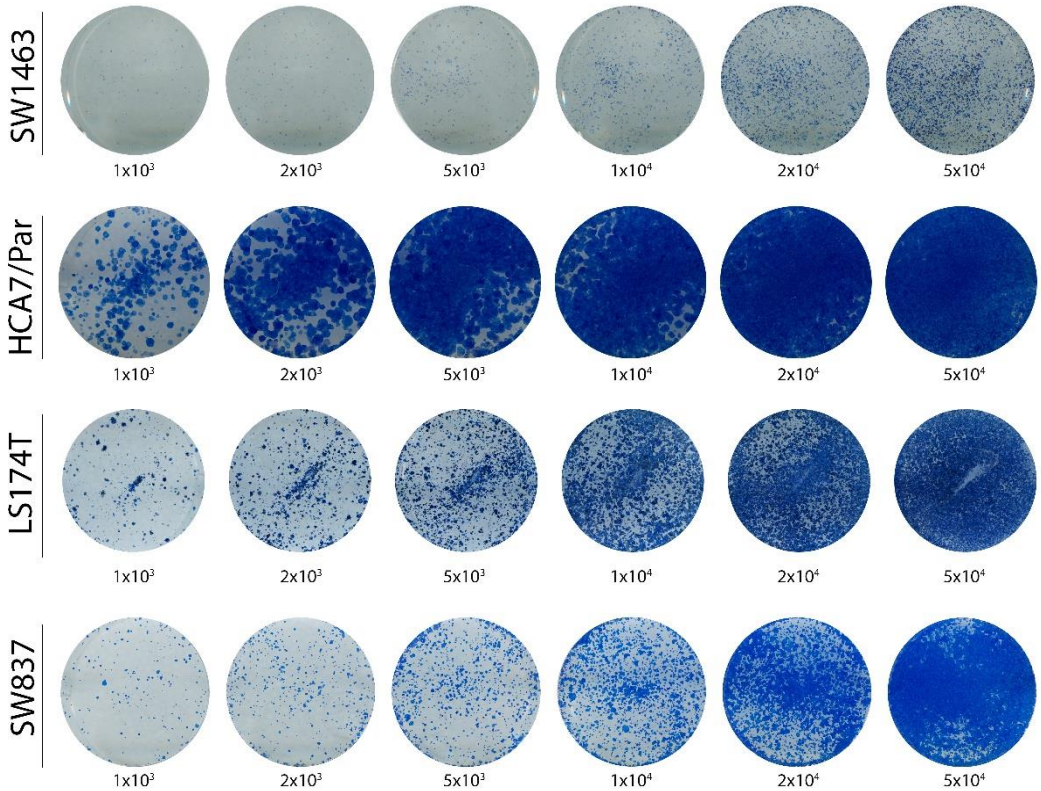

Figure 4.2 Seeding densities for crystal violet cell viability assay in colorectal tumour cells

Colorectal cancer cells SW1463, HCA7/P, LS174T and SW837 were seeded into 6-well plates at two weeks from seeding cells were fixed with 4 % paraformaldehyde and stained with crystal violet. Cell density was picked so that cells were not over or under confluent at the two week timepoint. Cultures were scanned using Epson V750Pro scanner.

Colorectal tumour cells SW1463, HCA7/P, LS174T and SW837 were seeded out in a series of increasing seeding densities into 6-well plates. Cells were grown for two weeks as I wanted to be able to analyse both the early and late effects of radiation on cell viability, following this growth phase cells were fixed with 4 % paraformaldehyde and stained with crystal violet (0.5 % w/v). Plates were scanned and assessed for confluence. It was observed that the seeding density required for each cell line would be cell line dependent. For future experiments cell lines were seeded at a density of between $0.5x10^4$ or $2x10^4$.

4.2.3 Radiation dose response rates in 4 colorectal cancer cell lines

As future experiments would combine BCL-3 suppression and irradiation, further experiments would determine the radiation dose that reduced the cell yield between 20-50 %. This would ensure a dose of radiation that did not result in too greater cell viability reduction and would facilitate measurement of the effect of BCL-3 suppression in conjunction with the effect of the radiation. Using the seeding densities obtained from previous experiments (Figure 4.2) further crystal violet cell viability assays were performed with a broad range of radiation doses (1, 2.5, 5 and 10 Gy). Cells were seeded into 6-well plates and grown for 2 days before being exposed to the specified doses of -γ-irradiation from a Cs^{137} source. After two further weeks of growth, cells were fixed with 4 % paraformaldehyde and stained with crystal violet (0.5 % v/v), crystal violet was eluted with acetic acid (10 % v/v) and absorbance measured with a microplate reader set at 594 nm. Results are summarised in Figure 4.3. Typically, 1 or 2.5 Gy resulted in between 20-50 % reduction in cell viability as measured by crystal violet. Interestingly, it was noted that the LS174T cell line were more radio-resistant than the other cell lines as 5 Gy resulted in a 10-50 % reduction in cell viability (depending on seeding concentration of cells) compared to SW1463, HCA7/P and SW837 cells where 5 Gy resulted in a >50 % reduction in cell viability. Additionally, it was noted that seeding density affected viable cells at the same radiation dose. LS174T cells treated with 5 Gy had a range of around 10 % reduction in cell viability when cells were seeded at $2x10^4$/well, but a 40-50 % reduction in cell viability when seeded at $0.5x10^4$/well. HCA7/P cells also showed a similar effect at both 2.5 and 5 Gy. These data show that irradiation response is both cell line and seeding concentration dependent and will be carefully controlled in future experiments.

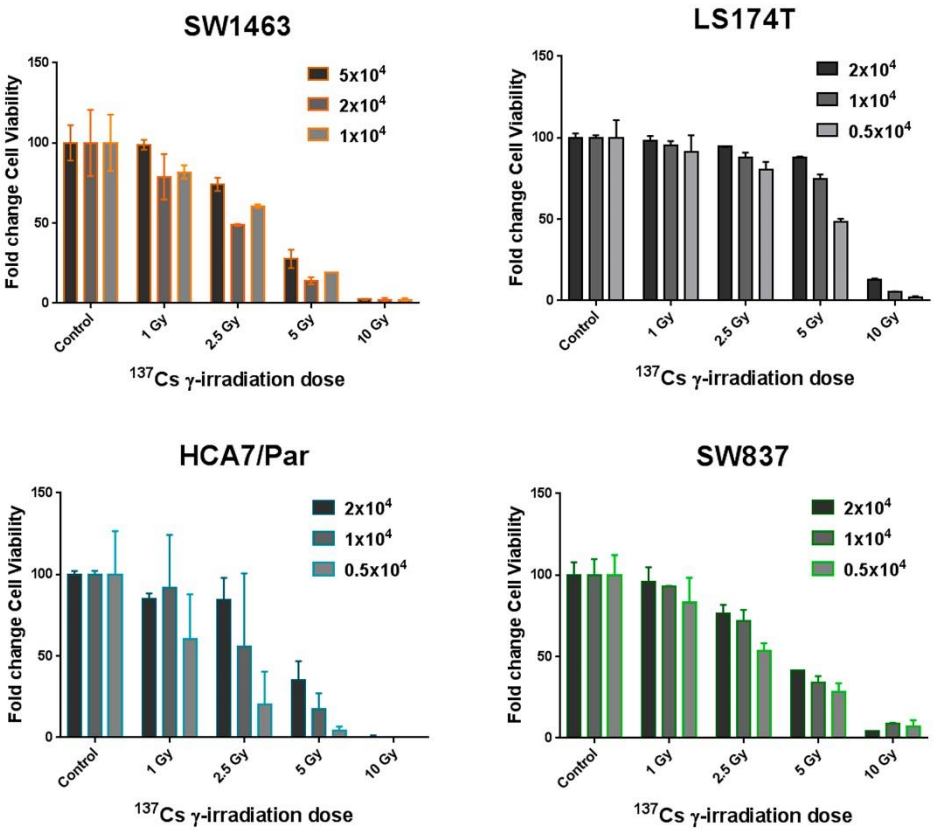

Figure 4.3 Sensitivity of colorectal cancer cells to γ-irradiation

To ascertain the sensitivity of colon and rectal cancer cells to γ-irradiation at different seeding doses, cells were seeded into 6-well plates and after 48 hours exposed to radiation from a Cs^{137} source. After 2 weeks cells were fixed with 4 % paraformaldehyde and a crystal violet cell viability assay was performed. Measurement of crystal violet absorbance was made at 594 nm using a microplate reader and normalised to the un-irradiated controls. It was noted that LS174T cells were consistently more resistant to irradiation that the other colorectal cancer cells. HCA7/P cells were relatively radiosensitive and therefore a higher seeding density was utilised. Results are means of n = 2 biological replicates with errors as standard deviations.

4.2.4 BCL-3 knockdown sensitises colorectal cells to γ-irradiation

BCL-3 has been shown to promote tumour cell survival in-vitro and over-expression, in the tumour, is known to confer worse survival in patients with colorectal cancer (240, 257). Previous work has identified that BCL-3 promotes survival in rectal cancer cells (Results 3.2). Patients with rectal cancers that are at high risk of local recurrence (Introduction 1.2.1) are typically treated with pre-operative chemo-radiation. The question remained as to whether BCL-3 expression protected colorectal cancer cells from the effects of irradiation. Using optimised conditions of seeding density and radiation dose from previous experiments (Figure 4.2 & Figure 4.3), colorectal tumour cells, with high BCL-3 expression (LS174T, HCA7/P and SW1463), were transfected with BCL-3 siRNA (50 nM) and 48 hours following transfection were exposed to γ-irradiation (1 and 2.5 Gy). Cells were then fixed with 4 % paraformaldehyde and a crystal violet cell viability assay performed. Protein lysates were collected at 48 hr from pairs of transfected cells to confirm efficiency of knockdown.

Results are summarised in Figure 4.4. It was observed that BCL-3 knockdown decreased cell viability, as shown previously. When colon and rectal cancer cells were subjected to combined γ-irradiation and BCL-3 suppression there was a significant additional reduction in cell viability compared to non-targeting siRNA controls (Figure 4.4). Data for LS174T and HCA7/P colon carcinoma cells showed the increase in radio-sensitivity was significant at both 1 and 2.5Gy (Figure 4.4 A &B); however, SW1463 rectal cancer cells showed significant increase in radio-sensitivity at 1 Gy but a non-significant increase in radio-sensitivity at 2.5 Gy (Figure 4.4 C). This may be due to the high sensitivity of SW1463 cells to BCL-3 knockdown. Western blot showed that BCL-3 expression was significantly reduced at the time-point when cells were irradiated.

Importantly, these data suggest that BCL-3 suppression may result in increased radio-sensitivity, at low doses of radiation (1 and 2.5 Gy). These data suggest that BCL-3 could play an important role in radioprotection of colorectal tumour cells corroborating the in-vivo observations from the ASPIRE trial.

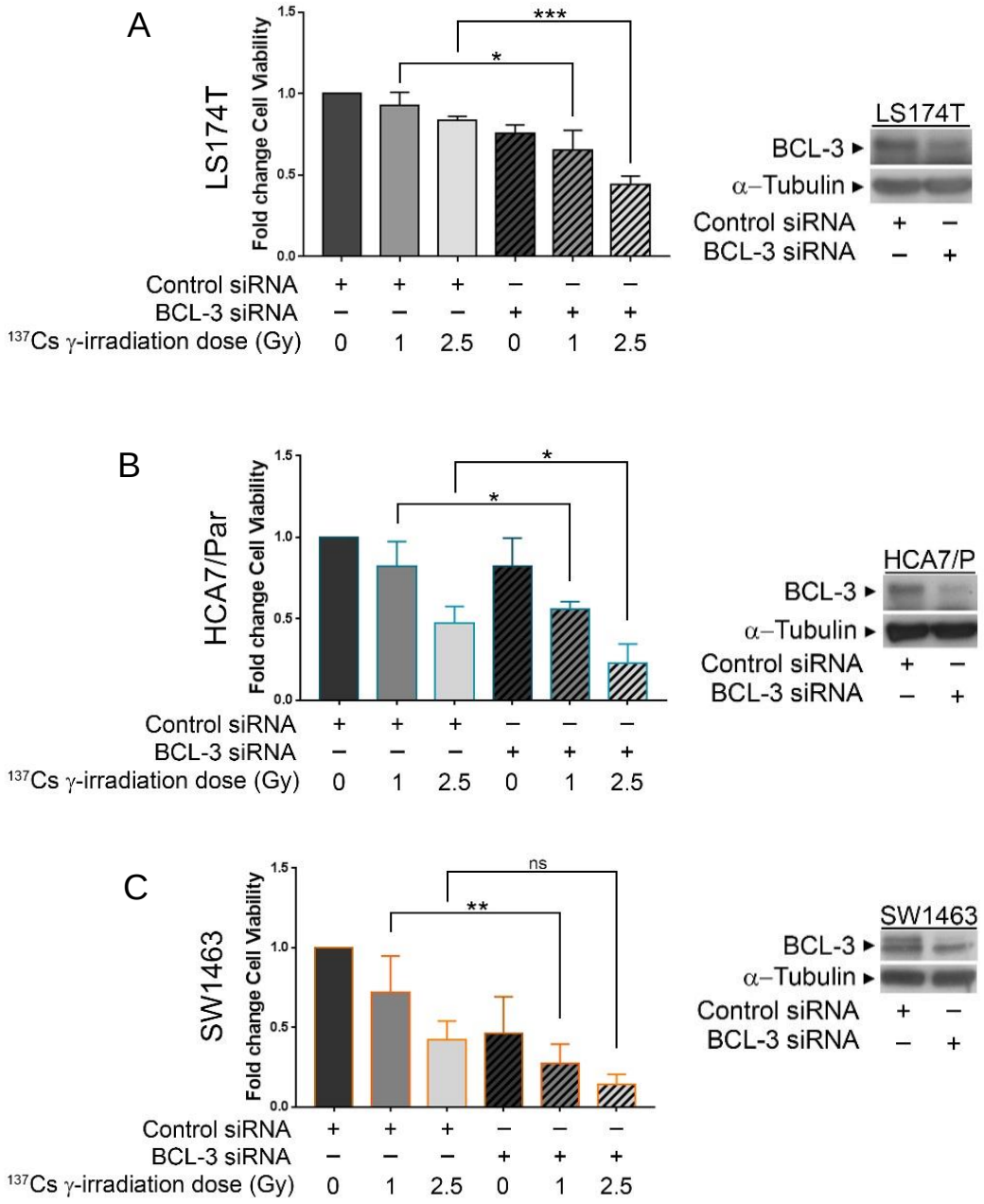

Figure 4.4 BCL-3 knockdown increases radio-sensitivity in colorectal cancer cells

Colorectal cancer cells LS174T, HCA7/P and SW1463 were transfected with BCL-3 siRNA (50 nM) and at 48 hours following transfection exposed to γ-irradiation from a Cs^{137} source. Cells were fixed at 2 weeks following transfection and a crystal violet cell viability assay was performed. Additionally, protein lysates were collected at 48 hours following transfection to assess for knockdown efficiency at the time of irradiation exposure. Results showed that BCL-3 siRNA reduced cell viability compared to control siRNA following γ-irradiation at two clinically relevant doses. Knockdown was confirmed using western blot. Graphs show means and SD of combined data from three independent experiments. Statistical analysis was performed on Graphpad Prism 7 software using ANOVA (*:P<0.05, **:P<0.01, ***:P<0.001, ns:non-significant)

4.2.5 BCL-3 suppression sensitises to oxaliplatin, a DNA damage inducing agent used in the management of rectal cancer

Clinically, oxaliplatin has been shown to be efficacious in the management of colorectal cancers (417). Oxaliplatin is a platinum-containing drug (other platinum-containing drugs include cis-platin or carboplatin, see Figure 2.2 Platinum-based chemotherapy compounds) that induces DNA inter and intra-strand crosslinks that lead to SSB or DSB if these SSB are encountered by replication forks (277). To examine if BCL-3 suppression decreased cell viability in combination with this alternative DNA damaging agent, rectal cancer cells (SW1463) were transfected with BCL-3 siRNA (50 nM) or non-targeting siRNA and then treated with oxaliplatin (1-100 μM) at 48 hr following transfection, for a duration of 24 hr after which medium was replaced with DMEM. At 1 week from transfection cells were fixed with 4 % paraformaldehyde and stained with 0.5 % v/v crystal violet (Methods 2.3.2). Measurements of absorbance were made at 594 nm and summarised in Figure 4.5. Results showed that BCL-3 knockdown reduced cell viability of SW1463 rectal cancer cells following low doses of oxaliplatin (1 μM) but not at higher doses of oxaliplatin (10-100 μM) (Figure 4.5 A). Western analysis was used to confirm suppression of BCL-3 protein at 48 hours following transfection (Figure 4.5 B).

These results in a single cell line suggest that the effect of BCL-3 suppression on cell viability following DNA damage may not be limited to γ-irradiation. This suggests that BCL-3 expression is important in DDR and understanding this role is important as it may have implications for patient response to therapy. To examine if radio-resistance could be induced by increasing BCL-3 expression, further experiments using over-expression systems were performed.

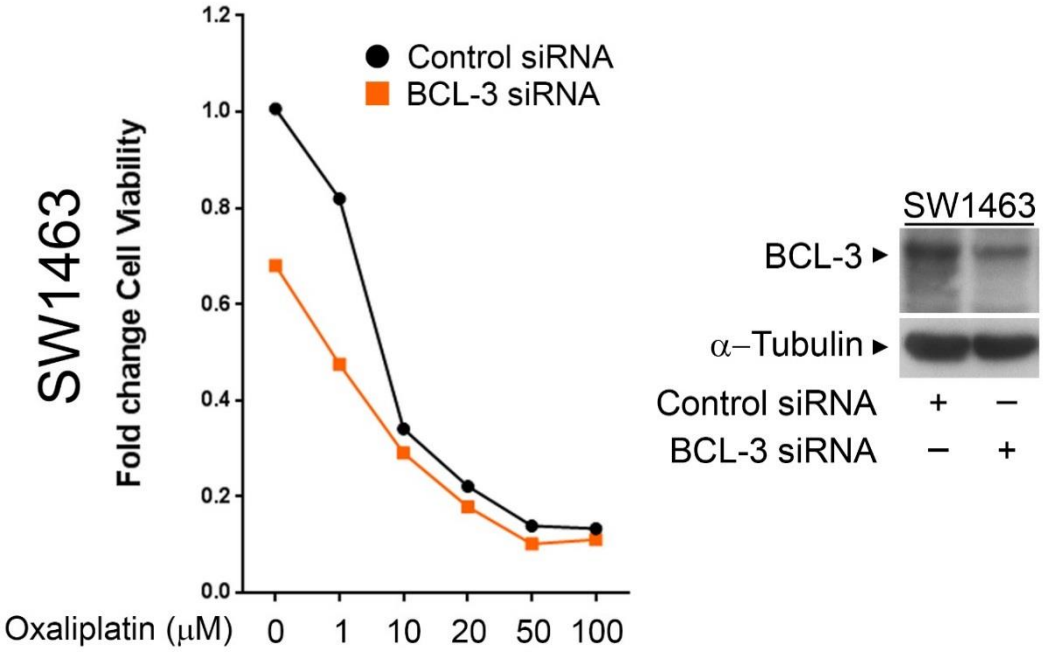

Figure 4.5 BCL-3 knockdown sensitises rectal cancer cells to an alternative DNA damaging agent, oxaliplatin.

SW1463 rectal cancer cells were treated, 48 hours following transfection (50 nM BCL-3 siRNA), with oxaliplatin for 24 hours total. Cells were fixed and stained with crystal violet at 72 hours following oxaliplatin treatment. Results identified that BCL-3 suppression sensitised to oxaliplatin at low doses (1 μM) but not at higher doses, where the effect of oxaliplatin on cell viability was more pronounced (A). Protein lysates were obtained at 48 hours following transfection and analysed using western blot to assess for knockdown efficiency (B). Graphs represent combined mean fold change in cell viability from 4 independent experiments. SD was not included for clarity.

4.2.6 BCL-3 stable overexpression in a low basal expressing BCL-3 rectal cancer cell line

SW837 rectal cancer cells have low basal expression of BCL-3 (Results 3.2.1) and so were used to determine if over-expression of BCL-3 resulted in resistance to radiation. Plasmids used were BCL-3^{WT}, BCL-$3^{ANK\ M123}$ (kind gift from Alain Chariot, Liege Belgium) and BCL-3^{GFP} in a pcDNA 3.1 plasmid (Origene, USA). Additionally, BCL-3^{WT} and BCL-$3^{ANK\ M123}$ constructs were FLAG tagged to enable efficient pulldown if IP experiments were to be performed. BCL-$3^{ANK\ M123}$ is a full length BCL-3 gene with 3 point mutations in the region of the 1^{st} and 2^{nd} ankyrin repeats, which inhibits binding of BCL-3 to p50 or p52 (218). BCL-3^{GFP} is a full length BCL-3 gene tagged with c-terminal turbo-GFP.

Plasmids were transfected into SW837 cells and cultured for three days (Methods 2.2.2). Thereafter, DMEM with 10 % FCS medium was supplemented with G418 400 µg/mL to select transfected cells followed by 200 µg/mL G418 to maintain cells long-term. Populations were grown up from an A flask and a B flask to create individual cell lines before being split and expanded. To assess expression of endogenous and exogenous protein, cell lysates were collected from each cell line generated, for each plasmid and western blot used to analyse BCL-3 expression. It was observed that BCL-3 was over-expressed in SW837 cells as shown in Figure 4.6. BCL-3^{WT} was expressed as a characteristic multi-band protein, at a significantly higher amount compared to endogenous expression in the empty vector cells. In comparison to BCL-3^{WT}, BCL-3^{GFP} was detected at a significantly slower migrating band, highlighting the GFP tagged protein was retarded in the gel. Expression of BCL-$3^{ANK\ M123}$ protein was shown to result in a faster migrating single band, which did not appear to undergo post-translational modification as reported by the Chariot group previously (201, 218).

Importantly, there was no observed differences in BCL-3 expression levels between clone A or B suggesting these cell lines could be considered as biological replicates for each other when validating future experimental results. In preliminary work it was observed that the BCL-3^{GFP} and the BCL-3$^{ANK\ M123}$ did not grow any differently to the BCL-3^{WT} cells and so it was decided that only the BCL-3^{WT} stable over-expression cells would be taken forward into future experiments.

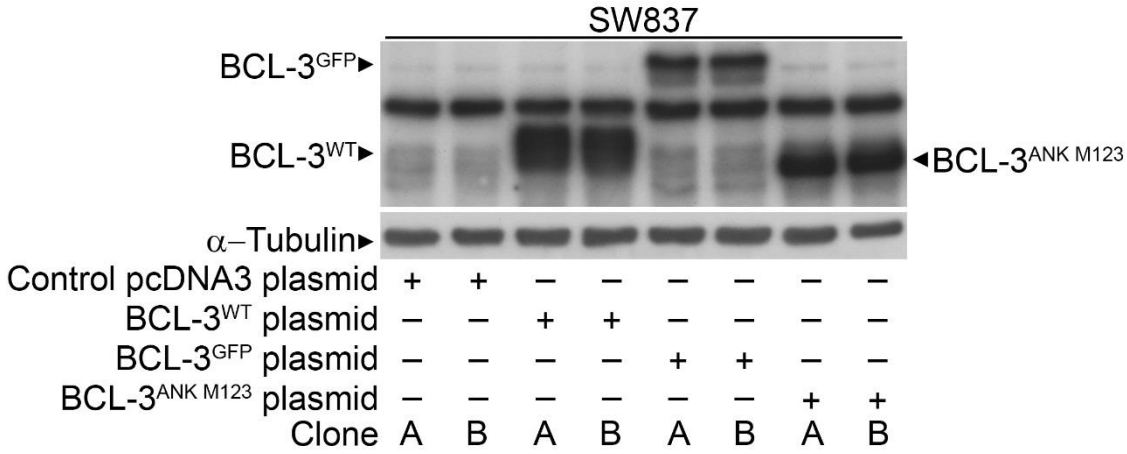

Figure 4.6 BCL-3 over-expression in the SW837 rectal cancer cell line

BCL-3 was stably over-expressed in the SW837 rectal cancer cell line, which has low basal levels of BCL-3. To achieve this, SW837 cells were transfected with a pcDNA3 plasmid with an empty vector, WT BCL-3, WT BCL-3 with GFP or mutant BCL-3. Plasmids contained a geneticin/neomycin (G418) selection vector and cell lines that had taken up the plasmid were selected with 400 µg/mL G418. Protein lysates were collected following selection of two individual cell lines (A & B) and analysed using western blot.

4.2.7 BCL-3 stable over-expression in rectal cancer cells does not alter cell viability following γ-irradiation

Using the SW837 BCL-3^{WT} cell line generated (Figure 4.6), it was possible to examine if BCL-3 over-expression had a radio-protective effect in rectal cancer cells. SW837 cells with either stably expressed control pcDNA3.1 plasmid or WT BCL-3 plasmid, were grown in 6-well plates at a seeding density of $1x10^4$ per well. Plates were then exposed to γ-irradiation (Cs^{137} source, 1 and 2.5 Gy) and medium was changed every 3-4 days. After 2 weeks of culture (mirroring previous experimental conditions Figure 4.4), plates were fixed with 4 % v/v paraformaldehyde and stained with crystal violet (0.5 %v/v). Absorbance was measured at 595 nm. Protein lysates were collected from parallel T25 flasks and western blot performed to confirm over-expression. Results showed that over-expression of BCL-3 did not confer statistically significant increase in radio-resistance to SW837 rectal cancer cells (Figure 4.7). Therefore, further experiments were not performed. It maybe that despite the over-expression of BCL-3 observed, that this was insufficient to cause altered radiation response.

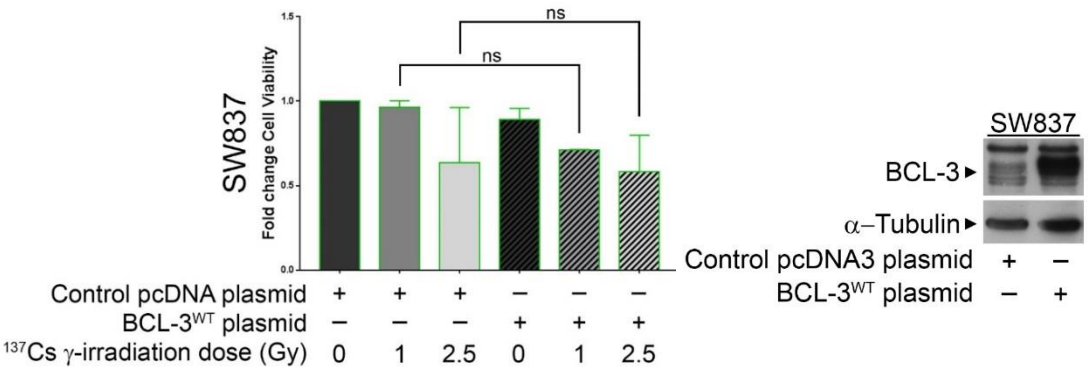

Figure 4.7 SW837 stably over-expressing BCL-3 does not protect cells against γ-irradiation induced cell death

Rectal cancer cells SW837 were stably transfected with WT BCL-3 pcDNA plasmid or control plasmid. Stably over-expressing SW837 cells were seeded into plates and 48 hours after seeding irradiated using a Cs^{137} source (1 and 2.5 Gy). Cells were cultured for 2 weeks following irradiation before being fixed with paraformaldehyde (4 % v/v) and stained with crystal violet (0.5 % v/v). Results show no statistical difference in sensitivity to either radiation dose, in SW837 cells over-expressing BCL-3. Protein lysates were collected from parallel flasks of BCL-3 WT and control plasmid cells and over-expression confirmed with western analysis. Data shown is mean and SD of n = 2 independent experiments. Statistical analysis was performed on GraphPad Prism 7 software using ANOVA (* :P<0.05, ** : P<0.01, *** : P<0.001, NS : non-significant).

4.2.8 Automated spheroid area analysis accurately measures colorectal cancer spheroids embedded in Matrigel and is comparable to manual spheroid diameter measurement

To test cellular response to irradiation in a model that better recapitulated aspects of the 3D tumour microenvironment by enabling cell polarisation (apical and basal cell polarity), cell-cell contact and cell-ECM contact, a 3D tumour spheroid model was utilised. These models are suggested to bridge the gap between 2D in-vitro models and in-vivo animal models (418). 3D spheroid models are commonly used to culture ex-vivo intestinal crypt cells as initially described by Sato et al (275). However, these models do not allow for quantification aside from rudimental analysis of spheroid diameter or a subjective assessment of size/number of spheroids. To facilitate these experiments, initially automation of the spheroid size assessment was developed; this would enable accurate, high throughput analysis of experimental data. Single cell suspensions of cancer cell lines were seeded into 50 µL Matrigel domes, in 24 well plates. Cells were allowed to form early organised spheroids before being imaged on a widefield microscope (schematic shown in Figure 4.8 A with an exemplary SW1463 spheroid shown in B). Z-stack images were obtained that ensured each spheroid within the microscope field was imaged with its widest diameter in focus. Images were then processed either manually to measure individual spheroid diameter or through a MATLAB script (Appendix 6) that measured each individual spheroid area. Optimisation of seeding density was performed for SW1463 cell lines, to enable analysis of individual spheroids, rather than spheroids clumped together. Results showed that spheroids seeded at a lower seeding density (200 cells/50 µL of Matrigel) were easier to analyse using the automated area analysis tool; it was also observed that spheroids at 200 cells/50 µL appear to grow faster after two weeks compared to spheroids seeded

at 400 cells/50 µL (Figure 4.8 C), which was likely to be due to media utilisation by the higher number of spheroids at the end of the experiment.

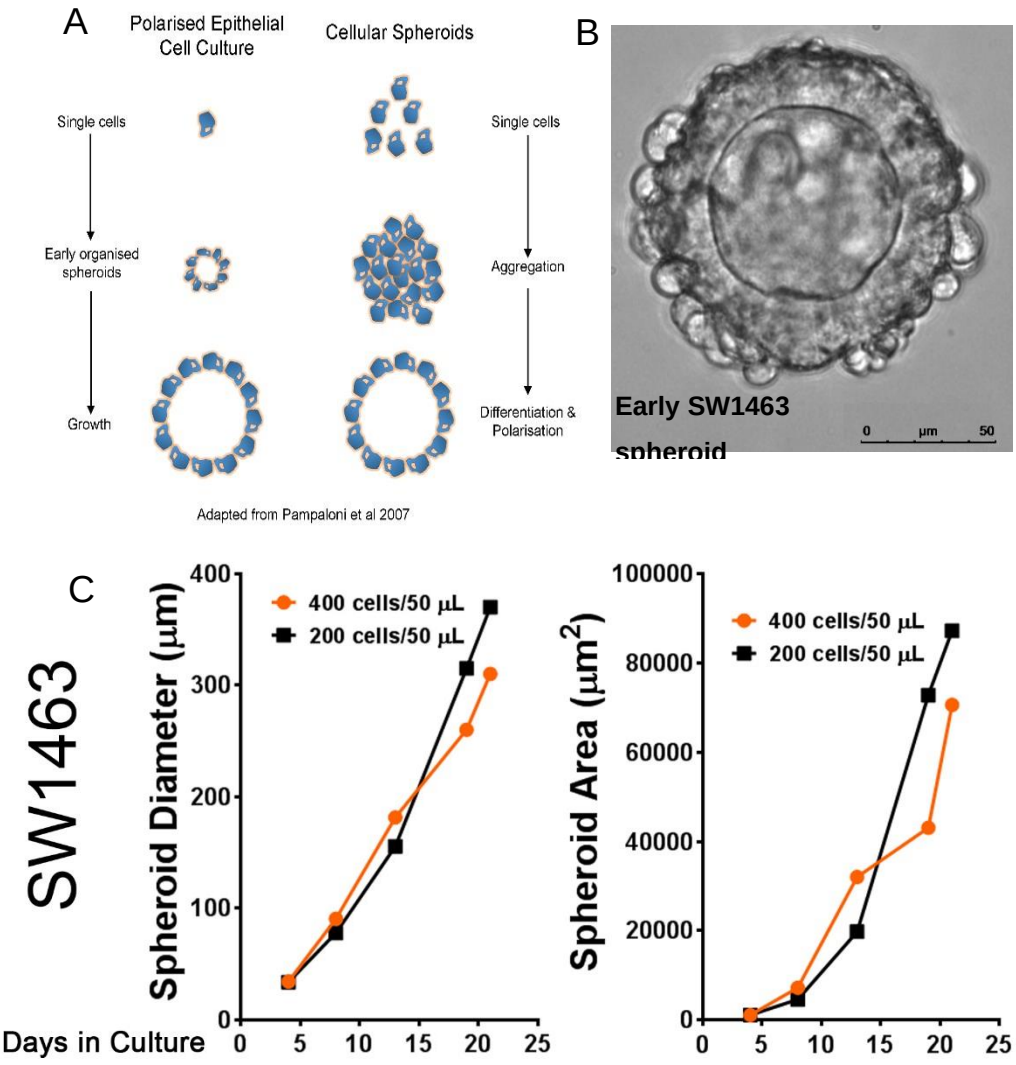

Figure 4.8 Automated spheroid area analysis in the rectal cancer cell line SW1463

SW1463 rectal cancer cells were grown as 3D spheroids in Matrigel. Single cell suspension was mixed with Matrigel to achieve a seeding density of either 200 or 400 cells per 50µL or Matrigel. Cells will form spheroids in Matrigel through a process of cell division combined with polarisation (A) (adapted from Pampaloni et al), leading to early organised SW1463 spheroids with a hollow lumen (B). To ascertain if the automated spheroid area analysis was comparable to the manual diameter measurement SW1463 rectal cancer cells were seeded into Matrigel (400 or 200 cells per 50 µL). Spheroids were measured using a digital ruler on the Leica Application Suite Lite software or a custom MATLAB script (Appendix 6) at day 4, 8, 13, 19 and 21. Results showed that there was no difference in relative size between the two seeding densities. Interestingly it was noted that the lower seeding density grew faster later in the experiment (day 19 and 21) (C). Data shown is the dual analysis of a single experiment with manual diameter measurement and automated area measurement (median (IQR not shown for clarity)).

4.2.9 BCL-3 expression in cells grown in 3D culture conditions

Following optimisation of the 3D culture conditions necessary for high throughput image analysis, I sought to determine if endogenous BCL-3 expression was altered when grown in 3D culture conditions and with 3D culture medium (275, 419). SW1463 and LS174T cells were grown initially in 2D culture but grown with either standard 2D medium of DMEM with 10 % FCS or 3D medium, Advanced DMEM (ADM/F12) supplemented with N2, B27 and N-acetylcysteine (NAC). Western analysis was performed on protein lysates collected form sub-confluent cells after 48 hr of growth in either medium. The results showed that growing cells in 3D culture medium (while in 2D culture flasks) did not change the expression of BCL-3 (Figure 4.9 A). Having observed that the 3D medium did not alter expression of BCL-3 in cells grown in flasks, investigations were performed to identify if BCL-3 expression in spheroid culture was altered. A panel of colon and rectal cancer cell lines (HCA7, HT29, HCT116, HCT15, SW480, SW620, LOVO, LS174T, SW837 and SW1463) were seeded from a single cell suspension into Matrigel (density of 500 cells per 50 µL) and allowed to grow for 14 days. Cells were harvested from the Matrigel (Methods 2.5.2.3) and lysed in cell lysis buffer as per 2D culture lysates. Western analysis was performed, where it was observed that relative BCL-3 expression between cell lines was comparable to the expression of BCL-3 observed in the 2D western blots (Figure 4.9 B). In 3D, high BCL-3 expressing cells were HCT116, LOVO, LS174T and SW1463; low BCL-3 expressing cells were HT29, HCT15, SW480, SW620 and SW837. These data suggest that relative expression between cancer cells lines in 3D is comparable to 2D cultures. As previous experiments showed that exogenous over-expression of BCL-3 failed to induce radio-resistance in rectal cancer cells; the aim was to analyse if stimulation of endogenous expression would result in radio-resistance. Understanding the

physiologically relevant stimulation of BCL-3 expression was considered important for further 3D investigations.

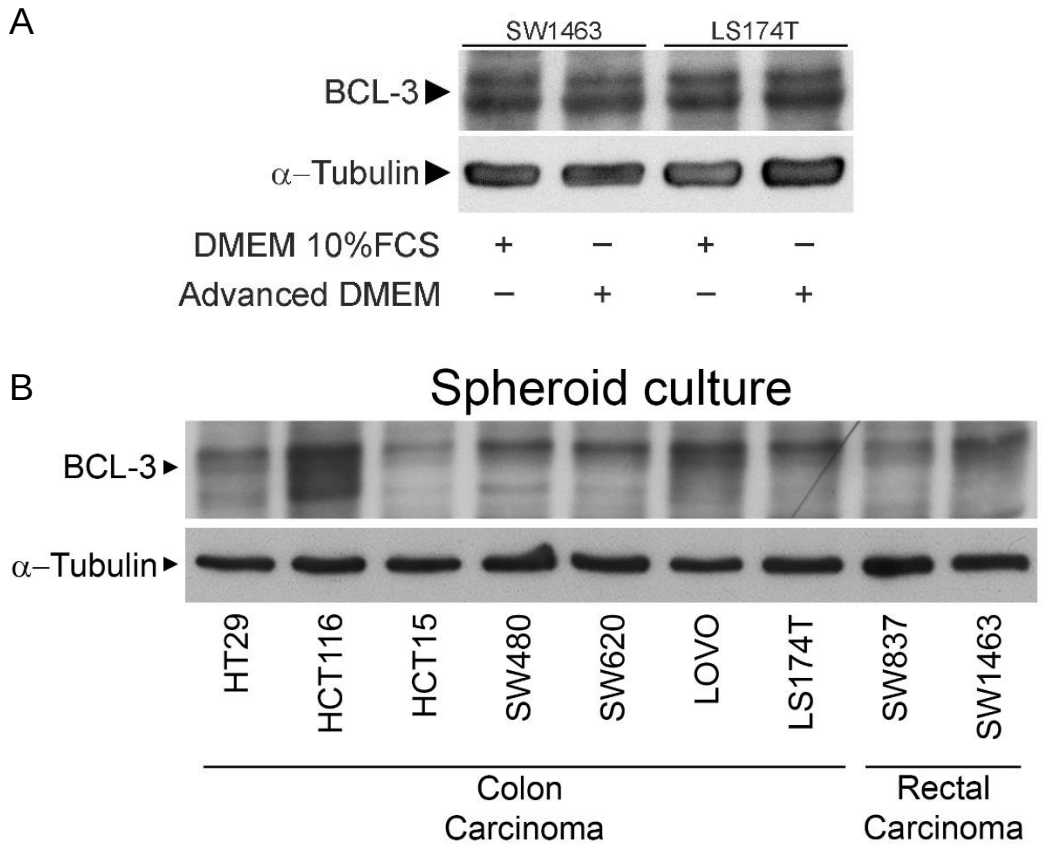

Figure 4.9 BCL-3 expression in 3D culture conditions in a panel of colon and rectal cancer cell lines

BCL-3 expression was initially examined in 2D flasks but using the 3D culture medium (ADM/F12 with N2, B27 and N-acetylcysteine) compared to standard medium (10% DMEM). Protein lysates were analysed by western blot and results showed that BCL-3 expression was not affected in SW1463 or LS174T colorectal cancer cells grown in either medium in 2D (NB both bands are BCL-3) (A). BCL-3 expression was then examined in colorectal cancer cells grown for 14 days in 3D culture. Cells were separated from the Matrigel extracellular matrix and protein lysates produced. Western analysis was performed, where it was observed that BCL-3 expression could be detected and that relative protein expression between cell lines was comparable to the 2D BCL-3 screen (Figure 3.1) (B). It should be noted that it was not possible to collect a protein lysate from HCA7/P colon cancer cells as growth in 3D was too slow to enable enough cell number for analysis.

4.2.10 Fibrosis is a principal component of response to radiation in rectal cancer

Fibrosis is a principal response to neoadjuvant radiation utilised in LARC (409). The assessment of proportion of fibrosis as a ratio to remaining tumour volume determines the regression grade of a tumour (TRG). Current guidance advocates the use of the AJCC/CAP (American Joint Committee on Cancer/College of American Pathologists) TRG for assessment of rectal cancers, where it has been shown to predict prognosis with tumours showing a good response (65, 420). The hypothesis was that radiation induces fibrosis in tumours which may lead to upregulation of BCL-3. To assess the proportion of rectal cancers that exhibited fibrosis following irradiation, tissue samples were used form the ASPIRE cohort study (IRAS 141548, REC 08/H0107/74, NIHR CRN portfolio ID16024). This study collected tissue from patients undergoing neo-adjuvant chemo-radiotherapy for locally advanced rectal cancers. Tumour response grade (TRG) is a histopathological grading system that measures the proportion of tumour replaced by fibrosis following neoadjuvant LCCRT. 92 specimens from the ASPIRE cohort study were assessed for their response to radiation by local pathologist and graded using the AJCC TRG system (TRG 0 no viable tumour cells, TRG 1 moderate response - single or small groups of tumour cells, TRG 2 minimal response - residual cancer outgrown by fibrosis, TRG 3 poor response – minimal or no tumour cells killed). Formalin-fixed paraffin-embedded (FFPE) samples were sectioned to 5 μm and stained with haematoxylin and eosin (H+E). A total of 92 patients were enrolled in the ASPIRE study. Results showed that TRG status correlated with Dukes stage (classification of tumours based on T, N and M-stage combined), T-stage and N-stage of resected tumours (Figure 4.10). Those tumours with a lower TRG had a much higher likelihood of being node negative and of a lower T-stage, which resulted in their lower Dukes classification. Fibrosis and fibroinflammatory

infiltrates were clearly seen in the majority of specimens examined. These results also highlight that residual tumour (TRG2 and TRG3, that has undergone incomplete regression) becomes incarcerated within fibrosis or fibro-inflammatory tissue (Figure 4.10). Previously shown data (Figure 4.1) identified that BCL-3 expression in tumour biopsies may predict response to LCCRT. Following irradiation, the role of the fibrotic stroma in promoting BCL-3 expression is unknown. In the 6-8 weeks of interval between LCRT and surgery it is highly likely that the ongoing interaction between tumour cells and the surrounding stromal cells is deleterious, but the biological result of this incarceration is incompletely understood. Remaining tumour cells are surrounded by fibrosis which may promote BCL-3 expression worsening patient prognosis. Therefore, the aim was to model this interaction in-vivo to understand the possible role of CAFs in BCL-3 expression and radiation response.

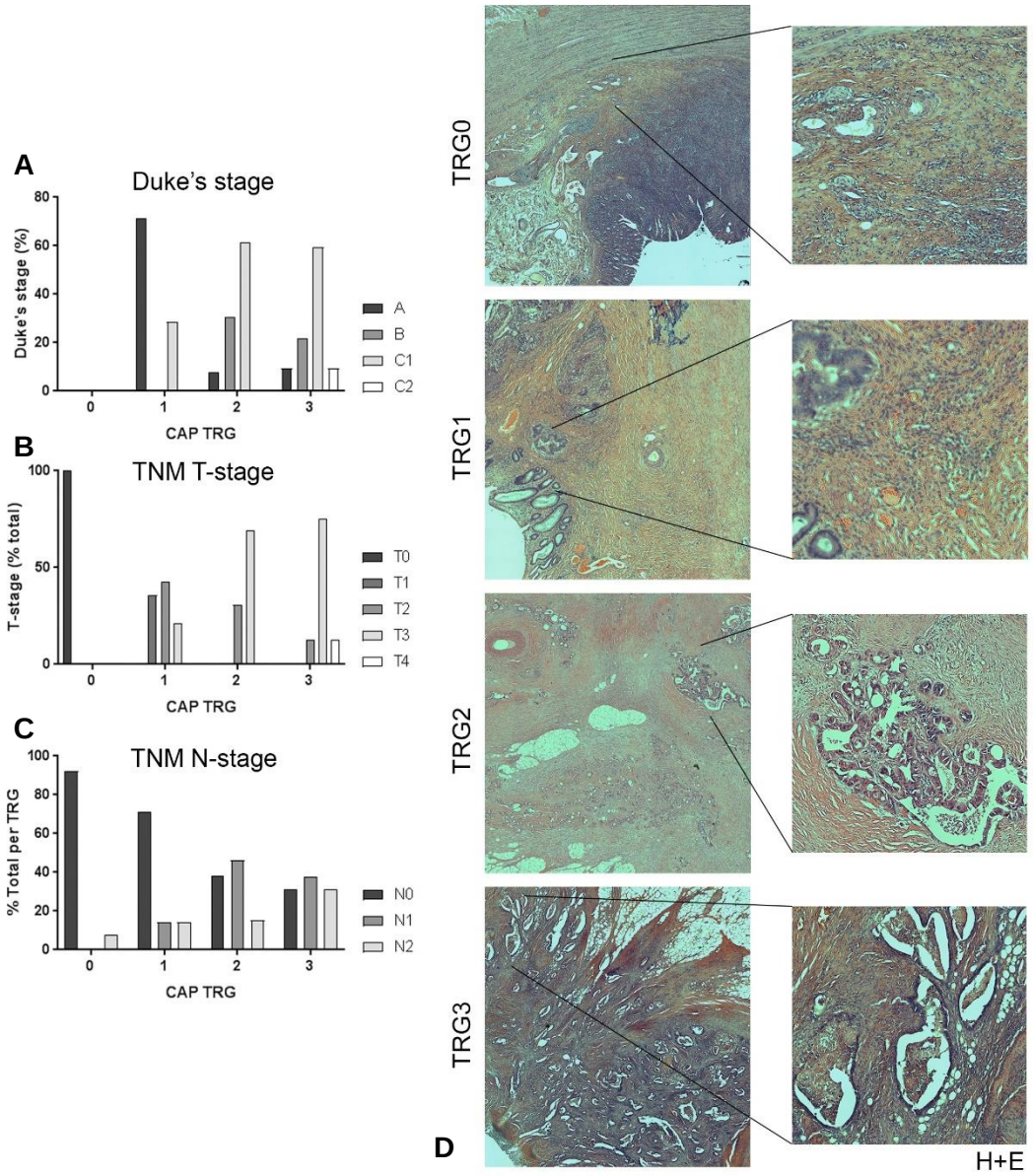

Figure 4.10 Fibrosis is a major component of the response to radiation in rectal cancer and closely related to pathological tumour stage

Samples and data from the ASPIRE prospective observational cohort study (IRAS 141548, REC 08/H0107/74, NIHR CRN portfolio ID16024) was analysed. 92 patients were enrolled and TRG, T-stage, N-stage and Dukes stage was determined in surgical resection specimens following LCRT. Results showed that TRG was closely related to pathological staging (A-C). As TRG increased there were Dukes stage increased with more C1 and C2 tumours in the TRG2 and TRG3 specimens (A), as well as more advanced T-stage (B) and fewer node negative specimens (C). H+E staining was performed on tumour specimens and exemplary slides shown for each grade with areas enlarged for comparison. Results of the staining highlight that with increasing response tumour tissue is replaced by fibrosis or fibroinflammatory tissue. TRG0 specimens show tumour completely replaced by fibrosis. TRG1 and TRG2 specimens show tumour surrounded by fibrosis. TRG3 are tumours with minimal or no response and very little fibrosis (D).

4.2.11 BCL-3 expression is upregulated by IL-6 in rectal cancer cells

BCL-3 is a target of STAT3 signalling and is therefore downstream of cytokines such as IL-6. IL-6 is considered to be one of the principle cytokines released by activated fibroblasts. The hypothesis was that BCL-3 expression is upregulated by IL-6 secretion by fibroblasts into the media. To analyse if BCL-3 expression was responsive to IL-6 cytokine treatment, rectal cancer cells were treated with IL-6 (25ng/mL). Cells were seeded in 2D and treated with IL-6 while still sub-confluent; cells were harvested for analysis 2, 4, 6, 8 and 24 hr following treatment and analysed for mRNA abundance and protein expression using qRT-PCR and western blot respectively. Results showed that there was a significant induction of BCL-3 mRNA following IL-6 treatment and increased protein expression of BCL-3. STAT3 phosphorylation was confirmed following IL-6 treatment. These results suggest that the rectal cancer cell line SW1463 is responsive to IL-6 treatment leading to upregulation of BCL-3, which is potentially due to STAT3 activation. CAFs present in irradiated tissue secrete IL-6, upregulating BCL-3; in spheroid cultures, it was hypothesised that CAFs may increase the growth of CRC spheroids and promote resistance to irradiation.

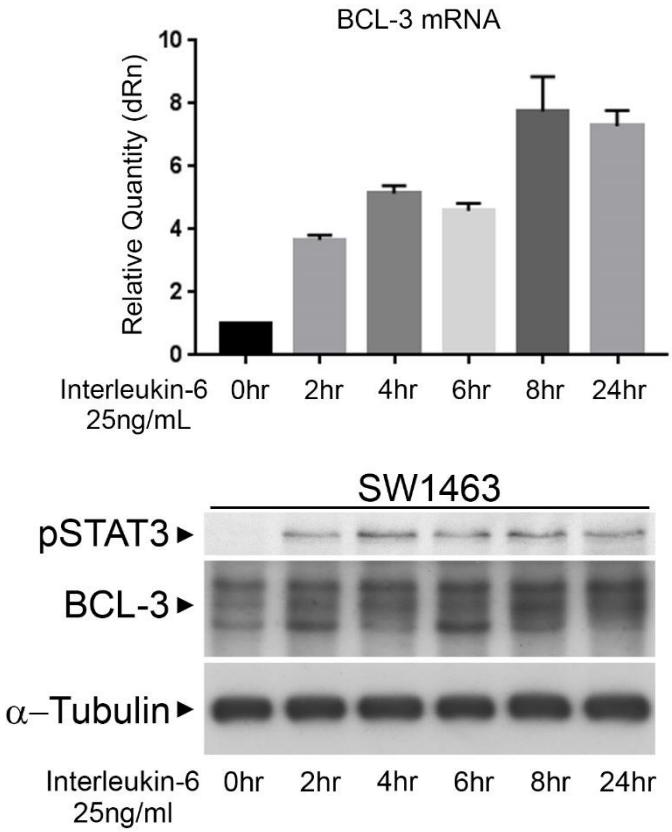

Figure 4.11 Rectal cancer cells upregulate BCL-3 in response to IL-6

SW1463 rectal cancer cells were treated with IL-6 (25ng/mL). mRNA and protein were analysed for upregulation at 2, 4, 6, 8 and 24 hr following IL-6 treatment. Results show that IL-6 induces BCL-3 expression at both the mRNA level and protein level particularly at the 8 and 24 hr post-treatment timepoints, n of 1. pSTAT3 was used to show activation of the IL-6 STAT3 pathway following treatment with cytokine. α-Tubulin was used as a loading control.

4.2.12 Investigating the role of CAFs on 3D growth and sensitivity to irradiation

Fibroblasts are a principle component of the TM. Predominantly, fibroblasts are found in the TM as the more aggressive CAF phenotype, which promotes tumour progression, growth and metastasis. Evidence suggests that CAFs modulate NF-κB signalling but with no investigation into the regulation of BCL-3 (410). To examine the effect of fibroblasts on BCL-3 expression in 3D culture, a co-culture model of colorectal cancer cells and fibroblasts is described. Co-culture of fibroblasts with colorectal cancer spheroids in collagen scaffolds is reported to mimic expression and morphology observed in in-vivo tissue (411). However, it was unknown if introducing colonic fibroblasts into the 3D CRC model, in Matrigel, would result in viable fibroblast cells and/or change in spheroid growth. There was scarce previous data regarding fibroblasts seeding density, therefore, low numbers of fibroblasts were seeded with the standard CRC 3D protocol (described previously) and spheroid growth was measured over time. Fibroblasts that had previously been isolated, by previous members of the group, from human colorectal cancers were grown until 50-60% confluent in T75 flasks before being made into a single-cell suspension. Fibroblasts were seeded into Matrigel at different densities (none, 25, 50, 100 and 200 fibroblasts per 50 μL) while CRC cells were seeded at the standard 200 cells per 50 μL Matrigel. Spheroids were measured at 7 and 11 days following seeding into Matrigel using widefield microscopy, as before, and analysed with an in-house spheroid area assessment programme. Results showed that spheroids from CRC cells (SW1463) grew no differently when co-cultured with and without fibroblasts (morphological images shown are exemplary images from day 11 spheroids). Spheroid growth was unaffected by the low numbers of fibroblasts seeded into co-culture as shown at day 7 and day 11 from seeding. Additionally, it was observed that fibroblasts

remained as single cells or becoming doublets whilst remaining embedded within the Matrigel. These data suggest it is possible to combine colonic fibroblasts within the current 3D CRC spheroid model and measure growth of the CRC spheroids as previously described. Further experiments were required to assess if increasing fibroblast cell number in co-culture altered spheroid growth.

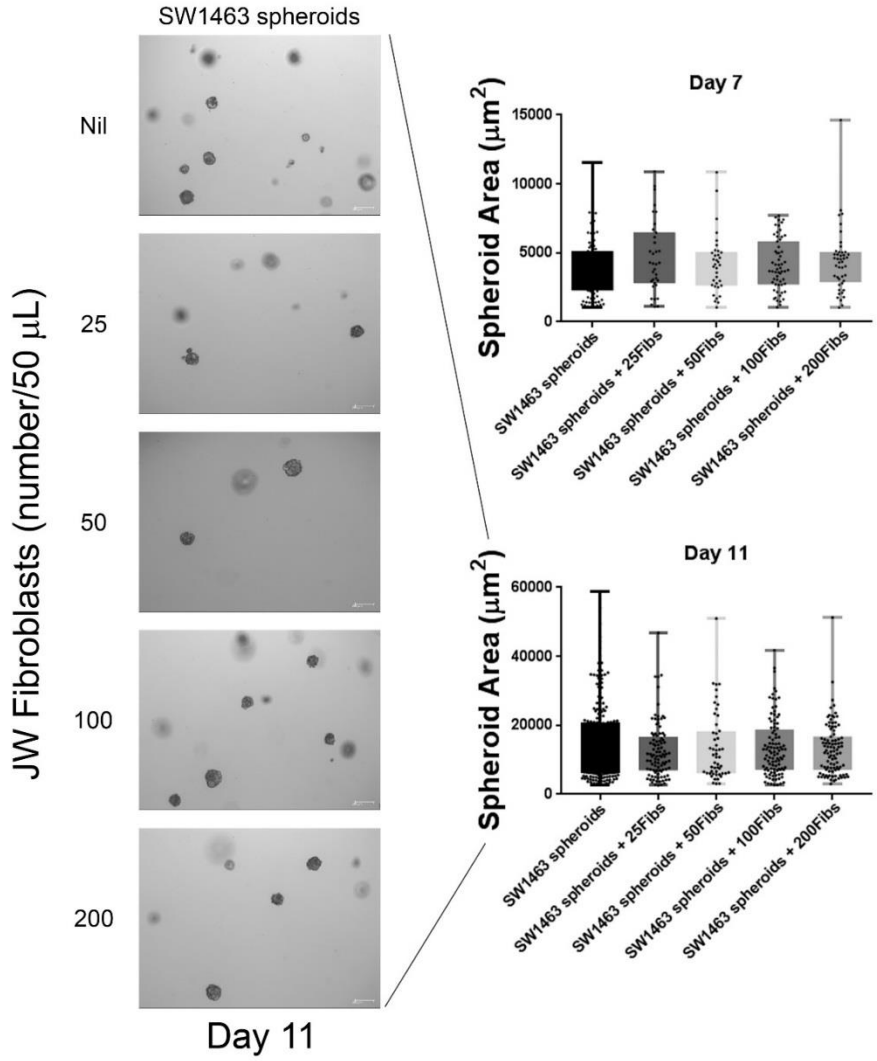

Figure 4.12 Colorectal cancer spheroids grow normally when co-cultured with low numbers of colon fibroblasts

Colorectal cancer cells SW1463 were co-cultured with colorectal fibroblasts JW. Cancer cells (200 cells/50 µL) and fibroblasts (0, 25, 50, 100 and 200 cells/50 µL) were suspended as a single cell suspension in Matrigel and supplemented with ADM/F12 media. Growth was assessed at 7, 11 and 14 days after seeding using widefield microscopy and an in-house automated spheroid assessment protocol. Data showed that low numbers of fibroblasts co-cultured with colorectal cancer cells did not alter the growth or formation of the cancer spheroids. Data shown here is from a single independent experiment with all data points shown. Data was log normally distributed and median and interquartile ranges were used as summary measures.

4.2.13 Growth of SW1463 colorectal cancer spheroids is increased in co-culture with fibroblasts

Having shown already that the addition of small numbers fibroblasts into a 3D spheroid model did not alter growth of spheroids, experiments were conducted to examine if increasing the number of fibroblasts in co-culture increased growth. SW1463 colorectal cancer cells (200 cells per 50 µL) were seeded with JW fibroblasts (500 cells per 50 µL) and spheroid growth was assessed at 7-, 11- and 14-days following seeding using widefield microscopy and an in-house automated imaging programme. Results showed that there was a small but consistent increase in spheroid size over the experimental time-period (Figure 4.13 A+B). It was observed that at the day 7 timepoint spheroids in co-culture with JW fibroblasts were significantly larger with a 40 % increase in growth compared to control (Figure 4.13 B). Growth of SW1463 spheroids increased when co-cultured with fibroblasts at day 11 and day 14 from seeding, which was not statistically significant, suggesting that fibroblasts may be able to enhance growth. However, as the number of epithelial cells increases the fibroblasts are overwhelmed, exhausting the growth effect. Given the small increases in growth observed in these experiments I wanted to know the effect of activating the fibroblasts (to a cancer-associated fibroblast phenotype) on spheroid growth.

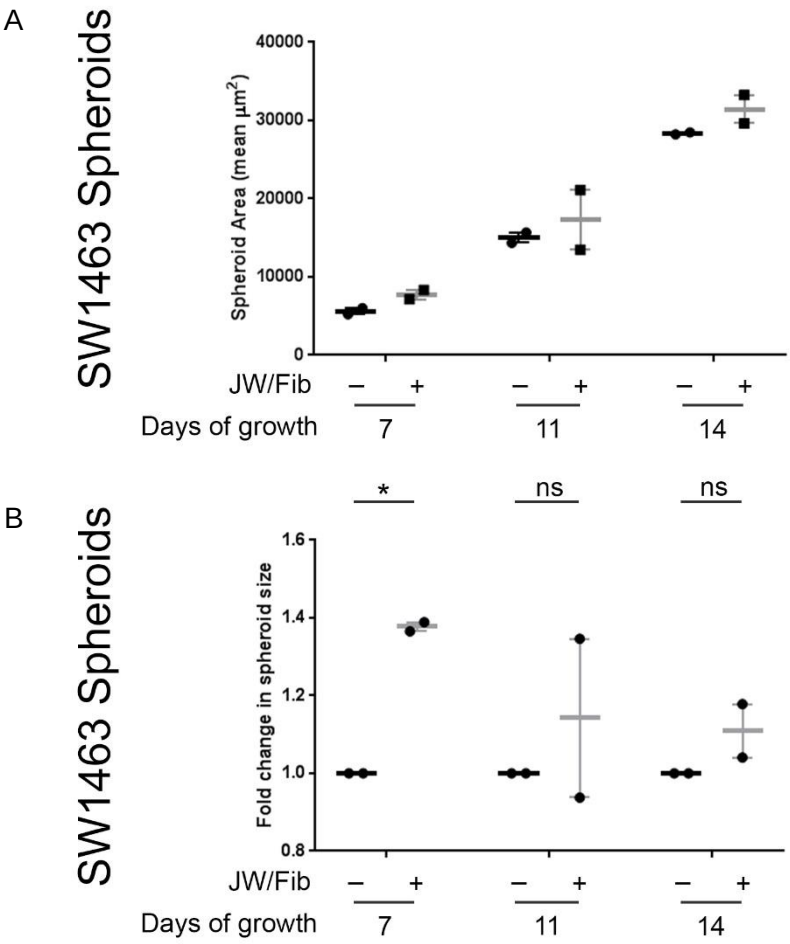

Figure 4.13 Colorectal cancer spheroids require higher numbers of fibroblasts in co-culture to initiate increases in spheroid growth

SW1463 colorectal cancer cells were seeded into 3D culture in Matrigel in conjunction with JW fibroblasts. Fibroblasts were seeded as single cells at 500 cells per 50 µL and SW1463 at 200 cells per 50 µL of Matrigel and supplemented with ADM/F12 media. Growth was assessed at 7, 11 and 14 days after seeding using widefield microscopy and an in-house automated spheroid assessment protocol. Data showed that there were small increases in spheroid size over the 2 weeks of culture which was significant at 7 days following seeding. Data shown here is the combined medians/ IQR from 2 independent experiments with >30 spheroids measured per experiment. Statistical analysis was performed on GraphPad Prism 7 software using ANOVA (* :P<0.05, ** : P<0.01, *** : P<0.001, NS : non-significant)

4.2.14 Growth of rectal cancer spheroids (SW1463 and SW837) is increased with activated fibroblasts

Cancer associated fibroblasts are activated through paracrine TGF-β signalling within the tumour microenvironment (421). This leads to upregulation of proteins that act as biomarkers for this activation, particularly αSMA. It is recognised that CAFs are the predominant phenotype of fibroblasts found within the TM. Previous experiments have shown that co-culture of fibroblasts with CRC spheroids resulted in a small, but statistically non-significant, increase in spheroid growth. To examine if activating fibroblasts increased growth of CRC spheroids co-culture experiments were designed with fibroblasts treated with TGFβ (10 ng/mL). Fibroblasts were pre-treated with TGFβ in T75 flasks for 72 hr prior to being trypsinised, counted and seeded (500 cells/50 µL) with SW1463 or SW837 (200 cells/50 µL) in co-culture (Methods 2.1.4). Co-cultures were supplemented with ADM/F12 media supplemented with N2, B27 and NAC (see methods) and changed three times a week. Additionally, fibroblasts treated with either TGFβ or vehicle control were collected for protein extraction and analysed using western blot to investigate fibroblast activation. Western blot confirmed that expression of αSMA was increased in fibroblasts treated with TGFβ compared to control fibroblasts. CRC spheroid growth was assessed using an in-house spheroid area assessment programme. Results showed that spheroid growth increased when co-cultured with TGFβ activated fibroblasts and compared to vehicle control treated fibroblasts. Results are summarised in (Figure 4.14). Statistical analysis of the data showed in SW1463 spheroids significantly increased growth with TGFβ treated fibroblasts compared to control at 14 days growth (Figure 4.14 A). SW837 spheroids also grew faster with TGFβ treated spheroids and showed significantly increased growth at day 11 (Figure 4.14 B). These data suggest that activated fibroblasts promote a small but significant increase in growth of spheroids in 3D culture

conditions. Further experiments were performed to assess if this was a single fibroblast cell line effect.

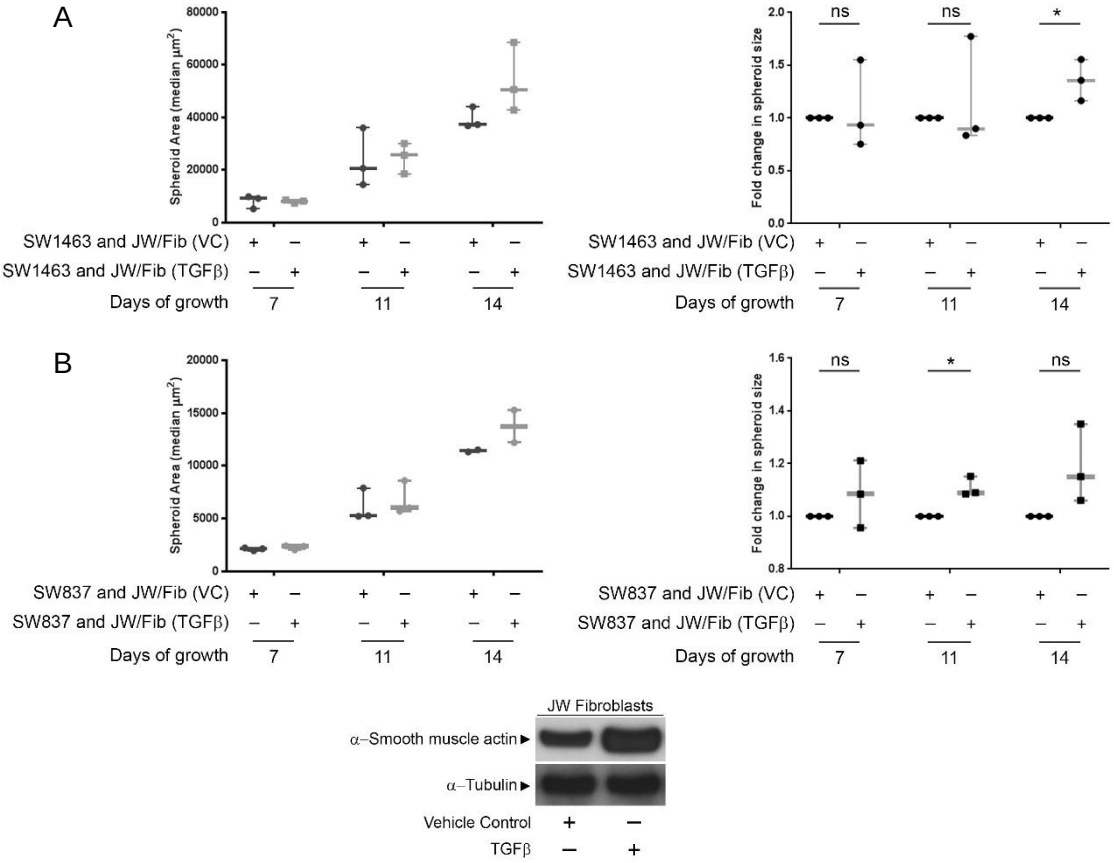

Figure 4.14 Rectal cancer cells co-cultured with activated fibroblasts have increased growth

Rectal cancer cells were co-cultured in Matrigel with activated fibroblasts or un-treated fibroblasts. JW fibroblasts were transformed into an activated phenotype using TGFβ (10 ng/mL) for 72hr prior to seeding into co-culture with colorectal cancer cells. CRC cells and fibroblasts were seeded as single cells in Matrigel and medium (ADM/F12 + supplements) was changed every 2 days to ensure that nutrients were not depleted by the co-culture conditions. Spheroids formed from rectal cancer cells and spheroid area was measured at days 7, 11 and 14 from seeding into Matrigel using an in-house automated spheroid area assessment tool. Data shown is from n=3 independent experiments (individual experiments measured >30 spheroids per condition per time-point). Median spheroid area was combined and fold change in spheroid area (TGFβ compared to control treated fibroblasts) at each time-point was analysed. Statistical analysis was performed on GraphPad Prism 7 software using students t-test (* :P<0.05, ** : P<0.01, *** : P<0.001, NS : non-significant)

4.2.15 Activated fibroblasts from normal and sporadic cancers potentially promote growth of SW1463 rectal spheroids

JW fibroblasts were isolated from a patient with a germline APC mutation, leading to FAP syndrome. To determine if activated fibroblasts from normal colon (SW fibroblasts) and from a sporadic colon carcinoma (SC and CM fibroblasts) also promoted spheroid growth further co-culture experiments were performed. Fibroblasts were seeded into T75 flasks and grown to 50-60 % confluence at which point the fibroblasts were supplemented with TGFβ or vehicle control. Fibroblasts were cultured for 72 hr in these media. For co-culture experiments in Matrigel, fibroblasts were trypsinised and counted prior to being seeded with SW1463. Fibroblasts were seeded at 500 cells per 50 µL Matrigel alongside cancer cells at 200 cells per 50 µL Matrigel. Co-cultures were supplemented with ADM/F12 media supplemented with N2, B27 and NAC (Methods 2.1.4) and changed three times a week. Spheroids were measured at day 7, 11 and 14 from seeding of the co-cultures and images analysed using the spheroid area assessment programme. As before, the results showed that the SW fibroblasts induced increased growth of SW1463 spheroids, particularly at the day 14 time-point following seeding (Figure 4.15). Co-culture with CM and SC fibroblasts resulted in a reduced effect. It should be noted that this data is the median values from single biological replicates and statistical analysis was not performed. These preliminary results suggest that the effect on spheroid growth from fibroblasts in 3D co-culture was not limited to JW fibroblasts and is likely to be independent of the germline mutation in APC that the JW fibroblasts harbour.

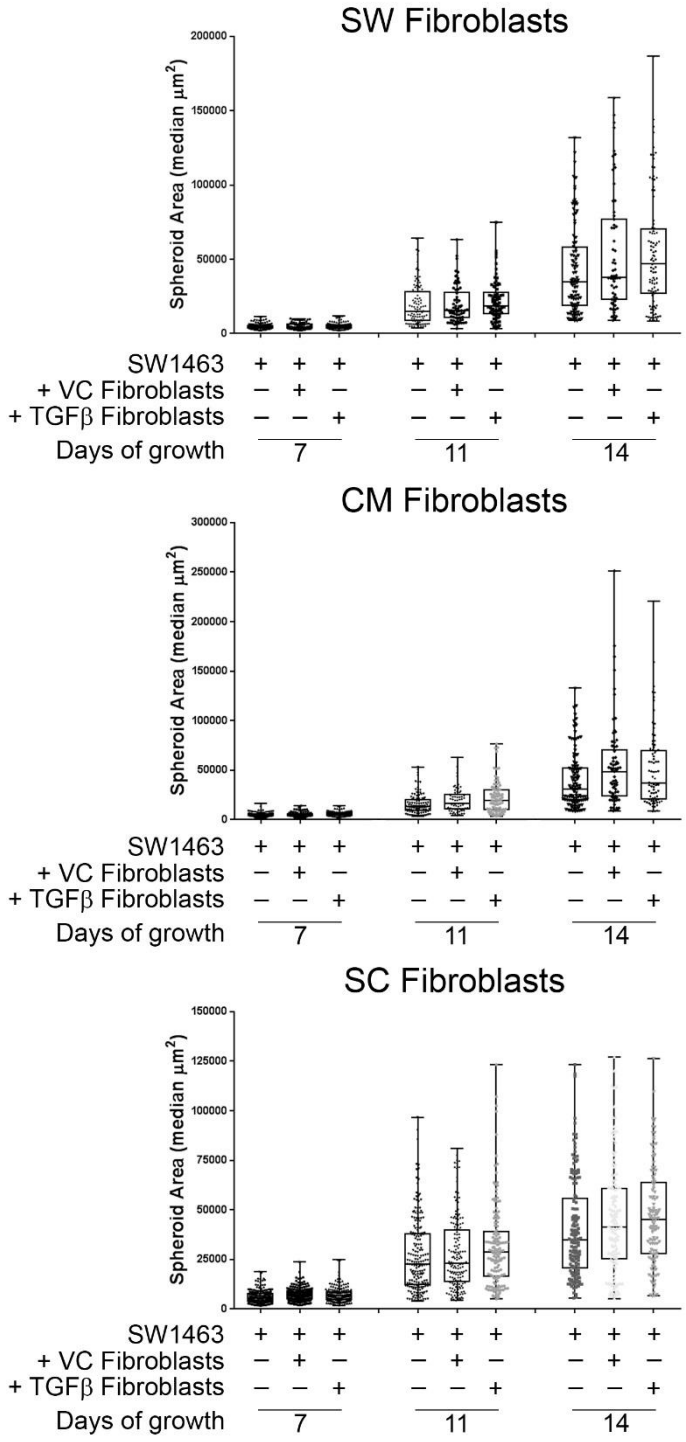

Figure 4.15 Co-culture of SW1463 rectal cancer spheroids with alternative fibroblasts results in increases in spheroid sizes.

Further fibroblast lines were assessed for their effect on spheroid growth when embedded in co-culture with SW1463 rectal cancer spheroids. CM (sporadic) and SW (normal) colonic fibroblasts were treated as previously with TGFβ or VC for 72 hr prior to being seeded at 500 cells per 50µL in Matrigel with SW1463 cells. Results showed that these alternative fibroblasts from non-FAP backgrounds induced increased growth of rectal cancer spheroids, particularly at day 14 from seeding. Data shown is preliminary data showing median values with interquartile range and all data points, from single experiments with >60 spheroids measured per condition at each time-point. Data was analysed in Graphpad Prism software. Statistical analysis was not performed as these were single independent experiments.

4.2.16 Co-culture of colorectal cancer spheroids with fibroblasts does not alter radiation sensitivity of the cancer spheroids

In irradiated tumours, fibroblasts undergo activation and secrete growth factors and cytokines that contribute to tumour proliferation and invasiveness (408). Additionally, previous data showed remaining tumour cells are surrounded by fibroblasts in rectal cancers, that have not had a pCR (Figure 4.10). Given that co-culture of fibroblasts increased tumour spheroid size, investigations were performed to determine if co-culture with fibroblasts altered the radiosensitivity of colorectal cancer cells in this 3D spheroid culture system. To test this, the rectal cancer cell line SW1463 was co-cultured with SW or SC fibroblasts in Matrigel. SW1463 cells were seeded at 200 cells per 50 μL alongside fibroblasts at 500 cells per 50 μL. ADM/F12 medium (supplemented with B12, N2 and NAC) was changed every two days throughout the course of the experiment. Spheroids were irradiated on day 7 of culture following initial imaging. Spheroids were then imaged on day 11 and day 14 (4 and 7 days following irradiation) to assess spheroid growth. Spheroid area was assessed using an in-house automated programme. Data showed conflicting results for each fibroblast cell line used. When SW1463 spheroids were co-cultured with SW fibroblasts, spheroids were more resistant to radiation when not activated by TGFβ (Figure 4.16). Whereas, spheroids co-cultured with SC fibroblasts showed greater resistance to radiation when fibroblasts had been activated by TGFβ, although both were non-significantly different to their un-irradiated controls. Firstly, this suggests that the role of activated fibroblasts depends on the origin of the fibroblast but also suggests that different fibroblasts may respond differently to irradiation itself leading to alterations in effect on the cancer cells. It may also suggest that TGFβ activation of fibroblasts is variable. Therefore, despite activation of fibroblasts in this co-culture system there was little effect on spheroid growth with radiation, and so experiments were

continued without co-culture of fibroblast, but with conditioned media, to increase the concentration of secreted factors.

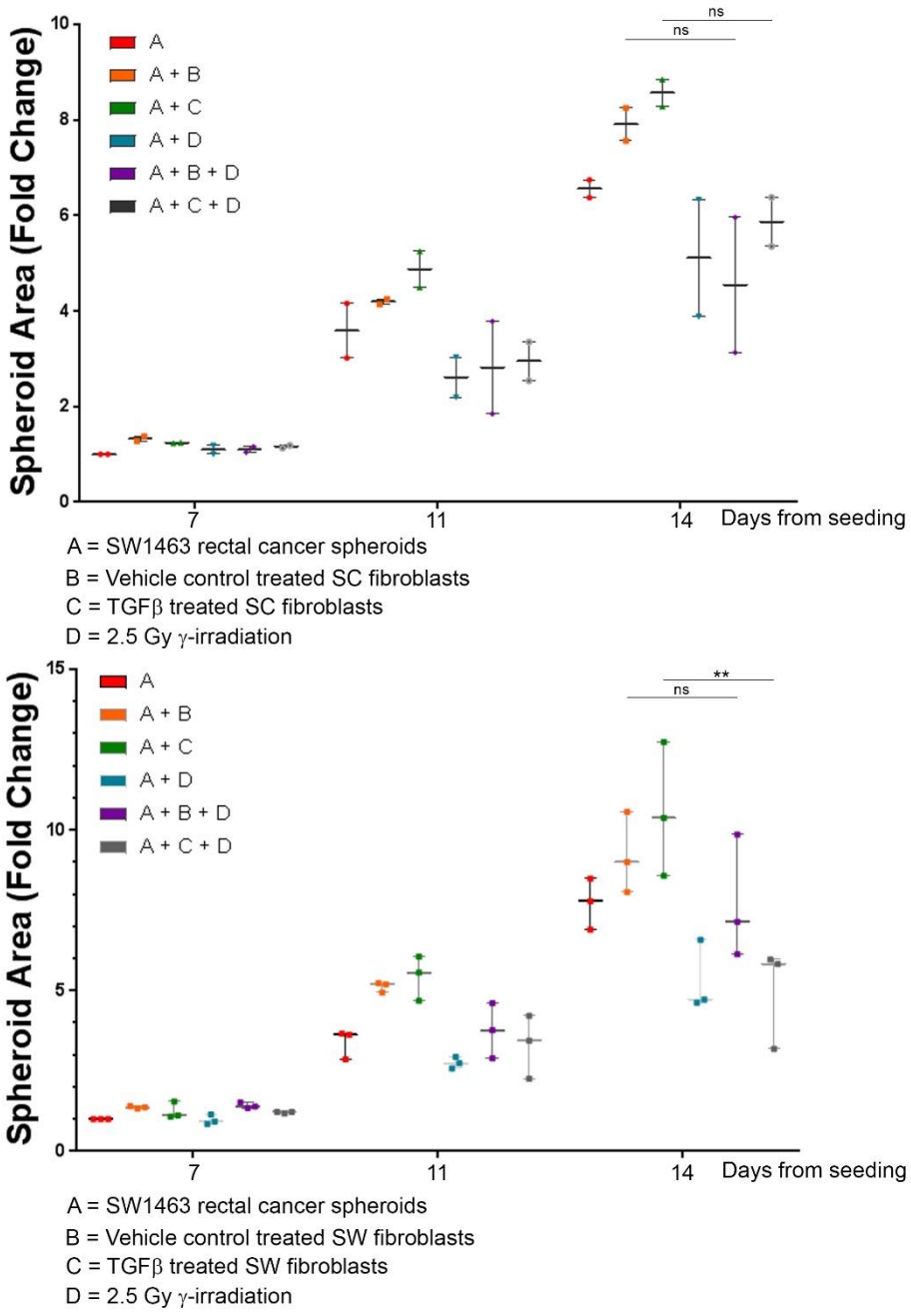

Figure 4.16 Rectal cancer spheroids co-cultured with fibroblasts have increased radioresistance

SW1463 rectal cancer cells were co-cultured as before with SW fibroblasts in Matrigel. Spheroid size was measured on days 7, 11 and 14 from seeding and analysed with an in-house spheroid assessment programme. Media was changed every 2 days through-out the experiment. Results showed that after 2 weeks growth in co-culture SW1463 spheroids grown with fibroblasts were more resistant to 2.5Gy radiation (Day 14 A+B+D). Co-culture with TGFβ treated fibroblasts resulted in Data shown is three independent experiments with each experiment containing two technical replicates (n=>30 spheroids measured per condition per time point). To determine fold change for each condition per time-point, values were compared to control spheroids at day 7. Statistical analysis was performed on GraphPad Prism 7 software using ANOVA (* :P<0.05, ** : P<0.01, *** : P<0.001, NS : non-significant)

4.2.17 Conditioned media from activated fibroblasts results in a small increase in growth of rectal cancer spheroids

Fibroblasts secrete a variety of factors that mediate epithelial tumour cell function in a paracrine mechanism (397). Due the limits of co-culture in Matrigel (Matrigel lost significant structure with high fibroblast numbers) conditioned media was used to increase the concentration of soluble factors in the media that could potentially regulate spheroid growth. Previous experiments showed around an 20% increase in spheroid growth when spheroids were co-cultured with fibroblasts after 2 weeks of growth. Data from other groups that has shown that fibroblasts embedded within 100% Matrigel signal in a predominantly paracrine manner to other cell types embedded within the Matrigel, as the fibroblasts have limited mobility in this ECM. To examine if the effect on spheroid growth was due to paracrine signalling within this 3D system conditioned medium was used. Conditioned media (CM) was collected from activated JW fibroblasts following treatment for 72 hr with TGFβ (creating TGFβ CM) or collected from non-activated fibroblasts treated with vehicle control only (VC CM). Fibroblasts were seeded into T75 flasks and grown to 50-60 % confluence (approx. $1x10^6$-$1x10^7$ cells) at which point the fibroblasts were supplemented with TGFβ or VC media. Fibroblasts were cultured for 72 hr in these media before being washed with 12 mL PBS (wash off media components and TGFβ not found in 3D media). Activated fibroblasts were then supplemented with 3D spheroid media (ADM/F12 and supplements) for 24 hr. Media was collected and centrifuged at 3000 rpm for 3 min to remove any cellular debris. Media was syringe filtered with a 20 µm filter to sterilise and stored at 4°C. SW1463 rectal cancer cells were seeded at 200 cells per 50 µL Matrigel and supplemented with TGFβ CM or VC CM. Results showed that there were increases in SW1463 spheroid area at all time points (7, 11- and 14-days following seeding) (Figure 4.17). Analysis of fold change in median spheroid area revealed statistically

significant increases in relative spheroid size at day 11 (TGFβ CM spheroids larger by 45 % SD +/-6 %, p=0.006 compared to VC CM) and day 14 (TGFβ CM spheroids larger by 20 % SD +/-4 %, p=0.016 compared to VC CM). Using CM allows for increased concentration of soluble factors from fibroblasts rather than the low levels produced from 500 fibroblast cells in co-culture, which resulted in increased spheroid growth. These results suggest that fibroblasts signal to tumour cells in a primarily paracrine manner in this 3D model system.

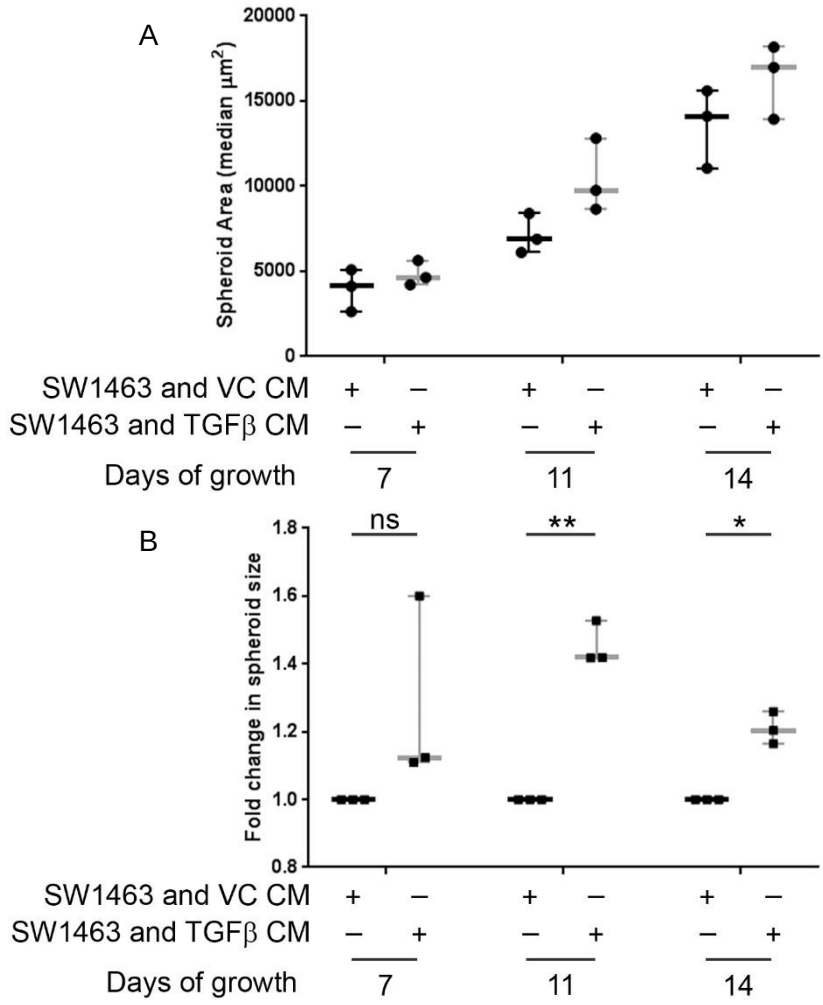

Figure 4.17 Conditioned media from activated fibroblasts increases growth of SW1463 rectal cancer spheroids

SW1463 were seeded into Matrigel at 200 cells per 50 µL and supplemented with conditioned media (CM) every 2 days for the duration of the experiment. Conditioned media was obtained from JW fibroblasts following 72 hr treatment with TGFβ (TGFβ CM) or vehicle control (VC CM) and sterilised using a 20 µm syringe filter. TGFβ CM and VC CM was stored at 4°C for the duration of the experiment. Spheroid growth was measured using widefield microscopy and assessed using an in-house automated programme. SW1463 spheroid areas increased with TGFβ CM compared to control (**A**). On days 11 and 14 from seeding fold change increased significantly in TGFβ CM treated spheroids (**B**). Data shown here is the combined median spheroid area (**A**) and the fold change in spheroid median spheroid size at each time-point (**B**) of n=3 independent experiments. Statistical analysis was performed on GraphPad Prism 7 software using ANOVA (* :P<0.05, ** : P<0.01, *** : P<0.001, NS : non-significant)

4.2.18 BCL-3 expression is promoted by treatment with conditioned media from fibroblasts in a rectal cancer cell line

Activated fibroblasts are recognised to secrete several pro-inflammatory cytokines and growth factors including IL-6. BCL-3 was shown to be upregulated by IL-6 (Figure 4.11), consistent with previous reports (195). Previous experiments showed that CM from fibroblasts resulted in increased spheroid growth of SW1463 cancer cells. To test if CM upregulated BCL-3, SW1463 rectal cancer cells were grown with either normal medium (10 % DMEM), ADM/F12 (supplemented with B12, N2 and NAC), conditioned media from vehicle control treated fibroblasts (VC CM) or conditioned media from TGFβ treated fibroblasts (TGFβ CM). Conditioned media was made as before by growing fibroblast cells in flasks until 50-60 % confluent, following which fibroblasts were treated with either vehicle control or TGFβ. After 72 hr incubation with drug, cells were washed twice with PBS and ADM/F12 (with supplements) was conditioned for 24 hr. SW1463 cells were seeded into flasks and grown to 50-60 % confluence at which point media was changed to experimental media as described. Cells were grown on experimental media for 24 hr before protein lysates were obtained. Lysates were analysed using western blot and blots probed with antibodies to BCL-3 and α-Tubulin. Results showed that BCL-3 expression was upregulated by treatment with both VC CM and TGFβ CM from the JW and SW fibroblast cell lines but not the SC fibroblasts, compared to spheroid medium control (Figure 4.18). These data suggest that BCL-3 is partially responsive to secreted factors from both non-activated and activated (TGFβ treated) fibroblasts in SW1463 rectal cancer cells. It may be that expression of BCL-3 in tumour cells is partially controlled by the stromal compartment in-vivo. It was of interest that BCL-3 was upregulated by both VC CM and TGFβ CM suggesting activation of fibroblasts with TGFβ is not required. It may also explain

why spheroid growth seen in earlier experiments is similar between activated (TGFβ treated) and non-activated (VC treated) fibroblasts.

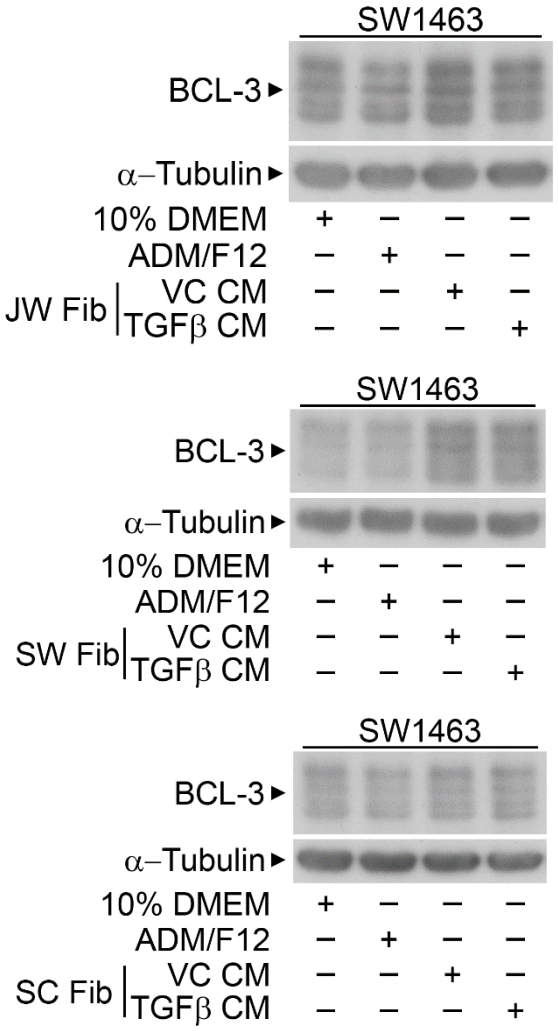

Figure 4.18 BCL-3 expression is increased following exposure to CM from VC or TGFβ treated fibroblasts

SW1463 rectal cancer cells were grown with either DMEM 10 %, ADM/F12 (supplemented), conditioned media from vehicle control treated fibroblasts (VC CM) or conditioned media from TGFβ treated fibroblasts (TGFβ CM) for 24 hr. Conditioned media was harvested from JW, SW and SC fibroblasts. At 24 hr protein was harvested for analysis using western blot. Results showed that there were increases in BCL-3 expression increased with both VC CM and TGFβ CM from the JW and SW fibroblasts lines. There was no increase in BCL-3 with either CM from SC fibroblasts. Western blots are exemplary blots from n=3 independent experiments.

4.2.19 BCL-3 suppression in 3D cultures was not possible using siRNA

Previous results had shown transient transfection with BCL-3 siRNA resulted in radiosensitivity of colorectal cancer cells in 2D (Results 3.2). To determine if siRNA transfection of BCL-3 in 3D spheroid cultures increased sensitivity to radiation, SW1463 rectal cancer cells were grown in Matrigel. Cells were cultured until spheroids formed and were subsequently transfected with BCL-3 siRNA (50 nM) vs control siRNA. 48 hr following transfection spheroid cultures were exposed to γ-irradiation (2.5 Gy) as per the 2D experimental methods (422). Spheroid areas were measured the day following radiation and every two to three days after. Protein and RNA was collected and analysed to verify suppression. Results showed that following transfection of spheroids in 3D there was a transient reduction in BCL-3 mRNA at 48 hr from start of transfection (Figure 4.19 A). BCL-3 protein expression was then examined following isolation of protein from spheroid cultures with results showing that BCL-3 expression was unchanged by siRNA transfection (Figure 4.19 B). Not surprisingly, when growth of spheroids was assessed following transfection with siRNA and combined with irradiation it was shown that there was a robust reduction in spheroid size with irradiation but siRNA transfection had no effect (Figure 4.19 C). These results suggest that BCL-3 transfection in 3D is currently not possible and further work is required to improve the efficiency of siRNA in 3D spheroid cultures. Additionally, shRNA in an inducible system failed to work, despite considerable effort (data not shown). Therefore, I investigated whether BCL-3 inhibitors could increase sensitivity to radiation in 3D.

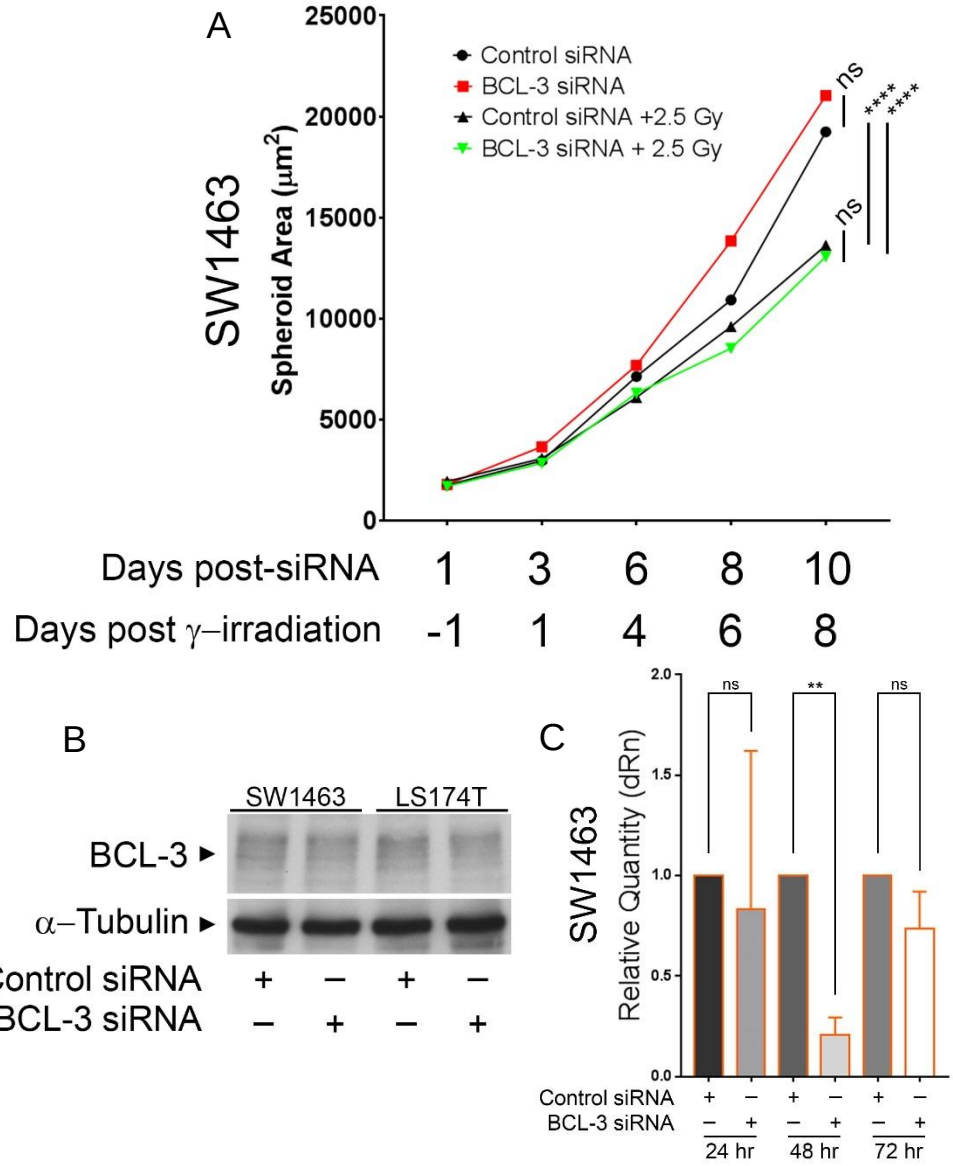

Figure 4.19 Transfection of spheroids with BCL-3 siRNA in 3D does not alter radiation sensitivity

BCL-3 was suppressed in 3D spheroid culture of SW1463 and LS174T. siRNA (50 nM) in lipofectamine RNAiMAX was placed on spheroids already in culture for 24 hr. Spheroids were irradiated 48 hr after initiation of transfection with 2.5 Gy γ-irradiation from a Cs^{137} source. Growth of spheroids was measured using widefield microscopy and an automated area assessment MATLAB code and showed that treatment with siRNA targetting BCL-3 confered no added radiosensitivity (A). There was clear statistically significant (***) decrease in spheroid size with radiation in both contol and BCL-3 siRNA treated spheroids compared to their un-irradiated controls. Western analysis of protein from 3D spheroid cultures showed that BCL-3 protein expression was not suppressed in SW1463 cells, which was confirmed with trial in a second cell line (LS174T) (B). Analysis of BCL-3 mRNA showed a statistically significant transient decrease in BCL-3 mRNA at 48 hr following transfection (C). Spheroid growth is exemplary data from n = 2 experiments (A). Western blots are exemplary from n = 2 experiments (B). mRNA abundance data is means with SD of n = 2 experiments (C). Statistical analysis was performed on GraphPad Prism 7 software (* :P<0.05, ** : P<0.01, *** : P<0.001, NS : non-significant).

4.2.20 BCL-3 inhibitors did not significantly reduce rectal cancer spheroid size

An alternative approach to suppression of BCL-3 signalling was to use novel inhibitors of BCL-3 (a kind gift from Dr. R Clarkson, Cardiff University). These inhibitors function by blocking the interaction of BCL-3 ankyrin repeat domain with either p50 or p52 NF-κB subunits (personal communication). Two inhibitors were obtained BCL-3iA and BCL-3iB. It was noted that BCL-3iB, but not BCL-3iA, was highly unstable as multiple freeze-thaw cycles resulted in reduced efficacy of the compound. Storage and use of BCL-3iB was tightly controlled as a result of these findings; however, it was not possible to obtain comparative biological replicates and therefore data for the BCL-3iB is not shown.

Initially, a dose response to BCL-3iA was performed in SW1463 rectal carcinoma cells grown in spheroid culture. SW1463 cells were seeded in Matrigel as a single cell suspension at 200 cells/50 μL Matrigel. Spheroids were allowed to organise before being treated with BCL-3iA every two days for the length of the experiment (14 days) and imaged on day 7, 11 and 14 from seeding. Spheroid area was assessed using an automated MATLAB script (Appendix 6). Results showed that there was a small, dose dependent but non-significant decrease in spheroid size most apparent at the final timepoint of 14 days (Figure 4.20 A). It was observed that there was a maximal level of spheroid growth suppression at 10 μM, suggesting that 10 μM would be the most appropriate dose to take forward into irradiation experiments.

Additionally, these data appeared to corroborate cell yield experiments performed in 2D culture that showed BCL-3 knockdown reduced cell yield (data not shown). As no significant effect on spheroid size could be determined using the inhibitors, further work is being performed with the focus ablating BCL-3 in colorectal cancer cells using CRISPR.

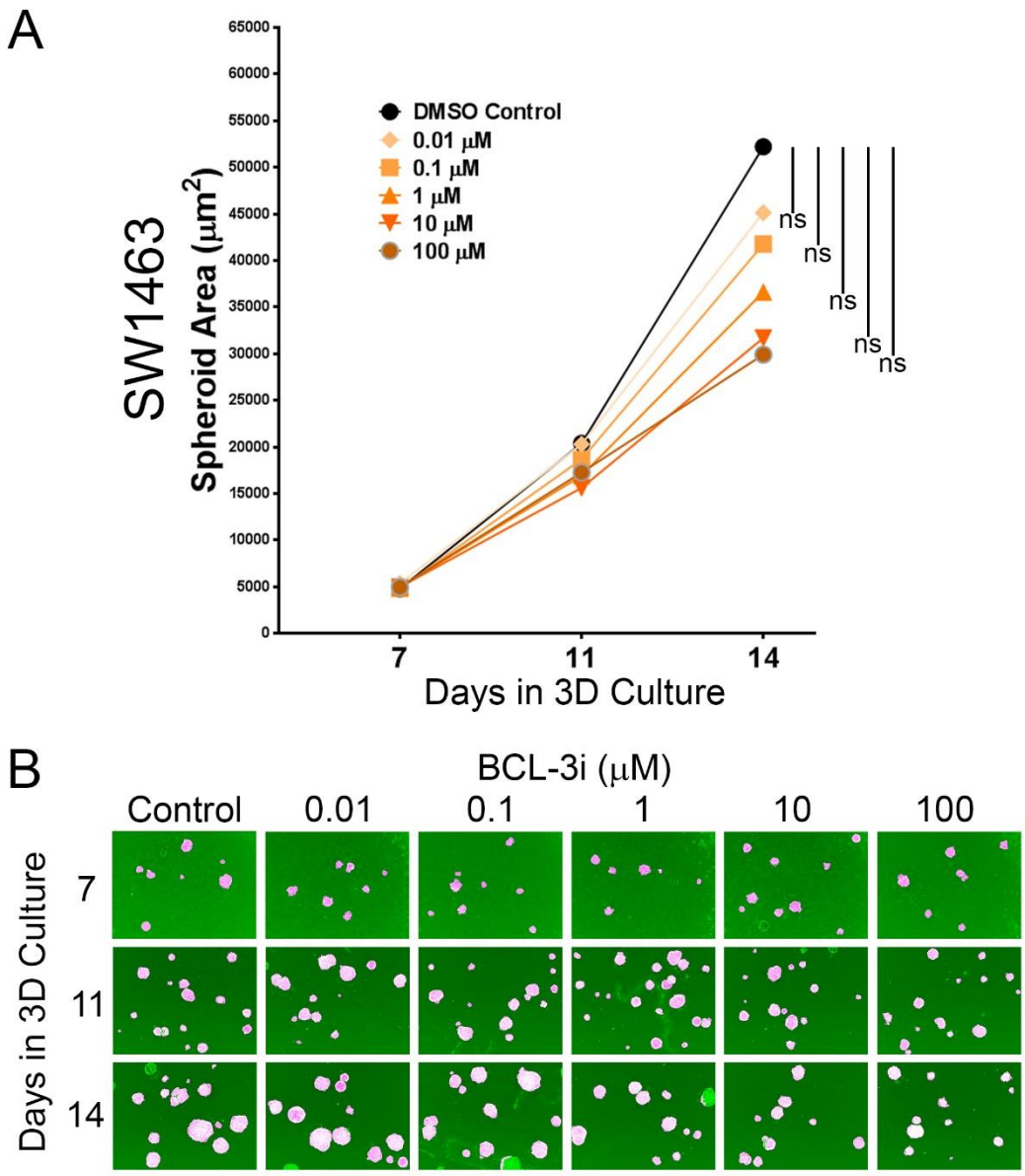

Figure 4.20 BCL-3 inhibitor non-significantly reduces growth of SW1463 rectal cancer spheroids

SW1463 cells were seeded into Matrigel and grown as 3D spheroids. Spheroids were treated every 48 hr, for the duration of the experiment with BCL-3 inhibitor (BCL-3i). Spheroids were imaged on day 7, 11 and 14 following initial seeding. It was observed that increasing concentrations of BCL-3iA reduced the area of SW1463 spheroids (A), however this was not significant for all doses compared to control (DMSO) treated spheroids. The data suggested the effect was most pronounced following 14 days of treatment and statistical analysis was performed at this timepoint. Exemplary images following automated image assessment are shown (spheroids over-layed in a pink mask following analysis) (B). Spheroid area data are means of 4 independent experiments. Image data are exemplary data from the automated image analysis pipeline (n=4). Statistical analysis was performed on GraphPad Prism 7 software using ANOVA (* :P<0.05, ** : P<0.01, *** : P<0.001, ns : non-significant).

4.2.21 Analysing the effect of BCL-3 expression on the DNA damage response

4.2.21.1 BCL-3 suppression promotes increased and persistent γH2AX foci formation following radiation in HCA7/P colon cancer cells

DNA damage results in the formation of irradiation induced foci (IRIF). Phosphorylation of H2AX occurs early in the cellular response to DSBs at the site of damage, and measurement of the γH2AX foci can be used as a measure of radiation sensitivity of cancer cells, as those cells with impaired DDR have persistent γH2AX foci formation (423). As such γH2AX foci formation provide a valuable and robust readout of DDR function.

Following difficulties in regulating BCL-3 in spheroid culture, it was decided to investigate the effect of BCL-3 expression on the DNA damage response (DDR) which could be performed in 2D culture. Therefore, the effect of BCL-3 suppression on the DNA damage response following γ-irradiation was analysed by assessing γH2AX foci formation. HCA7/P cells were chosen as they have high levels of BCL-3, are responsive to combined BCL-3 suppression and irradiation and are relatively easy to image due to their large nuclei (Figure 4.4). BCL-3 was suppressed using siRNA in HCA7/P cells grown on coverslips in 6 well plates (Methods 2.2.1). Cells were irradiated at 48 hr following transfection with 2.5 Gy and compared to control un-irradiated cells. Cells were fixed with 4 % paraformaldehyde for 10 minutes, permeabilised using 0.01 % TritonX for 5 minutes and blocked with 1 % BSA for 30 minutes, prior to being stained with γH2AX antibody and DAPI (1:10000). Coverslips were mounted onto slides using mowiol with DABCO and dried overnight in the dark. Cells were imaged using confocal microscopy and mean γH2AX foci per nucleus assessed and summarised in Figure 4.21. It was observed

that BCL-3 knockdown significantly increased the number of foci per nucleus at 30 min after radiation exposure compared to control (Figure 4.21). Interestingly, BCL-3 suppression appeared to increase both the speed at which foci were formed after radiation (0 min time-point) and led to persistent γH2AX foci (higher numbers of γH2AX foci in BCL-3 suppressed cells at 6 hr and 24 hr compared to control siRNA), although these data was not statistically significant at these later time-points. (Figure 4.21). Representative immunofluorescence images are shown for each condition analysed (Figure 4.21).

Therefore, these data show for the first time that BCL-3 suppression results in an increase in γH2AX foci formation at 30 min following γ-irradiation, which suggests that BCL-3 may be involved in DSB repair.

Figure 4.21 BCL-3 knockdown increases phosphorylated H2AX (γH2AX) foci formation following γ-irradiation

HCA7/P were transfected with BCL-3 siRNA or control siRNA on glass coverslips in 6 well plates and exposed to radiation 48 hr after transfection. Cells were fixed at the time-points shown 0 hr, 0.5 hr, 6 hr and 24 hr (0 hr time-point was placed on ice straight from irradiator and lysed immediately) and stained using γH2AX antibody and DAPI. Cells were imaging with a confocal microscope and γH2AX foci were counted per nuclei (n>30 nuclei per condition) and mean foci per nuclei analysed. Analysis of HCA7/P cells showed increases in initial foci formation, a higher maximal number of foci and prolonged foci formation in cells with BCL-3 suppression after treatment with irradiation. Only the 30 min maximal time-point was statistically significant for increased maximal foci formation in HCA7/P cells. Confocal images for HCA7/P represent foci formation at 30 min following exposure to irradiation in control and BCL-3 siRNA transfected cells. Data is from triplicate experiments combined. Statistical analysis was performed on GraphPad Prism 7 software using ANOVA (* :P<0.05, ** : P<0.01, *** : P<0.001, NS : non-significant).

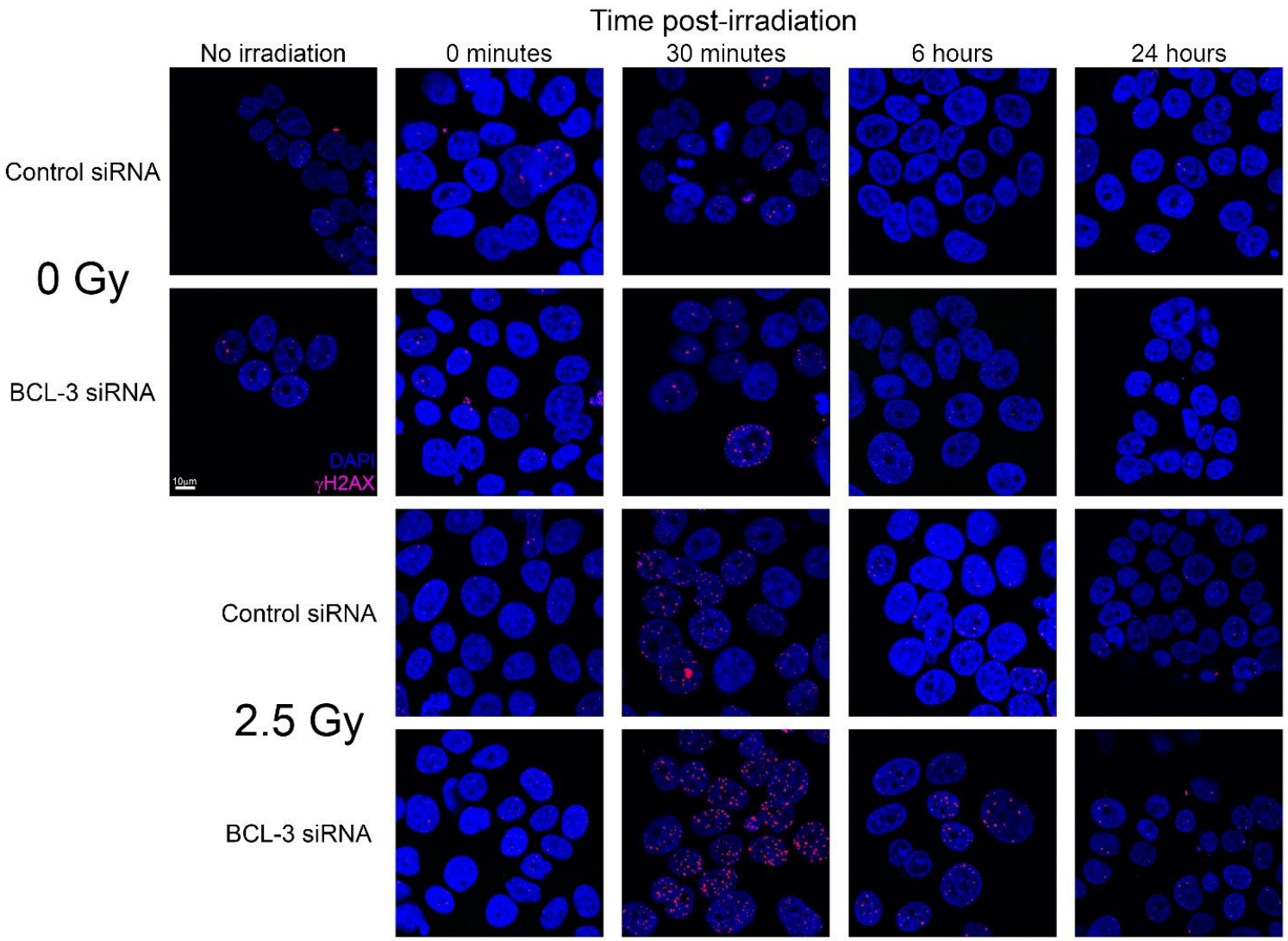
Time post-irradiation
No irradiation
0 minutes
30 minutes
6 hours
24 hours
Control siRNA
0 Gy
BCL-3 siRNA
DAPI
γH2AX
10μm
Control siRNA
2.5 Gy
BCL-3 siRNA

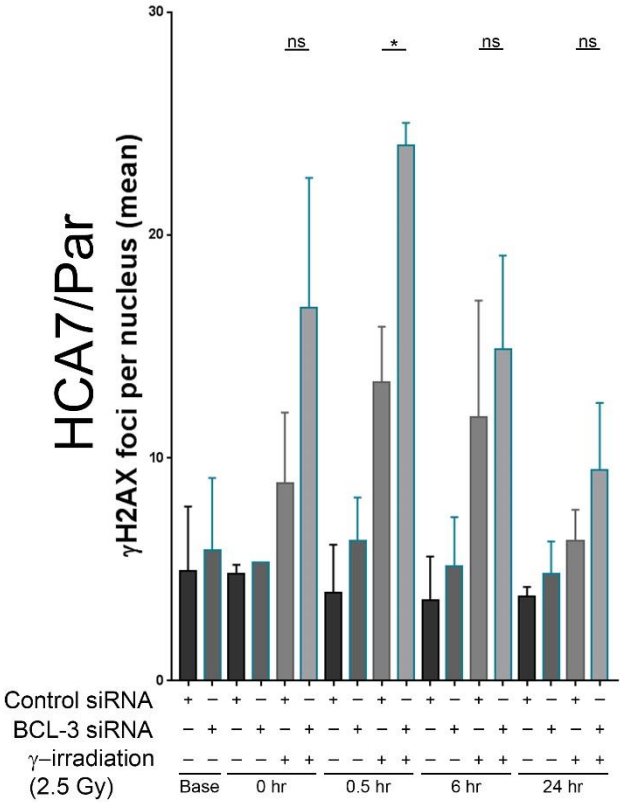
HCA7/Par
γH2AX foci per nucleus (mean)
30
20
10
0
ns
*
ns
ns
Control siRNA
BCL-3 siRNA
γ–irradiation
(2.5 Gy)
Base
0 hr
0.5 hr
6 hr
24 hr

4.2.21.2 BCL-3 suppression increases γH2AX formation in SW1463 cells

The role of BCL-3 is known to be context and cell type specific. Therefore, to determine whether this was a cell specific phenomenon a second colorectal cancer cell line was analysed. SW1463 rectal cancer cells were treated as previously (Results 4.2.21). In addition to the steps outlined before, coverslips were coated with poly-L-lysine due to SW1463 cells adhering poorly to coverslips. Coverslips were treated for 30 minutes with 0.001 % poly-L-lysine before being dried and used as above. SW1463 cells were fixed and analysed at the 30-minute post-irradiation time-point, the time-point were γH2AX foci formation was observed to be statistically significantly increased following BCL-3 suppression in the HCA7/P cell line. It was observed that BCL-3 suppression significantly increased the mean foci per nucleus in irradiated SW1463 cells. Interestingly, it was also noted that while unirradiated control siRNA cells showed very low numbers of γH2AX foci, unirradiated BCL-3 knockdown cells showed increased numbers of γH2AX foci. These data further support the evidence for BCL-3 playing an important role in the DDR.

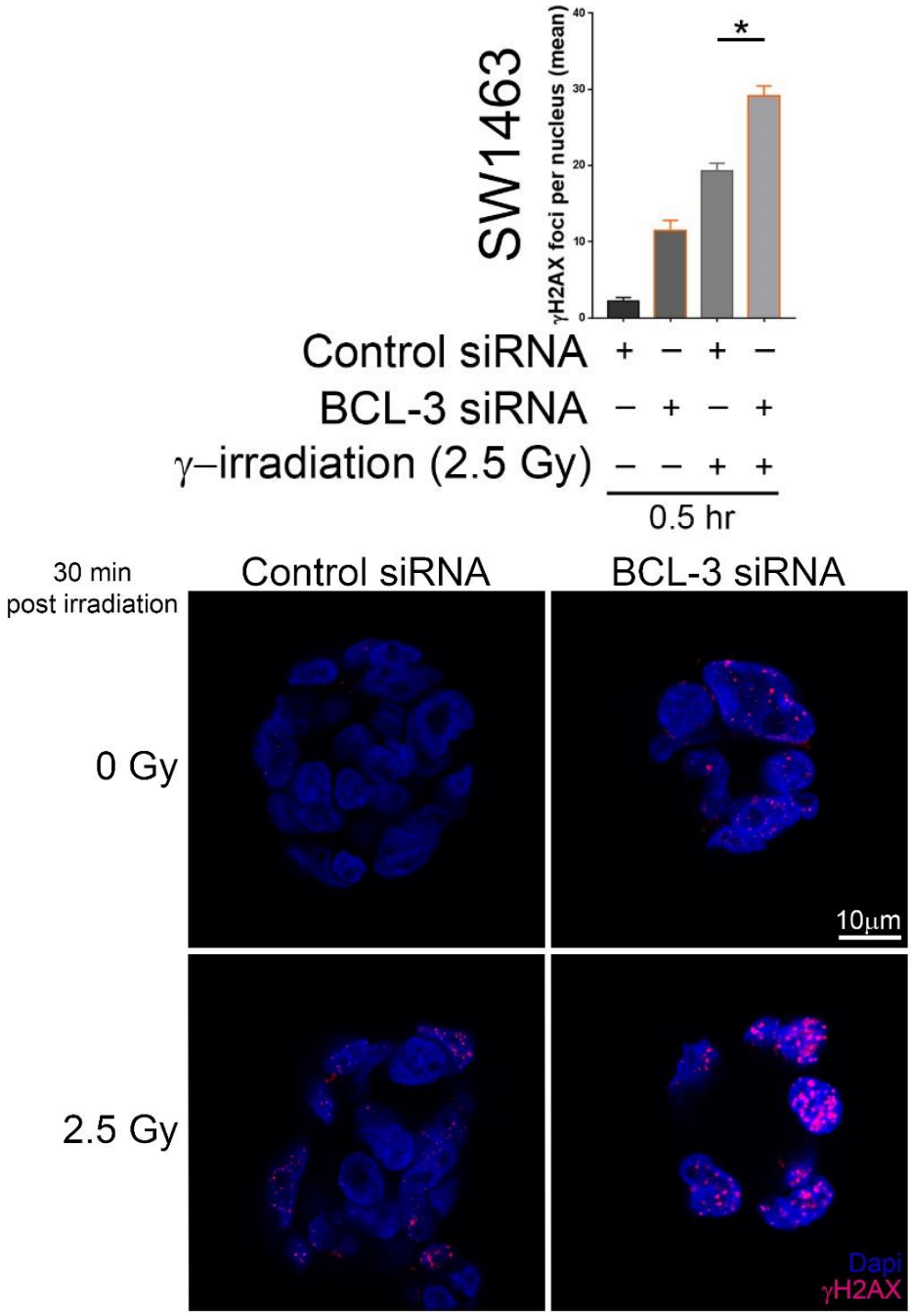

Figure 4.22 Rectal cancer cells SW1463 demonstrate increased γH2AX foci after BCL-3 suppression and irradiation.

SW1463 rectal cancer cells were transfected with BCL-3 siRNA or control siRNA on glass coverslips in 6 well plates and exposed to radiation (2.5 Gy) 48 hr after transfection. Cells were fixed at 0.5 hr following the end of irradiation. Cells were stained using γH2AX antibody and DAPI. After mounting coverslips on glass slides using mowiol, cells were imaging with a confocal microscope. γH2AX foci were counted per nuclei (n>30 nuclei per condition) and mean foci per nuclei analysed. Analysis of SW1463 cells showed increased foci/nuclei in cells with BCL-3 suppression after treatment with irradiation. Confocal images for SW1463 cells represent foci formation at 30 min following exposure to irradiation in control and BCL-3 siRNA transfected cells. Data is from two independent experiments combined. Statistical analysis was performed on GraphPad Prism 7 software using ANOVA (* :P<0.05, ** : P<0.01, *** : P<0.001, NS : non-significant).

4.2.21.3 Does BCL-3 inhibit homologous recombination?

Further investigations were performed to analyse the mechanism by which BCL-3 suppression increased radiation sensitivity. PARP inhibitors are known to be highly effective in cells with defective components of the HR DSB repair pathway (424). BCL-3 suppression was shown to increase the magnitude of γH2AX foci formation at 30 minutes following radiation, suggesting a defect in DSB repair. It was hypothesised that If BCL-3 suppression increased the sensitivity of cells to PARPi this may suggest that BCL-3 was regulating HR.

To test this hypothesis, BCL-3 was suppressed using siRNA (50 nM) in suspension in 24 well plates in SW1463 cells, as these cells were high BCL-3 expressing cells and showed increases in γH2AX foci following irradiation (Figure 4.22). At 48 hours following transfection cells were treated with the PARPi, veliparib (ABT-888), for 24 hours following which cells were transferred back onto normal medium. Cell viability was measured 96 hours following PARPi treatment (425), using a crystal violet stain (Methods 2.3.2) and quantified with a spectrophotometer at 594 nm. It was observed that BCL-3 suppression did not sensitise SW1463 cells to PARPi (Figure 4.23). PARPi treatment resulted in a reduction in cell viability at a dose of >10 μM in SW1463 for both non-targeting and BCL-3 siRNA treated cells.

These data suggest that as BCL-3 knockdown does not sensitise cells to PARPi, the mechanism by which BCL-3 suppression increases radiosensitivity may not be through HR. The mechanism by which BCL-3 promotes radiation resistance is yet to be determined and is the subject of future work.

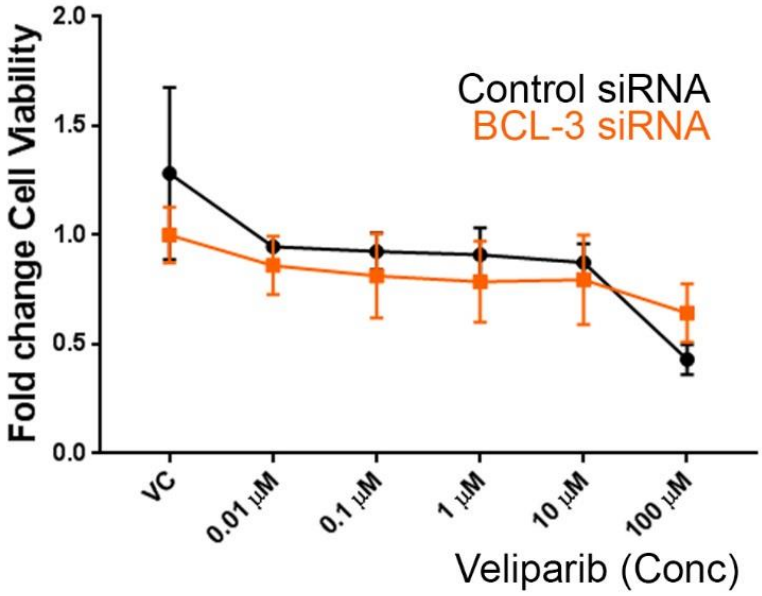

Figure 4.23 BCL-3 suppression does not sensitise rectal cancer cells to Veliparib (PARP inhibitor)

SW1463 rectal cancer cells were transfected with BCL-3 siRNA or control siRNA and following 48 hr of transfection treated with Veliparib (PARPi) or vehicle control. Veliparib was used at logarithmic concentrations (0.01, 0.1, 1, 10 and 100 μM). Cell viability was measured 4 days following drug treatment using a crystal violet assay. Results showed that BCL-3 suppression did not sensitise cells to PARPi. Data shown is combined data from n=2 independent experiments. Statistical analysis was performed on GraphPad Prism 7 software using ANOVA (* :P<0.05, ** : P<0.01, *** : P<0.001, NS : non-significant).

4.3 Discussion

The aim of this chapter was to investigate the role of BCL-3 in irradiation in rectal cancers using both ex-vivo tissue specimens, in-vitro and spheroid models of rectal cancer. Initial observations, from rectal cancer tissue biopsies collected as part of the ASPIRE study, suggested that BCL-3 expression in tumour biopsies correlated with the subsequent response of the tumour to LCCRT, as measured by the AJCC-CAP TRG (Appendix 3 American Joint Committee on Cancer/College of American Pathologists Tumour Regression Grade). These preliminary results from the ASPIRE study and work is ongoing to analyse the whole cohort of patients' biopsies to assess whether there is a correlation between BCL-3 expression and therapeutic response. However, this result was sufficiently interesting to investigate whether BCL-3 expression conferred resistance to irradiation induced cell death.

BCL-3 is thought to be upregulated by IL-6 through STAT3 (195). In the tumour microenvironment CAFs are recognised to secrete IL-6. Further data from the ASPIRE cohort study showed that in those tumours with a partial response to irradiation, cancer cells are surrounded by dense fibrotic tissue. 3D models of colorectal cancer are thought recapitulate some of the features found within the tumour microenvironment, including cell-cell interactions and cell matrix interactions (418). Therefore, to examine if BCL-3 was regulated by fibroblasts in-vitro, a cancer spheroid model was developed. Results from the cancer spheroid model showed that there were small increases in spheroid growth when co-cultured with fibroblasts or fibroblasts that had undergone activation with TGFβ. However, the co-culture of CAFs with cancer spheroids did not result in resistance to irradiation of the spheroids. Previous data has shown that stromal cells contribute to therapy resistance in-vivo and in-vitro (426). The model used in experiments presented here was limited as it was only possible to co-culture very

low numbers of fibroblasts with the tumour spheroids. This was due to utilisation of media components and disruption to the matrix with large number of fibroblasts (images not shown). Additionally, it was not possible to determine BCL-3 expression in the spheroids when in co-culture with fibroblasts due to being unable to separate the two cell types for western blot and being unable to examine BCL-3 expression by confocal due to antibody limitations. Given that the CAFs were thought to be signalling to the cancer spheroids in a paracrine mechanism (427), further investigation was performed to see if conditioned media from fibroblasts could promote growth of cancer spheroids in this 3D system. Results identified that conditioned media increased spheroid growth and that when cells were cultured with conditioned media in 2D there was a small increase in BCL-3 expression. Further investigation is necessary to analyse if BCL-3 is upregulated at the transcriptional level, using qRT-PCR, following growth in 2D or 3D spheroids with fibroblast conditioned media. Additionally, as CM experiments showed a greater effect on growth, work could be performed to analyse the effect of fibroblast conditioned media on the radiation response of rectal cancer spheroids. Although, this data would have to be interpreted with caution as the BCL-3 dependent effect on radiation response would likely be minimal given the small increases in BCL-3 expression observed after spheroids were grown in conditioned media.

The 3D spheroid model was also limited as it was not possible to knockdown BCL-3 using siRNA. As we described in the published report (422), it was possible to introduce fluorescently tagged siRNA into spheroids but this did not result in robust changes in mRNA levels (only at 48 hr) or importantly protein levels. The key feature of this model is to have spheroids that grow before inhibiting BCL-3 activity combined with irradiation. Therefore, methods that induce permanent knockdown (shRNA) or knockout (CRISPR) of BCL-3 may not be suitable for these experiments as recent work has shown that BCL-3 affects the colony forming

efficiency as well (Legge et al, 2018 accepted in Disease Models and Mechanisms with revisions). Ideally, an inducible system such as a doxycycline-inducible shRNA could be used to induce knockdown of BCL-3 prior to additional treatments such as irradiation. Additionally, it was found that over-expression of BCL-3 did not induce radioresistance within rectal or colon (preliminary data not shown) tumour cells. BCL-3 is a highly post-translationally modified protein, particularly by phosphorylation (203), and it could be that the over-expressed protein does not have the same level of modification in a saturated system. Alternatively, it could be that despite normal process and PTM of BCL-3, over-expression of BCL-3 occurs in a system where BCL-3 is already saturated, leading to no additional function with over-expression. The use of a novel BCL-3 inhibitor failed to increase radiation sensitivity in the rectal cancer spheroid model. These inhibitors are thought to inhibit the interaction between BCL-3 and atypical NF-κB homodimers. Currently, it is not clear if the effect of BCL-3 on radiation sensitivity is dependent on its function as a transcriptional co-regulator with atypical NF-κB subunits or through an alternative function. Given the BCL-3 inhibitor failed to induce sensitivity to radiation it is suggested that the mechanism of action may be NF-κB independent.

In summary, the 3D spheroid model is a useful model to examine the regulation of cancer spheroid growth by other cell types in conjunction with treatments such as irradiation. Further work also needs to be completed to examine the phenotype of CRC spheroids with fibroblast conditioned media and irradiation.

Following the observation from tumour biopsies that BCL-3 expression correlated to TRG, cell viability assays were performed using RNA interference of BCL-3 to investigate if suppression of BCL-3 in rectal cancer cells led to an increase in radiation sensitivity. Importantly, results from this chapter show that BCL-3 knockdown in-vitro induces radiosensitivity in rectal and colon cancer cells, supporting the hypothesis that BCL-3 promotes radiation resistance in rectal

cancers. This corroborates other published work which has shown that BCL-3 suppression sensitises cells to other types of DNA damaging agents, such as UV radiation (239) or alkylating chemotherapy (428). In one of these studies the mechanism was p53 dependent, which is unlikely to be the case in the cell lines investigated here, which have either WT or mutant p53. Interestingly, stable over-expression, performed in a rectal cancer cell line with low basal expression of BCL-3, failed to induce resistance to radiation. The reason why increased expression had no effect may principally be as a result of prior saturation of BCL-3 interacting partners such as atypical NF-κB homodimers (discussed in Introduction 1.6.5), alternative transcriptional regulators or possibly histone modifiers. Furthermore, to examine the effect of BCL-3 in radiation in more detail, experiments were performed to analyse γH2AX foci formation after irradiation in cells with loss of BCL-3. BCL-3 knockdown increased γH2AX foci significantly following irradiation compared to control. Phosphorylation of H2AX or γH2AX is a key regulatory event in the DDR (367, 368). γH2AX foci formation following irradiation are a critical measure of a cells' sensitivity to irradiation, as cancer cells that clear γH2AX foci quickly being more resistant to irradiation (429, 430).

The use of DNA damaging agents in rectal cancer is a mainstay of current therapy. However, there is significant failure of therapy in some patients with poor or absent response to therapy (Introduction 1.2.1.2). Local recurrence rates in rectal cancer have been significantly reduced with optimisation of surgical technique and addition LCCRT. However, overall survival and disease-free survival have not seen such significant improvements. Response to therapy is a marker of better prognosis for patients with rectal cancer and so perhaps now the focus should be on improving the TRG to give patients the best prognosis. The data presented here suggest that BCL-3 suppression in rectal cancers results in increased sensitivity to

radiation and other DNA damaging agents and therefore identifying clinically achievable BCL-3 suppression should remain a priority for future research.

5 Discussion

Colorectal cancer remains a major source of mortality in westernised nations, particularly the UK. Rectal cancer is the most common anatomical location of CRC and while surgery remains the principal therapeutic option, in LARC, patients are offered pre-operative chemoradiation. This therapy aims to reduce local recurrence and induce tumour regression, which confers with it an improved prognosis. Critically, a large proportion of patients fail to respond to this therapy, leaving them at risk of the side effects and the sequelae from therapy itself but also with a worse prognosis. Stratification of patients into those who will respond to therapy and those who will not respond would enable patient treatment to be tailored. Additional therapy could be instigated in those patients who were not expected to respond, improving treatment efficacy and tumour regression, leading to better prognosis. The atypical IκB protein, BCL-3, is a co-regulator of NF-κB transcription. It is known to be upregulated in a subset of colorectal cancers, with high expression of BCL-3 also known to confer a poorer prognosis for patients following therapy (240, 241); however, its role in the survival and response to treatment of rectal cancer was unknown. The aim of this project was to investigate the role of BCL-3 in evasion of apoptosis and therapy response in rectal cancer.

Data shown here identifies that suppression of BCL-3 expression (regulated by fibroblasts from the tumour microenvironment in a paracrine manner) could increase the therapeutic response in rectal cancer patients.

5.1 BCL-3 and apoptosis

The aim of the first chapter was to understand the role BCL-3 plays in apoptosis. Recent data, from this group, showed BCL-3 to be anti-apoptotic in colon cancer cells (257). Evasion of apoptosis is a critical hallmark of malignancies and enables cell proliferation to go unchecked (224). The investigations described here identified that BCL-3 is found at the BCL2L11 promoter alongside p52, where it potentially facilitates development of repressive chromatin, as marked by reduced

histone acetylation, leading to downregulation of Bim transcription and evasion of apoptosis. It has been shown previously that BCL-3 functions to repress transcription through interaction with HDACs (162, 219, 231). Interestingly, previous studies have shown that Bim transcription is repressed by non-canonical NF-κB heterodimers, p52:RelB, in association with HDAC4 (153). This led to resistance to apoptosis, promoting drug resistance (153) and propagated autoimmunity by blocking apoptosis in immune cells (431). There is also evidence from a BCL-3 knockout mouse model showing that activated T cells die rapidly, mediated via Bim upregulation (237). Given the various mechanisms by which BCL-3 has been shown to interact and alter the function of NF-κB homodimers there are several alternative mechanisms which may explain how BCL-3 may be repressing Bim.

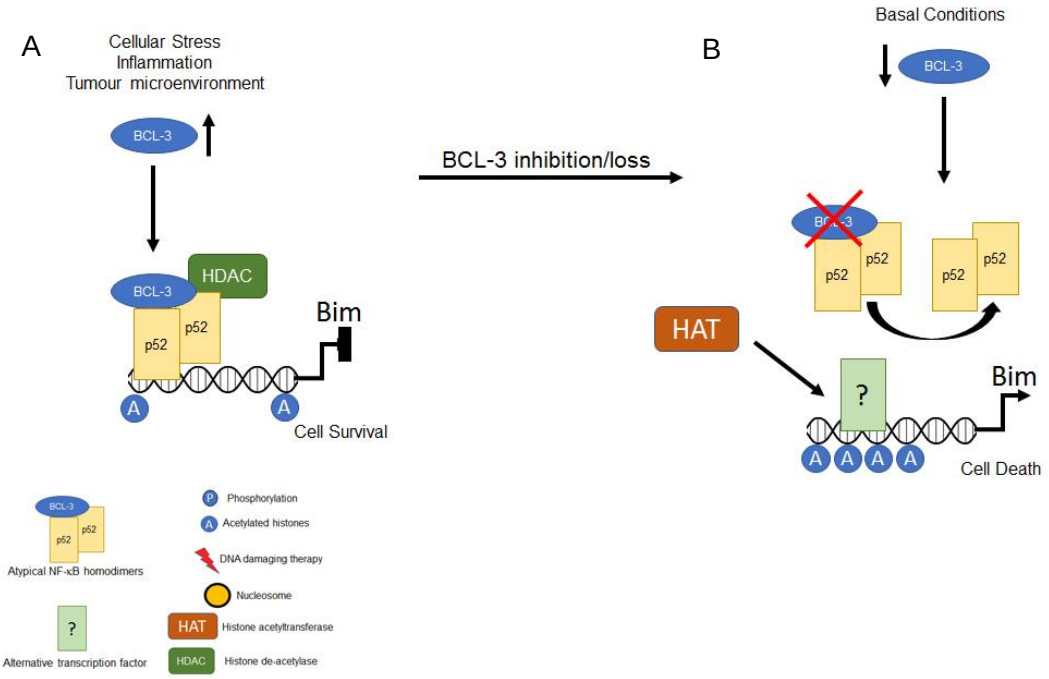

Figure 5.1 Model of BCL-3 function in apoptosis in colorectal cancer cells

A When highly expressed, BCL-3 represses gene transcription when bound to NF-κB homodimer subunit p52 at the Bim promoter. This is associated with lower levels of acetylated H3 at the Bim promoter. **B** Following BCL-3 loss/inhibition, Bim undergoes transcription with associated increases in acetylated H3 at the promoter, resulting in increased cell death.

It has been shown in multiple myeloma cells that the non-canonical NF-κB complex associate with the chromatin de-acetylase, HDAC4, maintaining repressive chromatin around the BCL2L11 gene and resulting in reduced Bim transcription (153). The preliminary data presented here shows that BCL-3 suppression increases levels of histone 3 acetylation. Acetylation of histones plays a fundamental role in several processes including gene transcription (432, 433). BCL-3 is known to act as a bridging protein to other cofactors, such as lysine acetylases or de-acetylases (216). Therefore, it is possible to hypothesise that BCL-3 could facilitate histone deacetylation leading to more repressive chromatin at the Bim promoter, which following the depletion of BCL-3 results chromatin decondensation and in Bim transcription. This could be NF-κB independent, as the increased histone acetylation could lead to better access for alternative transcription factors aside from NF-κB. Further work could investigate the dynamics of how BCL-3 regulates Bim transcription by performing ChIP with canonical NF-κB subunits to see if there was exchange of NF-κB dimers at the BCL2L11 promoter following BCL-3 suppression. Additionally, the putative role of BCL-3 and regulation of transcription via modulation of chromatin acetylation could be investigated in more detail. RNA-seq could be performed following BCL-3 suppression combined with histone acetyl transferases (HAT) or histone de-acetylases (HDAC) inhibition to assess sets of genes where BCL-3 interacted independently of histone acetylation and those where transcription of genes was controlled by BCL-3 and could be blocked or augmented by the inhibitors.

The role of BCL-3 as a co-regulator of gene transcription by the atypical NF-κB subunits is context dependent, with evidence suggestion repressive and activating roles with both p50 and p52 homodimers in differing cell types (169, 208, 211).

An alternative mechanism suggested to that above, is that BCL-3 suppression results in NF-κB dimer exchange at the Bim promoter, with repressive p52

homodimers exchanged for canonical heterodimers, leading to Bim transcription. This is plausible as p52 suppression also increases Bim expression. However, the data shown here does not delineate whether the effect of both BCL-3 and p52 knockdown on Bim is a joint effect or through separate mechanisms.

Blocking Bim expression may lead to a greater effect in cells with wild-type KRAS or BRAF, as it is known that tumours harbouring mutations in these genes constitutively activate ERK1/2 leading to Bim degradation (311). Interestingly, the greatest effect in this study was observed in the HCA7/P cell line, which lack either a KRAS or BRAF mutation. Further work could analyse apoptosis in additional KRAS WT cells following BCL-3 suppression. Understanding which pathways are important in the efficacy of BCL-3 targeting is important for future therapeutic development, and for identifying which patients would most benefit.

The fact that BCL-3 inhibition could alter chromatin accessibility also suggests that BCL-3 expression could be important in determining therapeutic resistance.

5.2 BCL-3 and irradiation

Results from the second chapter showed BCL-3 suppression sensitises cells to γ-irradiation, increasing the magnitude and persistence of γH2AX foci and could also be explained by BCL-3-induced modulation of chromatin acetylation. Chromatin acetylation plays an important role in the DDR (434). Inhibition of HDACs has been shown to radio-sensitise tumour cells and results in an increased and prolonged γH2AX foci formation (435); the results from chapter 2 replicate this phenotype. BCL-3 has been previously shown to interact with HATs and HDACs such as TIP60, CBP/p300 and HDAC1. Studies examining BCL-3 and HDAC1 show that gene transcription is repressed as a result of this interaction but did not analyse the function of this interaction in DDR (162, 219, 231). Interestingly, evidence suggests that inhibition of HDAC function reverses the effect of BCL-3 expression

on gene transcription (436). HDACs regulate DSB processing, checkpoint activation and degradation of DDR proteins and it could be that BCL-3 acts in conjunction with HDACs, such as HDAC1, to facilitate chromatin de-acetylation, resulting in abrogation of these functions (437). This would explain the phenotype that was observed in the study where loss of BCL-3 could impair the DDR leading to increased γH2AX foci formation and prolongation of γH2AX foci in nuclei following irradiation.

Conversely, BCL-3 interacts with HATs such as TIP60. BCL-3 bridges TIP60 to p50, through interaction with all 7 ARs, which leads to enhanced transcription by the BCL-3:p50 complex (216). TIP60/KAT5 is a lysine acetyl-transferase that has numerous substrates in the DDR, such as histones, ATM or NOTCH1; critically, TIP60 facilitates chromatin acetylation following DNA damage, particularly H4 acetylation, with inhibition of this function leading to impaired recruitment of DNA repair proteins to DNA damage (438, 439). Currently, it is unknown what regulates BCL-3 to perform these functions and given BCL-3 is primarily controlled by PTM, it may be PTM plays a role. Interestingly, NOTCH1 has seven AR, and undergoes acetylation following binding to TIP60. It could be that BCL-3 is also acetylated following binding with TIP60 after irradiation, in a manner similar to NOTCH1, possibly leading to inhibition of TIP60-induced chromatin acetylation (439). Furthermore, analysis of the BCL-3 protein sequence reveals it has two putative ATM phosphorylation sites, the first site sits within the second AR and the second site sits in the proline-serine rich region at the c-terminus. BCL-3 may be phosphorylated in a manner similar to p65, which is phosphorylated by ATM on conserved ATM-phosphorylation consensus sites, resulting in its activation (379). Recent work, analysing BCL-3 phosphorylation did not examine these sites but it may be that BCL-3 is phosphorylated as a result of DNA damage by activated ATM (203). ATM induced phosphorylation of BCL-3 has two outcomes. ARDs are well

recognised protein-protein binding motifs and it could be that by phosphorylating BCL-3, within an AR, alters the ability of BCL-3 to bind to other proteins, such as HDAC1 or TIP60. Alternatively, the C-terminal domain of BCL-3 is well recognised to contain other phosphorylation sites that lead to BCL-3 translocation, stability and its function as a cofactor with NF-κB subunits. It may be that ATM phosphorylation in the C-terminus primes BCL-3 for further phosphorylation by other kinases. Further investigation is required to understand the role of BCL-3 in chromatin remodelling, identify the protein interactions important for this function and the BCL-3 PTMs implicated in the DDR. This would lead to investigating whether targeting this function is important for sensitising to therapy.

There may be alternative mechanisms by which BCL-3 exerts its effects in radiation. The finding that BCL-3 knockdown promotes formation of γH2AX foci following γ-irradiation suggests alteration to the DDR. Cells with competent repair machinery are able to compensate to some extent for increasing damage, whilst also maintaining low levels of un-repaired DSBs resulting in lower levels of foci formation. However, evidence shows that cells with aberrant DDR machinery, had linear increases in un-repaired DSBs, marked by increased formation of γH2AX foci. A similar phenotype is observed when BCL-3 is suppressed, suggesting that BCL-3 suppression results in defects in DDR. Irradiation induced DNA damage leads to a variety of lesions clustered together (440, 441), resulting in significant γH2AX foci formation. Results showed that BCL-3 suppression increased γH2AX foci formation after irradiation. Increased or persistent γH2AX foci formation, after irradiation, is correlated with reduced cell survival as a result of unrepaired DNA damage (442). Additionally, increased duration and persistent of γH2AX foci is known to be a marker of more complex DSBs generated by physical or chemical insults (443). DSB complexity plays a role in cell survival after radiation, with more complex lesions resulting in prolonged repair kinetics which leads to cells choosing

to undergo increased IR-induced apoptosis (444). Therefore, it could be that BCL-3 is altering the repair (likely not to be through HR as BCL-3 suppression failed to induce sensitivity to PARPi) of a particular type of lesion resulting in increased complexity of the DSB, which would result in the observed alterations to γH2AX foci formation.

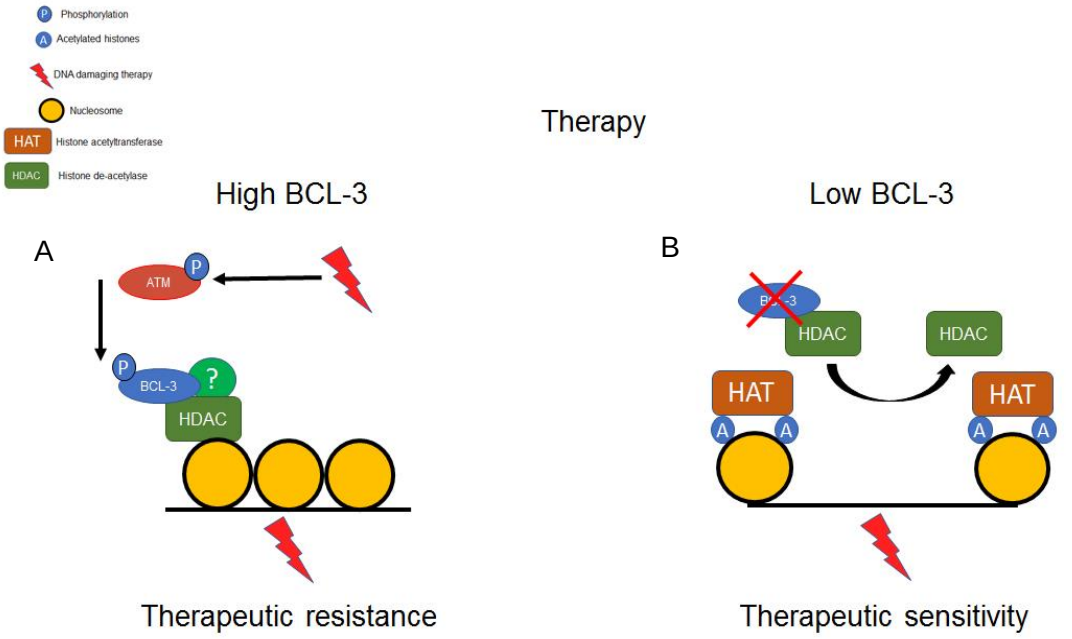

Figure 5.2 Model of BCL-3 function in DNA damaging therapy response

A In cells with high levels of BCL-3 promote increased resistance to DNA damaging therapies. Possibly through promoting inaccessable chromatin through association with histone de-acetylases. BCL-3 may also be phosphorylated by ATM following irradiation. **B** Following loss of BCL-3 there is increased sensitivity to DNA damaging agents. It is suggested that BCL-3 loss results in increased chromatin accessability leading to the observed response.

Other mechanisms involving BCL-3 in the response to DNA damage may include interaction with other members of DDR such as RAD1, part of the 9-1-1 complex that senses DNA lesions (376). Interestingly, in other species, BCL-3 has been shown to be evolutionarily upregulated in Tibetan boars living at high altitude as an adaption to high levels of DNA damage sustained from UV radiation in these animals (445). It may also be that BCL-3 modulates DNA damage-induced p53 activation through upregulation of HDM2 (239), however, this is unlikely in this model as p53 is both WT and mutated in the cells analysed, which show the same

response to BCL-3 suppression (LS174T – p53 WT; SW1463 and HCA7/P – p53 mutant). The data presented above showed that a novel BCL-3 inhibitor, which is designed to inhibit the interaction of BCL-3 with p50 or p52 did not result in increased radiosensitivity in the tumour spheroid model, potentially corroborating the evidence discussed above that BCL-3 may be functioning in a NF-κB independent manner in DDR.

In summary, this work suggests that high expression of BCL-3 in rectal cancers could lead to therapy resistance and that by targeting BCL-3 in tumours, this may offer an opportunity to sensitise tumours to current therapies. Further work is required to define interactions of BCL-3 and members of DDR and determine if inhibitors can disrupt this interaction or inhibitor the downstream outcomes of BCL-3 (HDAC inhibitors).

BCL-3 regulates both apoptosis and radiation resistance through different mechanisms in colorectal cancer. Clinically, the importance of this work is considerable. Significant benefits to patient prognosis can be achieved by improving response to therapy, which could be achieved by targeting BCL-3. Additionally, given that BCL-3 may predict response to neo-adjuvant LCCRT, expression of BCL-3 could have utility as a biomarker of response. As a biomarker it could be used to stratify those patients with low expression who could progress to LCCRT and those with high expression who would progress straight to surgery. Further work is required to assess this in detail. BCL-3 could also be used to stratify the use of adjuncts to LCCRT such as the putative use of HDAC inhibitors to block the downstream effects of BCL-3 upregulation.

In conclusion, BCL-3 is a potent survival factor in CRC and inhibition of BCL-3 may work to prevent tumour progression and increase sensitivity to conventional therapy.

6 Appendix

6.1 Appendix 1

6.1.1 ASPIRE STUDY PROTOCOL

Does aspirin increase the clinical response to pre-operative chemo-radiotherapy [CRT] in rectal cancer?

Prof Ann Williams: Professor of Experimental Oncology

Prof Chris Paraskeva: Professor of Experimental Oncology, Head of School

Mr Mike Thomas: Consultant Colorectal Surgeon, Bristol Royal Infirmary

Miss Katherine Gash: Clinical Research Fellow in Colorectal Surgery, Chief Investigator of the study

Summary

The overall purpose is to determine whether aspirin increases clinical response to chemo-radiotherapy [CRT], through targeting the Lgr5+ cancer stem cell population. *In vivo* and *in vitro* approaches will be combined to help understand the role of cancer stem cells in resistance to treatment and late relapse. Previous laboratory studies have shown that through inhibiting both the COX2/PGE_2 and BCL-3/NF-κB signalling pathways, aspirin is able to target cancer stem cells and hence we propose that the adjuvant use of aspirin will increase the therapeutic response of rectal tumours to CRT.

Background Information

Despite recent advances in treatment, more than 40% of patients who present with advanced colorectal cancer will be resistant to current therapies. Hence there is an urgent need not only to develop new treatments but also to find ways to improve the long term response to existing therapies. Importantly it is the colorectal cancer stem cell [CSC] population that is thought to be responsible for fuelling the growth of the tumour leading to metastatic disease. Up to very recently research on colorectal CSCs has been limited due to the lack of reliable cancer stem cell markers. However, the identification of the Leucine-rich repeat-containing G-protein coupled receptor 5 (Lgr5) and other putative intestinal stem cell markers has made possible the investigation of intestinal cancer stem cells in tumour response to conventional treatment [1]. As colorectal CSCs are able to remain dormant and to become resistant to the effects of chemo-radiotherapy (CRT), it is the CSC that are thought to be responsible for recurrence after R0 surgical resection. Importantly, recent work from our lab has shown that the COX2/PGE_2 and BCL-3/NF-κB signalling pathways can promote the stem cell phenotype [2, unpublished] and hence potentially confer resistance to therapies.

The link between chronic inflammation and cancer is widely accepted and the importance of the pro-inflammatory Cyclooxygenase-2 (COX-2) derived prostaglandin E2 (PGE_2) in

inflammation and cancer well established [3]. COX-2 is overexpressed in the majority of colorectal cancers and leads to elevated levels of PGE_2 which promote many hallmarks of cancer including tumour cell survival [4]. PGE_2 has been shown to enhance Wnt/β-catenin signalling in colorectal carcinoma cells and in normal haematopoietic stem cells, driving Lgr5 expression and stem cell function [5-7]. The important chemopreventive properties of NSAIDs such as aspirin, which act through inhibiting PGE_2, have been known for many years and one very striking clinical observation is their ability to cause adenoma regression in FAP patients [8]. Recent exciting data from our laboratory shows that PGE_2 promotes the growth and survival of Lgr5+ colorectal stem cells and suggests that NSAIDs would inhibit cancer stem cell survival through suppressing Lgr5 expression [2]. This led to the hypothesis that as NSAIDs including aspirin directly target the CSC population (which are the cells that become resistant to treatment and drive tumour growth), the use of NSAIDS in an adjuvant setting could improve therapeutic outcome.

The success of surgical resection of rectal tumours has improved significantly with the use of pre-operative chemo-radiotherapy, although the reason why some patients with rectal cancer respond better to CRT than others remains unknown. Interestingly, radiotherapy (RT) has been reported to enhance COX-2 protein expression as well as elevate PGE2 synthesis in human cancer cells [reviewed in 9]. As COX2-PGE2 signalling drives the survival of the CSC population, RT induced PGE2 may contribute to a poor response to CRT. Hence, one way of determining potential response to CRT may be through measuring PGE2 levels in the patients prior to therapy. PGE2 is an unstable compound that is rapidly metabolised by the 15-hydroxy prostaglandin dehydrogenase (15-PGDH) enzyme to the stable PGE-M. Interestingly PGE-M can be quantified in urine samples and has been shown to be a reliable indicator of systemic PGE2 levels in a number of studies [reviewed in 9]. For example breast cancer patients that received cytotoxic chemotherapy had significantly higher levels of urinary PGE-M compared to patients without chemotherapy [10]. Further, levels of urinary PGE-M have been shown to be a marker of pharmacological activity of NSAIDs [10-12] suggesting that the measurement of urinary PGE-M can not only be used as a surrogate marker for disease progression in COX-2 positive tumours but also as a marker for NSAID efficacy. Therefore measuring urinary levels of PGE-M will enable monitoring of the effect of NSAIDs on systemic levels of prostaglandins in rectal cancer patients. In addition, we propose to determine the efficacy of PGE-M monitoring compared to established markers such as CEA in relation to tumour recurrence after surgical resection.

As NSAIDs may in part reduce cancer risk through suppression of the inflammatory response, it is interesting that NSAIDs also target pro-survival NF-κB signalling in tumour cells [13]. In this context, it was of interest to note that aspirin but not the COX-2 specific inhibitor NS398 suppressed Bcl-3/NF-kB signalling in colorectal cancer cell lines (confidential, unpublished data). Although well characterised in haematopoietic system,

Bcl-3 signalling is now emerging as an important survival factor in a number of solid tumours [14-18]. Work in our laboratory has recently identified induction of Bcl-3 expression in epithelial cells in response to inflammatory cytokines and shown the Bcl-3/NF-kB homodimeric complex to promote survival through activation of the AKT pathway (Urban et al, *submitted*). Excitingly, recent data suggest that Bcl-3/NF-kB signalling also enhances the stem cell phenotype of colorectal tumour cells [confidential, unpublished data]. As aspirin represses both Bcl-3 expression and COX-2/PGE_2 activity, this combined effect suggests that aspirin could be particularly effective at targeting the Lgr5+ stem cells and hence able to increase therapeutic response to CRT.

The novel aspects of this work are therefore: i) identify whether the regular daily use of aspirin acts as an important novel adjuvant for colorectal cancer treatment by blocking both the PGE_2 and Bcl-3 pathways hence targeting carcinoma stem cell survival ii) the use of urinary PGE_2 as a possible novel cancer biomarker for tumour response, reporting efficacy of NSAID use in combination with CRT and for tumour recurrence.

The proposed research is highly original and exploits the CRUK group's recent novel discovery that prostaglandins (which enhance the Wnt/B Catenin pathway) and Bcl-3/NF-kB both up regulate the recently characterised intestinal stem cell marker Lgr5 (a Wnt target), thus promoting cancer stem cell survival. Hence, aspirin which works by lowering prostaglandin levels may have a dual role in targeting these pro-cell survival pathways and inhibiting intestinal cancer stem cell survival, which may be critical for chemoprevention and the development of novel therapies through targeting cancer stem cells.

Study Objective

Thus the aim of this study is to determine whether the use of aspirin can enhance the response to pre-operative CRT in rectal cancer patients. If this cohort study generates encouraging results then a larger study, likely to be a randomised trial, will be undertaken.

Aims

There are 3 aspects to this proposal:

1) To investigate whether aspirin can enhance the effect of pre-operative CRT in rectal cancer [using clinical end points]. Levels of the PGE_2 metabolite PGE-M will be monitored to assess efficacy of aspirin [or other daily NSAID use] on systemic PGE_2 levels.

2) To investigate the pre-operative levels of PGE-M during CRT (in patient urine samples) to determine whether therapeutic response correlates with prostaglandin levels. In addition, measure urinary PGE-M following surgery to investigate whether prostaglandin levels correlate with recurrent tumour burden (to assess utility as a biomarker compared with established serum markers such as CEA).

3) To determine whether aspirin [or daily use of NSAIDs] target the Lgr5+ cell population through the inhibition of the COX-2/PGE_2 and/or BCL-3 signalling pathways; this study will

allow us to determine the effect of NSAID activity on the survival of cancer stem cell population.

This study is a modification of a previous application (E5900) that was not completed due to the voluntary withdrawal of VIOXX (COX-2 specific NSAID). However experience from the previous trial has demonstrated feasibility of the study and patient compliance.

Study Site

Patients who are receiving treatment at Bristol Royal Infirmary, North Bristol NHS Trust, Cheltenham General Hospital, Royal Devon and Exeter NHS Foundation Trust, Abertawe Bro Morgannwg University Health Board, or Royal United Hospital Bath, will be invited to participate. This will be a cohort study involving **between 50 and 100 patients**. The research will commence in February 2014 and will last for 36 months.

The laboratory element of the research will be carried out in the Cancer Research UK Colorectal Tumour Biology Research Group in the Cancer Research Labs within the School of Cellular and Molecular Medicine, a Cancer Research UK group with more than 20 year continuous CRUK programme funding and renowned for producing high quality research. This group has direct involvement in clinical trials and a proven research track record as leaders in the field of colorectal cancer chemoprevention.

Subjects and Recruitment

The aim of this trial is to determine whether regular NSAID use, through suppressing systemic PGE_2 levels and Bcl-3 activity, can increase the therapeutic response to pre-surgery chemo-radiotherapy in rectal cancer patients.

As with normal NHS management: Patients will have been diagnosed with rectal cancer either at their outpatient clinic appointment (where the tumour can sometimes be felt on rectal examination or seen with a rigid sigmoidoscope), or at endoscopy. The probable diagnosis will have been discussed with them and biopsies taken. The patient will then re-attend clinic to receive the results of the histology and to discuss their management. Further investigations will then be requested, (as is routine management), such as an MRI scan +/- endo-anal ultrasound scan, staging CT scan.

At this point, patients will be approached about the study. The study will be fully explained to them in clinic and they will be given a Patient Information Sheet (PIS). The consultant surgeon in charge of their care will be carrying out this clinic consultation. Patients will not be asked to consent at this point, but will be invited to participate. The patients will then have the opportunity to go away and think about the study and any questions that they might have.

At their next hospital outpatient appointment when they return to discuss the results of their investigations, (likely to be within a couple of weeks of their previous appointment), the patient will once again be invited to participate in the study. If they are happy to be involved

in the research, they will be asked to sign the consent form. They will have the opportunity to ask questions and to discuss any concerns regarding the study. This consent process will be carried out by either the research fellow, or the consultant surgeon in charge of their care (who will all be fully briefed on the study). The consultant who has seen the patient in clinic and completed the consent process will inform the research fellow (via telephone) that the patient has been recruited.

Flowchart of Recruitment Process

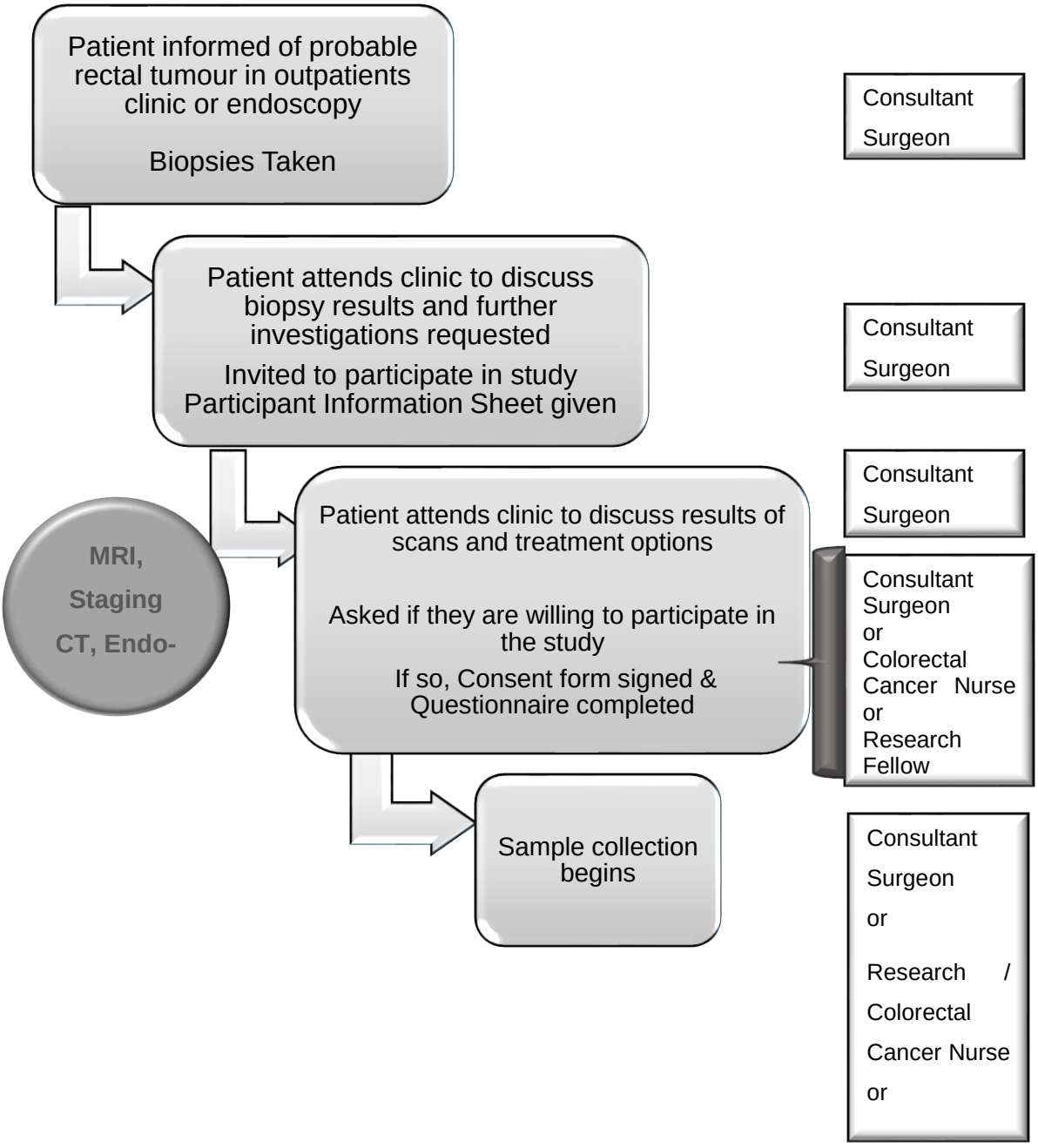

Inclusion criteria

Patients must be:

aged 18 years or over (no upper age limit)

newly diagnosed with primary rectal cancer

receiving treatment at Bristol Royal Infirmary, North Bristol NHS Trust, Cheltenham General Hospital, Exeter NHS Foundation Trust, Abertawe Bro Morgannwg University Health Board Wales, or Royal United Hospital Bath

medically fit enough to undergo pre-operative radiotherapy and surgery

willing to consent to this treatment (in accordance with the standard NHS management for rectal cancer).

Patients with metastatic disease will be included, as will those with previous colon (but not rectal) cancers.

Patients with synchronous colon tumours or other simultaneous cancers will be included.

Exclusion criteria

Patients will be excluded if:

they are aged 17 years and under

they are not fit enough for or not consenting to chemo-radiotherapy and surgery

they have recurrent rectal cancer.

Measures and materials

Having been identified and recruited as detailed above and after full informed consent is obtained, patients will be asked to complete a brief questionnaire enquiring about NSAID use. This will ask if the patient takes Aspirin or other NSAIDs (namely Diclofenac/Volterol, Ibuprofen, Naproxen, Indomethacin, Mefenamic acid, Celecoxib/Celebrex, Meloxicam, Ketorolac, Sulindac, Asasantin Retard or Etoricoxib). We will then ask about dose and frequency of NSAID use. If patients take no regular NSAIDs there will be no further questions for them to complete. It will be completed in outpatient's clinic with the help of the colorectal cancer nurse specialist, the research fellow or the consultant surgeon.

Based on the results of this questionnaire, patients will be stratified into three groups according to their regular NSAID use: those taking daily Aspirin; those taking daily NSAIDs other than Aspirin; those not taking daily NSAIDs (either because it has never been suggested or because they have contra-indication to their use).

As this study does not require additional treatment, all patients will undergo standard treatment of pre-operative chemo-radiotherapy plus surgery. Those that are on daily Aspirin / other NSAIDs will be asked to continue throughout the duration of their chemo-

radiotherapy (as would be normal clinical practice). They will be asked to inform the PI if, for any reason, they need to stop taking their medications. Patients will be free to withdraw at any time. It is important to determine whether patients treated with a combination of chemo-radiotherapy and NSAIDs respond better than those treated with chemo-radiotherapy alone. Patients will not be asked to change their pattern of medication to take part in this study.

Patients will be given Paracetamol or opiate based pain control after surgery as is required. Patient data collected will be stratified according to NSAID use (control / irregular NSAID use n≥20; daily NSAID use (non-Aspirin) n≥20; daily Aspirin n≥20).

Many patients in this age group take Aspirin or other NSAIDs and we would not expect significant problems. Nevertheless any patient showing common side-effects (for example dyspepsia) will be advised by their clinician and an external independent assessor will monitor detailed morbidity data after every 5 patients and compare this to known figures. Any adverse events will be reported as per the Sponsor's procedures, (http://www.bristol.ac.uk/red/research-governance/registration-sponsorship/specific-advice/adverseevent.html).

All patients recruited will be discussed at the colorectal multidisciplinary team meeting at their hospital, (Bristol Royal Infirmary/North Bristol Trust/Cheltenham General Hospital/ Exeter NHS Foundation Trust/ Abertawe Bro Morgannwg University Health Board/ Royal United Hospital Bath), as is the case for all colorectal cancer patients. The MDT will make the decision as to whether it is appropriate to offer them pre-operative chemo-radiotherapy prior to undergoing surgery. [The research fellow regularly attends these meetings].

Urine Samples

A single void urinary sample was requested from patients at the start of the study, when attending CRT appointments, and when attending their outpatient clinic appointments once they have completed the course of pre-operative chemo-radiotherapy. These specimens were collected and stored at -80'C. When the recruitment process is complete (ethical approval is valid until January 2017- a further 18 months), as part of the ongoing study, the level of PGE-M in urine samples will be determined as a surrogate for NSAID efficacy and levels analysed for biomarker potential.

Blood Samples

During the patients' routine treatment for rectal cancer, several blood tests are usually taken as part of their normal cancer management. We would ask that an extra blood sample bottle is filled on two occasions when they are already having blood taken. One sample would be requested prior to CRT and one post CRT. We will always endeavour to take the blood samples for research purposes at the same time as blood is being taken for the patient's routine cancer management. There is a small possibility that the patient may not be due a routine blood test when the sample is needed for the study and in that case we

would ask if they are willing to have an extra blood test (although this situation is unlikely). Similarly to the urine specimens, the blood samples were stored (having been spun in a centrifuge and the serum removed and deposited in an ependorf) and will undergo analysis once recruitment has closed.

Tissue Samples

All patients will be asked for their consent to provide tissue samples for use in the study.

1) Tissue from the biopsy specimen taken when the patient was originally diagnosed with rectal cancer will be requested from the pathologists.

2) Tissue from the resected tumour specimen (after surgery) will be taken, once the pathologists have complete their full analysis of the tumour and have determine the stage of cancer etc., so as to guide any future treatment. Only tissue which is surplus to requirements will be used.

3) Normal mucosa from within the surgical specimen resection margins will be collected and will act as an internal control.

Response to radiotherapy will be classified according to the pathology report from the excised tumour specimen (range: no response to complete therapeutic response). However, it is normal clinical practice for patients to undergo pre-radiotherapy MRI scans of the pelvis to aid in treatment planning. If patients in this study undergo pre or post-radiotherapy MRI scans (as part of their normal NHS care), we will ask for access to the data to aid assessment of the shrinkage in tumour volume. This will be done by the research fellow (via a hospital computer), reading the radiology report which details tumour measurements. The only data which we would need to obtain from this report is the graded response (by the radiologist) of the tumour to radiotherapy (e.g. no response, partial response etc.). The patients' actual medical case notes will not be looked at.

We will study tissue samples in the lab (at University of Bristol, Department of Cellular and Molecular Medicine). We will process the tissue to slides and the proliferative and apoptotic index of the tumour cells calculated pre and post-RT for both control and treatment groups. Immunohistochemical staining/in situ hybridisation will allow analysis of Lgr5+ cells, other CSC markers and surrogate markers of tumour response and normal mucosal healing to be assessed.

At post-surgery follow up clinics we will collect additional urine samples to monitor urinary levels of PGE-M enabling us to compare efficacy as a surrogate marker of tumour burden with more established markers such as CEA.

Laboratory experiments;

Tissue

COX1 and COX2, PGDH and PGT

Bcl-3, NF-κB FGFBP-1 and related co-factor Bag-1

Ki67 (proliferation associated antigen)

Apoptotic cell markers

E-cadherin (marker of cellular differentiation)

CSC markers including Lgr5

Reporters of wnt activity including B-catenin

PG receptor 1-4

Blood/Urine

PGE_2 metabolite PG-M

Tumour derived DNA

Markers including CEA and above

Safety Assessments

As the study will not alter the patients' clinical management there are no direct safety assessments required for patients. The research fellow and professors at the laboratory who will be handling specimens have all attended induction in the School of Cellular and Molecular Medicine, which covers aspects of safety. All students and staff are issued with a copy of the School's Safety Manual which makes reference to the relevant University Codes of Practice. This manual must be read and signed, along with relevant COSHH (Control Substances Hazardous to Health) regulations, prior to commencing work in the lab. The induction covers specific areas including use of radiochemicals, COSHH regulations, high-speed centrifuges and pathogenic micro-organisms. All laboratory staff have been immunised against Hepatitis B.

Study Personnel

The University of Bristol and the proposed academic supervisors, Prof Paraskeva & Prof Williams, have an established track record of collaboration with Bristol Royal Infirmary and the clinical supervisor Mr MG Thomas. The importance of research carried out in Bristol has been internationally recognised as providing unique human colorectal epithelial cell models for identifying the biological consequences of genetic changes associated with colorectal carcinogenesis [refer to 1,2]. A combined *in vivo* and *in vitro* approach is used to study the cellular and molecular biology of colorectal carcinogenesis. The group have a strong reputation in the field of chemoprevention supported by Cancer Research UK programme funding, with work form the laboratory contributing to the initiation of National and International clinical trials.

The research we propose will expand and develop earlier work done by the Cancer Research UK Colorectal Tumour Biology Group and address important questions in the

role of the COX2/prostaglandin and Bcl-2/NF-κB signalling pathway in promoting the survival of cancer stem cells.

This importance of this study relates to the fact that, despite the huge advances in the management of colorectal cancer, there are still patients who remain resistant to treatment: the aim of the project is to investigate ways of targeting the cancer stem cell population, thought to be critical in repopulating the tumour after therapy, leading to local recurrence after resection as well as late metastatic disease.

Monitoring

The study will be monitored and audited in accordance with the R&D governance procedures of the University of Bristol, who have delegated this role to UH Bristol. All study-related documents will be made available on request for monitoring and audit by the trust, University and REC.

Ethical considerations

It is not anticipated that there will be any major ethical issues for this study. Patients will all have participated with informed consent. Some patients may have up to one week to decide if they wish to participate in the trial due to the narrow window between diagnosis and surgery. This cohort is small and some patients may have longer than a week to consider their participation.

There is no risk of the study interfering with a patient's definitive treatment, (i.e. surgery), as prior to us receiving the tissue the sample will be examined by a pathologist at the hospital in which the patient is receiving treatment. The pathologist will record all of the information needed to stage the tumour / guide any further treatment. There is a chance of some discomfort from having blood samples taken, but as previously stated, we will endeavour take the patients' blood at the same time as it is being taken for their routine NHS investigations.

Ethics and R&D approval

The study will be performed subject to Research Ethics Committee (REC) approval and local Research and Development (R&D) approval.

Research governance

This study is sponsored by the University of Bristol.

Finance & Indemnity

This study is being funded by:

The Royal College of Surgeons- One Year Surgical Research Fellowship

The David Telling Charitable Trust

The Above and Beyond Charitable Trust.

These grants are administered through the University of Bristol and University Hospitals Bristol NHS Foundation Trust.

The laboratory is funded by a Cancer Research UK Programme Grant.

The University has Clinical Research Insurance to cover the liability of the University to research participants. In the event that something does go wrong and a participant is harmed during the research study there are no special compensation arrangements. If a participant is harmed and this is due to someone's negligence then they may have grounds for a legal action for compensation against Bristol University or the NHS Trust or one of the other parties to the research, but they may have to pay their own legal costs.

Reporting and Dissemination

It is anticipated that the results of the study will be disseminated in the form of peer reviewed publication and presented at scientific/academic meetings locally, nationally and internationally.

Conflicts of interest

We have no conflicts of interest.

6.2 Appendix 2

6.2.1 TNM staging of colorectal cancer

TNM staging of colorectal cancer – 8th edition			
AJCC stage	Tumour	Node	Metastasis
0	Tis	N0	M0
I	T1-T2	N0	M0
IIA	T3	N0	M0
IIB	T4a	N0	M0
IIC	T4b	N0	M0
IIIA	T1-T2	N1/N1c	M0
	T1	N2a	M0
IIIB	T3-T4a	N1/N1c	M0
	T2-T3	N2a	M0
	T1-T2	N2b	M0
IIIC	T4a	N2a	M0
	T3-T4a	N2b	M0
	T4b	N1-N2	M0
IVA	Any T	Any N	M1a
IVB	Any T	Any N	M1b
IVC	Any T	Any N	M1c

Tumour

Tx: Primary tumour cannot be assessed

T0: No evidence of primary tumour

Tis: carcinoma in-situ

T1: tumour invades submucosa (through muscularis mucosa but not into the muscularis propria)

T2: tumour invades muscularis propria

T3: tumour invades through the muscularis propria into the pericolorectal tissues

T4a: tumour invades through the visceral peritoneum

T4b: tumour directly invades or adheres to other adjacent structures or organs

Node (at least 12 regional lymph nodes recovered to be accurate)

Nx: regional lymph nodes (LN) cannot be assessed

N0: no regional LN metastasis

N1a: metastasis in 1 LN

N1b: metastasis in 2-3 LN

N1c: no regional lymph nodes are positive but there are tumour deposits in the subserosa, mesentery or nonperitonealised pericolic or perirectal/mesorectal tissues

N2a: metastasis in 4-6 LN

N2b: metastasis in 7 or more LN

Metastasis

M0: no distant metastasis

M1a: metastasis confined to 1 organ or site without peritoneal metastasis

M1b: metastasis to 2 or more sites without peritoneal metastasis

M1c: metastasis to the peritoneal surface with or without other metastasis

6.3 Appendix 3

6.3.1 Tumour regression grade (TRG) systems

Tumour regression grade (TRG) systems				
Response	AJCC	Dworak	Mandard	Ryan
Complete regression	No viable cancer cells (TRG 0)	No tumour cells (TRG 4)	No residual cancer cells (TRG 1)	No viable cancer cells or single cells or small groups of cancer cells (TRG 1)
Near complete regression	Single cells or rare small groups of cancer cells (TRG 1)	Very few tumour cells (TRG 3)	Rare residual cancer cells (TRG 2)	-
Moderate regression	Residual cancer with evident tumour regression but more than single cells or rare small groups of cancer cells (TRG 2)	Dominantly fibrotic changes with few tumour cells or groups (TRG 2)	Predominant fibrosis with increased number of residual cancer cells (TRG 3)	Residual cancer outgrown by fibrosis (TRG 2)
Minimal regression	Extensive residual cancer with no evident tumour regression (TRG 3)	Dominant tumour mass with obvious fibrosis (TRG 1)	Residual cancer outgrowing fibrosis (TRG 4)	Significant fibrosis outgrown by cancer or no fibrosis with extensive residual cancer (TRG 3)
No regression	-	No regression (TRG 0)	No regressive change (TRG 5)	-

6.4 Appendix 4

6.4.1 BCL2L11 gene sequence

NF-κB consensus sites marked in blue

Start codon highlighted in red

>hg19_refGene_NM_207002 range=chr2:111873491-111887423
atattgaaatctgcctcatttaattcctacctctggccctacgttctgtttttggcacca
gatagataaaacccatactctattttacactcattcaaatcattgtatttcccccaccgg
tgaatatattaccaaagttggttgagtttcataatgcaaacccaaagggaaaattatctt
gaataatcatatgacaatatgtggaaagtttaggggctgtgtacgccacctcatggtttt
gaactgtgtggttaaagacgttgagagttgacagattagtcagggatttttcaagagtat
taattacaaactttgaaatcttggtcagtgaaagttcattttagtgcatcttgcaaatac
gatcaaaggtcttttcagtactgatttgatgatgcttaaccacagtgtgtgaagaatgaa
gtttttcattagaaattactggtgtaatagagcacattttcagggaagatgtattgttgg
actattacaattcatgctcttcccccaccatatccctaccctctatattccccatcccct
atttcctccaccttcctccttgggacctcactgaaaacctgaaatgctctgaaaacctga
aatggcgttttggactgctgcaagggaaactgtgatcttaacaacatcagtgcggctcag
acatgaccaccatgtgagggcaaaggtggggctggtgtaagtgatgttgttaaacctgta
aaaataaaccatgaaaacctggggatttactgtgatttggggagtgaaacaaatttacca
ctggccgaaaacttgaaaaatggagtacaatgtgtagatcagaagaaaagaaagccgtcc
ctctgcccttgtgtagttttagaaaaacaatcttattagtttggtagctttttttcctga
aaataaaaaaaaaaatacattggcacctaagccatggaaaatgaaataaaaatacaccag
tgcagcttccaaaacactgacttgcatctccctctcctatccgccgggaatgtcttatcc
ctgccttccagtggctgccagaaccaagggcatccgcggcgttccttggcattggcgtta
acagcagatggattttccgcagcggccaggcggaagatgcctagcattggtccgccgtct
cactgtactgaatttcaagaatcatggcctactgccagccaggtcaggaccgaaggcgct
agtctggggagactggagcaggtctctagtggttcacctgttcggaggctcttcctgttc
agttccctctgcgcgccagagggtggcacccaggcactccagaggtggagaggaggggga
cgacaggggaggcaaagagagaggagcggagggaaggaccagggaggaaggaccaaggag
ggagctttaataaattctcagaccttggtctcgagttcccggctaatttgggggcaaagc
cgaccgaccccacgtccacgcccacccccttacgggaaaagccggggtttccactgggct
aggtgtcagagttgggaatgtctaaaacaaaaaaggcttccgagggttattcatggccaa
cagtttccacaggagaatccaaagggaaactagtttccggggccgctgtgtgtgcgggtg
cttggtgggctgaaagctgctgtcactagatggctgtaagtgtgccaacatctgacctgt
cccattgtgttgtgttttgcagttgctggatttgtgcgactcggtgaaggatgatgcccg
gagggtgatctcgacctttaacattccacacacctacctccacgcaccaatcgccggaat
ctccaacccgcgggccgcgtgggctttctaccctgcaccgctgcagccgcggccacggga
agaggcgcgctcccggcggcccaagctgggagccaagctctaacgggtgtggcgggaagt
gtggtggcccgccagcagctgccacgacgctcgctccaccgacgcccagagctgtggccg
aggccgggggctggcacccgctgggccgccactctcggggattttggtggcaaagcggag
gtcccgccgaggctggcgaggtgcgcggctggctgctaggaaagagatccagacggtcgc
ctggtgcgctggatccctgtgccctttccctgaaacccagcctggcctgactgcaacctc
tcccaacttcagtgccggatcccctagacaatcagggtgggctccccgctgcgagcgcgc
cccacagccgggtgccgccaaaggtctcctgctgttagcggtgactcacattcccagtga
tttagaaaaactgtggtgccgagtgaaagaaaaaaaaaaaagcaaacacccttagacaaa
agaaaaaagctccactctttccgcgagcgggaaaaaggtttggttcagcaagtgatgct
atttcagtgaatcagacgctctggggctctgcaaggaaacgcacggactgggagaaggaa
gtgggagcctagagttttgctctcggcaaaacaagaactcggcttgtcctcccaggccgg
cggtttccgtacggcaagacaaggcgcggaaaacatttttaccatctgacgctgtagtct
gtcctttagaagagaataggtgaaaagtttaataaagaaattaagcgatgtggaagtcgt
tcccgctgcttgcagagggtggggaggcgggcctgggcaatttcggaactaggagagacc
acgtcggcaaagcctgtggtcccgaacaagggccatggatttcccatttctcagatcccg
gctgcccgacttcattcttgtttctttcagcacaagccatcctcccttctccctccctcc

acgtctcttggcagagacagaaagggacaccgctctgcccgcgtccagcgcgaaggaggt
gacctaaaacccatgggcccttctcacactgcgttctctgcgctccggcccagttccggg
aggacctcccgacggcgcgggagaaggctgtaagggctcttggcccccgacgcggcctgg
gtctcgggggacgcatgaacccgccacctctggccggcttccttttagtgccccaaatag
cagcgcttagcccgttgcttcccccgactcttgtttttcaaagtgttcacagggtcgcga
gagcgagcgacgcgggggcggcgaggctgcaaggctgcacaggaacagacgacaagaaat
agggctttcttctgcgtggttcttttccggtccctgtctgagtcgcccgaccccgcgggg
agcgcggagcattgcggcgtgcggcgggcttcgggctctcagcccgcgcagcaagttgtg
ttgcttttccccgggtgcgacgcgggacggccgcgaagagcaaagttcgtccgcggtagg
aacttcgaggcccggttaggaccgatctccggcctccgagtctacttagccgtgtccacg
ctcgtgccttttccctcttgcagcgaaataactgggcggggcccgacgcgcgtcctccag
cgactccgggaacccaaggcctccttcacctcgctcaaaattcacccgaaaatgcgctga
gactttggcatggggctgcgctgtgtcccactgacgttacagaagcgcttatgaatttaa
aaactgctccaggcggccggacggcgggacaacgcctcctcacttgctcctctacggcaa
ggccccttccttctccctgccggctgcggtggtgtgtagggtggtccctttacagagttt
ccttaatccatctagcctgacctcacctgcgggatgttccatttcccgatccacctccca
caccccgctgcagttgtctagaagctggggctggggaactgaggcgcgggaggagcaga
caggagggccggggttggggcgccagccacgcgttgggagagcagacccgggtgcagact
cagaggactggagaggcggcatggagtttggtctcctgggaggtagagtgaggtgctgcg
gactccagggaggaaagggatgggtggggaggcgggaggggaggagggacggggtatttt
gcgctcccgcaccgcggcccgaactcagctgttctgccttcactggcctcagccagtcga
gggagctcctacgaggttatctgcgagcccagcaaatcttgggggtcctagccaaatgca
gtgcgcaacgttctctctcacttggaggccgccattcacctcgtttttttttttcctaaa
aggatttttttttctgagtgctttttcatttccctattttacctgctttgcacatgcct
cccgccctcacccgggaggcggcgaagacgcccactgggaccgcgcctggccgttttctg
ggcgcgtcctgcccccacggcctctgtctcttagggcgactgggcgcggaagaaaagctg
gagagcccctgcggggtggcaggaggagggtgcctgagtcccgcgagaggcccgggcgag
gaagatgcgcagcctgctgatccgcgtcccgcccggcgccagggaccctcagagggagga
gagctcaaagacctcgccccgcgccttcgcgaggaccaacccagtccccgcgcctgcccc
agagcggcttagaaactcagggcacagtgagagcgcagggcgcctcccgaggcttcacac
cgccggccgggccagcggaggctgtgaccggagcgccccctctgtgccgcgcacgccgcg
gccgccgccgggttggggtaggtgagcgggaggctagggtacacttcggggtgggggatg
ggcgcgcacatggccgccagcaggcagagttactccggtaaacacgccagggacggcggc
gcgcgcgggaggcaacccagcggggcaacccccgcctttacctgtccgagcctgcacgcg
ccggcggccgcggcgccgaggggggcggagcttgccagcccgcgcgccggggcgggacct
agcgggggcggggtccgcagtgattgggcgtaggagcggggccgccagccagagctgggc
tgcagggccgcgcaggtttcACTTCGCTCCGCGCAGCCGCCTGGTCTGCAGTTTGTTGGA
GCTCTGCGTCCAGCGCCGCTGCCGCTGCCGCCGCCGCCGCCGCCGCCGCCGCCGCCG
CCGCCGCCACTACCACCACTTGATTCTTGCAGCCACCCTGCGAACCCTGCCACACTGCGA
TCGCATCATCGCGGTATTCGGTTCGCTGCGTTCCCGCCGCCACCGCCTCGGCGCCCTTTC
TTGGCCCTTGTTCCCCCAAATGTCTGACTCTGACTCTCGGACTGAGAAACGCAAGgtaaa
tacctccaaatcccggggcgcgggcctggcaccgaaggaagactagcgctggagcccgaa
cggcaccacctactgcccgcttcccgtgcacgtgcgagcggagacgcttgcatcggcgcc
gcttgtcgccggcgggaggtggggatccgtgtggatcgggttccctctcgggcaggttct
ctttaaagaaaagtcgttcacgcggaacctgcaggctcttggccgaagtgcggcttggga
cgggatgctgcgcgcgggcctggtgaagggtcgtaggtccgggcaggaggagaggcagcg
cgtgcctttcggcgccggcccgggagctgaggacctgctcgtagtatcgggctgtgcgcc
cagctggaaagtctcgccgccggctccggcgccctcagagtagcggccgcgcagtgtgag
ggtgtttcgtgtcttggtttttggggcgcgtgggcctgttgcggaggatttgcggaact
gcggtggtgatttaactgacgagacacggcttttccttttactcattcaggccaaggttt
cggggccactgctgcgttcgctttctcaagcgtacctggggcccctgcttgctctgcagg
agtcctgcggcctgtgccatccgcacgattccctggcagcgagaaatctaggtcctcccc
tgaccacctggaccgcgcaggggactagtcgcggccggcagaacctgctcggtccctggg
ccgggctatcttagcggctcacgcatgcccgagcacacccgacccggttcgcggtgcagg
ctggcggcgccgtgccctctgggacctgttgccccagggttggcgctgctggtggagggc

ccgacggacgccagggcggagggtgtgaatttactcgatggtcgcggacgtgcgcgtccg
cggccaggggtggctcttcggctttgactcgtgtctgcggcgcaccaggagagagaggaa
gttgttggaggagaatagttgccacagccagggcggtgacggccgttagggtctgccccc
gacgggccaaaacaaggacaagtggcgaggactgggcctggggatggcccctgcgggtccg
ggcgcggcgcaagtcctgctttgtctccaggtgactggctgtccaggacggcgggagctg
ctaaggcttgtgtccggaaggagcacagggatgggcagggtggccgggccagccggccct
caaatcctccgacgaagcggcagccgccacgaccacggccagagcagcgctcggaggcga
gtttgtcaacaatcgcctcgcctttggcggcctgacccgtaggcgccgcccccaccgcgg
ctgccgattggctgcggcgcggagcgaccgcgcgcggaccaattgggaacgcgggcaccc
ggcgccagcggcgcggggaggtcggcggtgccggcggcggcgggcgcagagcgcgagggg
aggagcgggaggaggcggaggatgttcccggcggctgcggccggggcagcgcgggccaga
ggcgcggcgtgcggagccctcggctgcccggcggagcgcggcggcgggctggcgggaagg
cgcgggctttgcgctgcgccggggactctgaacccgagtcccgggctttgtctcctgcgc
tgctttcgtggtgacggtcaggggggcgcccggtcggcgaagggcgcgggccggacgccgc
ggggcttggtccctggcccggacgctgcgctctgaagggaaggcgcggacgtgagtttcg
gtgtgattgccttctgaggggagggtctgtgggatgaaggcggcgcggcgcgcaccggtg
tcgcctagcctgcggacctagttgtagaccttgcaggcgttcgcttcgtcgccctccgcc
gccccctccccatttagagatgtgcacctcacggtgtgcacctcagagaagttctgtctg
attcggtgcggcgtgcggtacgggagcgggagggagggagcacgggcggagagagcgcca
gagccgggccgagccgcgctggagttacaaactctattgtgacgcacttactacgactga
cggccgctgccagaccttccccagacttgctgccctcagcattttcggcaaacaatgggg
ccggagcagggaacgcggccagccgcctgcaatcgctgcatctgcgcccgctcctgtgct
ccggcgtcctacctaaccccgggaagtcagagccgctgggagtttctgacttactcgaag
aagtctgtcctgggcaaagagcacacacgaatagacttcagattagctgcttctctggaa
acgcatgtgtgtgtgcaccagttccgcaagctgttgacattgttactgtattttgtttggg
gggtacccctctaccaaaaaaaaattacacctttattattttaggtgcaatttttttattt
gggagattgtcagaaaagtatagaacaaagtatttgggattaaccctaagaatttttaat
cgctaggtgagagctaatttgtttattcatcgatttttttttttgcttaaaataatctta
gtttttattttacttgcagAAAAAAAGACCAAATGGCAAAGCAACCTTCTGATGTAAGTT
CTGAGTGTGACCGAGAAGGTAGACAATTGCAGCCTGCGGAGAGGCCTCCCCAGCTCAGAC
CTGGGGCCCCTACCTCCCTACAGACAGAGCCACAAGgtaatcctgaaggcaatcacggag
gtgaaggggacagctgcccccacggcagccctcagggcccgctggccccacctgccagcc
ctggccctttgctaccagatccccgcttttcatctttatgagaagatcctccctgctgt
ctcgatcctccagtgggtatttctcttttgacacagACAGGAGCCCAGCACCCATGAGTT
GTGACAAATCAACACAAACCCCAAGTCCTCCTTGCCAGGCCTTCAACCACTATCTCAGTG
CAATGGgtaagcaatgcctgggtaagaggcagttgacgtgtggatggttgaatctgcttg
aaggctgtgtgtggcatttaaaatccccttttaaaaccccgtaactgatttattccatct
ttagatgggaatggaggatgtgtcaaactatcaaaccaacttttttttttttttgaga
tgagtcttgctctgtcgcccaggctggagtgcagtggtgcaatctcagctcaccgcaagc
tccacctcccgggttcaagcaattctcctacctcagcctccagagtagctgggactacag
gcgcgtgccaccacgcccagctaatttttttctatttttggtagagatggggtttcaccgt
gttagccaggatggtctcaatctcctgaccttgtaatctgcctgtctcagcctcccaaag
tgctgggattacaggcgtgagccaccgcgcatggcccacatcaacatttttacaaagtta
ctaacttttgtggcagtgatgagttgaggtccaaacattagctttcaggtctgtcttcat
taagctaaagtgtgttttaaccaccaggctttacatagtaatgacattttgcttgaaagg
gaactgatcatttacagaaaatagcttaataatcaaaagtgtaaagaaagatgacaatca
tttttgaaaataacacttttaaaaaaatgaactagttcatgaaagcagtaccaacataga
accatgaaaatggtttgttttctgcctaaattcctctttgtgcttattgctcagagggtt
tggacatagtactaatcagattaggttgtaggtttttatttcagggattaaaggcagtag
tagggtttgaaccaagagtggctaacataaataccacagaggcccacagcaaaatcatgg
aaggaactgacctggtggagactggtaaattggagagtatttgccccttctatgtttggg
ccacacctaattgtggctgtgagggcatgtggtctcagggtgggttttcctatattgcaa
gataacctaggaatgcaaaattgatgccagataccctgtttcaacattgacagctgattc
agattttgaaaacattgtacaagctgaaaagaaacatctgcagacttgatttggcccttg
aacctacagcatgtgactttgggtacatactttgggtaaccttggtgaggggctgagtct

gtgttgatcgacttgctgttccccaccaatggaaaaggttcatgtcttgatcagtagtca
atcacattgaccatttgtccagattagcttgccatacatgaacaagatagaagtaagttg
gtagagttatcaattaggaaacccagtacagagtctattataatttagattgtacctcat
gatgaaggctaactcaacaaacccatcagaacagacactggaacaaaatgacatttctaa
ataccatccagctctgtcttcataggcttcagtgaggtaaatcaggcaggcctttgccca
tgttatagaattggaaagaacctcagagtggtggtcacttgtcagaggttgggcacacct
gtgaggtggtggggagaaatgacagacatcccagcagctacacatgctggctgcacgtct
cttgccaaatgccaggaggtaatttttttagggtccctccttagggaaaggggctggaagt
tttattattgctgttactactgctcgtgaactcatttcagccttagaagttcttggcttg
tagtttttgttgtactcatgaaaatgctcccccatatatatgatcattctcgcttactat
aacatccttgcttactaaatgagttaacagggctttatggtgtgtatcgtgaaacacacg
tgcattaaagaccctctggaaggtattagcttttcacactttcacaacaaaagcttcaca
cttgtggttattaagctattttctctaaccagttccctttcaagcaaaatgcatacattg
gtctctgtaggtgatgggttaatgcatggaaatagtttctccttccctggaactgggaat
agtgggtgagatagtgtatttttttaatgtaaagacaggcacaaatgctttttttgttgat
aaatactattttacaagctaattataagttaagcactgttacttgagatgaaatatacag
ggcttcaaagatcataatctaaataattatgcacagctaatggttatacctgtgaagtaa
agtagtggatcctgaggtgtaattttatagtattagctgcatttcagtagatggtgtgat
gaagagtttaatgcataggattaaatgagaagttacgaggagtttgtttaaagttaatgt
accgaggtaagttttcagtgttaagtttttgggagatttgttttgggagaggatgagttg
gggttgggggaggaaaggacttagccagatgtgagtttcttaaattgaagcataaaattt
acaatttatgtagtccataatttctctggacattctacagtcttagttcatgcctgaag
accactgaaataatgctgagttgataagtggttctcttgactttgtttagtattctttac
tcaaccctatccatgaagttcttcaatgaagcttttgataatttattgcaaaatacattt
tccacaaagaagtcattatgattggtttgaactagtggaacacaaatgtgaggttataaa
gaggttcgccttagccaggggctcctttagctgcaaagcagtttttgctcagcaacttg
gggtagagatcagtgtgtcttgaagttttgttttgcaaaactttgttctaatgagaaagt
caagtcttaggaggaatgtatagtagttgagtgtttgtattaacactgttttcatatttt
ccttttatgtctctgatttttctgaagacaagttcaaggaatatatttctctgtggggca
acagatacagtttttcacttttcctcaattttagtctccttacactctgggaggattaa
cttgacaaatgataccttagtgaataactgattatttttatcaaaatcactcacatgtgt
tggtttactgagtgccttttggatgagtgttttatgccatatgtgtttttaatggaaat
taaagtgtagtcagtacactaaagtgtagtcagtacaattggaaataagagttgagaaaa
gtcaggatatggaggaatgctccctagtgtcatgttagtaaatgtcttaaattttatact
tgttccctggcacattggaattcacagatgggagttaatggctttctttttttttttttt
tttttcctcagcgtcttgtgggtacttctcttatagctggtacttgtctgacccctcctt
tagtttgtgagctccctgggcggggaataatggcctgcagatgctagcgagtgcctgaca
aagaggagaagcccaggagatgttgagagtcagtccagctctgcctgttagcctttcaga
caaataaagttgaagaaggcaggtagcaagaaaaagatcctgacctctgctctgccaaag
tgtttttaattacctggatctagctgtaaggtttgccacgtagtggtgacagctgaggtc
tagctcagcactactcagcagggaagccacacatgcattaagcacttgacataggactag
tctgaactgagttgtgctgtcattattgatacacactggattttgaggagacaaaaaaga
atgcaaaatagtttaattgttttcatatgggttacatgttgaaatggtgttttaaatata
taggttaaataaaatataaacttgtattgcagttaaacacaaagcgtaaaatttaccatc
tgaaccatttatttctaagtgtactgttcagtagtgttaagtgcacttattttgttgtgc
ggccaatctccagaacttcttcaccttgcaaaacagaaattctgtactcattaaacaact
ccccatttccccctcccccagcttctgacaaccaccattctattttctgtctattaatt
tgacaacttcagataccttatataagtgaaatttatatagtatttgctcttccatgacag
gcttatttcacttagcgtaatgtcgtcagggttcatttatcttgcaacatgtcagaattt
ccttccttttaaggctgaaggttgttccagtgtgtgtatatcacatacttcatttatcc
attcatccatcaggagatacttgggttgcttccacttttggctattgtgagtagtgctg
ctatgaacatgggtatgcaaatatcttttgggggattctgctttgaatttttttggatat
atacttggaagtggaattgctggatcatatggtaattctatttttaatttttggggaac
catcatgctgttctccatagaggctgtgccatttacattcccaccaacagggcacaagg
gttccagtttctccacatacttaccaacacttttttttttttttttttaacagTAGTCAT

CCTAGAGGATATAGGTGATCTTTCACTGTGCTTTGGATTTATATTTACTGGCTTAGATTT
GTATGGCCACCACCATAGTCAAGATACAGAACAACTCAACCACAAGGATTTCTCATGATA
CCTTTTTATAGCCACAGCCACCTCTCTCCCTCTTCCTTGAGCATTTTGTCATATGGTCAT
TGGTGATTAAATAAAATGTATTTTAATATTGACtttctctgtttctttctacctttttaa
acatggctactagaaaaatgcacaattagatttgtggctggtgttctgtttcatctaaac
aggctggcctcacagaggagctggagtgtgcagtgctgctctagcaagccaggcttgact
cttcccactcagggcacatcacttccatgaagcttactccttgggttgtttggttgactt
aggagaatggaagtgattagcagaatcttgtaagcattttaaacattaaatgagcattgt
aaacagcggcattcttcaggcaaatacagttttgttttacctctttaaattccatggtat
attcggacttcaaaaagtagatggtagagcacatgctttctcagcaccttcaggctgcct
ggagcctcccaatagaggtgtcttcgagggagtcccagctctgtctctgaaaccccaaag
ttacttgtttgacaccaagagaaataaggaaacttttaggtcctaagtggggagagaaa
gtgctagaagagaaagatatttttctttactagttccaaacacatttattaattgttagt
tacccaattttaaatttacatcttaaaaaaatttttttttcagataattacagattcacat
gcatttataggaaataatacaaagaaattgtatatgccattcacccagtttcctacgatg
gtaacatcttgcctaattatagtatactgtcacaaccagcagttgacattaacagaatcc
atctactgtattgagatttcatcagtttcacatgcagtccatttcatgtgtctgtgagtg
tttacttctattcaggtttatcaaatgtgtagatttgtatggccgccaccacagtcaaga
tgcagaacaactccaccacaaggatttctcatggtacctttttatagccacagccacctt
tctgtctcttccttacccatgataaccactcatctgatctacatatctgtacttttgtca
tttcaaggatgct

6.5 Appendix 5

6.5.1 SDS-PAGE gel composition

Resolving Gel	15%	12.5%	9%	7.5%	Stack (4.5%)
30% acrylamide/l%bis	8.7	7.3	5.4	4.4	0.6
Resolving Buffer 1.5M Tris PH8.8/0.4% SDS	4.4	4.4	4.4	4.4	
Stack Buffer 0.5M Tris pH6.8/0.4% SDS					1.0
ddH20	4.4	5.8	7.7	8.7	2.2

Just before pouring

*Ammonium persulphate (0.5g/ml in distilled water)	110µl	110µl	110µl	110µl	29µl
TEMED	3.6µl	3.6µl	3.6µl	3.6µl	0.9µl

6.6 Appendix 6

6.6.1 Automated spheroid assessment MATLAB script

```
% Set up GUI
clc
clear all

%The main figure
ss = get(0,'ScreenSize');
h.h = figure('CloseRequestFcn', @closeWindowMode);
%h.h = figure;

set(h.h,'Position',[ss(3)/2-(ss(4)/2)-50  50  ss(4)+100  ss(4)-150],
'Visible','off');

%Two panels, one folgr\f gr the image, the other for the controls
%h.h_im_plain_p     =     uipanel('Position',[0.01     0.01     0.7
0.98],'FontSize',12);
h.h_im_cont_p      =     uipanel('Position',[0.01     0.01     0.7
0.98],'FontSize',12);
h.h_cont_tg  =  uitabgroup('Parent',h.h,'Position',[0.72  0.27  0.28
0.72]);
h.h_dis_p      =      uipanel('Position',[0.72      0.01      0.27
0.25],'FontSize',12);
h.h_det_t = uitab('Parent',h.h_cont_tg,'Title','<html><font size=4
color="black">Spheroid analysis transmitted light','Tag','1');
%h.h_fluor_t    =    uitab('Parent',h.h_cont_tg,'Title','<html><font
size=4 color="black">Fluorescence Image','Tag','2');
%  h.h_export_t  =  uitab('Parent',h.h_cont_tg,'Title','<html><font
size=4 color="black">Export','Tag','3');
h.h_im_cont_p_ax  =  axes('Parent',h.h_im_cont_p,'Position',[0  0  1
1],'Visible','on');
%h.h_im_plain_p_ax  =  axes('Parent',h.h_im_plain_p,'Position',[0  0
1  1],'Visible','off');

cont_top = 0.9;
bt_h = 0.055;
gap = bt_h + 0.015;
edit_offs = 0.01;


%%Load defaults & Global variables

kernelSize=50;
offset=-0.05;
size1=2000;
size2=2000;
se = strel('disk',2);
scaling=1;
L=[];
B=[];
mask5=[];
properties=[];
focusedProcessed=[];

%Set up Random Colourmap for images
x=[0:255];
T=rand(256,3);
```

```
map=T;
%map = interp1(x/256,T,linspace(1,1,256));
%map(255,:,:)=[0,0,0];
map(1,:,:)=[0,0,0];

%% Getting files
[im_fname,                    im_pname,load_cnd]                    =
uigetfile({'*.tif;*.tiff;*.jpg;*.jpeg;*.png;*.bmp;*.lif'},    'Load
image');
if load_cnd == 0
    return
end
cd(im_pname)



%bioformats open Lif
lif_name=strcat([im_pname, im_fname]);
[pathstr,lif_name,ext] = fileparts(lif_name);
if strcmp(ext,'.lif')
    lif_name=strcat(lif_name,'.lif');
    data=bfopen(char(lif_name));
    omeMeta = data{1, 4};
    numberOfChannels=omeMeta.getChannelCount(0);
    try

scaling=double(omeMeta.getPixelsPhysicalSizeX(0).getValue());
    catch
        scaling=double(omeMeta.getPixelsPhysicalSizeX(0).value());
    end
    if numberOfChannels==1
        im=data{1,1};
    else
        loadMultichannelLif
        data=allData;
        im=data{1,1};
    end

    preProcessImage;

elseif strcmp(ext,'.tif')
    im = imread(strcat([im_pname, im_fname]));
    if size(im,3) == 3
        im = rgb2gray(im);

    end
    data=1;
end
n_rows = size(im,1);
n_cols = size(im,2);

%Buttons and controls TRANS
set(h.h,'Position',[ss(3)/2-(ss(4)/2)-50  50  ss(4)+100  ss(4)-150],
'Visible','on');
pos = 0;
pos=pos;
fluorescence_text                                                    =
uicontrol('Parent',h.h_det_t,'Style','text','String','Fluorescence
```

```
image?','FontSize',12,'Units','normalized','HorizontalAlignment','
left','Position',[0.1, cont_top-gap*pos, 0.54, bt_h-edit_offs]);
fluorescence=uicontrol('Parent',h.h_det_t,'Style','checkbox','Font
Size',24,'Units','normalized','HorizontalAlignment','left','Enable
','on','Position',[0.75, cont_top-gap*pos, 0.54, bt_h-edit_offs]);
pos = pos + 1.2;
KS_text                                                          =
uicontrol('Parent',h.h_det_t,'Style','text','String','Kernel
Size:','FontSize',12,'Units','normalized','HorizontalAlignment','l
eft','Position',[0.1, cont_top-gap*pos, 0.54, bt_h-edit_offs]);
KS_edit                                                          =
uicontrol('Parent',h.h_det_t,'Style','edit','String',num2str(kerne
lSize),'FontSize',12,'Units','normalized','Position',[0.7,
cont_top-gap*pos, 0.22, bt_h]);
pos = pos + 1.2;
offset_text                                                      =
uicontrol('Parent',h.h_det_t,'Style','text','String','Offset:','Fo
ntSize',12,'Units','normalized','HorizontalAlignment','left','Posi
tion',[0.1, cont_top-gap*pos, 0.54, bt_h-edit_offs]);
offset_edit                                                      =
uicontrol('Parent',h.h_det_t,'Style','edit','String',num2str(offse
t),'FontSize',12,'Units','normalized','Position',[0.7,   cont_top-
gap*pos, 0.22, bt_h]);
pos = pos + 1.2;
sizeFilter1_text                                                 =
uicontrol('Parent',h.h_det_t,'Style','text','String','SizeFilter1
(pix):','FontSize',12,'Units','normalized','HorizontalAlignment','
left','Position',[0.1, cont_top-gap*pos, 0.54, bt_h-edit_offs]);
sizeFilter1_edit                                                 =
uicontrol('Parent',h.h_det_t,'Style','edit','String',num2str(size1
),'FontSize',12,'Units','normalized','Position',[0.7,    cont_top-
gap*pos, 0.22, bt_h]);
pos = pos + 1.2;
sizeFilter2_text                                                 =
uicontrol('Parent',h.h_det_t,'Style','text','String','SizeFilter2
(pix):','FontSize',12,'Units','normalized','HorizontalAlignment','
left','Position',[0.1, cont_top-gap*pos, 0.54, bt_h-edit_offs]);
sizeFilter2_edit                                                 =
uicontrol('Parent',h.h_det_t,'Style','edit','String',num2str(size2
),'FontSize',12,'Units','normalized','Position',[0.7,    cont_top-
gap*pos, 0.22, bt_h]);

%Change image slider and number
pos = pos + 1.5;
image_number                                                     =
uicontrol('Parent',h.h_det_t,'Style','slider','String','Image','Ca
llback',@changeImage,'Min',  1,  'Max',  size(data,1),  'Value',  1,
'SliderStep',                                          [1/size(data,1),
1/size(data,1)],'FontSize',12,'Units','normalized','Position',[0.1
, cont_top-gap*pos, 0.8, bt_h]);
pos = pos + 1.5;
cont_image_text                                                  =
uicontrol('Parent',h.h_det_t,'Style','text','String','Image
Number:','FontSize',12,'Units','normalized','HorizontalAlignment',
'left','Position',[0.1, cont_top-gap*pos, 0.54, bt_h-edit_offs]);
cont_image_edit                                                  =
uicontrol('Parent',h.h_det_t,'Style','edit','String',num2str(get(i
mage_number,'Value')),'Callback',@changeImageNumber,'FontSize',12,
'Units','normalized','Position',[0.7,    cont_top-gap*pos,    0.22,
bt_h]);
```

```
%Detect, reset and run all
pos = pos + 1.2;
Detect_button                                                    =
uicontrol('Parent',h.h_det_t,'Style','pushbutton','String','Detect
those
spheroids','FontSize',12,'Callback',@detect,'Units','normalized','
Position',[0.05, cont_top-gap*pos, 0.9, bt_h]);
pos = pos + 1.2;
Reset_button                                                     =
uicontrol('Parent',h.h_det_t,'Style','pushbutton','String','Clear
Outlines','FontSize',12,'Callback',@clearOutlines,'Units','normali
zed','Position',[0.05, cont_top-gap*pos, 0.9, bt_h]);
pos = pos + 1.2;
display_label_button                                             =
uicontrol('Parent',h.h_det_t,'Style','pushbutton','String','Displa
y
Labels','FontSize',12,'Callback',@displayLabels,'Units','normalize
d','Enable','off','Position',[0.05, cont_top-gap*pos, 0.9, bt_h]);
pos = pos + 1.2;
Run_All_button                                                   =
uicontrol('Parent',h.h_det_t,'Style','pushbutton','String','Run
All','FontSize',12,'Callback',@runAll,'Units','normalized','Positi
on',[0.05, cont_top-gap*pos, 0.9, bt_h]);


%Disco
pos=7;
disco_button                                                     =
uicontrol('Parent',h.h_dis_p,'Style','pushbutton','String','Disco?
','FontSize',12,'Callback',@runDisco,'Units','normalized','enable'
,'off','Position',[0.05, cont_top-gap*pos, 0.9, bt_h+0.1]);
pos=pos+3.5;
save_preview_button                                              =
uicontrol('Parent',h.h_dis_p,'Style','pushbutton','String','Save
Preview','FontSize',12,'Callback',@savePreview,'Units','normalized
','Position',[0.05, cont_top-gap*pos, 0.9, bt_h+0.1]);


curr_im = imshow(im,[],'Parent',h.h_im_cont_p_ax);
dcm = datacursormode(h.h);
set(dcm, 'UpdateFcn', @dcmCallback);
drawnow;

    function savePreview(~,~)
        mkdir(strcat(date,'_Analysis'));
        prompt = {'Input File Name (without extension):'};
        title = 'Save as...';
        dims = [1 35];
        definput = {'myFile'};
        fileName = inputdlg(prompt,title,dims,definput);
        fileName = strcat(char(fileName), '.png');
        fileName = strcat(date,'_Analysis/',fileName);
        imwrite(im,fileName);
    end

    function preProcessImage(~,~)
        im=fstack(im);
    end

    function changeImage(~,~)
```

```
        set(h.h, 'pointer', 'watch')
        drawnow;

set(cont_image_edit,'String',num2str(round(get(image_number,'Value
'))));
        im=data{round(get(image_number,'Value')),1};
        %metadata = data{1, 2};

        preProcessImage;

        curr_im = imshow(im,[],'Parent',h.h_im_cont_p_ax);
        set(display_label_button,'Enable','off');
        set(disco_button,'Enable','off');
        set(h.h, 'pointer', 'arrow')
    end


    function changeImageNumber(~,~)
        set(h.h, 'pointer', 'watch')
        drawnow;

set(image_number,'Value',(str2double(get(cont_image_edit,'String')
)));

        im=data{str2double(get(cont_image_edit,'String')),1};
        preProcessImage;

        curr_im = imshow(im,[],'Parent',h.h_im_cont_p_ax);
        set(display_label_button,'Enable','off');
        set(disco_button,'Enable','off');
        set(h.h, 'pointer', 'arrow')
    end

    function detect(~,~)
        set(h.h, 'pointer', 'watch')
        drawnow;
        curr_im = imshow(im,[],'Parent',h.h_im_cont_p_ax);

        focused=im;

        if get(fluorescence,'Value')==0
            focusedProcessed=imcomplement(focused);
        else
            focusedProcessed=focused;
        end

mask=adaptivethreshold(focusedProcessed,str2double(get(KS_edit,'St
ring')),str2double(get(offset_edit,'String')),0);
        mask=imdilate(mask,se);
        mask2=imfill(mask,'holes');
        %sizeSieve1In=sizeSieve1/(scaling*scaling);

mask3=bwareaopen(mask2,round(str2double(get(sizeFilter1_edit,'Stri
ng'))));
        D = -bwdist(~mask3);
        Ld = watershed(D);
        bw2 = mask3;
        bw2(Ld == 0) = 0;
        extendMin = imextendedmin(D,2.5);
```

```
        D2 = imimposemin(D,extendMin);
        Ld2 = watershed(D2);
        bw3 = mask3;
        bw3(Ld2 == 0) = 0;

        %sizeSieve2In=sizeSieve2/(scaling*scaling);


bw4=bwareaopen(bw3,round(str2double(get(sizeFilter2_edit,'String')
)));
        mask4=imclearborder(bw4);
        mask5=immultiply(focusedProcessed,mask4);

        [B,L,N,A] = bwboundaries(mask4);

properties=regionprops(L,focused,'Area','Centroid','Eccentricity',
'Perimeter','FilledArea','Solidity');

        hold on
        for k=1:length(B),
            boundary_Master = B{k};
            line(boundary_Master(:,2), boundary_Master(:,1),...
                'color','r','LineWidth',1,'Parent',
h.h_im_cont_p_ax);
        end
        hold off;

        %im=mask4;
        %curr_im = imshow(im,[],'Parent',h.h_im_cont_p_ax);
        set(h.h, 'pointer', 'arrow')
        set(display_label_button,'Enable','on');
    end

    function clearOutlines(~,~)
        set(h.h, 'pointer', 'watch')
        drawnow;
        clearvars B L properties mask5;
        im=data{str2double(get(cont_image_edit,'String')),1};
        preProcessImage;
        curr_im = imshow(im,[],'Parent',h.h_im_cont_p_ax);
        set(display_label_button,'Enable','off');
        set(disco_button,'Enable','off');
        set(h.h, 'pointer', 'arrow')
    end

    function displayLabels(~,~)
        figure('Visible','off'); temp=imshow(L,[]);
        %map(255,:,:)=[0,0,0];
        map(1,:,:)=[0,0,0];
        %colormap(map);

        %set(temp,'AlphaData',mask5);
        set(temp,'AlphaData',focusedProcessed);

        colormap(map);

        centroids = cat(1, properties.Centroid);

        hold on
```

```
        for k = 1:length(centroids)
            try
                text(centroids(k,1), centroids(k,2), sprintf('%d',
k),'FontSize',14);
            catch
            end

        end
        hold off
%         hold on
%         for k=1:length(B),
%             boundary_Master = B{k};
%             line(boundary_Master(:,2), boundary_Master(:,1),...
%                 'color','g','LineWidth',1);
%         end
%         hold off;

        drawnow
        img=getframe(gcf);
        curr_im = imshow(img.cdata,[],'Parent',h.h_im_cont_p_ax);
        set(disco_button,'Enable','on');
    end

    function runAll(~,~)
        progress = waitbar(0,'Processing bits and bobs');


        for allData=1:size(data,1);
            excelData=[];
            name=omeMeta.getImageName(allData-1);

            im=data{allData,1};
            preProcessImage;
            focused=im;

            if get(fluorescence,'Value')==0;
                focusedProcessed=imcomplement(focused);
            else
                focusedProcessed=focused;
            end


mask=adaptivethreshold(focusedProcessed,str2double(get(KS_edit,'St
ring')),str2double(get(offset_edit,'String')),0);
            mask=imdilate(mask,se);
            mask2=imfill(mask,'holes');
            %sizeSieve1In=sizeSieve1/(scaling*scaling);

mask3=bwareaopen(mask2,round(str2double(get(sizeFilter1_edit,'Stri
ng'))));
            D = -bwdist(~mask3);
            Ld = watershed(D);
            bw2 = mask3;
            bw2(Ld == 0) = 0;
            extendMin = imextendedmin(D,2.5);
            D2 = imimposemin(D,extendMin);
            Ld2 = watershed(D2);
            bw3 = mask3;
            bw3(Ld2 == 0) = 0;
```

```
            %sizeSieve2In=sizeSieve2/(scaling*scaling);
            get(sizeFilter1_edit);

bw4=bwareaopen(bw3,round(str2double(get(sizeFilter2_edit,'String')
)));
            mask4=imclearborder(bw4);
            mask5=immultiply(focusedProcessed,mask4);

            [B,L,N,A] = bwboundaries(mask4);

properties=regionprops(L,focused,'Area','Centroid','Eccentricity',
'Perimeter','FilledArea','Solidity');

            %scaling
            scaling;
            for i=1:length(properties);

properties(i).Area=(properties(i).Area)*(scaling*scaling);
            end

            %Data Export organisation
            nameList=cell(1,length(properties));
            for t=1:length(properties)
                nameList(t)=name;
            end

            propsEx=struct2cell(properties);
            propsEx=propsEx.';
            propsEx2=[nameList' propsEx];
            %propsEx2;

testExport=cell2table(propsEx2,'VariableNames',{'Image_Name'
'Area'                                          'Centroid'
'Eccentricity','Perimeter','FilledArea','Solidity'});

            %Save Data
            mkdir(strcat(date,'_Analysis'));

writetable(testExport,strcat(strcat(date,'_Analysis\'),strcat(date
,'_Analysis'),'.xlsx'),'sheet',strrep(char(name),'/','-'));


            figure('Visible','off'), temp=imshow(L,[]);
            %set(temp,'AlphaData',mask5);
            set(temp,'AlphaData',focusedProcessed);
            map(1,:,:)=[0,0,0];
            colormap(map);

            centroids = cat(1, properties.Centroid);

            hold on
            for k = 1:length(centroids);
                try
                    text(centroids(k,1),           centroids(k,2),
sprintf('%d', k),'FontSize', 14);
                catch
                end
            end
```

```
            hold off
            img=getframe(gcf);

imwrite(img.cdata,strcat(strcat(strcat(date,'_Analysis\'),strrep(c
har(name),'/','-'),'_',mat2str(allData),'.png')));

            waitbar(allData/size(data,1),progress);
        end
        if isvalid(progress)
            close(progress)
        end

    end

    function runDisco(~,~)

        for loop=1:25
            map=circshift(map,1);
            displayLabels;

        end

    end

    function loadMultichannelLif(~,~)

        prompt = {'Pick channel to analyse'};
        dlg_title = 'Channel Picker thing';
        num_lines = 1;
        defaultans = {'1'};
        channelAssignment                                          =
inputdlg(prompt,dlg_title,num_lines,defaultans);


        reader=bfGetReader(lif_name);
        omeMeta = reader.getMetadataStore();
        reader.setSeries(1);
        iPlaneEnd=reader.getIndex(reader.getSizeZ-
1,(str2double(channelAssignment{1}))-1,0)+1;
        iPlaneBeg=iPlaneEnd-(reader.getSizeZ-1);



        allData=cell(reader.getSeriesCount,1);
        for series=1:reader.getSeriesCount
            data2=data{series,1};
            data3=cell(reader.getSizeZ,2);
            j=1;
            for i=iPlaneBeg:iPlaneEnd;
                data3{j,1}=data2{i,1};
                j=j+1;
            end
            j=1;
            for i=iPlaneBeg:iPlaneEnd;
                data3{j,2}=data2{i,2};
                j=j+1;
            end
```

```
            allData{series}=data3;
            data3=[];
        end

    end

    function closeWindowMode(~,~)
        % Asking the user if the process should be repeated
        quest_res     =     questdlg('Analyse     another     Lif
File?','Continue?','Yes','No','Yes');
        switch quest_res
            case 'Yes'
                delete(h.h)
                clear all
                SpheroidMeasureTransmitted_2017_08_04
            case 'No'
                delete(h.h)
        end
    end

end
```

References

1. Todd RC, Lippard SJ. Inhibition of transcription by platinum antitumor compounds. Metallomics. 2009;1(4):280-91.

2. Urban B, Collard T, Eagle C, Southern S, Greenhough A, Hamdollah-Zadeh M, et al. BCL-3 expression promotes colorectal tumorigenesis through activation of AKT signalling. Gut. 2015;Epub ahead of print.

3. Jost PJ, Ruland J. Aberrant NF-kappa B signaling in lymphoma: mechanisms, consequences, and therapeutic implications. Blood. 2007;109(7):2700-7.

4. Perkins ND. Integrating cell-signalling pathways with NF-kappa B and IKK function. Nature Reviews Molecular Cell Biology. 2007;8(1):49-62.

5. CRUK. [Available from: http://www.cancerresearchuk.org/health-professional/cancer-statistics/statistics-by-cancer-type/bowel-cancer#heading-Six.

6. ONS. Cancer Survival in England: Adults Diagnosed 2008 to 2012, followed up to 2013. In: Statistics OfN, editor. London2014.

7. Siegel RL, Fedewa SA, Anderson WF, Miller KD, Ma J, Rosenberg PS, et al. Colorectal Cancer Incidence Patterns in the United States, 1974–2013. JNCI: Journal of the National Cancer Institute. 2017;109(8):djw322-djw.

8. Ionov Y, Peinado MA, Malkhosyan S, Shibata D, Perucho M. UBIQUITOUS SOMATIC MUTATIONS IN SIMPLE REPEATED SEQUENCES REVEAL A NEW

MECHANISM FOR COLONIC CARCINOGENESIS. Nature. 1993;363(6429):558-61.

9. Kinzler K, Vogelstein B. Lessons from hereditary colorectal cancer. Cell. 1996;87:159-70.

10. Byrne RM, Tsikitis VL. Colorectal polyposis and inherited colorectal cancer syndromes. Annals of Gastroenterology. 2018;31(1):24-34.

11. Syngal S, Brand RE, Church JM, Giardiello FM, Hampel HL, Burt RW. ACG Clinical Guideline: Genetic Testing and Management of Hereditary Gastrointestinal Cancer Syndromes. American Journal of Gastroenterology. 2015;110(2):223-62.

12. Hill MJ, Morson BC. ETIOLOGY OF ADENOMA - CARCINOMA SEQUENCE IN LARGE BOWEL. Lancet. 1978;1(8058):245-7.

13. Linnekamp JF, Hooff SRV, Prasetyanti PR, Kandimalla R, Buikhuisen JY, Fessler E, et al. Consensus molecular subtypes of colorectal cancer are recapitulated in in vitro and in vivo models. Cell Death Differ. 2018.

14. Haggar F, Boushey R. Colorectal cancer epidemiology: Incidence, Mortality, Survival and Risk Factors. Clinics in Colon and Rectal Surgery. 2009;22(4):191-7.

15. Li F-Y, Lai M. Colorectal cancer, one entity or three. Journal of Zhejiang University. 2009;10(3):219-29.

16. Muzny DM, Bainbridge MN, Chang K, Dinh HH, Drummond JA, Fowler G, et al. Comprehensive molecular characterization of human colon and rectal cancer. Nature. 2012;487(7407):330-7.

17. Evans J, Patel U, Brown G. Rectal cancer: primary staging and assessment after chemoradiotherapy. Semin Radiat Oncol. 2011;21(3):169-77.

18. NICE. Colorectal Cancer: The diagnosis and management of colorectal cancer CG131. NICE; 2014.

19. Gollins S, Sebag-Montefiore D. Neoadjuvant Treatment Strategies for Locally Advanced Rectal Cancer. Clinical Oncology. 2016;28(2):146-51.

20. Adam IJ, Mohamdee MO, Martin IG, Scott N, Finan PJ, Johnston D, et al. ROLE OF CIRCUMFERENTIAL MARGIN INVOLVEMENT IN THE LOCAL RECURRENCE OF RECTAL-CANCER. Lancet. 1994;344(8924):707-11.

21. Quirke P, Dixon MF, Durdey P, Williams NS. LOCAL RECURRENCE OF RECTAL ADENOCARCINOMA DUE TO INADEQUATE SURGICAL RESECTION - HISTOPATHOLOGICAL STUDY OF LATERAL TUMOR SPREAD AND SURGICAL EXCISION. Lancet. 1986;2(8514):996-9.

22. Nagtegaal ID, Quirke P. What is the role for the circumferential margin in the modern treatment of rectal cancer? Journal of Clinical Oncology. 2008;26(2):303-12.

23. Gollins S, West N, Sebag-Montefiore D, Myint AS, Saunders M, Susnerwala S, et al. Preoperative chemoradiation with capecitabine, irinotecan

and cetuximab in rectal cancer: significance of pre-treatment and post-resection RAS mutations. British Journal of Cancer. 2017;117(9):1286-94.

24. Brown G, Daniels IR, Heald RJ, Quirke P, Blomqvist L, Sebag-Montefiore D, et al. Diagnostic accuracy of preoperative magnetic resonance imaging in predicting curative resection of rectal cancer: prospective observational study. British Medical Journal. 2006;333(7572):779-82.

25. Morino M, Risio M, Bach S, Beets-Tan R, Bujko K, Panis Y, et al. Early rectal cancer: the European Association for Endoscopic Surgery (EAES) clinical consensus conference. Surg Endosc. 2015;29(4):755-73.

26. Heald R, Moran B, Ryall R, Sexton R, MacFarlane J. Rectal Cancer: the Basingstoke experience of Total Mesorectal Excision 1978-1997. Archives of Surgery. 1998;133(8):894-8.

27. MacFarlane JK, Ryall RDH, Heald RJ. Mesorectal excision for rectal cancer. The Lancet. 1993;341(8843):457-60.

28. Enker WE, Thaler HT, Cranor ML, Polyak T. TOTAL MESORECTAL EXCISION IN THE OPERATIVE TREATMENT OF CARCINOMA OF THE RECTUM. Journal of the American College of Surgeons. 1995;181(4):335-46.

29. Shirouzu K, Isomoto H, Kakegawa T. DISTAL SPREAD OF RECTAL-CANCER AND OPTIMAL DISTAL MARGIN OF RESECTION FOR SPHINCTER-PRESERVING SURGERY. Cancer. 1995;76(3):388-92.

30. Shimada Y, Takii Y, Maruyama S, Ohta T. Intramural and Mesorectal Distal Spread Detected by Whole-Mount Sections in the Determination of Optimal Distal Resection Margin in Patients Undergoing Surgery for Rectosigmoid or Rectal Cancer Without Preoperative Therapy. Diseases of the Colon & Rectum. 2011;54(12):1510-20.

31. de Lacy AM, Rattner DW, Adelsdorfer C, Tasende MM, Fernandez M, Delgado S, et al. Transanal natural orifice transluminal endoscopic surgery (NOTES) rectal resection: "down-to-up" total mesorectal excision (TME)-short-term outcomes in the first 20 cases. Surgical Endoscopy and Other Interventional Techniques. 2013;27(9):3165-72.

32. Lacy AM, Tasende MM, Delgado S, Fernandez-Hevia M, Jimenez M, De Lacy B, et al. Transanal Total Mesorectal Excision for Rectal Cancer: Outcomes after 140 Patients. Journal of the American College of Surgeons. 2015;221(2):415-23.

33. Penna M, Cunningham C, Hompes R. Transanal Total Mesorectal Excision: Why, When, and How. Clinics in Colon and Rectal Surgery. 2017;30(5):339-45.

34. Stearns MW, Deddish MR, Quan SHQ. PREOPERATIVE ROENTGEN THERAPY FOR CANCER OF THE RECTUM. Surgery Gynecology & Obstetrics. 1959;109(2):225-9.

35. Gunderson LL, Sosin H. AREAS OF FAILURE FOUND AT REOPERATION (SECOND OR SYMPTOMATIC LOOK) FOLLOWING CURATIVE SURGERY FOR ADENOCARCINOMA OF RECTUM -

CLINICOPATHOLOGIC CORRELATION AND IMPLICATIONS FOR ADJUVANT THERAPY. Cancer. 1974;34(4):1278-92.

36. Roswit B, Higgins GA, Keehn RJ. PREOPERATIVE IRRADIATION FOR CARCINOMA OF RECTUM AND RECTOSIGMOID COLON - REPORT OF A NATIONAL VETERANS ADMINISTRATION RANDOMIZED STUDY. Cancer. 1975;35(6):1597-602.

37. Kligerman MM. RADIOTHERAPY AND RECTAL CANCER. Cancer. 1977;39(2):896-900.

38. Tepper M, Vidone RA, Hayes MA, Lindenmuth WW, Kligerman MM. PREOPERATIVE IRRADIATION IN RECTAL CANCER - INITIAL COMPARISON OF CLINICAL TOLERANCE SURGICAL AND PATHOLOGIC FINDINGS. American Journal of Roentgenology Radium Therapy and Nuclear Medicine. 1968;102(3):587-+.

39. Ahmad NR, Marks G, Mohiuddin M. HIGH-DOSE PREOPERATIVE RADIATION FOR CANCER OF THE RECTUM - IMPACT OF RADIATION-DOSE ON PATTERNS OF FAILURE AND SURVIVAL. International Journal of Radiation Oncology Biology Physics. 1993;27(4):773-8.

40. Foster JD, Jones EL, Falk S, Cooper EJ, Francis NK. Timing of surgery after long-course neoadjuvant chemoradiotherapy for rectal cancer: a systematic review of the literature. Dis Colon Rectum. 2013;56(7):921-30.

41. Moertel CG. ACCOMPLISHMENTS IN SURGICAL ADJUVANT THERAPY FOR LARGE-BOWEL CANCER. Cancer. 1992;70(5):1364-71.

42. O'Connell M, Martenson JA, Wieand HS, Krook JE, Macdonald JS, Haller DG, et al. IMPROVING ADJUVANT THERAPY FOR RECTAL-CANCER BY COMBINING PROTRACTED-INFUSION FLUOROURACIL WITH RADIATION-THERAPY AFTER CURATIVE SURGERY. New England Journal of Medicine. 1994;331(8):502-7.

43. Krook JE, Moertel CG, Gunderson LL, Wieand HS, Collins RT, Beart RW, et al. EFFECTIVE SURGICAL ADJUVANT THERAPY FOR HIGH-RISK RECTAL-CARCINOMA. New England Journal of Medicine. 1991;324(11):709-15.

44. Group GTS. PROLONGATION OF THE DISEASE-FREE INTERVAL IN SURGICALLY TREATED RECTAL-CARCINOMA. New England Journal of Medicine. 1985;312(23):1465-72.

45. Wils JA. Adjuvant treatment in Dukes' B and C disease. Annals of Oncology. 2000;11:37-43.

46. Rider WD, Palmer JA, Mahoney LJ, Robertson CT. PREOPERATIVE IRRADIATION IN OPERABLE CANCER OF RECTUM - REPORT OF TORONTO TRIAL. Canadian Journal of Surgery. 1977;20(4):335-8.

47. Second Report of an MRC Working Party. The evaluation of low dose pre-operative X-ray therapy in the management of operable rectal cancer; results of a randomly controlled trial. Br J Surg. 1984;71(1):21-5.

48. Kapiteijn E, Marijnen CA, Nagtegaal ID, Putter H, Steup WH, Wiggers T, et al. Preoperative radiotherapy combined with total mesorectal excision for resectable rectal cancer. N Engl J Med. 2001;345(9):638-46.

49. Pahlman L, Glimelius B, Cedermark B, Lundell G, Rubio C, Rutqvist LE, et al. Improved survival with preoperative radiotherapy in resectable rectal cancer. New England Journal of Medicine. 1997;336(14):980-7.

50. Folkesson J, Birgisson H, Pahlman L, Cedermark B, Glimelius B, Gunnarsson U. Swedish rectal Cancer Trial: Long lasting benefits from radiotherapy on survival and local recurrence rate. Journal of Clinical Oncology. 2005;23(24):5644-50.

51. Peeters KCMJ, Marijnen CAM, Nagtegaal ID, Kranenbarg EK, Putter H, Wiggers T, et al. The TME Trial After a Median Follow-up of 6 Years. Annals of Surgery. 2007;246(5):693-701.

52. Sebag-Montefiore D, Stephens RJ, Steele R, Monson J, Grieve R, Khanna S, et al. Preoperative radiotherapy versus selective postoperative chemoradiotherapy in patients with rectal cancer (MRC CR07 and NCIC-CTG C016): a multicentre, randomised trial. The Lancet. 2009;373(9666):811-20.

53. Sauer R, Becker H, Hohenberger W, Rodel C, Wittekind C, Fietkau R, et al. Preoperative versus Postoperative Chemoradiotherapy for Rectal Cancer. New England Journal of Medicine. 2004;351(17):1731-40.

54. Roh MS, Colangelo LH, O'Connell MJ, Yothers G, Deutsch M, Allegra CJ, et al. Preoperative multimodality therapy improves disease-free survival in patients with carcinoma of the rectum: NSABP R-03. J Clin Oncol. 2009;27(31):5124-30.

55. Sauer R, Liersch T, Merkel S, Fietkau R, Hohenberger W, Hess C, et al. Preoperative versus postoperative chemoradiotherapy for locally advanced rectal cancer: results of the German CAO/ARO/AIO-94 randomized phase III trial after a median follow-up of 11 years. J Clin Oncol. 2012;30(16):1926-33.

56. Bosset JF, Collette L, Calais G, Mineur L, Maingon P, Radosevic-Jelic L, et al. Chemotherapy with preoperative radiotherapy in rectal cancer. N Engl J Med. 2006;355(11):1114-23.

57. Gerard JP, Conroy T, Bonnetain F, Bouche O, Chapet O, Closon-Dejardin MT, et al. Preoperative radiotherapy with or without concurrent fluorouracil and leucovorin in T3-4 rectal cancers: Results of FFCD 9203. Journal of Clinical Oncology. 2006;24(28):4620-5.

58. Bujko K, Nowacki MP, Nasierowska-Guttmejer A, Michalski W, Bebenek M, Kryj M. Long-term results of a randomized trial comparing preoperative short-course radiotherapy with preoperative conventionally fractionated chemoradiation for rectal cancer. Br J Surg. 2006;93(10):1215-23.

59. Rombouts AJM, Hugen N, Verhoeven RHA, Elferink MAG, Poortmans PMP, Nagtegaal ID, et al. Tumor response after long interval comparing 5x5Gy radiation therapy with chemoradiation therapy in rectal cancer patients. Ejso. 2018;44(7):1018-24.

60. Ceelen WP, Van Nieuwenhove Y, Fierens K. Preoperative chemoradiation versus radiation alone for stage II and III resectable rectal cancer. Cochrane Database of Systematic Reviews. 2009(1).

61. Dworak O, Keilholz L, Hoffmann A. Pathological features of rectal cancer after preoperative radiochemotherapy. International Journal of Colorectal Disease. 1997;12(1):19-23.

62. Mandard A-M, Dalibard F, Mandard J-C, Marnay J, Henry-Amar M, Petiot J-F, et al. Pathologic assessment of tumor regression after preoperative chemoradiotherapy of esophageal carcinoma. Clinicopathologic correlations. Cancer. 1994;73(11):2680-6.

63. Schrag D, Weiser MR, Goodman KA, Gonen M, Cercek A, Reidy DL, et al. Neoadjuvant FOLFOX-bev, without radiation, for locally advanced rectal cancer. Journal of Clinical Oncology. 2010;28(15).

64. Ryan R, Gibbons D, Hyland JMP, Treanor D, White A, Mulcahy HE, et al. Pathological response following long-course neoadjuvant chemoradiotherapy for locally advanced rectal cancer. Histopathology. 2005;47(2):141-6.

65. Trakarnsanga A, Gonen M, Shia J, Nash GM, Temple LK, Guillem JG, et al. Comparison of tumor regression grade systems for locally advanced rectal cancer after multimodality treatment. J Natl Cancer Inst. 2014;106(10).

66. Minsky BD, Rodel C. Identifying the Most Predictive Post-Chemoradiation TRG System for Rectal Cancer. Jnci-Journal of the National Cancer Institute. 2014;106(10).

67. Kong JC, Guerra GR, Warrier SK, Lynch AC, Michael M, Ngan SY, et al. Prognostic value of tumour regression grade in locally advanced rectal cancer: a systematic review and meta-analysis. Colorectal Disease. 2018;20(7):574-85.

68. Fokas E, Liersch T, Fietkau R, Hohenberger W, Beissbarth T, Hess C, et al. Tumor regression grading after preoperative chemoradiotherapy for locally advanced rectal carcinoma revisited: updated results of the CAO/ARO/AIO-94 trial. J Clin Oncol. 2014;32(15):1554-62.

69. Yeo SG, Kim DY, Kim TH, Chang HJ, Oh JH, Park W, et al. Pathologic complete response of primary tumor following preoperative chemoradiotherapy for locally advanced rectal cancer: long-term outcomes and prognostic significance of pathologic nodal status (KROG 09-01). Ann Surg. 2010;252(6):998-1004.

70. Kim SH, Chang HJ, Kim DY, Park JW, Baek JY, Kim SY, et al. What Is the Ideal Tumor Regression Grading System in Rectal Cancer Patients after Preoperative Chemoradiotherapy? Cancer Research and Treatment. 2016;48(3):998-1009.

71. Pettersson D, Lorinc E, Holm T, Iversen H, Cedermark B, Glimelius B, et al. Tumour regression in the randomized Stockholm III Trial ofradiotherapy regimens for rectal cancer. British Journal of Surgery. 2015;102(8):972-8.

72. Rodel C, Martus P, Papadoupolos T, Fuzesi L, Klimpfinger M, Fietkau R, et al. Prognostic significance of tumor regression after preoperative

chemoradiotherapy for rectal cancer. Journal of Clinical Oncology. 2005;23(34):8688-96.

73. Van der Valk M, Consortium I. The International Watch and Wait Database (IWWD) for rectal cancer, an update. European Journal of Cancer. 2017;72:S55-S6.

74. Habr-Gama A, Juliao GPS, Vailati BB, Castro I, Raffaele D. Management of the Complete Clinical Response. Clinics in Colon and Rectal Surgery. 2017;30(5):387-94.

75. Van der Valk M, Hilling D, Bastiaannet E, Kranenbarg E-K, Beets G, Figueiredo N, et al. Long-term outcomes of clinical complete responders after neoadjuvant treatment for rectal cancer in the International Watch & Wait Database (IWWD): an international multicentre registry study. Lancet. 2018;391:2537-45.

76. Peeters K, van de Velde CJH, Leer JWH, Martijn H, Junggeburt JMC, Kranenbarg EK, et al. Late side effects of short-course preoperative radiotherapy combined with total mesorectal excision for rectal cancer: Increased bowel dysfunction in irradiated patients - A dutch colorectal cancer group study. Journal of Clinical Oncology. 2005;23(25):6199-206.

77. Dahlberg M, Glimelius B, Graf W, Pahlman L. Preoperative irradiation affects functional results after surgery for rectal cancer - Results from a randomized study. Diseases of the Colon & Rectum. 1998;41(5):543-9.

78. Hu MH, Huang RK, Zhao RS, Yang KL, Wang H. Does neoadjuvant therapy increase the incidence of anastomotic leakage after anterior resection for mid and low rectal cancer? A systematic review and meta-analysis. Colorectal Disease. 2017;19(1).

79. Fearon E, Vogelstein B. A genetic model of colorectal tumourigenesis. Cell. 1990;61:759-67.

80. Binkley GE, Sunderland DA, Miller CJ, Stearns M, Deddish MR. CARCINOMA ARISING IN ADENOMAS OF COLON AND RECTUM. Jama-Journal of the American Medical Association. 1952;148(17):1465-9.

81. Danaei G, Vander Hoorn S, Lopez AD, Murray CJL, Ezzati M, Comparative Risk Assessment C. Causes of cancer in the world: comparative risk assessment of nine behavioural and environmental risk factors. Lancet. 2005;366(9499):1784-93.

82. Cho K, Vogelstein B. Genetic alterations in the adenoma-carcinoma sequence. Cancer. 1992;70(S4):1727-31.

83. Logan CY, Nusse R. The Wnt signaling pathway in development and disease. Annual Review of Cell and Developmental Biology. 2004;20:781-810.

84. Clevers H, Nusse R. Wnt/beta-Catenin Signaling and Disease. Cell. 2012;149(6):1192-205.

85. Dow L, O'Rourke K, Simon J, Tschaharganeh D, vanEs J, Clevers H, et al. Apc restoration promotes cellular differentiation and reestablishes crypt homeostasis in colorectal cancer. Cell. 2015;161:1539-52.

86. Moser AR, Pitot HC, Dove WF. A DOMINANT MUTATION THAT PREDISPOSES TO MULTIPLE INTESTINAL NEOPLASIA IN THE MOUSE. Science. 1990;247(4940):322-4.

87. Reya T, Clevers H. Wnt signalling in stem cells and cancer. Nature. 2005;434(7035):843-50.

88. Dhillon AS, Hagan S, Rath O, Kolch W. MAP kinase signalling pathways in cancer. Oncogene. 2007;26(22):3279-90.

89. Rajagopalan H, Bardelli A, Lengauer C, Kinzler KW, Vogelstein B, Velculescu VE. Tumorigenesis - RAF/RAS oncogenes and mismatch-repair status. Nature. 2002;418(6901):934-.

90. Fransen K, Klintenas M, Osterstrom A, Dimberg J, Monstein HJ, Soderkvist P. Mutation analysis of the BRAF, ARAF and RAF-1 genes in human colorectal adenocarcinomas. Carcinogenesis. 2004;25(4):527-33.

91. Hutchins G, Southward K, Handley K, Magill L, Beaumont C, Stahlschmidt J, et al. Value of Mismatch Repair, KRAS, and BRAF Mutations in Predicting Recurrence and Benefits From Chemotherapy in Colorectal Cancer. Journal of Clinical Oncology. 2011;29(10):1261-70.

92. Phipps AI, Buchanan DD, Makar KW, Win AK, Baron JA, Lindor NM, et al. KRAS-mutation status in relation to colorectal cancer survival: the joint impact of correlated tumour markers. British Journal of Cancer. 2013;108(8):1757-64.

93. Cunningham D, Humblet Y, Siena S, Khayat D, Bleiberg H, Santoro A, et al. Cetuximab monotherapy and cetuximab plus irinotecan in irinotecan-refractory metastatic colorectal cancer. New England Journal of Medicine. 2004;351(4):337-45.

94. Karapetis CS, Khambata-Ford S, Jonker DJ, O'Callaghan CJ, Tu D, Tebbutt NC, et al. K-ras mutations and benefit from cetuximab in advanced colorectal cancer. New England Journal of Medicine. 2008;359(17):1757-65.

95. Dewdney A, Cunningham D, Tabernero J, Capdevila J, Glimelius B, Cervantes A, et al. Multicenter Randomized Phase II Clinical Trial Comparing Neoadjuvant Oxaliplatin, Capecitabine, and Preoperative Radiotherapy With or Without Cetuximab Followed by Total Mesorectal Excision in Patients With High-Risk Rectal Cancer (EXPERT-C). Journal of Clinical Oncology. 2012;30(14):1620-7.

96. Lane DP. CANCER - P53, GUARDIAN OF THE GENOME. Nature. 1992;358(6381):15-6.

97. Donehower LA, Harvey M, Slagle BL, McArthur MJ, Montgomery CA, Butel JS, et al. MICE DEFICIENT FOR P53 ARE DEVELOPMENTALLY NORMAL BUT SUSCEPTIBLE TO SPONTANEOUS TUMORS. Nature. 1992;356(6366):215-21.

98. Merritt AJ, Potten CS, Kemp CJ, Hickman JA, Balmain A, Lane DP, et al. THE ROLE OF P53 IN SPONTANEOUS AND RADIATION-INDUCED APOPTOSIS IN THE GASTROINTESTINAL-TRACT OF NORMAL AND P53-DEFICIENT MICE. Cancer Research. 1994;54(3):614-7.

99. Kastenhuber ER, Lowe SW. Putting p53 in Context. Cell. 2017;170(6):1062-78.

100. Hollstein M, Sidransky D, Vogelstein B, Harris CC. P53 MUTATIONS IN HUMAN CANCERS. Science. 1991;253(5015):49-53.

101. Hamelin R, Laurentpuig P, Olschwang S, Jego N, Asselain B, Remvikos Y, et al. ASSOCIATION OF P53 MUTATIONS WITH SHORT SURVIVAL IN COLORECTAL-CANCER. Gastroenterology. 1994;106(1):42-8.

102. Rebischung C, Gerard JP, Gayet J, Thomas G, Hamelin R, Laurent-Puig P. Prognostic value of p53 mutations in rectal carcinoma. International Journal of Cancer. 2002;100(2):131-5.

103. Skeen VR, Paterson I, Paraskeva C, Williams AC. TGF-beta 1 Signalling, Connecting Aberrant Inflammation and Colorectal Tumorigenesis. Current Pharmaceutical Design. 2012;18(26):3874-88.

104. de Caestecker MP, Piek E, Roberts AB. Role of transforming growth factor-beta signaling in cancer. Journal of the National Cancer Institute. 2000;92(17):1388-402.

105. Massague J, Blain SW, Lo RS. TGF beta signaling in growth control, cancer, and heritable disorders. Cell. 2000;103(2):295-309.

106. Parsons R, Myeroff LL, Liu B, Willson JKV, Markowitz SD, Kinzler KW, et al. MICROSATELLITE INSTABILITY AND MUTATIONS OF THE TRANSFORMING GROWTH-FACTOR-BETA TYPE-II RECEPTOR GENE IN COLORECTAL-CANCER. Cancer Research. 1995;55(23):5548-50.

107. Watanabe T, Wu T, Catalano PJ, Ueki T, Satriano R, Benson AB, et al. Molecular predictors of survival after adjuvant chemotherapy for colon cancer. New England Journal of Medicine. 2001;344(16):1196-206.

108. Vanhaesebroeck B, Guillermet-Guibert J, Graupera M, Bilanges B. The emerging mechanisms of isoform-specific PI3K signalling. Nature Reviews Molecular Cell Biology. 2010;11(5):329-41.

109. Samuels Y, Diaz LA, Schmidt-Kittler O, Cummins JM, DeLong L, Cheong I, et al. Mutant PIK3CA promotes cell growth and invasion of human cancer cells. Cancer Cell. 2005;7(6):561-73.

110. Wang Q, Shi YL, Zhou K, Wang LL, Yan ZX, Liu YL, et al. PIK3CA mutations confer resistance to first-line chemotherapy in colorectal cancer. Cell Death & Disease. 2018;9:11.

111. Liao XY, Lochhead P, Nishihara R, Morikawa T, Kuchiba A, Yamauchi M, et al. Aspirin Use, Tumor PIK3CA Mutation, and Colorectal-Cancer Survival. New England Journal of Medicine. 2012;367(17):1596-606.

112. Wong J, Hawkins N, Ward R. Colorectal Cancer: A model for epigenetic tumorigenesis. Gut. 2007;56:140-8.

113. Vogelstein B, Papdopoulos N, Velculescu V, Zhou S, Diaz L, Kinzler K. Cancer Genome Landscapes. Science. 2013;339:1546-58.

114. Feinberg A, Vogelstein B. Hypomethylation distinguishes genes of some human cancers from their normal counterparts. Nature. 1983;301:89-92.

115. Kim H, Roh S, Ga I, Kim J, Yu C, Kim J. CpG island methylation as an early event during adenoma progression in carcinogenesis of sporadic colorectal cancer. Journal of Gastroenterology and Hepatology. 2005;20:1920-6.

116. Issa J-P. CpG island methylator phenotype in cancer. Nature Reviews Cancer. 2004;4:988-93.

117. Sen R, Baltimore D. INDUCIBILITY OF KAPPA-IMMUNOGLOBULIN ENHANCER-BINDING PROTEIN NF-KAPPA-B BY A POSTTRANSLATIONAL MECHANISM. Cell. 1986;47(6):921-8.

118. Pahl HL. Activators and target genes of Rel/NF-kappa B transcription factors. Oncogene. 1999;18(49):6853-66.

119. Zhang Q, Lenardo MJ, Baltimore D. 30 Years of NF-kappa B: A Blossoming of Relevance to Human Pathobiology. Cell. 2017;168(1-2):37-57.

120. Brach MA, Hass R, Sherman ML, Gunji H, Weichselbaum R, Kufe D. IONIZING-RADIATION INDUCES EXPRESSION AND BINDING-ACTIVITY OF THE NUCLEAR FACTOR-KAPPA-B. Journal of Clinical Investigation. 1991;88(2):691-5.

121. Karin M. Nuclear factor-kappaB in cancer development and progression. Nature. 2006;441(7092):431-6.

122. Colotta F, Allavena P, Sica A, Garlanda C, Mantovani A. Cancer-related inflammation, the seventh hallmark of cancer: links to genetic instability. Carcinogenesis. 2009;30(7):1073-81.

123. Hoesel B, Schmid JA. The complexity of NF-kappa B signaling in inflammation and cancer. Molecular Cancer. 2013;12.

124. Sau A, Lau R, Cabrita MA, Nolan E, Crooks PA, Visvader JE, et al. Persistent Activation of NF-kappa B in BRCA1-Deficient Mammary Progenitors Drives Aberrant Proliferation and Accumulation of DNA Damage. Cell Stem Cell. 2016;19(1):52-65.

125. Schmid RM, Perkins ND, Duckett CS, Andrews PC, Nabel GJ. CLONING OF AN NF-KAPPA-B SUBUNIT WHICH STIMULATES HIV TRANSCRIPTION IN SYNERGY WITH P65. Nature. 1991;352(6337):733-6.

126. Bours V, Burd PR, Brown K, Villalobos J, Park S, Ryseck RP, et al. A NOVEL MITOGEN-INDUCIBLE GENE-PRODUCT RELATED TO P50/P105-NF-KAPPA-B PARTICIPATES IN TRANSACTIVATION THROUGH A KAPPA-B SITE. Molecular and Cellular Biology. 1992;12(2):685-95.

127. Huxford T, Ghosh G. A Structural Guide to Proteins of the NF-kappa B Signaling Module. Cold Spring Harbor Perspectives in Biology. 2009;1(3).

128. Hoffmann A, Natoli G, Ghosh G. Transcriptional regulation via the NF-kappa B signaling module. Oncogene. 2006;25(51):6706-16.

129. Saccani S, Pantano S, Natoli G. Two waves of nuclear factor kappa B recruitment to target promoters. Journal of Experimental Medicine. 2001;193(12):1351-9.

130. Wan FY, Lenardo MJ. Specification of DNA Binding Activity of NF-kappa B Proteins. Cold Spring Harbor Perspectives in Biology. 2009;1(4).

131. Perkins ND, Schmid RM, Duckett CS, Leung K, Rice NR, Nabel GJ. DISTINCT COMBINATIONS OF NF-KAPPA-B-SUBUNITS DETERMINE THE SPECIFICITY OF TRANSCRIPTIONAL ACTIVATION. Proceedings of the National Academy of Sciences of the United States of America. 1992;89(5):1529-33.

132. Saccani S, Pantano S, Natoli G. Modulation of NF-kappa B activity by exchange of dimers. Molecular Cell. 2003;11(6):1563-74.

133. Siggers T, Chang AB, Teixeira A, Wong D, Williams KJ, Ahmed B, et al. Principles of dimer-specific gene regulation revealed by a comprehensive characterization of NF-kappa B family DNA binding. Nature Immunology. 2012;13(1):95-U123.

134. Perkins ND. Achieving transcriptional specificity with NF-kappa B. International Journal of Biochemistry & Cell Biology. 1997;29(12):1433-48.

135. Wong D, Teixeira A, Oikonomopoulos S, Humburg P, Lone IN, Saliba D, et al. Extensive characterization of NF-kappa B binding uncovers non-canonical motifs and advances the interpretation of genetic functional traits. Genome Biology. 2011;12(7).

136. Nijnik A, Mott R, Kwiatkowski DP, Udalova IA. Comparing the fine specificity of DNA binding by NF-kappa B p50 and p52 using principal coordinates analysis. Nucleic Acids Research. 2003;31(5):1497-501.

137. Wang VYF, Huang W, Asagiri M, Spann N, Hoffmann A, Glass C, et al. The Transcriptional Specificity of NF-kappa B Dimers Is Coded within the kappa B DNA Response Elements. Cell Reports. 2012;2(4):824-39.

138. O'Neill LAJ, Golenbock D, Bowie AG. The history of Toll-like receptors - redefining innate immunity. Nature Reviews Immunology. 2013;13(6):453-60.

139. Karin M, Cao Y, Greten FR, Li ZW. NF-kappaB in cancer: from innocent bystander to major culprit. Nat Rev Cancer. 2002;2(4):301-10.

140. Hayden MS, Ghosh S. NF-kappa B, the first quarter-century: remarkable progress and outstanding questions. Genes & Development. 2012;26(3):203-34.

141. Rothwarf DM, Zandi E, Natoli G, Karin M. IKK-gamma is an essential regulatory subunit of the IkappaB kinase complex. Nature. 1998;395(6699):297-300.

142. Viatour P, Merville MP, Bours V, Chariot A. Phosphorylation of NF-kappa B and I kappa B proteins: implications in cancer and inflammation. Trends in Biochemical Sciences. 2005;30(1):43-52.

143. DiDonato JA, Hayakawa M, Rothwarf DM, Zandi E, Karin M. A cytokine-responsive I kappa B kinase that activates the transcription factor NF-kappa B. Nature. 1997;388(6642):548-54.

144. Karin M, Greten FR. NF kappa B: Linking inflammation and immunity to cancer development and progression. Nature Reviews Immunology. 2005;5(10):749-59.

145. Greten FR, Eckmann L, Greten TF, Park JM, Li ZW, Egan LJ, et al. IKKbeta links inflammation and tumorigenesis in a mouse model of colitis-associated cancer. Cell. 2004;118(3):285-96.

146. Razani B, Reichardt AD, Cheng GH. Non-canonical NF-kappa B signaling activation and regulation: principles and perspectives. Immunological Reviews. 2011;244:44-54.

147. Malinin NL, Boldin MP, Kovalenko AV, Wallach D. MAP3K-related kinase involved in NF-kappa B induction by TNF, CD95 and IL-1. Nature. 1997;385(6616):540-4.

148. Bai XZ, x00Fc, Gf, Xie ST, Hu DH, Zhu XX, et al. [Reproduction of a model of heat injured keratinocyte in vitro and observation on its apoptosis rate]. Zhonghua Shao Shang Za Zhi. 2009;25(3):189-92.

149. Tao ZH, Fusco A, Huang DB, Gupta K, Kim DY, Ware CF, et al. p100/I kappa B delta sequesters and inhibits NF-kappa B through kappaBsome formation. Proceedings of the National Academy of Sciences of the United States of America. 2014;111(45):15946-51.

150. Senftleben U, Cao YX, Xiao GT, Greten FR, Krahn G, Bonizzi G, et al. Activation by IKK alpha of a second, evolutionary conserved, NF-kappa B signaling pathway. Science. 2001;293(5534):1495-9.

151. Fusco AJ, Savinova OV, Talwar R, Kearns JD, Hoffmann A, Ghosh G. Stabilization of RelB requires multidomain interactions with p100/p52. Journal of Biological Chemistry. 2008;283(18):12324-32.

152. Solan NJ, Miyoshi H, Carmona EM, Bren GD, Paya CV. RelB cellular regulation and transcriptional activity are regulated by p100. Journal of Biological Chemistry. 2002;277(2):1405-18.

153. Vallabhapurapu SD, Noothi SK, Pullum DA, Lawrie CH, Pallapati R, Potluri V, et al. Transcriptional repression by the HDAC4-RelB-p52 complex regulates multiple myeloma survival and growth. Nat Commun. 2015;6:8428.

154. Franzoso G, Carlson L, Poljak L, Shores EW, Epstein S, Leonardi A, et al. Mice deficient in nuclear factor (NF)-kappa B/p52 present with defects in humoral responses, germinal center reactions, and splenic microarchitecture. Journal of Experimental Medicine. 1998;187(2):147-59.

155. Bista P, Zeng WK, Ryan S, Bailly V, Browning JL, Lukashev ME. TRAF3 Controls Activation of the Canonical and Alternative NF kappa B by the Lymphotoxin Beta Receptor. Journal of Biological Chemistry. 2010;285(17):12971-8.

156. Xu Y, Cheng GH, Baltimore D. Targeted disruption of TRAF3 leads to postnatal lethality and defective T-dependent immune responses. Immunity. 1996;5(5):407-15.

157. Compagno M, Lim WK, Grunn A, Nandula SV, Brahmachary M, Shen Q, et al. Mutations of multiple genes cause deregulation of NF-kappa B in diffuse large B-cell lymphoma. Nature. 2009;459(7247):717-U124.

158. Ciana P, Neri A, Cappellini C, Cavallo F, Pomati M, Chang CC, et al. Constitutive expression of lymphoma-associated NFKB-2/Lyt-10 proteins is tumorigenic in murine fibroblasts. Oncogene. 1997;14(15):1805-10.

159. Wu ZH, Shi YL, Tibbetts RS, Miyamoto S. Molecular linkage between the kinase ATM and NF-kappa B signaling in response to genotoxic stimuli. Science. 2006;311(5764):1141-6.

160. Ryan KM, Ernst MK, Rice NR, Vousden KH. Role of NF-kappa B in p53-mediated programmed cell death. Nature. 2000;404(6780):892-7.

161. Kato T, Jr., Delhase M, Hoffmann A, Karin M. CK2 Is a C-Terminal IkappaB Kinase Responsible for NF-kappaB Activation during the UV Response. Mol Cell. 2003;12(4):829-39.

162. Wessells J, Baer M, Young HA, Claudio E, Brown K, Siebenlist U, et al. BCL-3 and NF-kappa B p50 attenuate lipopolysaccharide-induced inflammatory responses in macrophages. Journal of Biological Chemistry. 2004;279(48):49995-50003.

163. Southern SL, Collard TJ, Urban BC, Skeen VR, Smartt HJ, Hague A, et al. BAG-1 interacts with the p50-p50 homodimeric NF-kappa B complex: implications for colorectal carcinogenesis. Oncogene. 2012;31(22):2761-72.

164. Moorthy AK, Savinova OV, Ho JQ, Wang VYF, Vu D, Ghosh G. The 20S proteasome processes NF-kappa B1 p105 into p50 in a translation-independent manner. Embo Journal. 2006;25(9):1945-56.

165. Montano MA, Kripke K, Norina CD, Achacoso P, Herzenberg LA, Roy AL, et al. NF-kappa B homodimer binding within the HIV-1 initiator region and interactions with TFII-I. Proceedings of the National Academy of Sciences of the United States of America. 1996;93(22):12376-81.

166. Cao SJ, Zhang X, Edwards JP, Mosser DM. NF-kappa B1 (p50) homodimers differentially regulate pro- and anti-inflammatory cytokines in macrophages. Journal of Biological Chemistry. 2006;281(36):26041-50.

167. Udalova IA, Richardson A, Denys A, Smith C, Ackerman H, Foxwell B, et al. Functional consequences of a polymorphism affecting NF-kappa B p50-p50 binding to the TNF promoter region. Molecular and Cellular Biology. 2000;20(24):9113-9.

168. Plaksin D, Baeuerle PA, Eisenbach L. KBF1 (P50 NF-KAPPA-B HOMODIMER) ACTS AS A REPRESSOR OF H-2K(B) GENE-EXPRESSION IN METASTATIC TUMOR-CELLS. Journal of Experimental Medicine. 1993;177(6):1651-62.

169. Grundstrom S, Anderson P, Scheipers P, Sundstedt A. Bcl-3 and NF kappa B p50-p50 homodimers act as transcriptional repressors in tolerant CD4(+) T cells. Journal of Biological Chemistry. 2004;279(9):8460-8.

170. Bours V, Franzoso G, Azarenko V, Park S, Kanno T, Brown K, et al. THE ONCOPROTEIN BCL-3 DIRECTLY TRANSACTIVATES THROUGH KAPPA-B MOTIFS VIA ASSOCIATION WITH DNA-BINDING P50B HOMODIMERS. Clinical Research. 1993;41(2):A201-A.

171. Thornburg NJ, Pathmanathan R, Raab-Traub N. Activation of nuclear factor-kappa B p50 homodimer/Bcl-3 complexes in nasopharyngeal carcinoma. Cancer Research. 2003;63(23):8293-301.

172. Lessard L, Saad F, Le Page C, Diallo JS, Peant B, Delvoye N, et al. NF-kappa B2 processing and p52 nuclear accumulation after androgenic stimulation of LNCaP prostate cancer cells. Cellular Signalling. 2007;19(5):1093-100.

173. Wilson CL, Jurk D, Fullard N, Banks P, Page A, Luli S, et al. NF kappa B1 is a suppressor of neutrophil-driven hepatocellular carcinoma. Nature Communications. 2015;6.

174. Seufert B, Poole E, Whitton J, Xiao L, Makar K, Campbell P, et al. IkappaBKbeta and NFkappaB1, NSAID use and risk of colorectal cancer in the Colon Cancer Family Registry. Carcinogenesis. 2013;34:79-85.

175. Wulczyn FG, Naumann M, Scheidereit C. Candidate proto-oncogene bcl-3 encodes a subunit-specific inhibitor of transcription factor NF-kappa B. Nature. 1992;358(6387):597-9.

176. Ohno H, Takimoto G, McKeithan TW. The candidate proto-oncogene bcl-3 is related to genes implicated in cell lineage determination and cell cycle control. Cell. 1990;60(6):991-7.

177. Hatada EN, Nieters A, Wulczyn FG, Naumann M, Meyer R, Nucifora G, et al. The ankyrin repeat domains of the NF-kappa B precursor p105 and the protooncogene bcl-3 act as specific inhibitors of NF-kappa B DNA binding. Proceedings of the National Academy of Sciences of the United States of America. 1992;89(6):2489-93.

178. Rogers S, Wells R, Rechsteiner M. AMINO-ACID-SEQUENCES COMMON TO RAPIDLY DEGRADED PROTEINS - THE PEST HYPOTHESIS. Science. 1986;234(4774):364-8.

179. Michel F, Soler-Lopez M, Petosa C, Cramer P, Siebenlist U, Muller CW. Crystal structure of the ankyrin repeat domain of Bcl-3: a unique member of the I kappa B protein family. Embo Journal. 2001;20(22):6180-90.

180. Lin RT, Beauparlant P, Makris C, Meloche S, Hiscott J. Phosphorylation of I kappa B alpha in the C-terminal PEST domain by casein kinase iu affects intrinsic protein stability. Molecular and Cellular Biology. 1996;16(4):1401-9.

181. Rechsteiner M, Rogers SW. PEST sequences and regulation by proteolysis. Trends in Biochemical Sciences. 1996;21(7):267-71.

182. Zhang Q, Didonato JA, Karin M, McKeithan TW. BCL3 encodes a nuclear protein which can alter the subcellular location of NF-kappa B proteins. Mol Cell Biol. 1994;14(6):3915-26.

183. Koch CA, Anderson D, Moran MF, Ellis C, Pawson T. SH2 AND SH3 DOMAINS - ELEMENTS THAT CONTROL INTERACTIONS OF CYTOPLASMIC SIGNALING PROTEINS. Science. 1991;252(5006):668-74.

184. Pawson T. PROTEIN MODULES AND SIGNALING NETWORKS. Nature. 1995;373(6515):573-80.

185. Weyrich AS, Dixon DA, Pabla R, Elstad MR, McIntyre TM, Prescott SM, et al. Signal-dependent translation of a regulatory protein, Bcl-3, in activated human platelets. Proceedings of the National Academy of Sciences of the United States of America. 1998;95(10):5556-61.

186. McKeithan TW, Ohno H, Dickstein J, Hume E. Genomic structure of the candidate proto-oncogene BCL3. Genomics. 1994;24(1):120-6.

187. Brasier AR, Lu M, Hai T, Lu Y, Boldogh I. NF-kappa B-inducible BCL-3 expression is an autoregulatory loop controlling nuclear p50/NF-kappa B1 residence. Journal of Biological Chemistry. 2001;276(34):32080-93.

188. Tao Y, Liu Z, Hou Y, Wang S, Liu S, Jiang Y, et al. Alternative NF-kappaB signaling promotes colorectal tumorigenesis through transcriptionally upregulating Bcl-3. Oncogene. 2018.

189. Chan KK, Shen LJ, Au WY, Yuen HF, Wong KY, Guo TH, et al. Interleukin-2 induces NF-kappa B activation through BCL10 and affects its subcellular localization in natural killer lymphoma cells. Journal of Pathology. 2010;221(2):164-74.

190. Rebollo A, Dumoutier L, Renauld JC, Zaballos A, Ayllon V, Martinez AC. Bcl-3 expression promotes cell survival following interleukin-4 deprivation and is controlled by AP1 and AP1-like transcription factors. Molecular & Cellular Biology. 2000;20(10):3407-16.

191. Lotem J, Gal H, Kama R, Amariglio N, Gideon R, Domany E, et al. Inhibition of p53-induced apoptosis without affecting expression of p53-regulated genes. Proceedings of the National Academy of Sciences. 2003;100(11):6718-23.

192. Richard M, Louahed J, Demoulin JB, Renauld JC. Interleukin-9 regulates NF-kappaB activity through BCL3 gene induction. Blood. 1999;93(12):4318-27.

193. Muhlbauer M, Chilton PM, Mitchell TC, Jobin C. Impaired bcl3 up-regulation leads to enhanced lipopolysaccharide-induced interleukin (IL)-23P19 gene expression in IL-10(-/-) mice. Journal of Biological Chemistry. 2008;283(21):14182-9.

194. Tohyama M, Shirakata Y, Hanakawa Y, Dai XJ, Shiraishi K, Murakami M, et al. Bcl-3 induced by IL-22 via STAT3 activation acts as a potentiator of psoriasis-related gene expression in epidermal keratinocytes. European Journal of Immunology. 2018;48(1):168-79.

195. Brocke-Heidrich K, Ge B, Cvijic H, Pfeifer G, Loffler D, Henze C, et al. BCL3 is induced by IL-6 via Stat3 binding to intronic enhancer HS4 and represses its own transcription. Oncogene. 2006;25(55):7297-304.

196. Beurel E, Jope RS. Differential regulation of STAT family members by glycogen synthase kinase-3. Journal of Biological Chemistry. 2008;283(32):21934-44.

197. Kung CP, Raab-Traub N. Epstein-Barr virus latent membrane protein 1 induces expression of the epidermal growth factor receptor through effects on Bcl-3 and STAT3. Journal of Virology. 2008;82(11):5486-93.

198. Ge B, Li O, Wilder P, Rizzino A, McKeithan TW. NF-kappa B regulates BCL3 transcription in T lymphocytes through an intronic enhancer. Journal of Immunology. 2003;171(8):4210-8.

199. Chang TP, Vancurova I. Bcl3 regulates pro-survival and pro-inflammatory gene expression in cutaneous T-cell lymphoma. Biochim Biophys Acta. 2014;1843(11):2620-30.

200. Bundy DL, McKeithan TW. Diverse effects of BCL3 phosphorylation on its modulation of NF-kappa B p52 homodimer binding to DNA. Journal of Biological Chemistry. 1997;272(52):33132-9.

201. Keutgens A, Zhang X, Shostak K, Robert I, Olivier S, Vanderplasschen A, et al. BCL-3 Degradation Involves Its Polyubiquitination through a FBW7-independent Pathway and Its Binding to the Proteasome Subunit PSMB1. Journal of Biological Chemistry. 2010;285(33):25831-40.

202. Viatour P, Dejardin E, Warnier M, Lair F, Claudio E, Bureau F, et al. GSK3-Mediated BCL-3 phosphorylation modulates its degradation and its oncogenicity. Molecular Cell. 2004;16(1):35-45.

203. Wang VYF, Li YD, Kim D, Zhong XY, Du Q, Ghassemian M, et al. Bcl3 Phosphorylation by Akt, Erk2, and IKK Is Required for Its Transcriptional Activity. Molecular Cell. 2017;67(3):484-+.

204. Massoumi R, Chmielarska K, Hennecke K, Pfeifer A, Fassler R. Cyld inhibits tumor cell proliferation by blocking Bcl-3-dependent NF-kappaB signaling. Cell. 2006;125(4):665-77.

205. Matsuoka S, Rotman G, Ogawa A, Shiloh Y, Tamai K, Elledge SJ. Ataxia telangiectasia-mutated phosphorylates Chk2 in vivo and in vitro. Proceedings of the National Academy of Sciences of the United States of America. 2000;97(19):10389-94.

206. Naumann M, Wulczyn FG, Scheidereit C. The NF-kappa B precursor p105 and the proto-oncogene product Bcl-3 are I kappa B molecules and control nuclear translocation of NF-kappa B. EMBO Journal. 1993;12(1):213-22.

207. Nolan GP, Fujita T, Bhatia K, Huppi C, Liou HC, Scott ML, et al. The bcl-3 proto-oncogene encodes a nuclear I kappa B-like molecule that preferentially interacts with NF-kappa B p50 and p52 in a phosphorylation-dependent manner. Molecular & Cellular Biology. 1993;13(6):3557-66.

208. Franzoso G, Bours V, Azarenko V, Park S, TomitaYamaguchi M, Kanno T, et al. The oncoprotein Bcl-3 can facilitate NF-kappa B-mediated transactivation by removing inhibiting p50 homodimers from select kappa B sites (vol 12, pg 3893, 1993). Embo Journal. 1997;16(2):440-.

209. Kerr LD, Duckett CS, Wamsley P, Zhang Q, Chiao P, Nabel G, et al. The proto-oncogene bcl-3 encodes an I kappa B protein. Genes & Development. 1993;6(12A):2352-63.

210. Inoue J, Takahara T, Akizawa T, Hino O. Bcl-3, a member of the I kappa B proteins, has distinct specificity towards the Rel family of proteins. Oncogene. 1993;8(8):2067-73.

211. Franzoso G, Bours V, Park S, Tomita-Yamaguchi M, Kelly K, Siebenlist U. The candidate oncoprotein Bcl-3 is an antagonist of p50/NF-kappa B-mediated inhibition. Nature. 1992;359(6393):339-42.

212. Fujita T, Nolan GP, Liou HC, Scott ML, Baltimore D. The candidate proto-oncogene bcl-3 encodes a transcriptional coactivator that activates through NF-kappa B p50 homodimers. Genes & Development. 1993;7(7B):1354-63.

213. Bours V, Franzoso G, Azarenko V, Park S, Kanno T, Brown K, et al. The oncoprotein Bcl-3 directly transactivates through kappa B motifs via association with DNA-binding p50B homodimers. Cell.72(5):729-39.

214. Franzoso G, Bours V, Azarenko V, Park S, Tomita-Yamaguchi M, Kanno T, et al. The oncoprotein Bcl-3 can facilitate NF-kappa B-mediated transactivation by removing inhibiting p50 homodimers from select kappa B sites.[Erratum appears in EMBO J 1997 Jan 15;16(2):440]. EMBO Journal.12(10):3893-901.

215. Franzoso G, Bours V, Azarenko V, Park S, Tomitayamaguchi M, Kanno T, et al. THE ONCOPROTEIN BCL-3 CAN FACILITATE NF-THETA-B-MEDIATED TRANSACTIVATION BY REMOVING INHIBITING P50 HOMODIMERS FROM SELECT THETA-B SITES. Embo Journal. 1993;12(10):3893-901.

216. Dechend R, Hirano F, Lehmann K, Heissmeyer V, Ansieau S, Wulczyn FG, et al. The Bcl-3 oncoprotein acts as a bridging factor between NF-kappa B/Rel and nuclear co-regulators. Oncogene. 1999;18(22):3316-23.

217. Walker T, Adamson A, Jackson DA. BCL-3 Attenuation of TNFA Expression Involves an Incoherent Feed-Forward Loop Regulated by Chromatin Structure. Plos One. 2013;8(10).

218. Keutgens A, Shostak K, Close P, Zhang X, Hennuy B, Aussems M, et al. The repressing function of the oncoprotein BCL-3 requires CtBP, while its polyubiquitination and degradation involve the E3 ligase TBLR1. Molecular & Cellular Biology. 2010;30(16):4006-21.

219. Jamaluddin M, Choudhary S, Wang SF, Casola A, Huda R, Garofalo RP, et al. Respiratory syncytial virus-inducible BCL-3 expression antagonizes the STAT/IRF and NF-kappa B signaling pathways by inducing histone deacetylase 1 recruitment to the interleukin-8 promoter. Journal of Virology. 2005;79(24):15302-13.

220. Kiernan R, Bres V, Ng R, Coudart M-P, El Messaoudi S, Sardet C, et al. Post-activation turn-off of NF-kB dependent transcription is regulated by acetylation of p65. Journal of Biological Chemistry. 2003;278(4):2758-66.

221. Furia B, Deng L, Wu K, Baylor S, Kehn K, Li H, et al. Enhancement of Nuclear Factor-kB acetylation by coactivator p300 and HIV-1 TAT proteins. Journal of Biological Chemistry. 2002;277:4973-80.

222. O'Carroll C, Moloney G, Hurley G, Melgar S, Brint E, Nally K, et al. Bcl-3 deficiency protects against dextran-sodium sulphate-induced colitis in the mouse. Clinical & Experimental Immunology. 2013;173(2):332-42.

223. Kim J, Kim B, Cai L, Choi H, Ohgi K, Tran C, et al. Transcriptional regulation of metastasis suppressor gene by Tip60 and B-catenin complexes. Nature Letters. 2005;434:921-6.

224. Hanahan D, Weinberg R. Hallmarks of Cancer: The next generation. Cell. 2011;144(4):646-74.

225. Asghar U, Witkiewicz AK, Turner NC, Knudsen ES. The history and future of targeting cyclin-dependent kinases in cancer therapy. Nature Reviews Drug Discovery. 2015;14(2):130-46.

226. Liu ZJ, Jiang YH, Hou YY, Hu YM, Cao XW, Tao Y, et al. The I kappa B family member Bcl-3 stabilizes c-Myc in colorectal cancer. Journal of Molecular Cell Biology. 2013;5(4):280-2.

227. Tu KS, Liu ZK, Yao BW, Xue YM, Xu M, Dou CW, et al. BCL-3 promotes the tumor growth of hepatocellular carcinoma by regulating cell proliferation and the cell cycle through cyclin D1. Oncology Reports. 2016;35(4):2382-90.

228. Park SG, Chung C, Kang H, Kim JY, Jung GH. Up-regulation of cyclin D1 by HBx is mediated by NF-kappa B2/BCL3 complex through kappa B site of cyclin D1 promoter. Journal of Biological Chemistry. 2006;281(42):31770-7.

229. Massoumi R, Kuphal S, Hellerbrand C, Haas B, Wild P, Spruss T, et al. Down-regulation of CYLD expression by Snail promotes tumor progression in malignant melanoma. Journal of Experimental Medicine. 2009;206(1):221-32.

230. Westerheide SD, Mayo MW, Anest V, Hanson JL, Baldwin AS, Jr. The putative oncoprotein Bcl-3 induces cyclin D1 to stimulate G(1) transition. Molecular & Cellular Biology. 2001;21(24):8428-36.

231. Rocha S, Martin AM, Meek DW, Perkins ND. p53 Represses cyclin D1 transcription through down regulation of Bcl-3 and inducing increased association of the p52 NF-kappa B subunit with histone deacetylase 1. Molecular and Cellular Biology. 2003;23(13):4713-27.

232. Chen X, Cao XW, Sun XH, Lei R, Chen PF, Zhao YX, et al. Bcl-3 regulates TGF beta signaling by stabilizing Smad3 during breast cancer pulmonary metastasis. Cell Death & Disease. 2016;7.

233. Wakefield A, Soukupova J, Montagne A, Ranger J, French R, Muller WJ, et al. Bcl3 selectively promotes metastasis of ERBB2-driven mammary tumors. Cancer Research. 2013;73(2):745-55.

234. Ren XX, Song W, Liu WJ, Guan X, Miao F, Miao SY, et al. Rhomboid domain containing 1 inhibits cell apoptosis by upregulating AP-1 activity and its downstream target Bcl-3. Febs Letters. 2013;587(12):1793-8.

235. Choi HJ, Lee JM, Kim H, Nam HJ, Shin HJ, Kim D, et al. Bcl3-dependent stabilization of CtBP1 is crucial for the inhibition of apoptosis and tumor progression in breast cancer. Biochem Biophys Res Commun. 2010;400(3):396-402.

236. Garcia I, Cosio G, Lizarraga F, Martinez-Ruiz G, Melendez-Zajgla J, Ceballos G, et al. Bcl-3 regulates UVB-induced apoptosis. Human Cell. 2013;26(2):47-55.

237. Bauer A, Villunger A, Labi V, Fischer SF, Strasser A, Wagner H, et al. The NF-kappaB regulator Bcl-3 and the BH3-only proteins Bim and Puma control the death of activated T cells. Proceedings of the National Academy of Sciences of the United States of America. 2006;103(29):10979-84.

238. Hosono N, Kishi S, Iho S, Urasaki Y, Yoshida A, Kurooka H, et al. Glutathione S-transferase M1 inhibits dexamethasone-induced apoptosis in association with the suppression of Bim through dual mechanisms in a lymphoblastic leukemia cell line. Cancer Science. 2010;101(3):767-73.

239. Kashatus D, Cogswell P, Baldwin AS. Expression of the Bcl-3 proto-oncogene suppresses p53 activation. Genes & Development. 2006;20(2):225-35.

240. Puvvada SD, Funkhouser WK, Greene K, Deal A, Chu H, Baldwin AS, et al. NF-κB and Bcl-3 Activation Are Prognostic in Metastatic Colorectal Cancer. Oncology. 2010;78(3-4):181-8.

241. Saamarthy K, Bjorner S, Johansson M, Landberg G, Massoumi R, Jirstrom K, et al. Early diagnostic value of Bcl-3 localization in colorectal cancer. BMC Cancer. 2015;15:341-50.

242. O'Neil BH, Buzkova P, Farrah H, Kashatus D, Sanoff H, Goldberg RM, et al. Expression of nuclear Factor-kappaB family proteins in hepatocellular carcinomas. Oncology. 2007;72(1-2):97-104.

243. Gehrke N, Worns MA, Mann A, Huber Y, Hoevelmeyer N, Longerich T, et al. Hepatic B cell leukemia-3 suppresses chemically-induced hepatocarcinogenesis in mice through altered MAPK and NF-kappa B activation. Oncotarget. 2017;8(34):56095-109.

244. Perkins ND, Gilmore TD. Good cop, bad cop: the different faces of NF-kappa B. Cell Death and Differentiation. 2006;13(5):759-72.

245. Paxian S, Merkle H, Riemann M, Wilda M, Adler G, Hameister H, et al. Abnormal organogenesis of Peyer's patches in mice deficient for NF-kappa B1, NF-kappa B2, and Bcl-3. Gastroenterology. 2002;122(7):1853-68.

246. Song L, Wormann S, Ai J, Neuhofer P, Lesina M, Diakopoulos KN, et al. BCL3 Reduces the Sterile Inflammatory Response in Pancreatic and Biliary Tissues. Gastroenterology. 2015.

247. Tassi I, Rikhi N, Claudio E, Wang H, Tang WH, Ha HL, et al. The NF-kappa B regulator Bcl-3 modulates inflammation during contact hypersensitivity reactions in radioresistant cells. European Journal of Immunology. 2015;45(4):1059-68.

248. Carmody RJ, Ruan Q, Palmer S, Hilliard B, Chen YH. Negative regulation of toll-like receptor signaling by NF-kappaB p50 ubiquitination blockade. Science. 2007;317(5838):675-8.

249. Kuwata H, Watanabe Y, Miyoshi H, Yamamoto M, Kaisho T, Takeda K, et al. IL-10-inducible Bcl-3 negatively regulates LPS-induced TNF-alpha production in macrophages. Blood. 2003;102(12):4123-9.

250. Reissig S, Tang YL, Nikolaev A, Gerlach K, Wolf C, Davari K, et al. Elevated levels of Bcl-3 inhibits Treg development and function resulting in spontaneous colitis. Nature Communications. 2017;8.

251. Reissig S, Nikolaev A, Weigmann B, Gerlach K, Glasmacher E, Hovelmeyer N, et al. The transcriptional regulator Bcl-3 impaires the function of regulatory T cells leading to the development of intestinal inflammation. Journal of Immunology. 2016;196.

252. Meguro K, Suzuki K, Hosokawa J, Sanayama Y, Tanaka S, Furuta S, et al. Role of Bcl-3 in the Development of Follicular Helper T Cells and in the Pathogenesis of Rheumatoid Arthritis. Arthritis & Rheumatology. 2015;67(10):2651-60.

253. Tang WH, Wang HS, Claudio E, Tassi I, Ha HL, Saret S, et al. The Oncoprotein and Transcriptional Regulator Bcl-3 Governs Plasticity and Pathogenicity of Autoimmune T Cells. Immunity. 2014;41(4):555-66.

254. Ikeda O, Sekine Y, Mizushima A, Nakasuji M, Miyasaka Y, Yamamoto C, et al. Interactions of STAP-2 with Brk and STAT3 Participate in Cell Growth of Human Breast Cancer Cells. Journal of Biological Chemistry. 2010;285(49):38093-103.

255. Lin ZW, Hegarty JP, Yu W, Cappel JA, Chen X, Faber PW, et al. Identification of Disease-Associated DNA Methylation in B Cells from Crohn's Disease and Ulcerative Colitis Patients. Digestive Diseases and Sciences. 2012;57(12):3145-53.

256. Kreisel D, Sugimoto S, Tietjens J, Zhu JH, Yamamoto S, Krupnick AS, et al. Bcl3 prevents acute inflammatory lung injury in mice by restraining emergency granulopoiesis. Journal of Clinical Investigation. 2011;121(1):265-76.

257. Urban BC, Collard TJ, Eagle CJ, Southern SL, Greenhough A, Hamdollah-Zadeh M, et al. BCL-3 expression promotes colorectal tumorigenesis through activation of AKT signalling. Gut. 2016;65(7):1151-64.

258. Leibovitz A, Stinson J, McCombs W, McCoy C, Mazur K, Mabry N. Classification of human colorectal adenocarcinoma cell lines. Cancer Research. 1976;36:4562-9.

259. Carotenuto P, Roma C, Cozzolino S, Fenizia F, Rachiglio A, Tatangelo F, et al. Detection of KRAS mutations in colorectal cancer with Fast COLD-PCR. International Journal of Oncology. 2012;40:378-84.

260. Mouradov D, Sloggett C, Jorissen R, Love C, Li S, Burgess A, et al. Colorectal cancer cell lines are representative model of the main molecular subtypes of primary cancer. Cancer Research. 2014;74(12):3238-47.

261. Tom B, Rutzky L, Jakstys M, Oyasu R, Kaye C, Kahan B. Human colonic adenocarcinoma cells. I. Establishment and description of a new cell line. In Vitro. 1976;12(3):180-91.

262. Malkhosyan S, Rampino N, Yamamoto H, Perucho M. Frameshift mutator mutations. Nature. 1996;382:499-500.

263. NR. R, Rowan A, Smith M, Kerr I, Bodmer W, Gannon J, et al. p53 mutations in colorectal cancer. Proceedings of the National Academy of Sciences USA. 1990;87:7555-9.

264. Carethers J, Pham T. Mutations of transforming growth factor beta 1 type II receptor, BAX and insulin-like growth factor II receptor genes in microsatellite unstable cell lines. In Vitro. 2000;14:13-20.

265. Arcaroli J, Quackenbush K, Powell R, Pitts T, Spreafico A, Varella-Garcia M, et al. Common PIK3CA mutants and a novel 3' UTR mutation are associated with increased sensitivity to saracatinib. Clinical Cancer Research. 2012;18:2704-14.

266. Ilyas M, Tomlinson I, Rowan A, Pignatelli M, Bodmer W. Beta-catenin mutations in cell lines established from colorectal cancers. Proceedings of the National Academy of Sciences USA. 1997;94(19):10330-4.

267. Efstathiou J, Liu D, Wheeler J, Kim H, Beck N, Ilyas M, et al. Mutated epithelial cadherin is associated with increased tumorigenicity and loss of adhesion and of responsiveness to the motogenic trefoil factor 2 in colon carcinoma cells. Proceedings of the National Academy of Sciences USA. 1999;96:2316-21.

268. Kirkland S, Bailey I. Establishment and characterisation of six human colorectal adenocarcinoma cell lines. British Journal of Cancer. 1986;53(6):779-85.

269. Abdel-Rahman W, Lohi H, Knuutila S, Peltomaki P. Restoring mismatch repair does not stop the formation of reciprocal translocations in the colon cancer cell line HCA7 but further destabilises chromosome number. Oncogene. 2005;24:706-13.

270. Liu Y, Bodmer W. Analysis of P53 mutations and their expression in 56 colorectal cancer cell lines. Proceedings of the National Academy of Sciences USA. 2005;103(4):976-81.

271. Rowan AJ, Lamlum H, Ilyas M, Wheeler J, Straub J, Papadopoulou A, et al. APC mutations in sporadic colorectal tumors: A mutational "hotspot" and interdependence of the "two hits". Proceedings of the National Academy of Sciences of the United States of America. 2000;97(7):3352-7.

272. Paraskeva C, Corfield AP, Harper S, Hague A, Audcent K, Williams AC. COLORECTAL CARCINOGENESIS - SEQUENTIAL STEPS IN THE INVITRO IMMORTALIZATION AND TRANSFORMATION OF HUMAN COLONIC EPITHELIAL-CELLS (REVIEW). Anticancer Research. 1990;10(5A):1189-200.

273. Paraskeva C, Harper S, Williams AC. MULTIPLE EVENTS IN THE INVITRO TRANSFORMATION OF A HUMAN ADENOMA CELL-LINE TO A CARCINOMA CELL-LINE. Journal of Pathology. 1990;161(4):A351-A.

274. Paraskeva C, Buckle B, Sheer D, Wigley C. ESTABLISHMENT AND CHARACTERIZATION OF PREMALIGNANT AND MALIGNANT COLON EPITHELIAL-CELL LINES FROM POLYPOSIS COLI PATIENTS. Biology of the Cell. 1984;52(1):A45-A.

275. Sato T, Vries RG, Snippert HJ, van de Wetering M, Barker N, Stange DE, et al. Single Lgr5 stem cells build crypt-villus structures in vitro without a mesenchymal niche. Nature. 2009;459(7244):262-5.

276. Hague A, Manning A, Hanlon K, Huschtscha L, Hart D, Paraskeva C. Sodium butyrate induces apoptosis in human colonic tumour cell lines in a p53-independent pathway: implications for the possible role of dietary fibre in the prevention of large-bowel cancer. International Journal of Cancer. 1993;55(3):498-505.

277. Di Francesco AM, Ruggiero A, Riccardi R. Cellular and molecular aspects of drugs of the future: oxaliplatin. Cellular and Molecular Life Sciences. 2002;59(11):1914-27.

278. Boysen G, Pachkowski BF, Nakamura J, Swenberg JA. The formation and biological significance of N7-guanine adducts. Mutation Research-Genetic Toxicology and Environmental Mutagenesis. 2009;678(2):76-94.

279. Naugler WE, Karin M. The wolf in sheep's clothing: the role of interieukin-6 in immunity, inflammation and cancer. Trends in Molecular Medicine. 2008;14(3):109-19.

280. Wagman GH, Testa RT, Marquez JA, Weinstein MJ. ANTIBIOTIC G-418, A NEW MICROMONOSPORA-PRODUCED AMINOGLYCOSIDE WITH ACTIVITY AGAINST PROTOZOA AND HELMINTHS - FERMENTATION, ISOLATION, AND PRELIMINARY CHARACTERIZATION. Antimicrobial Agents and Chemotherapy. 1974;6(2):144-9.

281. Mroue R, Bissell MJ. Three-dimensional cultures of mouse mammary epithelial cells. Methods Mol Biol. 2013;945:221-50.

282. Laemmli U. Cleavage of structural proteins during the assembly of the head of bacteriophage T4. Nature. 1970;227:680-5.

283. Towbin H, Staehelin T, Gordon J. Electrophoretic transfer of proteins from polyacrylamide gels to nitrocellulose sheets: Procedure and some applications. Proceedings of the National Academy of Sciences of the USA. 1979;76(9):4350-4.

284. Untergasser A, Nijveen H, Rao X, Bisseling T, Geurts R, Leunissen JAM. Primer3Plus, an enhanced web interface to Primer3. Nucleic Acids Research. 2007;35:W71-W4.

285. Untergasser A, Cutcutache I, Koressaar T, Ye J, Faircloth BC, Remm M, et al. Primer3-new capabilities and interfaces. Nucleic Acids Research. 2012;40(15).

286. Korbie DJ, Mattick JS. Touchdown PCR for increased specificity and sensitivity in PCR amplification. Nature Protocols. 2008;3(9):1452-6.

287. Martin OA, Ivashkevich A, Choo S, Woodbine L, Jeggo PA, Martin RF, et al. Statistical analysis of kinetics, distribution and co-localisation of DNA repair foci in irradiated cells: cell cycle effect and implications for prediction of radiosensitivity. DNA Repair (Amst). 2013;12(10):844-55.

288. Cory S, Adams JM. The Bcl2 family: regulators of the cellular life-or-death switch. Nat Rev Cancer. 2002;2(9):647-56.

289. Kerr J, Wyllie A, Currie A. Apoptosis: A basic biological phenomenon with wide-ranging implications in tissue kinetics. British Journal of Cancer. 1972;26:239-57.

290. Riedl S, Shi Y. Molecular mechanisms of caspase regulation during apoptosis. Nature Reviews Molecular Cell Biology. 2004;5:897-907.

291. Vaux D, Weissman I, Kim S. Prevention of programmed cell death in Caenorhabditis elegans by human bcl-2. Science. 1992;258:1955-7.

292. Elmore S. Apoptosis: A review of programmed cell death. Toxicologic Pathology. 2007;35(4):495-516.

293. Youle RJ, Strasser A. The BCL-2 protein family: opposing activities that mediate cell death. Nature Reviews Molecular Cell Biology. 2008;9(1):47-59.

294. Mancini M, Nicholson DW, Roy S, Thornberry NA, Peterson EP, Casciola-Rosen LA, et al. The caspase-3 precursor has a cytosolic and mitochondrial distribution: implications for apoptotic signaling. J Cell Biol. 1998;140(6):1485-95.

295. Susin SA, Lorenzo HK, Zamzami N, Marzo I, Snow BE, Brothers GM, et al. Molecular characterization of mitochondrial apoptosis-inducing factor. Nature. 1999;397(6718):441-6.

296. Li P, Nijhawan D, Budihardjo I, Srinivasula S, Ahmad M, Alnemri E, et al. Cytochrome c and dATP-Dependent formation of Apaf-1/Caspase-9 complex initiates an apoptotic protease cascade. Cell. 1997;91:479-89.

297. Kluck RM, Bossy-Wetzel E, Green DR, Newmeyer DD. The release of cytochrome c from mitochondria: a primary site for Bcl-2 regulation of apoptosis. Science. 1997;275(5303):1132-6.

298. Giam M, Huang DCS, Bouillet P. BH3-only proteins and their roles in programmed cell death. Oncogene. 2008;27:S128-S36.

299. Gavathiotis E, Suzuki M, Davis M, Pitter K, Bird G, Katz S, et al. BAX activation is initiated at a novel interaction site. Nature. 2008;455:1076-82.

300. Willis SN, Fletcher JI, Kaufmann T, van Delft MF, Chen L, Czabotar PE, et al. Apoptosis initiated when BH3 ligands engage multiple Bcl-2 homologs, not Bax or Bak. Science. 2007;315(5813):856-9.

301. Letai A, Bassik MC, Walensky LD, Sorcinelli MD, Weiler S, Korsmeyer SJ. Distinct BH3 domains either sensitize or activate mitochondrial apoptosis, serving as prototype cancer therapeutics. Cancer Cell. 2002;2(3):183-92.

302. Chen L, Willis SN, Wei A, Smith BJ, Fletcher JI, Hinds MG, et al. Differential targeting of prosurvival Bcl-2 proteins by their BH3-only ligands allows complementary apoptotic function. Mol Cell. 2005;17(3):393-403.

303. Cartron PF, Gallenne T, Bougras G, Gautier F, Manero F, Vusio P, et al. The first alpha helix of Bax plays a necessary role in its ligand-induced activation by the BH3-only proteins bid and PUMA. Molecular Cell. 2004;16(5):807-18.

304. Certo M, Moore VD, Nishino M, Wei G, Korsmeyer S, Armstrong SA, et al. Mitochondria primed by death signals determine cellular addiction to antiapoptotic BCL-2 family members. Cancer Cell. 2006;9(5):351-65.

305. Merino D, Giam M, Hughes PD, Siggs OM, Heger K, O'Reilly LA, et al. The role of BH3-only protein Bim extends beyond inhibiting Bcl-2-like prosurvival proteins. J Cell Biol. 2009;186(3):355-62.

306. O'Connor L, Strasser A, O'Reilly LA, Hausmann G, Adams JM, Cory S, et al. Bim: a novel member of the Bcl-2 family that promotes apoptosis. Embo j. 1998;17(2):384-95.

307. Kuwana T, Bouchier-Hayes L, Chipuk JE, Bonzon C, Sullivan BA, Green DR, et al. BH3 domains of BH3-only proteins differentially regulate bax-mediated mitochondrial membrane permeabilization both directly and indirectly. Molecular Cell. 2005;17(4):525-35.

308. Puthalakath H, Huang DC, O'Reilly LA, King SM, Strasser A. The proapoptotic activity of the Bcl-2 family member Bim is regulated by interaction with the dynein motor complex. Mol Cell. 1999;3(3):287-96.

309. Lei K, Davis R. JNK phosphorylation of Bim-related members of the Bcl2 family induces Bax-dependent apoptosis. Procedures of the National Academy of Sciences of the United States of America. 2003;100(5):2432-7.

310. Puthalakath H, Strasser A. Keeping killers on a tight leash: transcriptional and post-translational control of the pro-apoptotic activity of BH3-only proteins. Cell Death Differ. 2002;9(5):505-12.

311. Wickenden JA, Jin H, Johnson M, Gillings AS, Newson C, Austin M, et al. Colorectal cancer cells with the BRAF(V600E) mutation are addicted to the ERK1/2 pathway for growth factor-independent survival and repression of BIM. Oncogene. 2008;27(57):7150-61.

312. Greenhough A, Wallam C, Hicks D, Moorghen M, Williams A, Paraskeva C. The proapoptotic BH3-only protein Bim is downregulated in a subset of colorectal cancers and is repressed by antiapoptotic COX-2/PGE2 signalling in colorectal adenoma cells. Oncogene. 2010;29:3398-410.

313. Ramesh S, Qi XJ, Wildey GM, Robinson J, Molkentin J, Letterio J, et al. TGF beta-mediated BIM expression and apoptosis are regulated through SMAD3-dependent expression of the MAPK phosphatase MKP2. Embo Reports. 2008;9(10):990-7.

314. Qi XJ, Wildey GM, Howe PH. Evidence that Ser(87) of Bim(EL) is phosphorylated by Akt and regulates BimEL apoptotic function. Journal of Biological Chemistry. 2006;281(2):813-23.

315. Puthalakath H, O'Reilly LA, Gunn P, Lee L, Kelly PN, Huntington ND, et al. ER stress triggers apoptosis by activating BH3-only protein Bim. Cell. 2007;129(7):1337-49.

316. Yang Y, Zhao Y, Liao W, Yang J, Wu L, Zheng Z, et al. Acetylation of FoxO1 activates Bim expression to induce apoptosis in response to histone deacetylase inhibitor depsipeptide treatment. Neoplasia. 2009;11(4):313-24.

317. Essafi A, Fernandez de Mattos S, Hassen YA, Soeiro I, Mufti GJ, Thomas NS, et al. Direct transcriptional regulation of Bim by FoxO3a mediates STI571-induced apoptosis in Bcr-Abl-expressing cells. Oncogene. 2005;24(14):2317-29.

318. Luo H, Yang Y, Duan J, Wu P, Jiang Q, Xu C. PTEN-regulated AKT/FoxO3a/Bim signalling contributes to reative oxygen species-mediated apoptosis in selenite-treated colorectal cancer. Cell Death and Disease. 2013;4:e481.

319. Stahl M, Dijkers PF, Kops GJ, Lens SM, Coffer PJ, Burgering BM, et al. The forkhead transcription factor FoxO regulates transcription of p27Kip1 and Bim in response to IL-2. J Immunol. 2002;168(10):5024-31.

320. Dijkers PF, Medema RH, Lammers JW, Koenderman L, Coffer PJ. Expression of the pro-apoptotic Bcl-2 family member Bim is regulated by the forkhead transcription factor FKHR-L1. Curr Biol. 2000;10(19):1201-4.

321. Zhao Y, Tan J, Zhuang L, Jiang X, Liu ET, Yu Q. Inhibitors of histone deacetylases target the Rb-E2F1 pathway for apoptosis induction through activation of proapoptotic protein Bim. Proc Natl Acad Sci U S A. 2005;102(44):16090-5.

322. Maldonado V, Melendez-Zajgla J. Role of Bcl-3 in solid tumors. Molecular Cancer.10:152.

323. Lazebnik YA, Kaufmann SH, Desnoyers S, Poirier GG, Earnshaw WC. Cleavage of poly(ADP-ribose) polymerase by a proteinase with properties like ICE. Nature. 1994;371(6495):346-7.

324. Caserta TM, Smith AN, Gultice AD, Reedy MA, Brown TL. Q-VD-OPh, a broad spectrum caspase inhibitor with potent antiapoptotic properties. Apoptosis. 2003;8(4):345-52.

325. Adams JM, Cory S. Bcl-2-regulated apoptosis: mechanism and therapeutic potential. Curr Opin Immunol. 2007;19(5):488-96.

326. Chen CL, Edelstein LC, Gelinas C. The Rel/NF-kappa B family directly activates expression of the apoptosis inhibitor Bcl-x(L). Molecular and Cellular Biology. 2000;20(8):2687-95.

327. Bouillet P, Zhang LC, Huang DCS, Webb GC, Bottema CDK, Shore P, et al. Gene structure, alternative splicing, and chromosomal localization of pro-apoptotic Bcl-2 relative Bim. Mammalian Genome. 2001;12(2):163-8.

328. Rampino N, Yamamoto H, Ionov Y, Li Y, Sawai H, Reed JC, et al. Somatic frameshift mutations in the BAX gene in colon cancers of the microsatellite mutator phenotype. Science. 1997;275(5302):967-9.

329. Carthew RW, Sontheimer EJ. Origins and Mechanisms of miRNAs and siRNAs. Cell. 2009;136(4):642-55.

330. Jackson AL, Bartz SR, Schelter J, Kobayashi SV, Burchard J, Mao M, et al. Expression profiling reveals off-target gene regulation by RNAi. Nature Biotechnology. 2003;21(6):635-7.

331. Sunters A, Fernandez de Mattos S, Stahl M, Brosens JJ, Zoumpoulidou G, Saunders CA, et al. FoxO3a transcriptional regulation of Bim controls apoptosis in paclitaxel-treated breast cancer cell lines. J Biol Chem. 2003;278(50):49795-805.

332. Greer EL, Brunet A. FOXO transcription factors at the interface between longevity and tumor suppression. Oncogene. 2005;24(50):7410-25.

333. Lorenz TC. Polymerase Chain Reaction: Basic Protocol Plus Troubleshooting and Optimization Strategies. Jove-Journal of Visualized Experiments. 2012(63).

334. Strahl BD, Allis CD. The language of covalent histone modifications. Nature. 2000;403(6765):41-5.

335. Komarnitsky P, Cho EJ, Buratowski S. Different phosphorylated forms of RNA polymerase II and associated mRNA processing factors during transcription. Genes & Development. 2000;14(19):2452-60.

336. Krajewska M, Moss SF, Krajewski S, Song K, Holt PR, Reed JC. Elevated expression of Bcl-X and reduced bak in primary colorectal adenocarcinomas. Cancer Research. 1996;56(10):2422-7.

337. Krajewska M, Kim H, Kim C, Kang HY, Welsh K, Matsuzawa S, et al. Analysis of apoptosis protein expression in early-stage colorectal cancer suggests opportunities for new prognostic biomarkers. Clinical Cancer Research. 2005;11(15):5451-61.

338. Zaanan A, Okamoto K, Kawakami H, Khazaie K, Huang SB, Sinicrope FA. The Mutant KRAS Gene Up-regulates BCL-XL Protein via STAT3 to Confer Apoptosis Resistance That Is Reversed by BIM Protein Induction and BCL-XL Antagonism. Journal of Biological Chemistry. 2015;290(39):23838-49.

339. Oltersdorf T, Elmore SW, Shoemaker AR, Armstrong RC, Augeri DJ, Belli BA, et al. An inhibitor of Bcl-2 family proteins induces regression of solid tumours. Nature. 2005;435(7042):677-81.

340. Savinova OV, Hoffmann A, Ghosh G. The Nfkb1 and Nfkb2 Proteins p105 and p100 Function as the Core of High-Molecular-Weight Heterogeneous Complexes. Molecular Cell. 2009;34(5):591-602.

341. Scherr AL, Gdynia G, Salou M, Radhakrishnan P, Duglova K, Heller A, et al. Bcl-x(L) is an oncogenic driver in colorectal cancer. Cell Death & Disease. 2016;7.

342. Sinicrope FA, Ruan SB, Cleary KR, Stephens LC, Lee JJ, Levin B. BCL-2 AND P53 ONCOPROTEIN EXPRESSION DURING COLORECTAL TUMORIGENESIS. Cancer Research. 1995;55(2):237-41.

343. Huang SB, Sinicrope FA. BH3 mimetic ABT-737 potentiates TRAIL-mediated apoptotic signaling by unsequestering bim and bak in human pancreatic cancer cells. Cancer Research. 2008;68(8):2944-51.

344. Chen S, Dai Y, Pei XY, Grant S. Bim Upregulation by Histone Deacetylase Inhibitors Mediates Interactions with the Bcl-2 Antagonist ABT-737: Evidence for Distinct Roles for Bcl-2, Bcl-x(L), and Mcl-1. Molecular and Cellular Biology. 2009;29(23):6149-69.

345. Okumura K, Huang SB, Sinicrope FA. Induction of Noxa Sensitizes Human Colorectal Cancer Cells Expressing Mcl-1 to the Small-Molecule Bcl-2/Bcl-X-L Inhibitor, ABT-737. Clinical Cancer Research. 2008;14(24):8132-42.

346. Souers AJ, Leverson JD, Boghaert ER, Ackler SL, Catron ND, Chen J, et al. ABT-199, a potent and selective BCL-2 inhibitor, achieves antitumor activity while sparing platelets. Nature Medicine. 2013;19(2):202-8.

347. Flatmark K, Nome RV, Folkvord S, Bratland A, Rasmussen H, Ellefsen MS, et al. Radiosensitization of colorectal carcinoma cell lines by histone deacetylase inhibition. Radiation Oncology. 2006;1.

348. Hoeijmakers JHJ. Genome maintenance mechanisms for preventing cancer. Nature. 2001;411(6835):366-74.

349. Bunz F, Dutriaux A, Lengauer C, Waldman T, Zhou S, Brown JP, et al. Requirement for p53 and p21 to sustain G(2) arrest after DNA damage. Science. 1998;282(5393):1497-501.

350. Zhou BBS, Elledge SJ. The DNA damage response: putting checkpoints in perspective. Nature. 2000;408(6811):433-9.

351. Modrich P, Lahue R. Mismatch repair in replication fidelity, genetic recombination, and cancer biology. Annual Review of Biochemistry. 1996;65:101-33.

352. Wang ML, Wu WZ, Wu WQ, Rosidi B, Zhang LH, Wang HC, et al. PARP-1 and Ku compete for repair of DNA double strand breaks by distinct NHEJ pathways. Nucleic Acids Research. 2006;34(21):6170-82.

353. Ward JF. DNA DAMAGE PRODUCED BY IONIZING-RADIATION IN MAMMALIAN-CELLS - IDENTITIES, MECHANISMS OF FORMATION, AND REPARABILITY. Progress in Nucleic Acid Research and Molecular Biology. 1988;35:95-125.

354. Hustedt N, Durocher D. The control of DNA repair by the cell cycle. Nature Cell Biology. 2017;19(1):1-9.

355. Symington LS, Gautier J. Double-Strand Break End Resection and Repair Pathway Choice. Annual Review of Genetics, Vol 45. 2011;45:247-71.

356. Ceccaldi R, Rondinelli B, D'Andrea AD. Repair Pathway Choices and Consequences at the Double-Strand Break. Trends in Cell Biology. 2016;26(1):52-64.

357. Kastan MB, Bartek J. Cell-cycle checkpoints and cancer. Nature. 2004;432(7015):316-23.

358. Kennedy RD, D'Andrea AD. DNA repair pathways in clinical practice: Lessons from pediatric cancer susceptibility syndromes. Journal of Clinical Oncology. 2006;24(23):3799-808.

359. Ceccaldi R, Liu JC, Amunugama R, Hajdu I, Primack B, Petalcorin MIR, et al. Homologous-recombination-deficient tumours are dependent on Pol theta-mediated repair. Nature. 2015;518(7538):258-U306.

360. Yang G, Liu C, Chen SH, Kassab MA, Hoff JD, Walter NG, et al. Super-resolution imaging identifies PARP1 and the Ku complex acting as DNA double-strand break sensors. Nucleic Acids Res. 2018.

361. Aleksandrov R, Dotchev A, Poser I, Krastev D, Georgiev G, Panova G, et al. Protein Dynamics in Complex DNA Lesions. Mol Cell. 2018;69(6):1046-61.e5.

362. Sun YL, Jiang XF, Chen SJ, Fernandes N, Price BD. A role for the Tip60 histone acetyltransferase in the acetylation and activation of ATM. Proceedings of the National Academy of Sciences of the United States of America. 2005;102(37):13182-7.

363. Paull TT. Mechanisms of ATM Activation. Annual Review of Biochemistry, Vol 84. 2015;84:711-38.

364. Burma S, Chen BP, Murphy M, Kurimasa A, Chen DJ. ATM phosphorylates histone H2AX in response to DNA double-strand breaks. Journal of Biological Chemistry. 2001;276(45):42462-7.

365. Ward IM, Chen JJ. Histone H2AX is phosphorylated in an ATR-dependent manner in response to replicational stress. Journal of Biological Chemistry. 2001;276(51):47759-62.

366. Stiff T, O'Driscoll M, Rief N, Iwabuchi K, Lobrich M, Jeggo PA. ATM and DNA-PK function redundantly to phosphorylate H2AX after exposure to ionizing radiation. Cancer Research. 2004;64(7):2390-6.

367. Paull TT, Rogakou EP, Yamazaki V, Kirchgessner CU, Gellert M, Bonner WM. A critical role for histone H2AX in recruitment of repair factors to nuclear foci after DNA damage. Current Biology. 2000;10(15):886-95.

368. Rogakou EP, Pilch DR, Orr AH, Ivanova VS, Bonner WM. DNA double-stranded breaks induce histone H2AX phosphorylation on serine 139. Journal of Biological Chemistry. 1998;273(10):5858-68.

369. Morrison AJ, Highland J, Krogan NJ, Arbel-Eden A, Greenblatt JF, Haber JE, et al. INO80 and gamma-H2AX interaction links ATP-dependent chromatin remodeling to DNA damage repair. Cell. 2004;119(6):767-75.

370. Shen XT, Mizuguchi G, Hamiche A, Wu C. A chromatin remodelling complex involved in transcription and DNA processing. Nature. 2000;406(6795):541-4.

371. Stucki M, Clapperton JA, Mohammad D, Yaffe MB, Smerdon SJ, Jackson SP. MDC1 directly binds phosphorylated histone H2AX to regulate cellular responses to DNA double-strand breaks. Cell. 2005;123(7):1213-26.

372. Kolas NK, Chapman JR, Nakada S, Ylanko J, Chahwan R, Sweeney FD, et al. Orchestration of the DNA-damage response by the RNF8 ubiquitin ligase. Science. 2007;318(5856):1637-40.

373. Mailand N, Bekker-Jensen S, Faustrup H, Melander F, Bartek J, Lukas C, et al. RNF8 ubiquitylates histones at DNA double-strand breaks and promotes assembly of repair proteins. Cell. 2007;131(5):887-900.

374. Huen MSY, Grant R, Manke I, Minn K, Yu XC, Yaffe MB, et al. RNF8 transduces the DNA-damage signal via histone ubiquitylation and checkpoint protein assembly. Cell. 2007;131(5):901-14.

375. Goldberg M, Stucki M, Falck J, D'Amours D, Rahman D, Pappin D, et al. MDC1 is required for the intra-S-phase DNA damage checkpoint. Nature. 2003;421(6926):952-6.

376. Boulton S, Gartner A, Reboul J, Vaglio P, Dyson N, Hill D, et al. Combined functional genomic maps of the C. elegans DNA Damage Response. Science. 2002;295:127-31.

377. Massoumi R, Chmielarska K, Hennecke K, Pfeifer A, Fassler R. Cyld inhibits tumor cell proliferation by blocking Bcl-3-dependent NF-kappa B signaling. Cell. 2006;125(4):665-77.

378. Miyamoto S. Nuclear initiated NF-kappa B signaling: NEMO and ATM take center stage. Cell Research. 2011;21(1):116-30.

379. Piret B, Schoonbroodt S, Piette J. The ATM protein is required for sustained activation of NF-kappa B following DNA damage. Oncogene. 1999;18(13):2261-71.

380. Lee SJ, Dimtchev A, Lavin MF, Dritschilo A, Jung M. A novel ionizing radiation-induced signaling pathway that activates the transcription factor NF-kappa B. Oncogene. 1998;17(14):1821-6.

381. Liu XJ, Li F, Huang Q, Zhang ZX, Zhou L, Deng Y, et al. Self-inflicted DNA double-strand breaks sustain tumorigenicity and stemness of cancer cells. Cell Research. 2017;27(6):764-83.

382. Huang TT, Wuerzbrger-Davis SM, Wu ZH, Miyamoto S. Sequential modification of NEMO/IKK gamma by SUMO-1 and ubiquitin mediates NF-kappa B activation by genotoxic stress. Cell. 2003;115(5):565-76.

383. Stilmann M, Hinz M, Arslan SC, Zimmer A, Schreiber V, Scheidereit C. A Nuclear Poly(ADP-Ribose)-Dependent Signalosome Confers DNA Damage-Induced I kappa B Kinase Activation. Molecular Cell. 2009;36(3):365-78.

384. Schmitt AM, Crawley CD, Kang SJ, Raleigh DR, Yu XH, Wahlstrom JS, et al. p50 (NF-kappa B1) Is an Effector Protein in the Cytotoxic Response to DNA Methylation Damage. Molecular Cell. 2011;44(5):785-96.

385. Schmitt A, Crawley C, Kang S, Raleigh D, Weichselbaum R, Yamini B. O6-methylguanine DNA Damage Signals Through Nfkb1/p50 to Potentiate DNA Strand Break-induced Cytotoxicity. International Journal of Radiation Oncology Biology Physics. 2012;84(3):S674-S.

386. O'Neil BH, Funkhouser WK, Calvo BF, Meyers MO, Kim HJ, Goldberg RM, et al. NUCLEAR FACTOR kappa-LIGHT CHAIN-ENHANCER OF ACTIVATED B CELLS IS ACTIVATED BY RADIOTHERAPY AND IS PROGNOSTIC FOR OVERALL SURVIVAL IN PATIENTS WITH RECTAL CANCER TREATED WITH PREOPERATIVE FLUOROURACIL-BASED CHEMORADIOTHERAPHY. International Journal of Radiation Oncology Biology Physics. 2011;80(3):705-11.

387. Lewander A, Gao JF, Adell G, Zhang H, Sun XF. Expression of NF-kappa B p65 phosphorylated at serine-536 in rectal cancer with or without preoperative radiotherapy. Radiology and Oncology. 2011;45(4):279-84.

388. Voboril R, Rychterova V, Voborilova J, Kubecova M, Fanta J, Dvorak J. NF-kappa B/p65 expression before and after treatment in rectal cancer patients undergoing neoadjuvant (chemo)radiotherapy and surgery: prognostic marker for disease progression and survival. Neoplasma. 2016;63(3):462-70.

389. Bhat KPL, Balasubramaniyan V, Vaillant B, Ezhilarasan R, Hummelink K, Hollingsworth F, et al. Mesenchymal Differentiation Mediated by NF-kappa B Promotes Radiation Resistance in Glioblastoma. Cancer Cell. 2013;24(3):331-46.

390. Dzhugashvili M, Luengo-Gil G, Garcia T, Gonzalez-Conejero R, Conesa-Zamora P, Escolar PP, et al. Role of genetic polymorphisms in NFKB-mediated inflammatory pathways in response to primary chemoradiation therapy for rectal cancer. Int J Radiat Oncol Biol Phys. 2014;90(3):595-602.

391. Karban AS, Okazaki T, Panhuysen CIM, Gallegos T, Potter JJ, Bailey-Wilson JE, et al. Functional annotation of a novel NFKB1 promoter polymorphism that increases risk for ulcerative colitis. Human Molecular Genetics. 2004;13(1):35-45.

392. Hanahan D, Coussens L. Accessories to the Crime: Functions of cells recruited to the Tumor Microenvironment. Cancer Cell. 2012;21:309-22.

393. Bhowmick NA, Moses HL. Tumor-stroma interactions. Current Opinion in Genetics & Development. 2005;15(1):97-101.

394. Hutchins GGA, Treanor D, Wright A, Handley K, Magill L, Tinkler-Hundal E, et al. Intratumoral stromal morphometry predicts disease recurrence but not response to 5-fluorouracilresults from the QUASAR trial of colorectal cancer. Histopathology. 2018;72(3):391-404.

395. Lohr M, Schmidt C, Ringel J, Kluth M, Muller P, Nizze H, et al. Transforming growth factor-beta 1 induces desmoplasia in an experimental model of human pancreatic carcinoma. Cancer Research. 2001;61(2):550-5.

396. Pena C, Cespedes MV, Lindh MB, Kiflemariam S, Mezheyeuski A, Edqvist PH, et al. STC1 Expression By Cancer-Associated Fibroblasts Drives Metastasis of Colorectal Cancer. Cancer Research. 2013;73(4):1287-97.

397. Bhowmick NA, Neilson EG, Moses HL. Stromal fibroblasts in cancer initiation and progression. Nature. 2004;432(7015):332-7.

398. Kalluri R, Zeisberg M. Fibroblasts in cancer. Nature Reviews Cancer. 2006;6:392-401.

399. Sun YQ, Wang RF, Qiao M, Xu YC, Guan WB, Wang LF. Cancer associated fibroblasts tailored tumor microenvironment of therapy resistance in gastrointestinal cancers. Journal of Cellular Physiology. 2018;233(9):6359-69.

400. Tommelein J, Verset L, Boterberg T, Demetter P, Bracke M, De Wever O. Cancer-associated fibroblasts connect metastasis-promoting communication in colorectal cancer. Frontiers in Oncology. 2015;5.

401. Xing F, Saidou J, Watabe K. Cancer associated fibroblasts (CAFs) in tumor microenvironment. Front Biosci (Landmark Ed). 2010;15:166-79.

402. Nishishita R, Morohashi S, Seino H, Wu YY, Yoshizawa T, Haga T, et al. Expression of cancer-associated fibroblast markers in advanced colorectal cancer. Oncology Letters. 2018;15(5):6195-202.

403. Herrera M, Herrera A, Dominguez G, Silva J, Garcia V, Garcia JM, et al. Cancer-associated fibroblast and M2 macrophage markers together predict outcome in colorectal cancer patients. Cancer Science. 2013;104(4):437-44.

404. Schneider S, Park DJ, Yang DY, El-Khoueiry A, Sherrod A, Groshen S, et al. Gene expression in tumor-adjacent normal tissue is associated with recurrence in patients with rectal cancer treated with adjuvant chemoradiation. Pharmacogenetics and Genomics. 2006;16(8):555-63.

405. Saigusa S, Toiyama Y, Tanaka K, Yokoe T, Okugawa Y, Fujikawa H, et al. Cancer-associated fibroblasts correlate with poor prognosis in rectal cancer after chemoradiotherapy. International Journal of Oncology. 2011;38(3):655-63.

406. Saigusa S, Toiyama Y, Tanaka K, Inoue Y, Mori K, Ide S, et al. Prognostic relevance of stromal CD26 expression in rectal cancer after chemoradiotherapy. International Journal of Clinical Oncology. 2016;21(2):350-8.

407. Tommelein J, De Vlieghere E, Verset L, Melsens E, Leenders J, Descamps B, et al. Radiotherapy-Activated Cancer-Associated Fibroblasts Promote Tumor Progression through Paracrine IGF1R Activation. Cancer Research. 2018;78(3):659-70.

408. Ohuchida K, Mizumoto K, Murakami M, Qian LW, Sato N, Nagai E, et al. Radiation to stromal fibroblasts increases invasiveness of pancreatic cancer cells through tumor-stromal interactions. Cancer Research. 2004;64(9):3215-22.

409. Shia J, Guillem JG, Moore HG, Tickoo SK, Qin J, Ruo L, et al. Patterns of morphologic alteration in residual rectal carcinoma following preoperative chemoradiation and their association with long-term outcome. Am J Surg Pathol. 2004;28(2):215-23.

410. Erez N, Truitt M, Olsen P, Hanahan D. Cancer-associated fibroblasts are activated in incipient neoplasia to orchestrate tumour-promoting inflammation in an NF-kB-dependant manner. Cancer Cell. 2010;17(2):135-47.

411. Dolznig H, Rupp C, Puri C, Haslinger C, Schweifer N, Wieser E, et al. Modeling Colon Adenocarcinomas in Vitro A 3D Co-Culture System Induces Cancer-Relevant Pathways upon Tumor Cell and Stromal Fibroblast Interaction. American Journal of Pathology. 2011;179(1):487-501.

412. Taga T, Hibi M, Hirata Y, Yamasaki K, Yasukawa K, Matsuda T, et al. Interleukin-6 triggers the association of its receptor with a possible signal transducer, gp130. Cell. 1989;58(3):573-81.

413. Garbers C, Heink S, Korn T, Rose-John S. Interleukin-6: designing specific therapeutics for a complex cytokine. Nat Rev Drug Discov. 2018;17(6):395-412.

414. Mao Y, Zhang Y, Qu Q, Zhao M, Lou Y, Liu J, et al. Cancer-associated fibroblasts induce trastuzumab resistance in HER2 positive breast cancer cells. Molecular Biosystems. 2015;11:1029-40.

415. Nagasaki T, Hara M, Nakanishi H, Takahashi H, Sato M, Takeyama H. Interleukin-6 released by colon cancer-associated fibroblasts is critical for tumour angiogenesis: anti-interleukin-6 receptor antibody suppressed angiogenesis and inhibited tumour-stroma interaction. British Journal of Cancer. 2014;110:469-78.

416. Brenne AT, Fagerli UM, Shaughnessy JD, Vatsveen TK, Ro TB, Hella H, et al. High expression of BCL3 in human myeloma cells is associated with increased proliferation and inferior prognosis. European Journal of Haematology. 2009;82(5):354-63.

417. Rodel C, Graeven U, Fietkau R, Hohenberger W, Hothorn T, Arnold D, et al. Oxaliplatin added to fluorouracil-based preoperative chemoradiotherapy and postoperative chemotherapy of locally advanced rectal cancer (the German CAO/ARO/AIO-04 study): final results of the multicentre, open-label, randomised, phase 3 trial. Lancet Oncol. 2015.

418. Pampaloni F, Reynaud EG, Stelzer EH. The third dimension bridges the gap between cell culture and live tissue. Nat Rev Mol Cell Biol. 2007;8(10):839-45.

419. Sato T, Stange DE, Ferrante M, Vries RG, Van Es JH, Van den Brink S, et al. Long-term expansion of epithelial organoids from human colon, adenoma, adenocarcinoma, and Barrett's epithelium. Gastroenterology. 2011;141(5):1762-72.

420. Jager T, Neureiter D, Urbas R, Klieser E, Hitzl W, Emmanuel K, et al. Applicability of American Joint Committee on Cancer and College of American Pathologists regression grading system in rectal cancer. Diseases of the Colon and Rectum. 2017;60(8):757-873.

421. Ronnovjessen L, Petersen OW. INDUCTION OF ALPHA-SMOOTH MUSCLE ACTIN BY TRANSFORMING GROWTH-FACTOR-BETA-1 IN QUIESCENT HUMAN BREAST GLAND FIBROBLASTS - IMPLICATIONS FOR MYOFIBROBLAST GENERATION IN BREAST NEOPLASIA. Laboratory Investigation. 1993;68(6):696-707.

422. Morgan RG, Chambers AC, Legge DN, Coles SJ, Greenhough A, Williams AC. Optimized delivery of siRNA into 3D tumor spheroid cultures in situ. Scientific Reports. 2018;8.

423. Lobrich M, Shibata A, Beucher A, Fisher A, Ensminger M, Goodarzi AA, et al. gamma H2AX foci analysis for monitoring DNA double-strand break repair Strengths, limitations and optimization. Cell Cycle. 2010;9(4):662-9.

424. McCabe N, Turner NC, Lord CJ, Kluzek K, Bialkowska A, Swift S, et al. Deficiency in the repair of DNA damage by homologous recombination and sensitivity to poly(ADP-ribose) polymerase inhibition. Cancer Research. 2006;66(16):8109-15.

425. Wiltshire TD, Lovejoy CA, Wang T, Xia F, O'Connor MJ, Cortez D. Sensitivity to Poly(ADP-ribose) Polymerase (PARP) Inhibition Identifies Ubiquitin-specific Peptidase 11 (USP11) as a Regulator of DNA Double-strand Break Repair. Journal of Biological Chemistry. 2010;285(19):14565-71.

426. Junttila MR, de Sauvage FJ. Influence of tumour micro-environment heterogeneity on therapeutic response. Nature. 2013;501(7467):346-54.

427. Mueller MM, Fusenig NE. Friends or foes - Bipolar effects of the tumour stroma in cancer. Nature Reviews Cancer. 2004;4(11):839-49.

428. Wu LT, Bernal GM, Cahill KE, Pytel P, Fitzpatrick CA, Mashek H, et al. BCL3 expression promotes resistance to alkylating chemotherapy in gliomas. Science Translational Medicine. 2018;10(448).

429. Banath JP, MacPhail SH, Olive PL. Radiation sensitivity, H2AX phosphorylation, and kinetics of repair of DNA strand breaks in irradiated cervical cancer cell lines. Cancer Research. 2004;64(19):7144-9.

430. Taneja N, Davis M, Choy JS, Beckett MA, Singh R, Kron SJ, et al. Histone H2AX phosphorylation as a predictor of radiosensitivity and target for radiotherapy. Journal of Biological Chemistry. 2004;279(3):2273-80.

431. Wang Z, Zhang BC, Yang LQ, Ding J, Ding HF. Constitutive production of NF-kappa B2 p52 is not tumorigenic but predisposes mice to inflammatory autoimmune disease by repressing bim expression. Journal of Biological Chemistry. 2008;283(16):10698-706.

432. Kurdistani SK, Tavazoie S, Grunstein M. Mapping global histone acetylation patterns to gene expression. Cell. 2004;117(6):721-33.

433. Eberharter A, Becker PB. Histone acetylation: a switch between repressive and permissive chromatin - Second in review series on chromatin dynamics. Embo Reports. 2002;3(3):224-9.

434. Masumoto H, Hawke D, Kobayashi R, Verreault A. A role for cell-cycle-regulated histone H3 lysine 56 acetylation in the DNA damage response. Nature. 2005;436(7048):294-8.

435. Munshi A, Tanaka T, Hobbs ML, Tucker SL, Richon VM, Meyn RE. Vorinostat, a histone deacetylase inhibitor, enhances the response of human tumor

cells to ionizing radiation through prolongation of gamma-H2AX foci. Molecular Cancer Therapeutics. 2006;5(8):1967-74.

436. Hishiki T, Ohshima T, Ego T, Shimotohno K. BCL3 acts as a negative regulator of transcription from the human T-cell leukemia virus type 1 long terminal repeat through interactions with TORC3. Journal of Biological Chemistry. 2007;282(39):28335-43.

437. Robert T, Vanoli F, Chiolo I, Shubassi G, Bernstein KA, Rothstein R, et al. HDACs link the DNA damage response, processing of double-strand breaks and autophagy. Nature. 2011;471(7336):74-9.

438. Murr R, Loizou JI, Yang YG, Cuenin C, Li H, Wang ZQ, et al. Histone acetylation by Trrap-Tip60 modulates loading of repair proteins and repair of DNA double-strand breaks. Nature Cell Biology. 2006;8(1):91-U36.

439. Kim MY, Ann EJ, Kim JY, Mo JS, Park JH, Kim SY, et al. Tip60 histone acetyltransferase acts as a negative regulator of notch1 signaling by means of acetylation. Molecular and Cellular Biology. 2007;27(18):6506-19.

440. Mavragani IV, Nikitaki Z, Souli MP, Aziz A, Nowsheen S, Aziz K, et al. Complex DNA Damage: A Route to Radiation-Induced Genomic Instability and Carcinogenesis. Cancers. 2017;9(7).

441. Ward JF. THE COMPLEXITY OF DNA-DAMAGE - RELEVANCE TO BIOLOGICAL CONSEQUENCES. International Journal of Radiation Biology. 1994;66(5):427-32.

442. Dikomey E, Dahm-Daphi I, Brammer R, Martensen B. Correlation between cellular radiosensitivity and non-repaired double-strand breaks studied in nine mammalian cell lines. International Journal of Radiation Biology. 1998;73(3):269-78.

443. Schipler A, Iliakis G. DNA double-strand-break complexity levels and their possible contributions to the probability for error-prone processing and repair pathway choice. Nucleic Acids Research. 2013;41(16):7589-605.

444. Jezkova L, Zadneprianetc M, Kulikova E, Smirnova E, Bulanova T, Depes D, et al. Particles with similar LET values generate DNA breaks of different complexity and reparability: a high-resolution microscopy analysis of gamma H2AX/53BP1 foci. Nanoscale. 2018;10(3):1162-79.

445. Li MZ, Tian SL, Jin L, Zhou GY, Li Y, Zhang Y, et al. Genomic analyses identify distinct patterns of selection in domesticated pigs and Tibetan wild boars. Nature Genetics. 2013;45(12):1431-U180.